Molecular and Functional Characterization of the Novel Lectin EclA from the *Enterobacter cloacae* Complex

Dissertation

Zur Erlangung des Grades des Doktors der Naturwissenschaften der Naturwissenschaftlich-Technischen Fakultät der Universität des Saarlandes

von Mario Fares, MSc.

Saarbrücken, 2025

Tag des Kolloquiums:	11.03.2026
Dekan:	Prof. Dr.-Ing. Dirk Bähre
Berichterstatter:	Prof. Dr. Alexander Titz Prof. Dr. Markus Bischoff
Vorsitz:	Prof. Dr. Claus-Michael Lehr
Akad. Mitglied:	Dr. Jennifer Herrmann

I. Summary

Bacterial lectins are carbohydrate-binding proteins that contribute to pathogenesis, making them attractive anti-virulence targets. The *Enterobacter cloacae* complex (ECC), a group of opportunistic pathogens with rising antibiotic resistance, requires such alternative strategies. This thesis presents the first functional characterization of EclA, a newly identified two-domain lectin in ECC species and structurally related to the virulence-associated lectin LecA of *Pseudomonas aeruginosa*.

Targeted gene deletions in *E. cloacae* subsp. *dissolvens* and subsp. *cloacae* showed that EclA is a key driver of aggregation in subsp. *dissolvens*, a process central to biofilm development. Loss of *eclA* abolished aggregation in this subspecies but had no detectable effect in subsp. *cloacae* under the conditions tested. EclA did not act as a primary host adhesin: recombinant protein bound selected host glycans and human type O^+ red blood cells in vitro, but this activity was absent in whole-cell assays under the conditions tested, suggesting a role focused on bacterial community interactions.

A *Galleria mellonella* infection model established here now enables direct assessment of EclA's contribution to virulence and its potential as an anti-virulence target. The findings also open new research avenues, including the role of the plasmid-borne TeR cluster in stress-induced aggregation and evidence for an unidentified hemagglutinating lectin, offering deeper insight into ECC pathophysiology.

II. Zusammenfassung

Bakterielle Lektine sind kohlenhydratbindende Proteine, die zur Pathogenese beitragen und daher als Anti-Virulenz-Ziele vielversprechend sind. Der *Enterobacter-cloacae*-Komplex (ECC), eine Gruppe opportunistischer Erreger mit steigender Antibiotikaresistenz, macht solche Alternativen notwendig. Diese Arbeit liefert die erste funktionelle Charakterisierung von EclA, einem neu identifizierten zweidomainigen Lektin in ECC-Arten, das strukturell LecA von *Pseudomonas aeruginosa* ähnelt.

Gezielte Genlöschungen in *E. cloacae* subsp. *dissolvens* und subsp. *cloacae* zeigten, dass EclA in subsp. *dissolvens* ein zentraler Treiber der Aggregation und damit der Biofilmbildung ist. Der Verlust von *eclA* hob diese Aggregation auf, hatte jedoch unter den getesteten Bedingungen keinen Effekt in subsp. *cloacae*. EclA fungierte nicht als primäres Wirtsadhäsin: Rekombinantes Protein band zwar ausgewählte Glykane und humane Erythrozyten des Typs O^+ in vitro, doch diese Aktivität fehlte in Vollzellassays, was auf eine vorwiegend innerbakterielle Funktion hinweist.

Ein etabliertes *Galleria-mellonella*-Infektionsmodell ermöglicht nun die direkte Untersuchung des Beitrags von EclA zur Virulenz und seines Potenzials als Anti-Virulenz-Ziel. Zudem weisen die Ergebnisse auf neue Forschungsansätze hin, darunter die Rolle des plasmidkodierten TeR-Clusters bei stressinduzierter Aggregation und Hinweise auf ein bislang unbekanntes hämagglutinierendes Lektin.

III. Acknowledgments

First and foremost, I would like to express my sincere gratitude to **Prof. Dr. Alexander Titz**, my main supervisor. He has been an exceptional mentor whose insight across both chemistry and biology continues to inspire me. While chemists may see him as a chemist, I have always seen him as a biologist at heart, effortlessly bridging both worlds. Beyond science, I deeply appreciated the cohesive and warm atmosphere he fostered in the group, whether during summer BBQs, Christmas dinners, or regular outings. Our discussions on science, geopolitics, and Lebanese food were always a pleasure. He is a true inspiration.

I would also like to thank **Prof. Dr. Markus Bischoff**, my co-supervisor, for his valuable insights and for warmly welcoming me to the UKS together with **Ben Wieland**. While our meetings were not always frequent, they were always impactful, including a memorable six-hour marathon session. I truly appreciate his time, proactive involvement, and thoughtful follow-up throughout the project.

I would like to sincerely thank **Prof. Dr. Andriy Luzhetskyy** and **Dr. Nikolas Peter Eckert** for kindly welcoming me into their lab and generously providing their molecular biology expertise regarding the problematic mutator plasmid. My time in their lab was both enjoyable and insightful. Additionally, I am grateful to **Dr. Markus Koch** for providing the SEM microscopy data. A special thanks goes to **Dr. Sari Rasheed** for his training in zebrafish handling and infection model.

To the department members: First, **Simone Amann**, for her constant support, humor, and positive spirit. I also thank **Jeannine Jung** and all other technical assistants for their contributions. I extend my gratitude to **Roya Shafiei** and **Dr. Atanaz Shams** for their kindness and support in introducing me to *Galleria mellonella* handling. A heartfelt thank you as well to **Nicole Klein Ramos** and **Bahareh Kadkhodazadeh** for their efficient and cheerful help with all the administrative tasks.

To my colleagues and friends:

Dirk Hauck, for the endless supply of Prinzen cookies and snacks that kept our office alive, and for always being a reliable and knowledgeable guide whenever I ventured into the chemistry lab as a biologist. Thanks for the help, especially with complicated orderings, shipments, and logistics.

Then, the first generation of office 2.25: **Dr. Stefanie Wagner**, who was my postdoc mentor when I first joined and helped me find my footing in the lab and research. **Dr. Joscha Meiers**, an exceptional scientist whose knowledge spans chemistry and biology, thank you for

launching the beach volleyball tradition and for taking the initiative to establish other ones. Thank you for the help in the chemistry lab, and all the insightful discussions. Thanks also to **Dr. Olga Metelkina** for contributing to the atmosphere in our office.

The second generation of office 2.25, known for keeping the snack shelf well stocked, and also for annihilating it: **Johanna Steinhagen**, a wonderful friend and my unofficial German tutor, thank you for your big heart. **Beshoy Tawfik**, a kind and knowledgeable soul, now carrying on with the EclA project. **Steffen Leusmann**, an exceptional pharmacist, tea expert, kicker and food buddy, thank you for the countless döner runs, Lebanese meal outings, Mensa lunches, late rides home from HIPS, or Mcces/BK, and for your intelligent, calm, and thoughtful conversations on everything from science to space. **Lisa-Marie Denig**, my biology buddy in a chemist's group, thanks for helping me get started in the lab during the Corona days, for all the practical advice, and for always being there. I'll always remember our lunches in the sun with Aldi salads, iced coffee breaks, and the endless memes and laughs we shared. Your support in science and in life meant a lot and made this whole journey lighter.

To our neighbors in office 2.24: **Hanna Perius**, always cheerful and ready for a drink, thank you for being thoughtful, thanks for your energy, the kicker matches, Planwagenfahrt planning and night outs. **Dr. Lorenzo Rossi**, top tier group guest, thank you for the good times, beers, laughs, and intense kicker competitions. I also thank **Marta Czekańska**, **Dr. Thorsten Kinsinger**, **Omar Zareei**, and **Qiuyu Zhu** for their team spirit.

Finally, and most importantly, I thank my family. To my parents, **Marie and Toni**, whom I owe everything to, thank you for your endless love, sacrifices, and encouragement. To my brother **John**, whose achievements and dedication always inspired me. And to **Rudy**, the best support system I could ever ask for, thank you for your constant motivation, care, and presence in every aspect of my life. Thank you for visiting me often with **Laetitia**, and for simply being you.

IV. Publications included in the thesis

-Bacterial Lectins: Multifunctional Tools in Pathogenesis and Possible Drug Targets

Authors: Mario Fares, Anne Imberty, and Alexander Titz*

Published in: *Trends in Microbiology*, 2025, 33, 8, P839-852

DOI: 10.1016/j.tim.2025.03.007

-A Fucose-Binding Superlectin from *E. cloacae* with High Lewis and ABO Blood group Antigen Specificity

Authors: Ghamdan Beshr, Asfandyar Sikandar, Julia Gläser, **Mario Fares**, Roman Sommer, Stefanie Wagner, Jesko Köhnke*, and Alexander Titz*

Published in: *Journal of Biological Chemistry*, 2025, 301, 2, 108151

DOI: 10.1016/j.jbc.2024.108151

-Molecular and Functional Characterization of the Novel Lectin EclA from the *Enterobacter cloacae* Complex

Authors: **Mario Fares**, Stefanie Wagner, Markus Bischoff, Alexander Titz

Manuscript in preparation

Other publications:

-Dual inhibitors of *Pseudomonas aeruginosa* virulence factors LecA and LasB

Authors: Olga Metelkina, Jelena Konstantinović, Andreas Klein, Roya Shafiei, **Mario Fares**, Alaa Alhayek, Samir Yahiaoui, Walid A. M. Elgaher, Jörg Haupenthal, Alexander Titz* and Anna K. H. Hirsch*

Published in: *Chemical Science*, 2024, 15, 13333-13342

DOI: 10.1039/d4sc02703e

-Toward Dual-Target Glycomimetics against Two Bacterial Lectins to Fight *Pseudomonas aeruginosa-Burkholderia cenocepacia* Infections: A Biophysical Study

Authors: Giulia Antonini, **Mario Fares**, Dirk Hauck, Patrycja Mała, Emilie Gillon, Laura Belvisi, Anna Bernardi, Alexander Titz*, Annabelle Varrot*, Sarah Mazzotta*.

Published in: *Journal of Medicinal Chemistry*, 2025, 68, 9, 9681-9693

DOI: 10.1021/acs.jmedchem.5c00405

V. Contributions report

Chapter 1.1: Bacterial Lectins: Multifunctional Tools in Pathogenesis and Possible Drug Targets

Authors: Mario Fares, Anne Imberty, and Alexander Titz*

Published in: *Trends in Microbiology*, 2025, 33, 8, P839-852

DOI: 10.1016/j.tim.2025.03.007

M.F. conceived the outline and drafted the manuscript with continuous revisions based on feedback from A.I. and A.T. A.I. contributed to the bacterial lectin classification section and crystallography figures. A.T. supervised the overall concept and finalization of the manuscript.

Chapter 1.2: A Fucose-Binding Superlectin from *E. cloacae* with High Lewis and ABO Blood group Antigen Specificity

Authors: Ghamdan Beshr, Asfandyar Sikandar, Julia Gläser, **Mario Fares**, Roman Sommer, Stefanie Wagner, Jesko Köhnke*, and Alexander Titz*

Published in: *Journal of Biological Chemistry*, 2025, 301, 2, 108151

DOI: 10.1016/j.jbc.2024.108151

M.F., A.S., A.T., J.K., and S.W. writing-review & editing; M.F., G.B., J.K., and A.T. writing-original draft; G.B., A.S., J.K., and S.W. visualization; G.B., J.K., A.T., and S.W. validation; G.B., J.K., A.T., and S.W. supervision; G.B., A.S., J.G., J.K., and S.W. investigation; G.B., A.S., J.G., J.K., A.T., and S.W. formal analysis; G.B., J.G., J.K., and A.S. data curation; J.K., A.T., A.S., G.B., and S.W. methodology; A.T., J.K., and R.S. resources; A.T. project administration; A.T. funding acquisition; A.T. conceptualization.

Chapter 3.1: Molecular and Functional Characterization of the Novel Lectin EclA from the *Enterobacter cloacae* Complex.

Authors: **Mario Fares**, Stefanie Wagner, Markus Bischoff, Alexander Titz

Manuscript in preparation

M.F., M.B., A.T. writing, review & editing; M.F. writing-original draft; S.W., M.B., A.T. supervision; M.F., S.W., M.B., A.T. investigation; M.F., S.W., M.B., A.T. formal analysis M.F. data curation; M.F., S.W., M.B., A.T. methodology; M.B. and A.T. resources and funding acquisition.

VI. Abbreviations

aap	Accumulation-associated protein
bp	Base pairs
CDS	Coding DNA sequence
CFU	Colony forming unit
CREC	Carbapenem-resistant *Enterobacter cloacae* complex
dpf	Days post fertilization
ECC	*Enterobacter cloacae* complex
EclA	*Enterobacter cloacae* lectin A
ESBL	Extended-spectrum β-lactamase
FITC	Fluorescein isothiocyanate
Gm	Gentamicin
GmR	Gemtamicin resistance
HK	Heat-killed
hpf	Hours post fertilization
hpi	Hours post infection
LDH	Lactate dehydrogenase
Le^a	Lewis A blood group antigen
Le^b	Lewis B blood group antigen
Le^c	Lewis C blood group antigen
LPS	Lipopolysaccharide
MSHA	Mannose-sensitive hemagglutination
MRHA	Mannose-resistant hemagglutination
NCBI	National center for biotechnology information
NICU	Neonatal intensive care unit
ONT	Oxford nanopore technology
ORF	Open reading frame
PCR	Polymerase chain reaction
PCV	Post caudal vein
RBC	Red blood cells
rt	Room temperature
SEM	Scanning electron microscopy
SmR	Streptomycin resistance
T3SS	Type 3 secretion system
T6SS	Type 6 secretion system
TeR	Tellurite resistance
WGS	Whole-genome sequencing
WT	Wild-type

VII. Table of Content

1. Introduction

This introductory section provides the essential scientific background required to contextualize the research presented in this thesis. It is designed to be informative, moving from a broad overview of the field to the specific components of this thesis. Chapter 1.1 begins by presenting a peer-reviewed article on the multifunctional roles of bacterial lectins in pathogenesis and their potential as therapeutic targets. The focus then narrows in Chapter 1.2 to introduce the central molecule of this study: the novel fucose-binding superlectin, EclA, detailing its discovery and unique structural characteristics. Finally, Chapter 1.3 provides a comprehensive background on the bacterial group central to this work, the *Enterobacter cloacae* complex (ECC), covering its intricate taxonomy, clinical relevance as an opportunistic group, and established virulence factors. Together, these chapters provide the necessary context for understanding the aim and hypothesis that drive the subsequent research.

1.1. Bacterial Lectins: Multifunctional Tools in Pathogenesis and Possible Drug Targets

To establish the broader scientific context for the research presented in this thesis, this first chapter provides a comprehensive overview of bacterial lectins. The following work is a peer-reviewed article, authored as part of this doctoral work, which explores the multifunctional roles of these carbohydrate-binding proteins in pathogenesis. It details their classification, their mechanisms of action in host adhesion, biofilm formation, cytotoxicity, and immune evasion, and discusses their emergence as promising targets for novel anti-virulence therapies. This foundational knowledge is essential for understanding the specific investigation into the novel lectin EclA, which forms the core of this thesis.

Authors: **Mario Fares**, Anne Imberty, and Alexander Titz
Published in: *Trends in Microbiology*, 2025, 33, 8, P839-852
DOI: 10.1016/j.tim.2025.03.007

Figures in this chapter are numbered independently from those in the rest of the dissertation. All references cited in this article are listed at the end of this chapter.

Trends in Microbiology

CellPress OPEN ACCESS

Review

Bacterial lectins: multifunctional tools in pathogenesis and possible drug targets

Mario Fares [1,2,3], Anne Imberty [4], and Alexander Titz [1,2,3,*]

Glycans are vital macromolecules with diverse biological roles, decoded by lectins – specialized carbohydrate-binding proteins crucial in pathogenesis. The WHO identifies bacterial antimicrobial resistance (AMR) as a critical global health challenge, necessitating innovative strategies that also target non-antibiotic pathways. Recent studies highlight bacterial lectins as key players in pathogenesis and promising therapeutic targets, with early clinical success using glycomimetics and vaccines to treat and prevent AMR-related infections. This review covers the current knowledge on bacterial lectins, their classifications, and roles in host recognition and adhesion, biofilm formation, cytotoxicity, and host immune evasion, with examples of well-characterized lectins. It also explores their therapeutic potential and highlights novel lectins with unknown functions, encouraging further research.

Highlights

Bacteria often utilize their lectins to promote pathogenesis. With the rise in antimicrobial resistance, targeting lectins with inhibitors presents a promising opportunity to enhance the host's ability to clear the pathogen.

Ongoing research continues to uncover a growing range of functions for bacterial lectins in pathogenesis, such as host recognition and adhesion, biofilm formation, cytotoxicity, and host immune evasion, with individual lectins often playing multiple roles in these processes.

Recent advances in targeting lectins with glycomimetics and vaccination saw early clinical success, consolidating their potential as drug targets.

Underexplored and novel lectins present a gap in the literature, with their biological functions still poorly understood.

Revisiting bacterial lectins in the era of antimicrobial resistance

Carbohydrates play essential roles in biological systems. They provide structural support such as in cell walls and protein stability, serve as energy sources, and function as information carriers in molecular recognition processes through carbohydrate–carbohydrate interactions or by acting as ligands for glycan-binding proteins (GBPs) [1]. Lectins, among the GBPs, are found in all biological systems [2]. Their ubiquitous presence highlights their evolutionary importance and functional versatility in terms of cell recognition, intracellular glycoprotein trafficking, adhesion of infectious agents to host cells, recruitment of immune cells to infection sites, malignancy, and metastasis [3]. Lectins lack catalytic activity and bind to mono- and oligosaccharides in a reversible and specific manner [4]. The binding strength of most lectins to glycans is in the μM to mM range, and is facilitated by hydrogen bonds, van der Waals forces, ionic interactions, and occasionally calcium ions [5]. Both calcium ions and hydrogen bonds enhance specificity by targeting the precise stereochemistry of carbohydrate hydroxyl groups [6].

Human pathogenic bacteria use their lectins as virulence factors to promote pathogenesis by interacting with host-exposed glycan ligands – such as cell surface receptors, N- and O-linked glycans, glycolipids, and glycosaminoglycans. For example, histo-blood group oligosaccharides – including ABH and Lewis antigens – are often exploited by pathogens that have evolved to target specific antigens, resulting in a higher risk of infection for individuals expressing them [7,8]. The resulting lectin–antigen interactions facilitate tissue recognition and adhesion, immune evasion, persistence via biofilm formation, and the promotion of cytotoxic effects (Figure 1, Table 1).

Bacterial antimicrobial resistance (AMR) poses a critical global health challenge in the 21st century; it was linked to 4.7 million deaths in 2021 – a number expected to rise to 8.2 million by 2050 [9]. Over the same period, the economic burden on healthcare is projected to surpass US$1 trillion [10]. ESKAPE pathogens – a group of multidrug-resistant bacteria comprising *Enterococcus*, *Staphylococcus*, *Klebsiella*, *Acinetobacter*, *Pseudomonas*, and *Enterobacter* known for 'escaping'

[1]Helmholtz Institute for Pharmaceutical Research Saarland (HIPS), Helmholtz Centre for Infection Research, D-66123 Saarbrücken, Germany
[2]Deutsches Zentrum für Infektionsforschung (DZIF), Standort Hannover-Braunschweig, Germany
[3]Department of Chemistry, PharmaScienceHub (PSH), Saarland University, D-66123 Saarbrücken, Germany
[4]University Grenoble Alpes, CNRS, CERMAV, 601 rue de la chimie, Grenoble 38000, France

*Correspondence: alexander.titz@helmholtz-hzi.de (A. Titz).

Trends in Microbiology, August 2025, Vol. 33, No. 8 https://doi.org/10.1016/j.tim.2025.03.007 839

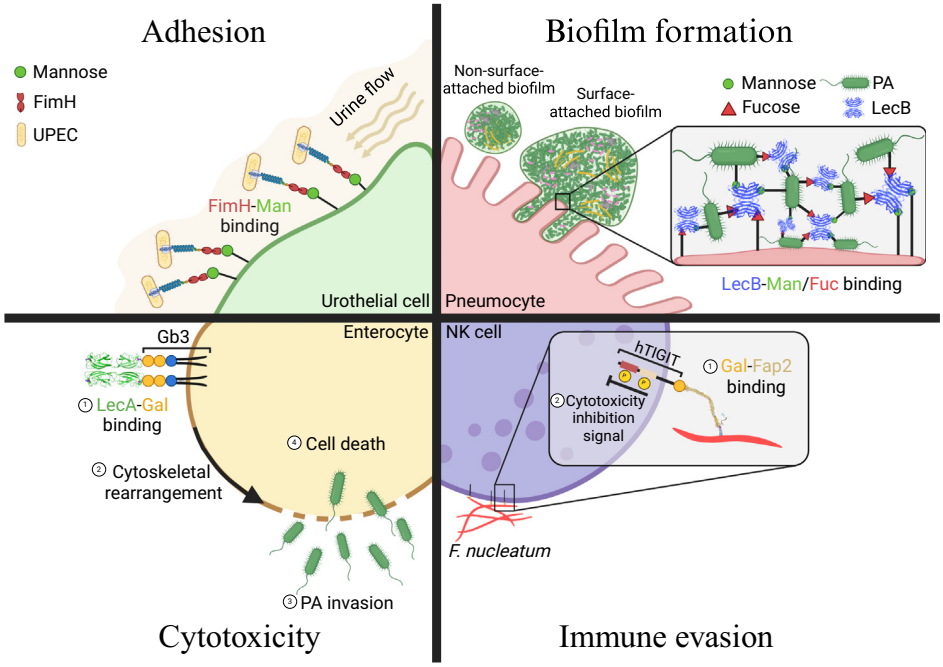

Figure 1. The roles of bacterial lectins in pathogenesis (selected examples). Adhesion. Uropathogenic *Escherichia coli* (UPEC) uses its FimH adhesin to bind to mannose-presenting uroplakin on urothelial cells, facilitating attachment and helping the bacteria resist clearance by urine flow during miction [17]. Biofilm formation. *Pseudomonas aeruginosa* (PA) forms and stabilizes its biofilms by using its mannose- and fucose-binding LecB to crosslink the glycans present on biofilm exopolysaccharides, on the host, or the bacterial surfaces [18]. Cytotoxicity. LecA from PA binds the glycosphingolipid Gb3, thereby rearranging the cytoskeleton of enterocytes and increasing their susceptibility to PA invasion which leads to cell death [19]. Immune evasion. *Fusobacterium nucleatum* uses its galactose-sensitive adhesin Fap2 to inhibit natural killer (NK) cell effector functions by binding the human T cell immunoreceptor with immunoglobulin and immunoreceptor tyrosine-based inhibition motif domain (hTIGIT) and triggering a biochemical cascade to downregulate NK cell function [20].

antibiotics – are significant contributors to nosocomial infections [11]. To address this growing threat, there is an urgent need for research and development of new treatments with innovative mechanisms of action that circumvent established resistances and replace existing antibiotic therapies that have become ineffective due to misuse and overuse [12,13].

Carbohydrate-based drugs, called glycomimetics, can target disease-causing lectins, preventing their harmful effects in infections, immune responses, cancer, and inflammation, by mimicking the structure and function of their natural carbohydrates [14]. In infectious diseases, these anti-virulence agents are emerging as a new class of antimicrobials that disarm bacteria without provoking resistance. They achieve this by targeting non-essential virulence traits, in contrast to antibiotics, which disrupt essential metabolic processes or directly kill bacteria, thereby exerting high evolutionary pressure [15]. As a result, anti-virulence agents can enhance immune clearance of pathogens and increase bacterial sensitivity to conventional antibiotics, offering a strategy to boost antibiotic effectiveness when used in combination [16].

This review revisits the classification of bacterial lectins and covers their roles in pathogenesis, highlighting examples of well-established lectins in each context. Furthermore, it explores their therapeutic targeting strategies, and concludes with a discussion of significant yet understudied lectins whose biological roles remain to be elucidated.

Table 1. Overview of the bacterial lectins discussed with regard to their respective pathogens, role in pathogenesis, and carbohydrate specificity[a]

Pathogen	Lectin	Host–pathogen adhesion	Biofilm formation	Cytotoxicity	Host immune evasion	Carbohydrate specificity
A. baumannii	Ata	x	x			Gal/GlcNAc/Gal(β1–3/4)GlcNAc
B. cenocepacia	BC2L-A	Spec	x			Man
B. cenocepacia	BC2L-B	Spec	x			–
B. cenocepacia	BC2L-C	Spec	x		x	Man/Hep/Fuc
B. ambifaria	BambL	x		x	x	Fuc
C. botulinum	BoNT			x		Polysialogangliosides
C. tetani	TeNT			x		Polysialogangliosides
E. cloacae	EclA	Spec	Spec			Fuc
E. coli (AIEC)	FimH	x		x		Man
E. coli (ETEC)	EtpA	x		x		GalNAc
E. coli (ETEC)	Stx	x		x		Gb3
E. coli (NMEC)	FimH	x		x		Man
E. coli (UPEC)	FmlH	x				Gal/GalNAc
E. coli (UPEC)	FimH	x	x	x	x	Man
E. coli (UPEC)	PapG	x	x			Gal
F. nucleatum	Fap2	x			x	Gal/GalNAc
H. pylori	BabA	x				Fuc
H. pylori	SabA	x				Sialylated antigens
M. tuberculosis	sMTL-13			Spec		–
M. tuberculosis	HBHA	x				Heparin
P. asymbiotica	PHL	x		Spec		Fuc
P. luminescens	PLL	Spec				Fuc
P. luminescens	PllA	Spec	Spec			Gal
P. aeruginosa	CdrA	x	x			Man, Psl polysaccharide
P. aeruginosa	LecA	x	x	x		Gal
P. aeruginosa	LecB	x	x	x	x	Man/Fuc
S. aureus	SasG-I	x	x			N-glycans
S. aureus	SasG-II	x	x			N-glycans/Core 2 O-glycans
S. epidermidis	Aap	x	x			GlcNAc/glucosamines
S. mitis	LLY	x		x		Fuc
S. pneumoniae	CbpA	x	x			LNnT/sialic acids
V. cholerae	CT			x		GM1
V. cholerae	Bap1	x	x			Anionic/linear polysaccharides
V. cholerae	RbmC	x	x			N-glycans/mucin
V. vulnificus	VVH	x		x		Gal/GalNAc/LacNAc

[a]Abbreviations: Hep, heptose; Spec, speculative role; x, confirmed in the literature; –, not yet elucidated.

Classification of bacterial lectins

Bacterial lectins are found intracellularly or on bacterial cell surfaces, and can be classified as either surface-bound or soluble [21]. Surface-bound lectins are part of multisubunit appendages, such as fimbriae or pili, which extend hundreds of nanometers from the bacterial surface to interact with host cells [22]. Some soluble lectins function as part of toxins and are secreted through

various mechanisms. For example, cholera toxin has dedicated secretion pathways, while others, like the Shiga toxin, depend on cell lysis [23,24]. In contrast, the release mechanisms of the soluble lectins from *Pseudomonas aeruginosa* have not yet been elucidated.

Lectins recognize glycans through binding sites that are generally localized in well delimited carbohydrate recognition domains (CRDs). While lectins can have one or several CRDs, they are typically multivalent, with several of these domains resulting from oligomerization, or tandem repeats on the same polypeptide chain. A classification has been proposed based on this architecture, distinguishing monovalent merolectins from multivalent hololectins [25]. In chimerolectins, an additional domain, with a different function, is linked to the CRD, such as the mannose-specific adhesin FimH of the uropathogenic *Escherichia coli* that presents a mannose-binding CRD linked to another domain responsible for the stability of the pilin structure [26].

Lectins can also be part of multiprotein complexes, such as AB_5 bacterial toxins that contain an enzymatic peptide responsible for cytotoxicity and five CRDs as targeting domains [22]. An example is the pertussis toxin (PTX) which binds to glycoproteins on host cell surfaces, while its catalytic domain disrupts intracellular signaling pathways, leading to immune suppression [27]. Superlectins are capable of recognizing multiple distinct carbohydrate structures due to the presence of different CRDs within the same protein, allowing them to exhibit broad specificity in their binding activity such as the mannose/fucose specific BC2L-C from the pathogen *Burkholderia cenocepacia* [28]. The ability to have multiple CRDs increases lectin binding strengths through avidity, and allows them to enhance their cross-linking activity and specificity by binding different kinds of glycans. Additionally, bacterial lectins have been recently classified based on their 3D-structural fold and sequence similarity (Table 2) [29]. Indeed, a large number of bacterial lectins have been crystallized, giving access to details about their architecture, topology, and binding sites. Figure 2 shows a selection of the lectins discussed in this review, illustrating the variety of secondary structures that converge for sugar recognition.

The role of bacterial lectins in host recognition and tissue adhesion

In its initial stages, bacterial pathogenesis is primarily facilitated by the adhesion of bacteria to their target host cells [30]. The glycocalyx is a complex layer of glycan structures and other biochemical molecules that envelops every living cell which bacteria exploit for adhesion [31]. Tissue specificity depends on the interaction of bacterial lectins with a specific glycome signature presented by the host, helping bacteria to thrive in environments they favor or to which they are specifically adapted [32]. These environments generally enable bacteria to grow, to evade the immune system, to exploit available resources, and to outcompete surrounding microbial communities [33]. Moreover, lectin interactions can also adapt to changes in the host glycome caused by environmental conditions and disease states [32].

For example, *Helicobacter pylori* is able to survive and colonize in the acidic conditions of the stomach by producing urease, an enzyme which neutralizes stomach acid [34]. Its lectins, BabA and SabA, support colonization by interacting with fucosylated Lewis B and sialylated antigens present on the stomach lining [35]. *H. pylori* can also switch between the two adhesins depending on the host glycome to maintain attachment under varying conditions. It uses BabA for adhesion in a healthy stomach lining, in contrast to using SabA during chronic inflammation where sialylated antigens are upregulated [36].

Another example is the Siglec-like adhesins, which mediate streptococcal binding to sialylated host glycoproteins [37]. Streptococci exploit the mutability of these adhesins through genetic recombination, allowing them to switch host receptors and adapt to diverse sialoglycan structures.

Table 2. 3D classification of structurally characterized lectins from human pathogenic bacteria

Classes (or super class)	Lectins	Species	Exemplary PDB code
Factor H binding protein	SadP	*Streptococcus suis*	5BOA
HOP-OMP adhesins	BabA, SabA	*Helicobacter pylori*	5F7M
Mycoplasma adhesins	MgpC/P110 adhesin P40/P90 adhesin	*Mycoplasma genitalium, M. pneumoniae*	6TM0
AB_5 toxins[a]	CTB, LTB, CTXB, STX1, STX2, PTX, PltB, ArtB, SubB,	*Vibrio cholerae, Escherichia coli, Citrobacter freundii, Shigella dysenteriae, Bordetella pertussis, Salmonella typhi, S. enterica*	2CHB
Staphylococcal enterotoxin and superantigen[a]	SEC2, SSL3, SSL4, SSL5, SSL11	*Staphylococcus aureus*	1SE3
OAA-like	BOA, PTL	*Burkholderia oklahomensis, Pseudomonas taiwanensis*	7DC4
Toxin repetitive domain	TcdA	*Clostridium difficile*	2G7C
Vibrio β-prism	RbmC, VCC	*Vibrio cholerae*	5V6F
Monocot-lectin like	Pyocin, MSMEG_3662	*Pseudomonas aeruginosa, Mycobacterium smegmatis*	4LEA
β-propeller[a]	BambL, BP39L, CV39L, PLL, PHL, PLL2	*Burkholderia ambifaria, B. pseudomallei, Chromobacterium violaceum, Photorhabdus luminescens, P. asymbiotica, P. laumondii*	3ZZV
2 calcium lectin	LecB, Bc2L-A, Bc2L-C, CV2L	*P. aeruginosa, B. cenocepacia, C. violaceum*	1W8H
L-type bacterial	SraP, SasG, Pls, Aap	*S. aureus, S. epidermis*	4M00
1 calcium lectin	LecA, PIIA, EclA-N	*P. aeruginosa, P. luminescens, Enterobacter cloacae*	1OKO
Stranded exchange sheet	EclA-C	*E. cloacae*	6YF6
F-type lectin	Lectinolysin	*Streptococcus mitis*	3LEK
Siglec-like adhesin	GspB, HSA, SrpA, SK1, HSA-like	*Streptococcus gordonii, S. sanguinis, S. mitis*	6EFD
Pilus adhesins[a]	CfaE, GafD/F17G, FaeG, FedF/F18, FimH, FlmH, PapG, PsaA, UclD, UcaD	*E. coli*; *Yersinia pestis, Proteus mirabilis*	2HB0
TNFα-like	Bc2LC-Nter	*B. cenocepacia*	6TID
Clostridial hemagglutinin	HA1, HA3	*Clostridium botulinum*	4LO5
Clostridial toxin	BoNT/B, TeNT	*C. botulinum, C. tetani*	2VU9
Ricin-like	VVH hemolysin, HA33 of HA1	*Vibrio vulnificus, C. botulinum*	4OWK

Abbreviation: PDB, Protein Data Bank.
[a]Includes several classes.

This adaptability extends to different glycosylation patterns in humans, where point mutations can shift host receptor preferences from saliva to plasma [38].

Furthermore, uropathogenic *E. coli* (UPEC) uses its pilus or non-pilus adhesins, lipopolysaccharide (LPS), flagella, and secreted toxins, all of which contribute to its colonization of various parts of the urinary tract [39]. Its fimbrial lectins FimH and PapG reinforce adhesion by respectively binding to the exposed mannosylated glycoproteins of urinary tract epithelia and bladder, and glycosphingolipids in kidneys [17]. FimH also displays remarkable plasticity in its binding pocket, allowing it to adapt to different environmental conditions such as shear stress during miction by binding to its mannose ligand with 20-fold greater strength through a catch bond mechanism [40].

FmlH, another UPEC adhesin, plays a crucial role in adhesion during chronic urinary tract infections (UTIs) by enhancing colonization. It specifically binds to Gal/GalNAc epitopes strictly on inflamed urothelial and naïve or inflamed kidney epithelial cells, helping UPEC to adapt to host glycome alterations [41].

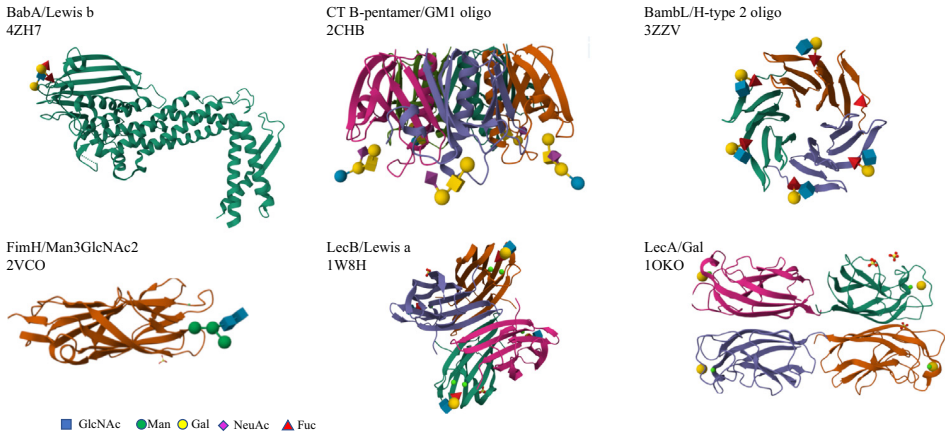

Figure 2. Crystal structures of selected lectins from Table 2 in complex with human glycans. Proteins are represented as ribbons colored by peptide chains. Glycans are represented by the indicated symbols, and calcium ions are represented by small light-green spheres.

The role of bacterial lectins in biofilm formation

Biofilms are structured communities of bacteria embedded in an extracellular polymeric substance (EPS) matrix. They protect bacteria from the external environment, host immune responses, and antibiotic treatment, thereby promoting chronic infections and complicating therapies [42]. Clinically, biofilms contribute to the persistence of bacteria on medical devices, such as catheters, as well as on host tissues – for example, skin and wounds, respiratory, digestive, and urogenital tracts [42]. The EPS matrix consists of a complex mixture of biopolymers primarily encompassing bacterial exopolysaccharides, along with nucleic acids, lipids, proteins, and other organic compounds [43]. Among these matrix proteins are bacterial lectins. Through their multivalence, many lectins play a significant role in facilitating biofilm formation and stabilization by cross-linking glycan chains on the exopolysaccharides, bacteria, and host tissue.

Besides their important role in host adhesion, the role of LecA and LecB of *P. aeruginosa* in biofilm formation is well established as both are integral components of its matrix. LecA supports the architecture and maturation of *P. aeruginosa* biofilms across various environmental conditions by cross-linking galactosides within the EPS, as well as on bacterial surfaces and host cells [44]. Similarly, LecB, which is commonly present in clinical *P. aeruginosa* isolates, supports and stabilizes the biofilm matrix by binding to Psl, a main polysaccharide component of the EPS in *P. aeruginosa,* containing mannose [45,46]. LecB generally binds to fucose or mannose residues that are ubiquitously present on host tissue and the bacterial O-antigen polysaccharides [45,47].

Another example of lectin involvement in biofilm formation is the choline binding protein CbpA from *Streptococcus pneumoniae* which is instrumental in adhesion and biofilm formation by having lectin domains that bind lacto-N-neotetraose and sialic acid, two pneumococcal ligands on eukaryotic cells [48].

The biofilm matrix proteins of *Vibrio cholerae* Bap1 and RbmC that show lectin activities were found to be essential in biofilm formation and biofilm adhesion to abiotic surfaces [49]. Though the unique specificity of their lectin activity requires further investigation, their ligands have been identified as polysaccharides in the *Vibrio* EPS and complex N-glycans on eukaryotic cells [50,51].

The role of bacterial lectins in facilitating cytotoxicity

Bacterial lectins play a crucial role in promoting cytotoxicity by enabling pathogens to invade host cells through disrupting membranes via pore formation or glycolipid rearrangement, and to deliver toxins.

In addition to its roles in adhesion and biofilm formation, LecA has also been identified to promote intracellular uptake of bacteria. Its interaction with the glycosphingolipid Gb3 modifies the shape of the host cell membranes, creating invaginations referred to as 'lipid zipper' mechanism, thereby facilitating the entry of *P. aeruginosa* into host cells [52,53]. This interaction also disrupts membranes and increases host cell permeability in mice, making gastrointestinal epithelial cells more vulnerable to cytotoxic effectors like exotoxin A, ultimately leading to cell death [19].

LecB was also found to have a similar effect to LecA in increasing alveolar barrier permeability as demonstrated in both an *in vitro* model with A549 cells, and an experimental murine acute lung injury model. The presence of these lectins exacerbated lung injury and increased mortality in mice [54].

FimH also plays a key role in the invasion of neonatal meningitis *E. coli* (NMEC) into cells forming the blood–brain barrier [55]. By attaching to microvascular endothelial cells, FimH triggers an increase in intracellular Ca^{2+} that stimulates actin rearrangements [56]. These changes provide NMEC with a pathway to penetrate the central nervous system, where it can cause edema, inflammation, and neural damage.

The EtpA lectin, located at the flagellar tip of enterotoxigenic *E. coli* (ETEC), binds to N-acetylgalactosamine, particularly targeting individuals with blood group A [57]. The expression of blood group A-related glycans on their intestinal epithelium enhances bacterial interaction and promotes the efficient delivery of ETEC enterotoxins, which has been shown to intensify diarrheal symptoms. However, the precise mechanism by which EtpA contributes to this effect remains unknown [58].

Several lectins are associated with a toxin peptide and are involved in the cell attachment mechanism. AB_5 toxins are six-component protein complexes in which the A subunit carries out the toxin's enzymatic and toxic activity, while the five B subunits, which are lectins, enable adhesion of the complex to its specific tissue via host cell receptors and facilitate the delivery of the toxic A subunit into the target host cell [59]. As an example, the Shiga toxin from *Shigella dysenteriae* and *E. coli* uses its B subunits to bind to the glycosphingolipid Gb3 on the surface of kidney or intestinal cells, enabling its A subunit to inhibit protein synthesis, leading to cell death [60]. Another example is cholera toxin (CT) from the bacterium *V. cholerae* and ETEC, where the B subunits bind to the ganglioside GM1, a glycolipid found on enterocytes [61]. CT also binds to histo-blood group oligosaccharides, rationalizing the observation of individuals of blood group O experiencing the most severe symptoms [62]. Once internalized, the ADP-ribosyltransferase A subunit ultimately activates adenylate cyclase, raising cyclic AMP levels. This disrupts ion transport in cells and leads to severe diarrhea [63]. Botulinum (BoNT) and tetanus (TeNT) neurotoxins, which respectively contribute to flaccid or spastic paralysis, also utilize lectin domains for ganglioside-mediated entry in neurons [64].

Other types of cytotoxic lectin activities include pore formation. The fucose-binding lectin domain of the lectinolysin toxin from *Streptococcus mitis* enhances its pore formation activity by concentrating toxin molecules at fucose-rich sites, forming pre-pore oligomers on the surface of host cells, eventually leading to cell death [65]. Similarly, the galactose-binding lectin domain of the hemolysin (VVH) toxin of the severe food poisoning and septicemia-causing *Vibrio vulnificus* assists

in its targeting towards host membranes, leading to the oligomerization of the toxins and the formation of transmembrane channels, resulting in cell death [66].

The role of bacterial lectins in host immune evasion

Bacterial lectins play a significant role in immune evasion, helping pathogens to thrive and persist within the host. As mentioned earlier, biofilm formation significantly contributes to shielding bacteria from the immune system.

One mechanism of immune evasion involves inhibiting the migration of immune cells to infection sites by blocking their movement across endothelial barriers. It was shown that LecB inhibited the migration of dendritic cells from the skin through lymphatic vessels to the lymph nodes, resulting in a reduced T cell response [67].

Another mechanism of immune evasion is through immunomodulation. LecB has also shown the ability to modulate neutrophil responses by either inducing or inhibiting intracellular reactive oxygen species (ROS) production based on yet-to-be-determined factors, through binding to several fucosylated or mannosylated epitopes on granules and plasma membranes of neutrophils [68]. An additional example of immunomodulation is the lectin Fap2 from *Fusobacterium nucleatum*, which binds and activates the human glycosylated T cell immunoglobulin and immunoreceptor tyrosine-based inhibitory motif (hTIGIT) on both natural killer cells and T lymphocytes, and inhibits their cytotoxic activities by disrupting kinase signaling [20,69].

A further strategy for immune evasion is the indirect killing of immune cells. Fap2 has also been shown to be responsible of *Fusobacterium*-induced human T lymphocyte death, although the exact mechanism remains unknown [70]. Another example of lectin-induced cytotoxicity in immune cells involves type I fimbriae, such as FimH from UPEC, which is essential for inducing human neutrophil apoptosis through a ROS-dependent pathway [71].

Bacterial lectins in infections: therapeutic targets for exploitation

The multifunctional role of bacterial lectins has made them a critical area of research, garnering significant attention due to their implications in diagnosing, treating, and preventing infectious diseases. For example, in diagnostics, fluorescent mannose-targeted polymers can be used to target the lectins LecB and CdrA. Since these lectins are abundant in *P. aeruginosa* biofilms and play a key role in their stability, they are valuable markers for identifying them [72]. In addition, low-molecular-weight, high-affinity ligands of LecA or LecB, coupled with fluorescent dyes, have proven suitable for imaging *P. aeruginosa* biofilms and lung infections in mice [73,74]. These works paved the way for the development of lectin-specific ligands to localize and treat infections by pathogen- and tissue-directed therapy. In this approach, LecA or LecB probes conjugated to an antibiotic delivered their drug cargo to *P. aeruginosa*, thereby potentially diminishing collateral damage on the host and the microbiome [75].

Furthermore, inhibition of lectins with glycomimetics blocked their deleterious effects in various infection models. Glycomimetics with higher affinity for the lectin than the natural oligosaccharide ligands are often obtained by substituting part of the sugar with (hetero)cycles [5] (Figure 3). For example, targeting LecA with potent glycomimetics inhibited the ability of *P. aeruginosa* to adhere to and invade lung epithelial cells, restored efficient cell culture wound model closure, significantly reduced biofilm formation, and reduced virulence in infected mice [76–79]. Targeting LecB with glycomimetics restored T cell immune responses, inhibited *P. aeruginosa* biofilm formation, and proved beneficial in murine lung infections [67,79,80]. Inhibition of *E. coli* FimH with mannosides has become a widely explored therapeutic alternative to antibiotics for treating UTIs

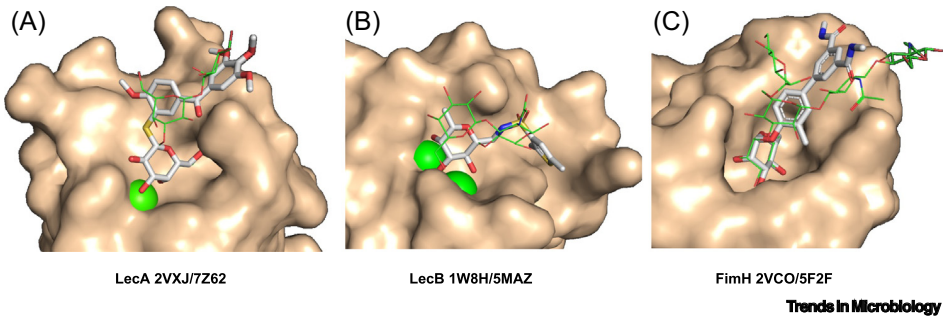

Figure 3. Crystal structures of complexes of several bacterial lectins with high-affinity glycomimetics. Glycomimetics are represented by sticks, natural ligands are superimposed as green lines, and green spheres represent Ca^{2+} ions. References: A [76], B [93], C [94].

and Crohn's disease [81–83]. By obstructing this interaction, these inhibitors block UPEC and adherent invasive *E. coli* (AIEC) strains from attaching to host-mannosylated antigens, thereby reducing the likelihood of infection. One such orally administered inhibitor, Sibofimloc of Enterome, has shown potential to block AIEC penetration into the intestinal wall, thereby suppressing a possible trigger in intestinal inflammation while preserving the balance of the gut microbiota [84]. After the pathoblocker was shown to be safe and tolerated in Phase 1a (NCT02998190) and 1b (NCT03709628) clinical trials, Phase 2 (NCT03943446) failed due to the inability to recruit a sufficient number of patients. Another promising candidate, GSK3882347 of Fimbrion/GlaxoSmithKline, targets FimH adhesion in UPEC. This agent offers a prospective treatment or prevention strategy for uncomplicated UTIs. It has passed Phase 1a clinical trials (NCT04488770) and is currently recruiting for Phase 1b (NCT05138822). Galactoside inhibitors against FmlH were shown to significantly reduce bacterial burdens in kidneys and bladders of infected mice, warranting further attention [85]. Recently, the development of these FmlH antagonists led to a promising lead with nanomolar activity and an improved 53% oral bioavailability in mice, up from initially less than 1% [86]. This compound thus holds significant promise and merits further optimization to enhance its potency, as well as evaluation in advanced preclinical models targeting chronic UTIs affecting the bladder and kidney.

In another context of prevention, bacterial lectins could serve as antigens for vaccines. Upon exposure to the pathogen, antibodies generated would bind to these lectins, blocking their mechanisms of infection. A vaccine formulation, including both LecA and LecB purified from a *P. aeruginosa* strain, showed a full protective effect in mice challenged with the homologous strain, and partial to full protection against other strains displaying lectin activities [87]. Through reverse vaccinology, three novel lectins were also identified as vaccine candidates against *P. aeruginosa*. One of these lectins (GenBank AAG08725.1) specifically binds ABO blood group antigens and terminal β-linked galactose. When included in vaccine formulations alongside other single *P. aeruginosa* antigens, remarkable efficacy in protecting challenged mice was demonstrated, improving survival rates by up to 50% [88,89]. To date, FimH-based vaccines are the only lectin-based vaccines that have entered clinical trials after showing promising results in mice and non-human primates by resisting bladder colonization and cystitis caused by UPEC [90]. Sequoia Sciences successfully completed Phase 1a clinical trials of their vaccine, SEQ-400, which combines the FimCH antigen with a glycolipid adjuvant, demonstrating high immunogenicity and tolerability [91]. In subsequent Phase 1b trials, the vaccine reduced recurrent UTIs and *E. coli*-caused UTIs by approximately 70%, and will advance to Phase 2 trials. Although the vaccine demonstrated clear therapeutic potential in clinical studies, improvements in its bioprocessing, antigen design, and immunogenicity is ongoing at Pfizer [92]. Building on the success of the FimH vaccine in mice, vaccination with purified FmlH combined with an adjuvant significantly protected

mice from chronic cystitis by reducing bacterial burden and colonization following the acute infection stage [41]. These findings highlight the potential of combining FmlH and FimH in a single vaccine formulation to enhance efficacy against UPEC infections.

Unexplored and novel lectins: biological roles that remain to be elucidated

Advances in bioinformatics, structural biology, and medicinal chemistry are uncovering novel lectins with potential as therapeutic targets while also accelerating the discovery of diverse inhibitors against them for the treatment of multidrug-resistant pathogens. However, the development and optimization of these compounds often outpaces the understanding of their respective lectin functions in pathogenesis. This disparity highlights a critical gap that urgently needs to be addressed. A selection of lectins that merit further attention follows:

Enterobacter cloacae, an ESKAPE pathogen, is a major cause of hospital outbreaks causing lung, wound, central nervous system, urinary tract, and catheter or orthopedic implant infections [95]. *E. cloacae* lectin A (EclA), has been recently identified and characterized. It is a superlectin composed of a dimer of a two-domain polypeptide, resulting in the presentation of two fucose-binding and two LecA domains. While the N-terminal LecA domain was initially expected to bind galactose, its specific ligand remains unknown [96]. The specificity of EclA for the Lewis A blood group and H-type II antigens suggests its potential as a drug target, given the high prevalence of *E. cloacae* outbreaks in neonatal intensive care units [97] and the ubiquity of Lewis A in 90% of newborns [98]. The role of EclA in biofilm formation as a congener of LecA and its role in adherence of *E. cloacae* to host cells is therefore yet to be determined.

Acinetobacter baumannii, a highly problematic ESKAPE pathogen, produces the autotransporter adhesin Ata, which binds to collagen, laminin, and fibronectin on host cells, and contributes to biofilm formation [99–101]. Its specific ligands were recently discovered to be galactose, N-acetylglucosamine, and galactose (β1–3/4) N-acetylglucosamine, facilitating the development of glycomimetics that would block host adherence and biofilm formation once the key host ligands recognized by Ata are clearly determined [101].

The cell wall anchored (CWA) protein SasG from *Staphylococcus aureus*, another ESKAPE pathogen, contains a lectin subdomain essential for adhesion to healthy human corneocytes and nasal epithelial cells, as well as for biofilm formation [102–104]. Recently, two major SasG alleles, SasG-I and SasG-II, were identified, with the latter exhibiting broader ligand-binding capabilities. While both bind N-linked glycans, SasG-II also recognized core 2 O-glycans [103].

Beyond the ESKAPE pathogen lectins, others also merit attention for either being homologs of pathogenic ones or holding promise in unraveling new lectin functions or therapies. An ortholog of SasG, the accumulation association protein (Aap) from *Staphylococcus epidermidis*, relies on its lectin A subdomain for adherence to host glycans on corneocytes, human skin, and other host surfaces [105]. Recently, it was shown that this lectin subdomain specifically binds to *N*-acetyl-D-glucosamine and mediates cell-cell adhesion via heterophilic interactions [106]. The fibrillar B domain of Aap is anchored to the cell wall of *S. epidermidis* and contributes to biofilm formation through interactions between its homophilic B domain regions, which form rope-like, antiparallel twisted structures with B domains on neighboring bacteria [107]. Therefore, the lectin A domain has been hypothesized to facilitate rapid binding upon cell-to-cell contact, while the B domains establish strong homophilic bonds to reinforce the connection [106]. Additionally, the lectin A domain may have a broader role in binding any cell displaying N-acetylglucosamine on its surface [106]. Determining the ligand identities and glycoprotein structures of SasG and Aap is therefore needed for the development of potential inhibitors.

Photorhabdus luminescens, an entomopathogenic bacterium with occasional reports in human infection, has a LecA-like galactose-binding soluble lectin, *P. luminescens* lectin A (PllA). Although PllA is suspected to bind the antigen Gal-α-1,3-GalNAc in the nematode symbiont of *P. luminescens* and infected insects, its precise role remains speculative [108]. However, it would be interesting to investigate the function of PllA orthologs in *Photorhabdus asymbiotica*, a bacterium found in the human intestinal microbiota with pathogenic potential. In fact, the novel fucose-binding β-propeller lectin PHL from *P. asymbiotica* has also been reported, and while initial studies have been conducted on human and insect cells, its function remains enigmatic [109]. PLL is a novel homotetrameric L-fucose-binding β-propeller lectin also from *P. luminescens*. It showed the ability to bind to the surface of nematodes and to insect hemocytes. It also was able to hemagglutinate human blood group A erythrocytes, thereby showing infectious potential [110].

Additionally, further important pathogens involved in lung infections, such as *Mycobacterium tuberculosis* and *Burkholderia* spp., have shown a strong rise in antibiotic resistance. They generally produce lectins potentially involved in their adhesion to airway epithelia.

BambL is an understudied soluble lectin produced by *Burkholderia ambifaria*, a member of the *Burkholderia cepacia* complex (Bcc) and an opportunistic human pathogen known to cause severe acute and chronic lung infections [111]. *Burkholderia* species are capable of forming robust biofilms and demonstrate significant resistance to most antibiotics [112]. Recent studies have shown that BambL exhibits cytotoxicity by acting as a superantigen, inducing activation-triggered cell death through binding to the B cell antigen receptor complex and other fucosylated ligands on the B cell surface [113,114]. However, much remains to be uncovered regarding its full range of biological functions and its potential as a therapeutic drug target.

Other understudied lectins within the Bcc include the three LecB homologs BC2L-A, -B, and -C from *B. cenocepacia* [115]. Inactivation of the genes encoding these soluble lectins resulted in biofilms with hollow microcolonies, highlighting their role in shaping biofilm architecture [116]. Furthermore, the ligands and structures of only BCL2-A and BC2L-C have been elucidated so far. LecB-like BC2L-A is a mannose-specific homodimer with two ligand-binding sites, and speculated to play a role in cell adhesion [115,117]. BC2L-C is a hexameric superlectin, featuring three LecB-like mannose/heptose-binding C-terminal domain dimers and additional trimeric N-terminal domains each having a TNF-α-like fold that shows specificity to fucosylated human histo-blood group antigens and triggers IL-8 production in cultured airway epithelial cells [28,118].

Mycobacterial lectins remain poorly studied, despite *Mycobacterium tuberculosis* (*Mtb*), the causative agent of tuberculosis (TB), being the leading bacterial cause of death worldwide [119]. sMTL-13 is a lectin-like protein found in patients with active tuberculosis, though its function and carbohydrate ligands are still unknown [120]. Bioinformatics also suggested the presence of lectin genes in *Mtb*, including several potential lectin-like D-arabinose-sensitive proteins important for aggregation and adhesion of mycobacteria to macrophages, although these have not been characterized further [121,122]. The heparin-binding hemagglutinin (HBHA) is the most studied lectin from *Mtb*; it is present on the mycobacterial surface, mediates the adhesion to phagocytes and auto-aggregation, promotes bacilli dissemination from the site of primary infection, and manipulates actin polymerization to promote survival and escape from phagocytes [123]. As a potential *Mtb* vaccine and biomarker, the precise role of HBHA in both latent and active tuberculosis patients still needs to be fully elucidated [124].

Concluding remarks

Understanding the mechanisms of action, roles in pathogenesis, and specific binding interactions of underexplored and novel lectins remains a priority in advancing our ability to design precise and effective treatments to neutralize these key virulence factors and circumvent AMR. To support lectin research, UniLectin has been developed as a comprehensive database that compiles known lectins from diverse species, along with their structure and carbohydrate specificities [125]. This tool also includes many predicted lectins from genomes, providing an excellent starting point for the biological elucidation of these intriguing proteins. However, the absence of a database focused on the various biological functions of lectins creates a bottleneck. This gap may stem from the various and often overlapping functions attributed to lectins as we observed during the development of this review, and would be of high value if addressed. Last, the rapid development of more complex *in vitro* models will also accelerate the discovery of lectins' physiological functions, such as the recently uncovered specific adhesion of *P. aeruginosa* mediated by LecA to distinct cells inside the epithelial barrier of a human airway organoid infection model [126].

Outstanding questions

How can we drive microbiology and infection research to catch up on the backlog of understudied lectins in pathogenesis? Are there any experiments that could streamline this process?

As new roles of bacterial lectins in pathogenesis continue to emerge, what unexplored mechanisms drive their influence on host–pathogen interactions and disease progression?

Many bacterial lectins remain undiscovered in bacterial pathogens. Which advanced biochemical and genomic approaches could aid in their identification?

Beyond clinically studied FimH, which bacterial lectins are promising targets for therapeutic intervention, and what systematic approaches can be used to assess their therapeutic potential?

How can novel glycomimetic inhibitors be designed to better target bacterial lectins and combat infections in light of the AMR crisis?

Acknowledgements

A.T. acknowledges support from Saarland University for a TANDEM PhD scholarship for M.F. Support from EU COST Action CA21145 EureStop to A.T. and A.I. is kindly acknowledged.

Declaration of interests

A.I. and A.T. are named as inventors on patents covering tools and inhibitors focusing on bacterial lectins.

References

1. Gagneux, P. *et al.* (2022) Biological functions of glycans. In *Essentials of Glycobiology* (4th edn) (Varki, A. *et al.*, eds), pp. 79–92, Cold Spring Harbor Laboratory Press
2. Taylor, M.E. *et al.* (2022) Discovery and classification of glycan-binding proteins. In *Essentials of Glycobiology* (4th edn) (Varki, A. *et al.*, eds), pp. 375–386, Cold Spring Harbor Laboratory Press
3. Lis, H. and Sharon, N. (1998) Lectins: carbohydrate-specific proteins that mediate cellular recognition. *Chem. Rev.* 98, 637–674
4. Goldstein, I.J. *et al.* (1980) What should be called a lectin? *Nature* 285, 66
5. Leusmann, S. *et al.* (2023) Glycomimetics for the inhibition and modulation of lectins. *Chem. Soc. Rev.* 52, 3663–3740
6. Angulo, J. *et al.* (2022) Structural biology of glycan recognition. In *Essentials of Glycobiology* (4th edn) (Varki, A. *et al.*, eds), pp. 403–418, Cold Spring Harbor Laboratory Press
7. Heggelund, J.E. *et al.* (2017) Histo-blood group antigens as mediators of infections. *Curr. Opin. Struct. Biol.* 44, 190–200
8. Cooling, L. (2015) Blood groups in infection and host susceptibility. *Clin. Microbiol. Rev.* 28, 801–870
9. Naghavi, M. *et al.* (2024) Global burden of bacterial antimicrobial resistance 1990–2021: a systematic analysis with forecasts to 2050. *Lancet* 404, 1199–1226
10. Jonas, O.B. *et al.* (2017) *Drug-resistant Infections: a Threat to Our Economic Future*, Final Report (English) Vol. 2. World Bank Group [Online]. Available: http://documents.worldbank.org/curated/en/323311493396993758/final-report
11. Miller, W.R. and Arias, C.A. (2024) ESKAPE pathogens: antimicrobial resistance, epidemiology, clinical impact and therapeutics. *Nat. Rev. Microbiol.* 22, 598–616
12. World Health Organization (2024) *2023 Antibacterial Agents in Clinical and Preclinical Development: an Overview and Analysis*, WHO
13. Miethke, M. *et al.* (2021) Towards the sustainable discovery and development of new antibiotics. *Nat. Rev. Chem.* 5, 726–749
14. Meiers, J. *et al.* (2019) Lectin antagonists in infection, immunity, and inflammation. *Curr. Opin. Chem. Biol.* 53, 51–67
15. Ogawara, H. (2021) Possible drugs for the treatment of bacterial infections in the future: anti-virulence drugs. *J. Antibiot. (Tokyo)* 74, 24–41
16. Gadar, K. and McCarthy, R.R. (2023) Using next generation antimicrobials to target the mechanisms of infection. *NPJ Antimicrob. Resist.* 1, 11
17. Klein, R.D. and Hultgren, S.J. (2020) Urinary tract infections: microbial pathogenesis, host–pathogen interactions and new treatment strategies. *Nat. Rev. Microbiol.* 18, 211–226
18. Tielker, D. *et al.* (2005) *Pseudomonas aeruginosa* lectin LecB is located in the outer membrane and is involved in biofilm formation. *Microbiology (N Y)* 151, 1313–1323
19. Laughlin, R.S. *et al.* (2000) The key role of *Pseudomonas aeruginosa* PA-I lectin on experimental gut-derived sepsis. *Ann. Surg.* 232, 133–142
20. Gur, C. *et al.* (2015) Binding of the Fap2 protein of *Fusobacterium nucleatum* to human inhibitory receptor TIGIT protects tumors from immune cell attack. *Immunity* 42, 344–355
21. Sharon, N. and Ofek, I. (2007) Microbial lectins. In *Comprehensive Glycoscience* (Kamerling, H., ed.), pp. 623–659, Elsevier
22. Lewis, A.L. *et al.* (2022) Microbial lectins: hemagglutinins, adhesins, and toxins. In *Essentials of Glycobiology* (4th edn) (Varki, A. *et al.*, eds), pp. 505–516, Cold Spring Harbor Laboratory Press
23. Sandkvist, M. *et al.* (1997) General secretion pathway (eps) genes required for toxin secretion and outer membrane biogenesis in *Vibrio cholerae*. *J. Bacteriol.* 179, 6994–7003
24. Mauro, S.A. and Koudelka, G.B. (2011) Shiga toxin: expression, distribution, and its role in the environment. *Toxins (Basel)* 3, 608–625
25. Tsaneva, M. and Van Damme, E.J.M. (2020) 130 years of plant lectin research. *Glycoconj. J.* 37, 533–551
26. Sauer, M.M. *et al.* (2016) Catch-bond mechanism of the bacterial adhesin FimH. *Nat. Commun.* 7, 10738
27. Wong, W. and Rosoff, P.M. (1996) Pharmacology of pertussis toxin B-oligomer. *Can. J. Physiol. Pharmacol.* 74, 559–564
28. Šulák, O. *et al.* (2011) *Burkholderia cenocepacia* BC2L-C is a super lectin with dual specificity and proinflammatory activity. *PLoS Pathog.* 7, e1002238
29. Bonnardel, F. *et al.* (2019) UniLectin3D, a database of carbohydrate binding proteins with curated information on 3D structures and interacting ligands. *Nucleic Acids Res.* 47, D1236–D1244

30. Parreira, P. and Martins, M.C.L. (2021) The biophysics of bacterial infections: adhesion events in the light of force spectroscopy. *Cell Surf.* 7, 100048
31. Möckl, L. (2020) The emerging role of the mammalian glycocalyx in functional membrane organization and immune system regulation. *Front. Cell Dev. Biol.* 8, 253
32. Moonens, K. and Remaut, H. (2017) Evolution and structural dynamics of bacterial glycan binding adhesins. *Curr. Opin. Struct. Biol.* 44, 48–58
33. Soni, J. *et al.* (2024) Understanding bacterial pathogenicity: a closer look at the journey of harmful microbes. *Front. Microbiol.* 15, 1370818
34. Montecucco, C. and Rappuoli, R. (2001) Living dangerously: how *Helicobacter pylori* survives in the human stomach. *Nat. Rev. Mol. Cell Biol.* 2, 457–466
35. Doohan, D. *et al.* (2021) *Helicobacter pylori* BabA–SabA key roles in the adherence phase: the synergic mechanism for successful colonization and disease development. *Toxins (Basel)* 13, 485
36. Mahdavi, J. *et al.* (2002) *Helicobacter pylori* SabA adhesin in persistent infection and chronic inflammation. *Science* 297, 573–578
37. Gaytán, M.O. *et al.* (2021) A novel sialic acid-binding adhesin present in multiple species contributes to the pathogenesis of Infective endocarditis. *PLoS Pathog.* 17, e1009222
38. Bensing, B.A. *et al.* (2022) Origins of glycan selectivity in streptococcal Siglec-like adhesins suggest mechanisms of receptor adaptation. *Nat. Commun.* 13, 2753
39. Terlizzi, M.E. *et al.* (2017) Uropathogenic *Escherichia coli* (UPEC) infections: virulence factors, bladder responses, antibiotic, and non-antibiotic antimicrobial strategies. *Front. Microbiol.* 8, 1566
40. Carlucci, L.A. *et al.* (2024) FimH-mannose noncovalent bonds survive minutes to hours under force. *Biophys. J.* 123, 3038–3050
41. Conover, M.S. *et al.* (2016) Inflammation-induced adhesin-receptor interaction provides a fitness advantage to uropathogenic *E. coli* during chronic infection. *Cell Host Microbe* 20, 482–492
42. Bjarnsholt, T. (2013) The role of bacterial biofilms in chronic infections. *APMIS* 121, 1–58
43. Karygianni, L. *et al.* (2020) Biofilm matrixome: extracellular components in structured microbial communities. *Trends Microbiol.* 28, 668–681
44. Diggle, S.P. *et al.* (2006) The galactophilic lectin, LecA, contributes to biofilm development in *Pseudomonas aeruginosa*. *Environ. Microbiol.* 8, 1095–1104
45. Sommer, R. *et al.* (2016) The virulence factor LecB varies in clinical isolates: consequences for ligand binding and drug discovery. *Chem. Sci.* 7, 4990–5001
46. Passos da Silva, D. *et al.* (2019) The *Pseudomonas aeruginosa* lectin LecB binds to the exopolysaccharide Psl and stabilizes the biofilm matrix. *Nat. Commun.* 10, 2183
47. Mitchell, E. *et al.* (2002) Structural basis for oligosaccharide-mediated adhesion of *Pseudomonas aeruginosa* in the lungs of cystic fibrosis patients. *Nat. Struct. Biol.* 9, 918–921
48. Rosenow, C. *et al.* (1997) Contribution of novel choline-binding proteins to adherence, colonization and immunogenicity of *Streptococcus pneumoniae*. *Mol. Microbiol.* 25, 819–829
49. Huang, X. *et al.* (2023) Vibrio cholerae biofilms use modular adhesins with glycan-targeting and nonspecific surface binding domains for colonization. *Nat. Commun.* 14, 2104
50. De, S. *et al.* (2018) Structural basis of mammalian glycan targeting by *Vibrio cholerae* cytolysin and biofilm proteins. *PLoS Pathog.* 14, e1006841
51. Kaus, K. *et al.* (2019) The 1.9 Å crystal structure of the extracellular matrix protein Bap1 from *Vibrio cholerae* provides insights into bacterial biofilm adhesion. *J. Biol. Chem.* 294, 14499–14511
52. Zheng, S. *et al.* (2017) The *Pseudomonas aeruginosa* lectin LecA triggers host cell signalling by glycosphingolipid-dependent phosphorylation of the adaptor protein CrkII. *Biochimica et Biophysica Acta (BBA) - Molecular. Cell Res.* 1864, 1236–1245
53. Sych, T. *et al.* (2023) The bacterial lectin LecA from *P. aeruginosa* alters membrane organization by dispersing ordered domains. *Commun. Phys.* 6, 153
54. Chemani, C. *et al.* (2009) Role of LecA and LecB lectins in *Pseudomonas aeruginosa*-induced lung injury and effect of carbohydrate ligands. *Infect. Immun.* 77, 2065–2075
55. Khan, N.A. *et al.* (2007) FimH-mediated *Escherichia coli* K1 invasion of human brain microvascular endothelial cells. *Cell. Microbiol.* 9, 169–178
56. Maruvada, R. *et al.* (2008) *Escherichia coli* interaction with human brain microvascular endothelial cells induces signal transducer and activator of transcription 3 association with the C-terminal domain of Ec-gp96, the outer membrane protein A receptor for invasion. *Cell. Microbiol.* 10, 2326–2338
57. Ntui, C.M. *et al.* (2023) Structural and biophysical characterization of the secreted, β-helical adhesin EtpA of Enterotoxigenic *Escherichia coli*. *PLoS One* 18, e0287100
58. Kumar, P. *et al.* (2016) Dynamic interactions of a conserved enterotoxigenic *Escherichia coli* adhesin with intestinal mucins govern epithelium engagement and toxin delivery. *Infect. Immun.* 84, 3608–3617
59. Brown, P.I. *et al.* (2023) The diverse landscape of AB5-type toxins. *Eng. Microbiol.* 3, 100104
60. Johannes, L. (2017) Shiga toxin – a model for glycolipid-dependent and lectin-driven endocytosis. *Toxins (Basel)* 9, 340
61. Merritt, E.A. *et al.* (1994) Crystal structure of cholera toxin B-pentamer bound to receptor GM1 pentasaccharide. *Protein Sci.* 3, 166–175
62. Heggelund, J.E. *et al.* (2012) Both El Tor and classical cholera toxin bind blood group determinants. *Biochem. Biophys. Res. Commun.* 418, 731–735
63. Sánchez, J. and Holmgren, J. (2005) Virulence factors, pathogenesis and vaccine protection in cholera and ETEC diarrhea. *Curr. Opin. Immunol.* 17, 388–398
64. Kitamura, M. (1999) Gangliosides are the binding substances in neural cells for tetanus and botulinum toxins in mice. *Biochim. Biophys. Acta (BBA) Mol. Cell Biol. Lipids* 1441, 1–3
65. Bouyain, S. and Geisbrecht, B.V. (2012) Host glycan recognition by a pore forming toxin. *Structure* 20, 197–198
66. Kaus, K. *et al.* (2014) Glycan specificity of the *Vibrio vulnificus* hemolysin lectin outlines evolutionary history of membrane targeting by a toxin family. *J. Mol. Biol.* 426, 2800–2812
67. Sponsel, J. *et al.* (2023) *Pseudomonas aeruginosa* LecB suppresses immune responses by inhibiting transendothelial migration. *EMBO Rep.* 24, e55971
68. Sanchez Klose, F.P. *et al.* (2024) The *Pseudomonas aeruginosa* lectin LecB modulates intracellular reactive oxygen species production in human neutrophils. *Eur. J. Immunol.* 54, e2350623
69. Schöpf, F. *et al.* (2024) Structural basis of *Fusobacterium nucleatum* adhesin Fap2 interaction with receptors on cancer and immune cells. *bioRxiv* https://doi.org/10.1101/2024.02.28.582045
70. Kaplan, C.W. *et al.* (2010) *Fusobacterium nucleatum* outer membrane proteins Fap2 and RadD induce cell death in human lymphocytes. *Infect. Immun.* 78, 4773–4778
71. Blomgran, R. *et al.* (2004) Uropathogenic *Escherichia coli* triggers oxygen-dependent apoptosis in human neutrophils through the cooperative effect of type 1 fimbriae and lipopolysaccharide. *Infect. Immun.* 72, 4570–4578
72. Limqueco, E. *et al.* (2020) Mannose conjugated polymer targeting *P. aeruginosa* biofilms. *ACS Infect. Dis.* 6, 2866–2871
73. Wagner, S. *et al.* (2017) Covalent lectin inhibition and application in bacterial biofilm imaging. *Angew. Chem. Int. Ed. Engl.* 56, 16559–16564
74. Zahorska, E. *et al.* (2024) High-affinity lectin ligands enable the detection of pathogenic *Pseudomonas aeruginosa* biofilms: implications for diagnostics and therapy. *JACS Au* 4, 4715–4728
75. Meiers, J. *et al.* (2022) Lectin-targeted prodrugs activated by *Pseudomonas aeruginosa* for self-destructive antibiotic release. *J. Med. Chem.* 65, 13988–14014
76. Bruneau, A. *et al.* (2023) Discovery of potent 1,1-diarylthiogalactoside glycomimetic inhibitors of Pseudomonas aeruginosa LecA with antibiofilm properties. *Eur. J. Med. Chem.* 247, 115025
77. Metelkina, O. *et al.* (2024) Dual inhibitors of *Pseudomonas aeruginosa* virulence factors LecA and LasB. *Chem. Sci.* 15, 13333–13342
78. Zahorska, E. *et al.* (2023) Neutralizing the impact of the virulence factor LecA from *Pseudomonas aeruginosa* on human

cells with new glycomimetic inhibitors. *Angew. Chem. Int. Ed.* 62, e202215535
79. Boukerb, A.M. *et al.* (2014) Antiadhesive properties of glycoclusters against *Pseudomonas aeruginosa* lung infection. *J. Med. Chem.* 57, 10275–10289
80. Sommer, R. *et al.* (2018) Glycomimetic, orally bioavailable LecB inhibitors block biofilm formation of *Pseudomonas aeruginosa*. *J. Am. Chem. Soc.* 140, 2537–2545
81. Cusumano, C.K. *et al.* (2011) Treatment and prevention of urinary tract infection with orally active fimH inhibitors. *Sci. Transl. Med.* 3, 109ra115-109ra115
82. Mydock-McGrane, L.K. *et al.* (2017) Rational design strategies for FimH antagonists: new drugs on the horizon for urinary tract infection and Crohn's disease. *Expert Opin. Drug Discov.* 12, 711–731
83. Hatton, N.E. *et al.* (2021) Developments in mannose-based treatments for uropathogenic *Escherichia coli*-induced urinary tract infections. *ChemBioChem* 22, 613–629
84. Chevalier, G. *et al.* (2021) Blockage of bacterial FimH prevents mucosal inflammation associated with Crohn's disease. *Microbiome* 9, 176
85. Kalas, V. *et al.* (2018) Structure-based discovery of glycomimetic FmlH ligands as inhibitors of bacterial adhesion during urinary tract infection. *Proc. Natl. Acad. Sci. U. S. A.* 115, E2819–E2828
86. Maddirala, A.R. *et al.* (2024) Discovery of orally bioavailable FmlH lectin antagonists as treatment for urinary tract infections. *J. Med. Chem.* 67, 3668–3678
87. Sudakevitz, D. and Gilboa-Garber, N. (1987) Immunization of mice against various strains of *Pseudomonas aeruginosa* by using *Pseudomonas* lectin vaccine. *FEMS Microbiol. Lett.* 43, 313–315
88. Bianconi, I. *et al.* (2019) Genome-based approach delivers vaccine candidates against *Pseudomonas aeruginosa*. *Front. Immunol.* 9, 3021
89. Day, C.J. *et al.* (2019) Lectin activity of *Pseudomonas aeruginosa* vaccine candidates PSE17-1, PSE41-5 and PSE54. *Biochem. Biophys. Res. Commun.* 513, 287–290
90. Chorro, L. *et al.* (2024) A cynomolgus monkey *E. coli* urinary tract infection model confirms efficacy of new FimH vaccine candidates. *Infect. Immun.* 92, e0016924
91. Eldridge, G.R. *et al.* (2021) Safety and immunogenicity of an adjuvanted *Escherichia coli* adhesin vaccine in healthy women with and without histories of recurrent urinary tract infections: results from a first-in-human phase 1 study. *Hum. Vaccin. Immunother.* 17, 1262–1270
92. Silmon de Monerri, N.C. *et al.* (2025) Structure-based design of an immunogenic, conformationally stabilized FimH antigen for a urinary tract infection vaccine. *PLoS Pathog.* 21, e1012325
93. Sommer, R. *et al.* (2019) Anti-biofilm agents against *Pseudomonas aeruginosa* : a structure–activity relationship study of *C*-glycosidic LecB inhibitors. *J. Med. Chem.* 62, 9201–9216
94. Jarvis, C. *et al.* (2016) Antivirulence isoquinolone mannosides: optimization of the biaryl aglycone for FimH lectin binding affinity and efficacy in the treatment of chronic UTI. *ChemMedChem* 11, 367–373
95. Garinet, S. *et al.* (2018) Elective distribution of resistance to beta-lactams among Enterobacter cloacae genetic clusters. *J. Infect.* 77, 178–182
96. Beshr, G. *et al.* (2024) A fucose-binding superlectin from *Enterobacter cloacae* with high Lewis and ABO blood group antigen specificity. *J. Biol. Chem.* 301, 108151
97. Girlich, D. *et al.* (2021) Uncovering the novel *Enterobacter cloacae* complex species responsible for septic shock deaths in newborns: a cohort study. *Lancet Microbe* 2, e536–e544
98. Arcilla, M.B. and Sturgeon, P. (1971) Perinatal expression of the Lewis and secretor blood group systems. *Pediatr. Res.* 5, 422–423
99. Bentancor, L.V. *et al.* (2012) Identification of Ata, a multifunctional trimeric autotransporter of *Acinetobacter baumannii*. *J. Bacteriol.* 194, 3950–3960
100. Tram, G. *et al.* (2021) The *Acinetobacter baumannii* autotransporter adhesin Ata recognizes host glycans as high-affinity receptors. *ACS Infect. Dis.* 7, 2352–2361
101. Flannery, A. *et al.* (2020) Glycomics microarrays reveal differential in situ presentation of the biofilm polysaccharide poly-N-acetylglucosamine on *Acinetobacter baumannii* and *Staphylococcus aureus* cell surfaces. *Int. J. Mol. Sci.* 21, 2465
102. Mills, K.B. *et al.* (2022) Staphylococcal corneocyte adhesion: assay optimization and roles of Aap and SasG adhesins in the establishment of healthy skin colonization. *Microbiol. Spectr.* 10, e0246922
103. Mills, K.B. *et al.* (2024) *Staphylococcus aureus* skin colonization is mediated by SasG lectin variation. *Cell Rep.* 43, 114022
104. Corrigan, R.M. *et al.* (2007) The role of *Staphylococcus aureus* surface protein SasG in adherence and biofilm formation. *Microbiology (N Y)* 153, 2435–2446
105. Roy, P. *et al.* (2021) Glycan-dependent corneocyte adherence of *Staphylococcus epidermidis* mediated by the lectin subdomain of Aap. *mBio* 12, e02908-20
106. Wang, C. *et al.* (2022) The staphylococcal biofilm protein Aap mediates cell–cell adhesion through mechanically distinct homophilic and lectin interactions. *PNAS Nexus* 1, pgac278
107. Conrady, D.G. *et al.* (2013) Structural basis for Zn^{2+}-dependent intercellular adhesion in staphylococcal biofilms. *Proc. Natl. Acad. Sci.* 110, E202–E211
108. Beshr, G. *et al.* (2017) *Photorhabdus luminescens* lectin A (PllA): a new probe for detecting α-galactoside–terminating glycoconjugates. *J. Biol. Chem.* 292, 19935–19951
109. Jančařiková, G. *et al.* (2017) Characterization of novel bangle lectin from Photorhabdus asymbiotica with dual sugar-binding specificity and its effect on host immunity. *PLoS Pathog.* 13, e1006564
110. Kumar, A. *et al.* (2016) A novel fucose-binding lectin from *Photorhabdus luminescens* (PLL) with an unusual heptabladed β-propeller tetrameric structure. *J. Biol. Chem.* 291, 25032–25049
111. Audfray, A. *et al.* (2012) Fucose-binding lectin from opportunistic pathogen *Burkholderia ambifaria* binds to both plant and human oligosaccharidic epitopes. *J. Biol. Chem.* 287, 4335–4347
112. Gunardi, W.D. *et al.* (2021) Biofilm targeting strategy in the eradication of *Burkholderia* infections: a mini-review. *Open Microbiol. J.* 15, 51–57
113. Frensch, M. *et al.* (2021) Bacterial lectin BambL acts as a B cell superantigen. *Cell. Mol. Life Sci.* 78, 8165–8186
114. Wilhelm, I. *et al.* (2019) Carbohydrate-dependent B cell activation by fucose-binding bacterial lectins. *Sci. Signal.* 12, eaao7194
115. Lameignere, E. *et al.* (2008) Structural basis for mannose recognition by a lectin from opportunistic bacteria *Burkholderia cenocepacia*. *Biochem. J.* 411, 307–318
116. Inhülsen, S. *et al.* (2012) Identification of functions linking quorum sensing with biofilm formation in *Burkholderia cenocepacia* H111. *Microbiologyopen* 1, 225–242
117. Marchetti, R. *et al.* (2012) *Burkholderia cenocepacia* lectin A binding to heptoses from the bacterial lipopolysaccharide. *Glycobiology* 22, 1387–1398
118. Šulák, O. *et al.* (2010) A TNF-like trimeric lectin domain from *Burkholderia cenocepacia* with specificity for fucosylated human histo-blood group antigens. *Structure* 18, 59–72
119. Kolbe, K. *et al.* (2019) Lectins of *Mycobacterium tuberculosis* – rarely studied proteins. *Beilstein J. Org. Chem.* 15, 1–15
120. Nogueira, L. *et al.* (2010) *Mycobacterium tuberculosis* Rv1419 encodes a secreted 13kDa lectin with immunological reactivity during human tuberculosis. *Eur. J. Immunol.* 40, 744–753
121. Singh, Desh Deepak and Jeyakani, Justin (2007) Scanning the genome of *Mycobacterium tuberculosis* to identify potential lectins. *Protein Pept. Lett.* 14, 683–691
122. Anton, V. *et al.* (1996) Identification of the sugars involved in mycobacterial cell aggregation. *FEMS Microbiol. Lett.* 144, 167–170
123. Esposito, C. *et al.* (2011) Heparin-binding hemagglutinin HBHA from *Mycobacterium tuberculosis* affects actin polymerisation. *Biochem. Biophys. Res. Commun.* 410, 339–344
124. De Maio, F. *et al.* (2019) The mycobacterial HBHA protein: a promising biomarker for tuberculosis. *Curr. Med. Chem.* 26, 2051–2060
125. Imberty, A. *et al.* (2021) UniLectin, a one-stop-shop to explore and study carbohydrate-binding proteins. *Curr. Protoc.* 1, e305
126. Laborda, P. *et al.* (2024) Mutations in the efflux pump regulator MexZ shift tissue colonization by *Pseudomonas aeruginosa* to a state of antibiotic tolerance. *Nat. Commun.* 15, 2584

1.2. A Fucose-Binding Superlectin from *E. cloacae* with High Lewis and ABO Blood group Antigen Specificity

The following chapter presents the introductory section of a peer-reviewed article detailing the discovery of the fucophilic lectin EclA from *E. cloacae* subsp. *cloacae*, identified through its sequence similarity to the orthologue LecA in *P. aeruginosa*. The abstract and introductory sections of the article presented were contributed by the author of this thesis during the manuscript preparation.

Authors: Ghamdan Beshr, Asfandyar Sikandar, Julia Gläser, **Mario Fares**, Roman Sommer, Stefanie Wagner, Jesko Köhnke, and Alexander Titz
Published in: *Journal of Biological Chemistry,* 2024, *301, 2, 108151*
DOI: 10.1016/j.jbc.2024.108151

All references cited in this article section are listed at the end of this chapter.

Abstract

Bacteria frequently employ carbohydrate-binding proteins, so-called lectins, to colonize and persist in a host. Thus, bacterial lectins are attractive targets for the development of new anti-infectives. To find new potential targets for anti-infectives against pathogenic bacteria, we searched for homologs of *Pseudomonas aeruginosa* lectins and identified homologs of LecA in *Enterobacter* species. Here, we recombinantly produced and biophysically characterized a homolog that comprises one LecA domain and one additional, novel protein domain. This protein was termed *Enterobacter cloacae* lectin A (EclA) and found to bind L-fucose. Glycan array analysis revealed a high specificity for the LewisA antigen and the type II H-antigen (blood group O) for EclA, while related antigens LewisX, Y, and B, as well as blood group A or B were not bound. We developed a competitive binding assay to quantify blood group antigen-binding specificity in solution. Finally, the crystal structure of EclA could be solved in complex with methyl α-L-selenofucoside. It revealed the unexpected binding of the carbohydrate ligand to the second domain, which comprises a novel fold that dimerizes *via* strand-swapping resulting in an intertwined beta sheet.

Introduction

Bacterial infections are increasingly threatening as a consequence of antimicrobial resistance development against standard-of-care antibiotics, which have been on the market for many decades. Therefore, new treatment options are needed to fight the inevitable spread of multidrug resistant pathogens rendering current medicines ineffective (1). The World Health Organization has classified, especially, Gram-negative bacteria from the resistance-prone ESKAPE group as outstandingly important due to a lack of treatments with new modes of action, able to circumvent established antimicrobial resistance (2).

For the critical priority Gram-negative bacterium *Pseudomonas aeruginosa*, many new approaches are actively being studied, such as new classes of antibiotics and alternative approaches interfering with bacterial virulence and pathogenicity (1, 3). Among the so-called pathoblockers or antivirulence agents (4, 5), interference with biofilm formation—a major determinant of drug resistance—is of particular interest to restore the pathogen's susceptibility to treatments (6). Numerous bacteria employ carbohydrate-binding proteins, so-called lectins, to adhere to host tissue and establish and maintain biofilms (7-9). It has been demonstrated that the *Pseudomonas* lectins LecA and LecB can be targeted with defined carbohydrates, small glycomimetics, and dendrimers to prevent biofilms and interfere with bacterial virulence (10-21).

Inspired by these data, we searched for orthologs of LecA in other bacteria. We previously identified many LecA orthologs in the genomes of several *Photorhabdus, Xenorhabdus*, and *Enterobacter* species and experimentally characterized PllA from *Photorhabdus luminescens*, an insect pathogen (22).

The *Enterobacter cloacae* complex is part of the ESKAPE pathogens infecting humans and comprises numerous species classified within 12 genetic clusters (2, 23, 24). Bacteria associated with this complex are usually found in soil, sewage, and drinking water reservoirs and are also part of the human intestinal microbiota (25). *E. cloacae* and *Enterobacter hormaechei* constitute the most frequently isolated *Enterobacter* species from human clinical specimens (24). Outbreaks of *E. cloacae* and the trigger to change from a commensal bacterium to a virulent one can be sporadic and often happens in the intensive care units of hospitals and causes either localized infections, such as lung, wound, central nervous system, urinary tract, and catheter, or orthopedic implant-associated infections, or systemic infections, such as bacteremia and sepsis (25, 26). It is also well-established that *E. cloacae* is a culprit of outbreaks and fatalities in neonatal intensive care units of hospitals (27). In their virulence

arsenal, *E. cloacae* species employ many virulence factors like enterotoxins, α-hemolysin, and thiol-activated pore-forming cytotoxins similar to Shiga-like toxin II after adhesion to epithelial cells (28). In some clinical strains of *E. cloacae*, type III secretion system was also seen to be employed to destroy phagocytes and epithelial cells to facilitate host colonization (29). Further, a type VI secretion system also showed to be instrumental in biofilm formation and adherence to epithelial cells (30). Like other Gram-negative bacilli, the virulence of *E. cloacae* also depends on the presence of its outer membrane lipopolysaccharide, which can help in avoiding opsonophagocytosis or initiate an inflammation cascade in the host cell leading to sepsis (31). *E. cloacae* are multidrug resistant due to their chromosomally encoded and induced and/or constitutively expressed AmpC β-lactamase with increased resistance rates following treatment with either β-lactams or first, second, and third generation cephalosporins (31). Fourth generation cephalosporins may be suitable against the AmpC β-lactamase strains if extended-spectrum β-lactamases are not present, in which case a combination therapy of colistin or aminoglycosides and carbapenems in a double regimen is used (31). Due to the prevalence of extended-spectrum β-lactamases and carbapenemases in this species, *E. cloacae* has become the third most common broad-spectrum *Enterobacteriaceae* involved in nosocomial infections, following *Escherichia coli* and *Klebsiella pneumoniae* (32). For these reasons, the World Health Organization identified carbapenem-resistant *Enterobacteriaceae* as a critical priority on its list of antibiotic-resistant bacteria in 2017, highlighting the urgent need for the development of new antibiotics. The characterization of LecA homologs in *Enterobacter* spp. as possible antivirulence targets is therefore of interest.

Here, we report the identification, biophysical and structural characterization of the first two-domain ortholog of LecA found in *E. cloacae* subsp. *cloacae* (type strain: ATCC 13047), an important member of the *E. cloacae* complex. This strain was isolated from human cerebrospinal fluid and is the first completely sequenced member of the *E. cloacae* species. It possesses many virulence properties, encodes more than 50 antibiotic resistance genes, and has been extensively studied and used as a reference strain (33-36).

The lectin termed *Enterobacter cloacae* lectin A (EclA) consists of an N-terminal LecA domain and a C-terminal domain reminiscent of carbohydrate binding modules. In this work, we established the l-fucose binding of EclA via its C-terminal domain while we did not succeed in identifying a ligand for the LecA-homologous N terminus despite intense efforts. EclA forms homodimers resulting in the presentation of two N termini toward one end and two C termini toward the opposite end in its structure. This orientation suggests a function as a cross-linker for two carbohydrate ligands, one of which remains elusive. The unprecedented high specificity

of EclA's C-terminal domain for l-fucosides in mammalian blood group H-type II and LewisA antigens over related A/B-antigens or isomeric LewisX suggests a link to host binding specificity and pathophysiology.

Article findings and implications

The article goes on to present its significant findings. Structurally, EclA is a unique fusion protein composed of two distinct parts: an N-terminal domain that is homologous to the LecA protein family and a C-terminal domain featuring a novel protein fold that also functions as a carbohydrate-binding module. This protein forms homodimers, where two identical EclA chains pair together. The dimerization is characterized by an unusual "β-strand swap" within the C-terminal domains, which results in a twisted β-zipper structure. This specific arrangement causes the two C-terminal binding domains to face one direction and the two N-terminal domains to face the opposite direction, suggesting a potential role in cross-linking different molecular and biological components. Interestingly, the full-length protein and/or its individual domains were also found in ECC and *Pseudomonas* species. Functionally, biophysical analysis demonstrated that EclA binds to the sugar L-fucose, an activity specifically located within its C-terminal domain and stabilized by a calcium ion in the binding pocket. Glycan array analyses further revealed a remarkable specificity for two human blood group antigens: the LewisA (Le^a) antigen and the H-type II antigen, which is the precursor to the O blood group. Notably, EclA does not bind to closely related structures like Lewis X, Lewis Y, Lewis B, or the antigens for blood groups A and B, highlighting its high degree of selectivity. Despite extensive testing, the specific ligand for the N-terminal domain could not be determined, leaving its precise function enigmatic. Essentially, this work provided the basis for the functional characterization of EclA as a standalone protein and as a protein in *E. cloacae*.

References

1. Miethke, M., Pieroni, M., Weber, T., Brönstrup, M., Hammann, P., Halby, L., et al. (2021) Towards the sustainable discovery and development of new antibiotics. Nat. Rev. Chem. 5, 726-749
2. Miller, W. R., and Arias, C. A. (2024) ESKAPE pathogens: antimicrobial resistance, epidemiology, clinical impact and therapeutics. Nat. Rev. Microbiol. 22, 598-616
3. Wagner, S., Sommer, R., Hinsberger, S., Lu, C., Hartmann, R. W., Empting, M., et al. (2016) Novel Strategies for the treatment of Pseudomonas aeruginosa infections. J. Med. Chem. 59, 5929-5969

4. Calvert, M. B., Jumde, V. R., and Titz, A. (2018) Pathoblockers or antivirulence drugs as a new option for the treatment of bacterial infections. Beilstein J. Org. Chem. 14, 2607-2617
5. Dickey, S. W., Cheung, G. Y. C., and Otto, M. (2017) Different drugs for bad bugs: antivirulence strategies in the age of antibiotic resistance. Nat. Rev. Drug Discov. 16, 457-471
6. Poole, K. (2011) Pseudomonas aeruginosa: resistance to the max. Front. Microbiol. 2, 65
7. Sharon, N. (2006) Carbohydrates as future anti-adhesion drugs for infectious diseases. Biochim. Biophys. Acta 1760, 527-537
8. Lis, H., and Sharon, N. (1998) Lectins: carbohydrate-specific proteins that mediate cellular recognition. Chem. Rev. 98, 637-674
9. Imberty, A., and Varrot, A. (2008) Microbial recognition of human cell surface glycoconjugates. Curr. Opin. Struct. Biol. 18, 567-576
10. Zahorska, E., Rosato, F., Stober, K., Kuhaudomlarp, S., Meiers, J., Hauck, D., et al. (2023) Neutralizing the impact of the virulence factor LecA from Pseudomonas aeruginosa on human cells with new glycomimetic inhibitors. Angew. Chem. Int. Ed. Engl. 62, e202215535
11. Sommer, R., Wagner, S., Rox, K., Varrot, A., Hauck, D., Wamhoff, E.-C.,et al. (2018) Glycomimetic, orally bioavailable LecB inhibitors block biofilm formation of Pseudomonas aeruginosa. J. Am. Chem. Soc. 140, 2537-2545
12. Sommer, R., Rox, K., Wagner, S., Hauck, D., Henrikus, S. S., Newsad, S.,et al. (2019) Anti-biofilm agents against Pseudomonas aeruginosa: a structure-activity relationship study of C-glycosidic LecB inhibitors. J. Med. Chem. 62, 9201-9216
13. Kadam, R. U., Bergmann, M., Hurley, M., Garg, D., Cacciarini, M., Swiderska, M. A., et al. (2011) A glycopeptide dendrimer inhibitor of the galactose-specific lectin LecA and of Pseudomonas aeruginosa biofilms.Angew. Chem. Int. Ed. Engl. 50, 10631-10635
14. Reymond, J.-L., Bergmann, M., and Darbre, T. (2013) Glycopeptide dendrimers as Pseudomonas aeruginosa biofilm inhibitors. Chem. Soc. Rev. 42, 4814-4822
15. Johansson, E. M. V., Crusz, S. A., Kolomiets, E., Buts, L., Kadam, R. U., Cacciarini, M., et al. (2008) Inhibition and dispersion of Pseudomonas aeruginosa biofilms by glycopeptide dendrimers targeting the fucosespecific lectin LecB. Chem. Biol. 15, 1249-1257
16. Sponsel, J., Guo, Y., Hamzam, L., Lavanant, A. C., Pérez-Riverón, A., Partiot, E., et al. (2023) Pseudomonas aeruginosa LecB suppresses immune responses by inhibiting transendothelial migration. EMBO Rep. 24, e55971
17. Boukerb, A. M., Rousset, A., Galanos, N., Méar, J.-B., Thepaut, M., Grandjean, T., et al. (2014) Anti-adhesive properties of glycoclusters against Pseudomonas aeruginosa lung infection. J. Med. Chem. 57, 10275-10289
18. Chemani, C., Imberty, A., de Bentzmann, S., Pierre, M., Wimmerová, M., Guery, B. P., et al. (2009) Role of LecA and LecB lectins in Pseudomonas aeruginosa-induced lung injury and effect of carbohydrate ligands. Infect. Immun. 77, 2065-2075
19. Leusmann, S., Ménová, P., Shanin, E., Titz, A., and Rademacher, C. (2023) Glycomimetics for the inhibition and modulation of lectins. Chem. Soc. Rev. 52, 3663-3740
20. Bucior, I., Abbott, J., Song, Y., Matthay, M. A., and Engel, J. N. (2013) Sugar administration is an effective adjunctive therapy in the treatment of Pseudomonas aeruginosa pneumonia. Am. J. Physiol. Lung Cell Mol. Physiol 305, L352-L363
21. Hauber, H.-P., Schulz, M., Pforte, A., Mack, D., Zabel, P., and Schumacher, U. (2008) Inhalation with fucose and galactose for treatment of Pseudomonas aeruginosa in cystic fibrosis patients. Int. J. Med. Sci. 5, 371-376

22. Beshr, G., Sikandar, A., Jemiller, E.-M., Klymiuk, N., Hauck, D., Wagner, S., et al. (2017) Photorhabdus luminescens lectin A (PllA) - a new probe for detecting a-galactoside-terminating glycoconjugates. J. Biol. Chem.292, 19935-19951
23. Liu, S., Chen, L., Wang, L., Zhou, B., Ye, D., Zheng, X., et al. (2022) Cluster differences in antibiotic resistance, biofilm formation, mobility, and virulence of clinical Enterobacter cloacae complex. Front. Microbiol.13, 814831
24. Mezzatesta, M. L., Gona, F., and Stefani, S. (2012) Enterobacter cloacae complex: clinical impact and emerging antibiotic resistance. Future Microbiol. 7, 887-902
25. Garinet, S., Fihman, V., Jacquier, H., Corvec, S., Le Monnier, A., Guillard, T., et al. (2018) Elective distribution of resistance to beta-lactams among Enterobacter cloacae genetic clusters. J. Infect. 77, 178-182
26. Bousquet, A., van der Mee-Marquet, N., Dubost, C., Bigaillon, C., Larréché, S., Bugier, S., et al. (2017) Outbreak of CTX-M-15-producing Enterobacter cloacae associated with therapeutic beds and syphons in an intensive care unit. Am. J. Infect. Control 45, 1160-1164
27. Girlich, D., Ouzani, S., Emeraud, C., Gauthier, L., Bonnin, R. A., Le Sache, N., et al. (2021) Uncovering the novel Enterobacter cloacae complex species responsible for septic shock deaths in newborns: a cohort study. Lancet Microbe 2, e536-e544
28. Barnes, A. I., Ortiz, C., Paraje, M. G., Balanzino, L. E., and Albesa, I. (1997) Purification and characterization of a cytotoxin from Enterobacter cloacae. Can. J. Microbiol. 43, 729-733
29. Krzyminska, S., Mokracka, J., Koczura, R., and Kaznowski, A. (2009) Cytotoxic activity of Enterobacter cloacae human isolates. FEMS Immunol. Med. Microbiol. 56, 248-252
30. Soria-Bustos, J., Ares, M. A., Gómez-Aldapa, C. A., González-y-Merchand, J. A., Girón, J. A., and De la Cruz, M. A. (2020) Two type VI secretion systems of Enterobacter cloacae are required for bacterial competition, cell adherence, and intestinal colonization. Front. Microbiol.11, 560488
31. Ramirez, D., and Giron, M. (2024) Enterobacter Infections, StatPearls Publishing
32. Davin-Regli, A., and PagÃ€s, J.-M. (2015) Enterobacter aerogenes and Enterobacter cloacae; versatile bacterial pathogens confronting antibiotic treatment. Front. Microbiol. 6, 392
33. Ren, Y., Ren, Y., Zhou, Z., Guo, X., Li, Y., Feng, L., et al. (2010) Complete genome sequence of Enterobacter cloacae subsp. cloacae type strain ATCC 13047. J. Bacteriol. 192, 2463-2464
34. Pantel, L., Guérin, F., Serri, M., Gravey, F., Houard, J., Maurent, K., et al. (2022) Exploring cluster-dependent antibacterial activities and resistance pathways of NOSO-502 and colistin against Enterobacter cloacae complex species. Antimicrob. Agents Chemother. 66, e0077622
35. Bhar, S., Edelmann, M. J., and Jones, M. K. (2021) Characterization and proteomic analysis of outer membrane vesicles from a commensal microbe, Enterobacter cloacae. J. Proteomics 231, 103994
36. Frutos-Grilo, E., Kreling, V., Hensel, A., and Campoy, S. (2023) Hostpathogen interaction: Enterobacter cloacae exerts different adhesion and invasion capacities against different host cell types. PLoS One 18, e0289334

1.3. The *Enterobacter cloacae* Complex

1.3.1. An Overview of the ECC: Origin, Detection, and Composition

The *Enterobacter cloacae* complex (ECC) is a group of genetically related but distinct bacterial species that are widely found in nature, including in soil, sewage, and the gastrointestinal tracts of humans and animals. While often existing as commensal organisms, they have emerged as significant opportunistic and nosocomial pathogens. The complex is genomically heterogeneous and its taxonomy is continuously updated (Davin-Regli et al., 2019; Mezzatesta et al., 2012; Sutton et al., 2018).

A primary source of confusion in clinical and research settings is the distinction between *E. cloacae* as a species and the *Enterobacter cloacae* complex. In routine clinical laboratories, isolates are frequently identified only to the complex level and reported as "*E. cloacae*" (Garinet et al., 2018; Sutton et al., 2018). This is because common phenotypic identification methods, such as API 20E and VITE K2, as well as MALDI-TOF MS, cannot reliably differentiate between the various species within this complex (Mezzatesta et al., 2012). Analysis of the 16S rRNA is also not efficient in accurate species identification, as the results represent 60% similarity within all species of ECC (Hoffmann & Roggenkamp, 2003). This confusion persists in clinical reporting and GenBank submissions, highlighting the need for improved molecular diagnostics in routine laboratories (Sutton et al., 2018). Consequently, the term *E. cloacae* is often used ambiguously to refer to the entire ECC, which represents a heterogeneous group of species rather than a single, well-defined species. This misnaming was documented by Hoffmann and Roggenkamp (2003), and has confounded the true genomic identity and clinical significance of individual species, such as *E. cloacae* subsp. *cloacae* and subsp. *dissolvens*, which belong to clusters XI and XII, respectively. These subspecies represent a small fraction of the ECC and are rarely encountered in clinical cases, as shown in numerous studies. (Akbari et al., 2016; Garinet et al., 2018; Kremer & Hoffmann, 2012; Krzymińska et al., 2010; S. Liu et al., 2022; Morand et al., 2009).

The most robust and widely cited method for classifying members of the ECC is through sequence analysis of a fragment of the *hsp60* gene. This molecular technique, pioneered by Hoffmann and Roggenkamp, divides the ECC into 12 genetic clusters (I-XII) and one unstable sequence crowd (XIII) (Hoffmann & Roggenkamp, 2003). Many of these clusters have been assigned specific species or subspecies names (Sutton et al., 2018) (Table 1).

Table 1: Cluster and species classification of the *Enterobacter cloacae* complex.

Cluster	Species Name
Cluster I	*E. asburiae*
Cluster II	*E. kobei*
Cluster III	*E. hormaechei* subsp. *hoffmani*
Cluster IV	*E. roggenkampii*
Cluster V	*E. ludwigii*
Cluster VI	*E. hormaechei* subsp. *oharae*
Cluster VII	*E. hormaechei* subsp. *hormaechei*
Cluster VIII	*E. hormaechei* subsp. *steigerwaltii*
Cluster IX	*E. bugandensis*
Cluster X	*E. nimipressuralis*
Cluster XI	*E. cloacae* subsp. *cloacae*
Cluster XII	*E. cloacae* subsp. *dissolvens*
Cluster XIII	*E. cloacae* sequence crowd

1.3.2. Notable Clinical Species within ECC

Several species and clusters within ECC have emerged as particularly significant in clinical contexts:

- ***E. hormaechei* (Clusters III, VI, VII, VIII):** This species is now recognized as the predominant member of ECC recovered from clinical samples worldwide (Ganbold et al., 2023; S. Liu et al., 2022; Sutton et al., 2018). It demonstrates a significantly higher prevalence of extended-spectrum β-lactamase (ESBL) production and resistance to third-generation cephalosporins compared to other clusters (Garinet et al., 2018).
- ***E. bugandensis* (Cluster IX):** This species has been identified as a hypervirulent pathogen responsible for fatal septic shock in newborns (Girlich et al., 2021).

Enterobacter species are among the ESKAPE group which also comprises the opportunistic pathogens *Enterococcus faecium*, *Staphylococcus aureus*, *Klebsiella pneumoniae*, *Acinetobacter baumannii*, and *P. aeruginosa*, that are known to cause a wide array of nosocomial infections, particularly in immunocompromised patients, those in intensive care units, and individuals with prolonged hospital stays (Davin-Regli et al., 2019). Common infections include: Urinary tract infections, bacteremia and sepsis, pneumonia and other lower respiratory tract infections, surgical site, skin, and soft tissue infections, osteomyelitis and infections of orthopedic implants, and neonatal meningitis and sepsis in neonatal intensive care units (NICU) of hospitals (Akbari et al., 2016; Farfour et al., 2022; Farsiani et al., 2019; Frutos-Grilo et al., 2023; Girlich et al., 2021; Kremer & Hoffmann, 2012; Krzymińska et al., 2009; Mezzatesta et al., 2012; Morand et al., 2009).

The presence of ECC in NICUs is of particular concern. Outbreaks have been linked to contaminated medical equipment, such as incubators, which can act as long-term reservoirs for cross-transmission (Girlich et al., 2021; Mezzatesta et al., 2012). Risk factors in neonates include low birth weight, premature birth, and the use of intravenous catheters (Farsiani et al., 2019).

1.3.3. *E. cloacae* subsp. *cloacae* and *E. cloacae* subsp. *dissolvens*

Within the ECC, the two *E. cloacae* subspecies used in the experimental phase of the thesis were *E. cloacae* subsp. *cloacae* (cluster XI) and *E. cloacae* subsp. *dissolvens* (cluster XII), since EclA was identified in both (Beshr et al., 2025).

- ***E. cloacae* subsp. *cloacae* (cluster XI):** *E. cloacae* subsp. *cloacae*, whose type strain ATCC 13047/DSM 30054 was isolated from human cerebrospinal fluid, has been extensively used as the model strain for ECC (Bhar et al., 2021; Debroy & Ramaiah, 2023; Frutos-Grilo et al., 2023; Mustafa et al., 2020; Rayner et al., 1998; Soria-Bustos et al., 2020), despite being genomically distinct from other clusters (Hoffmann & Roggenkamp, 2003; Ren et al., 2010). Its complete genome sequence reveals a multitude of genes associated with virulence, including seven loci for fimbrial biosynthesis, six genes for adhesin/invasin proteins, genes for iron acquisition and hemolysins, 37 multidrug efflux proteins, 7 antimicrobial peptide resistance proteins, and 11 β-lactamases, suggesting a broad range in antibiotic resistance (Ren et al., 2010). Despite this genetic potential for virulence, cluster XI appears to be the least isolated from clinical samples compared to the more dominant cluster *E. hormaechei* (Kremer & Hoffmann, 2012)
- ***E. cloacae* subsp. *dissolvens* (cluster XII):** To date, human infections caused by this cluster (XII) have been rarely reported, or were entirely absent in several of the referenced studies, suggesting limited capacity to cause disease in humans (Akbari et al., 2016; Garinet et al., 2018; Kremer & Hoffmann, 2012; S. Liu et al., 2022). The type strain ATCC 23373/DSM 16657 used in this study has been isolated from an infected corn plant (Rosen H.R, 1922).

In summary, both subspecies are formally part of ECC, *E. cloacae* subsp. *cloacae* is rarely isolated in clinical settings, while *E. cloacae* subsp. *dissolvens* is even less common and appears to play a more prominent role as an environmental organism, frequently associated with plant soils (Ramesh et al., 2014).

The taxonomic distinction between *E. cloacae* subsp. *cloacae* and *E. cloacae* subsp. *dissolvens* remained for a long time a subject of ongoing investigation. Originally classified in the genus *Erwinia*, *E. cloacae* subsp. *dissolvens* was later reassigned to *Enterobacter* as *E. dissolvens*, though its status as a separate species from *E. cloacae* was debated (Brenner et al., 1986). Early DNA-DNA hybridization studies highlighted their close genomic similarity, showing 60% to 82% relatedness with ΔTm values well below the 5 °C threshold for species differentiation (Grimont & Grimont, 2006; Lindh & Ursing, 1991). However, despite this high similarity, more recent phylogenetic assessments based on multiple housekeeping genes (*hsp60*, *rpoB*, *hemB*) indicated that they consistently form distinct evolutionary lineages, suggesting potential species-level divergence (Hoffmann & Roggenkamp, 2003). As the definitive resolution of their classification was still pending, phenotypic characterizations with API20E, Biotype 100 provided the conclusive evidence by differentiating the genovars (*E. cloacae* and *E. dissolvens*) based on their ability to hydrolyze the glycoside esculin. Knowing that phenotypically different genovars of one species are generally considered subspecies (Moore et al., 1987), *E. dissolvens* was transferred to *E. cloacae* as subspecies *dissolvens*, and *E. cloacae* was reassigned to *E. cloacae* subspecies *cloacae* (Hoffmann et al., 2005).

1.3.4. Virulence Factors and Antibiotic Resistance in ECC

ECC has emerged in clinical settings through its multifunctional pathogenic traits that encompass host colonization, tissue invasion, immune evasion, and antibiotic resistance (Davin-Regli & Pagès, 2015; Farsiani et al., 2019).

Adhesion and biofilm formation

The initial and most critical stage of infection is the ability of the bacteria to colonize host surfaces, a process mediated by a variety of adhesins and the capacity to form resilient communities.

- **Adhesion and invasion:** All ECC species were shown in a study to adhere human epithelial cell type 2, and most of them (70%) showed invasive activities (Keller et al., 1998; Krzymińska et al., 2010). Additionally, *E. cloacae* subsp. *cloacae* exhibits tissue-specific patterns of adhesion and invasion, which further reflects its clinical target specificity as a pathogen (Frutos-Grilo et al., 2023).
- **Type 1 pili and other fimbriae:** Adhesion in ECC is often mediated by fimbriae, with type 1 pili being the most common, facilitating mannose-sensitive hemagglutination (MSHA) (Adegbola & Old, 1983; Keller et al., 1998). The genome of the *E. cloacae*

subsp. *cloacae* contains seven distinct loci for fimbrial biosynthesis (Ren et al., 2010). The functionality of these pili is dependent on the major subunit, FimA, and the adhesin FimH, both of which are essential for attachment to human bladder cells (Frutos-Grilo et al., 2023). Some *Enterobacter* species also express type 3 fimbriae, which mediate mannose-resistant hemagglutination (MRHA), and are antigenically distinct from type 1 pili (Adegbola & Old, 1983).

- **Curli fimbriae and biofilm formation:** Curli are highly aggregated amyloid fibers encoded by the *csg* operons, that correlated with the ability of ECC to form robust, mature biofilms on inert surfaces (Kim et al., 2012). Interestingly, while essential for biofilm architecture, curli fimbriae were found to be dispensable for the initial adhesion of *E. cloacae* to bladder cells, suggesting that different adhesins are deployed for different stages of infection and tissue types (Frutos-Grilo et al., 2023).

Toxin delivery and bacterial warfare

ECC employs secretion systems to deliver toxins and effector proteins that can damage host cells:

- **Cytotoxins and hemolysins:** ECC is known to secrete a variety of cellular toxins, including enterotoxins, pore-forming toxins, and hemolysins (Davin-Regli & Pagès, 2015; Farsiani et al., 2019). The genome of *E. cloacae* subsp. *cloacae* contains three genes for hemolysin-like proteins (Ren et al., 2010). A significant percentage (70%) of clinical isolates produce thiol-activated cytotoxic toxins capable of destroying epithelial (Vero) cells and killing phagocytes such as macrophages, however, the expression of these toxins can be variable, as cytotoxic activity in certain strain collections was not detected (Keller et al., 1998; Krzymińska et al., 2009).
- **Secretion systems:** The delivery of such cytotoxins and hemolysins is often mediated by specialized secretion systems. A low percentage (27%) of ECC clinical isolates have been found to possess genes for a type III secretion system (T3SS), acting as a key marker of pathogenicity (Krzymińska et al., 2009). More recently, the type VI secretion system (T6SS) has been identified as another critical virulence factor in *Enterobacter* (Soria-Bustos et al., 2020). The T6SS delivers a diverse array of toxic effectors to compete with other bacteria and also serves to adhere to epithelial cells, colonize intestinal cells, and form biofilms (Soria-Bustos et al., 2020). Genomic analyses show that *E. cloacae* subsp. *cloacae* along other *E. cloacae* strains, typically possess multiple

T6SS gene clusters and a wide range of effectors, including peptidoglycan-targeting amidases, DNases, and an anti-eukaryotic catalase (Anderson et al., 2023).

Immune evasion and host survival

As ECC can cause systemic infections, it must overcome host immune defenses.

- **Apoptosis induction:** Following invasion of host cells, ECC strains can trigger apoptosis, or programmed cell death (Krzymińska et al., 2010). This mechanism may serve as a strategy to create tissue damage, evade phagocytic cells, and facilitate bacterial spread within the host (Krzymińska et al., 2010).
- **Serum resistance and iron acquisition**: The majority of *E. cloacae* isolates (over 92%) are resistant to the bactericidal effects of human serum, a critical trait for surviving in the bloodstream (Keller et al., 1998). To acquire iron in the restrictive host environment, many strains produce the siderophore aerobactin. The genome of *E. cloacae* subsp. *cloacae* confirms this capability, containing two loci for iron-chelating compounds (Keller et al., 1998; Ren et al., 2010).
- **Antiphagocytic and anti-complement mechanisms**: In addition to directly killing macrophages via cytotoxins, ECC can evade the immune system through molecular mimicry. The O-antigen gene cluster has also been found in *E. cloacae* subsp. *cloacae* and encodes enzymes for the biosynthesis of pseudaminic acid, a sugar that may mimic host cell structures, thereby downregulating complement-mediated killing and gaining a survival advantage (Ren et al., 2010).

Antibiotic resistance

The clinical challenge posed by ECC also lies within its intrinsic and acquired resistance to a wide range of antibiotics.

- **Intrinsic and inducible resistance:** ECC possesses a chromosomally encoded *ampC* gene product, which provides intrinsic resistance to ampicillin, first-generation cephalosporins, and cefoxitin (Annavajhala et al., 2019; Mezzatesta et al., 2012). Under selective pressure from antibiotics like third-generation cephalosporins, mutations (e.g., in the *ampD* gene) can lead to the stable derepression and hyperproduction of this AmpC β-lactamase, conferring high-level resistance to most cephalosporins (Annavajhala et al., 2019; Davin-Regli & Pagès, 2015).
- **Acquired enzymatic resistance:** ECC readily acquires mobile genetic elements carrying additional resistance genes.

- **ESBLs:** The acquisition of plasmid-mediated families of β-lactamases, such as CTX-M (Cefotaximase, Munich), SHV (Sulfhydryl Variable), and TEM (Temoniera) types, renders ECC resistant to most penicillins and cephalosporins (Annavajhala et al., 2019).
- **Carbapenemases:** The emergence of carbapenem-resistant ECC (CREC) is a major global threat (Annavajhala et al., 2019). Resistance is primarily driven by the acquisition of genes encoding carbapenemases, including *Klebsiella pneumoniae* carbapenemase (bla_{KPC}), New Delhi metallo-β-lactamase (bla_{NDM}), oxacillinases ($bla_{OXA\text{-}48\text{-}like}$), and Verona integron-encoded metallo-β-lactamase (bla_{VIM}) (Annavajhala et al., 2019; Davin-Regli & Pagès, 2015; Merhi et al., 2023). These genes are typically located on highly mobile plasmids, facilitating their rapid spread (Merhi et al., 2023).

- **Membrane-mediated resistance:** Resistance is also achieved by controlling the intracellular concentration of antibiotics.
  - **Porin Loss:** Reduced expression or mutation of outer membrane ECC porins (homologs of OmpF and OmpC) decreases the influx of β-lactams, especially carbapenems. This mechanism often acts synergistically with AmpC or ESBL production to confer high-level resistance (Annavajhala et al., 2019; Davin-Regli & Pagès, 2015; Merhi et al., 2023).
  - **Efflux Pumps:** ECC utilizes multi-drug efflux pumps, such as the AcrAB-TolC system, to actively expel a wide range of antimicrobial agents, including fluoroquinolones and tetracyclines (Davin-Regli & Pagès, 2015). The expression of these pumps is tightly controlled by a network of transcriptional regulators, which can be activated by environmental stressors, including the antibiotics themselves (Davin-Regli & Pagès, 2015).

As a summary, ECC is highly heterogeneous. Its genetic diversity leads to wide variation in virulence and resistance traits, preventing the assignment of a single phenotype to the group. For example, only ~27% of strains carry a Type III Secretion System, and Type VI systems vary similarly. ESBL production is notably higher in *E. hormaechei* than in other clusters, and even traits like biofilm formation are inconsistently observed. As such, referring to all ECC members simply as "*E. cloacae*" could confound their distinct pathogenic and resistance profiles. The pathogenic potential of ECC is multifaceted. Its success as a nosocomial pathogen relies on a toolkit of virulence factors that enable it to colonize host surfaces, form resilient biofilms, acquire essential nutrients, and evade antibiotics or destroy host immune cells.

2. Aim and Hypothesis

The primary aim of this PhD thesis was to elucidate the biological function of the novel two-domain lectin EclA, which has been found in *E. cloacae* subsp. *cloacae* and subsp. *dissolvens*. Although these two subspecies are not the most predominant human pathogens within the highly heterogeneous ECC, they harbor EclA, and their investigation is crucial. First, infections involving these subspecies are still documented, and assessing the contribution of potential virulence factors like EclA remains important. Second, EclA contains a domain orthologous to LecA from *P. aeruginosa*, a well-characterized virulence factor, yet this domain in EclA remains unexplored. Finally, and more broadly, this work provides a fundamental characterization of a lectin whose domains are widespread across bacterial species, including more virulent clinical isolates (e.g., ECC and *Pseudomonas* species). By establishing a functional blueprint for EclA in these genetically tractable systems, this research aimed to generate insights into the general mechanisms of EclA function.

To achieve this, the investigation was designed to characterize EclA both as a standalone protein and within the contexts of *E. cloacae* subsp. *dissolvens* and *E. cloacae* subsp. *cloacae*, with three key objectives:

1. Determining the role of EclA in key virulence-associated phenotypes, particularly bacterial autoaggregation and biofilm formation.
2. Investigating the function of EclA as a potential adhesin mediating interactions with host cell structures, such as blood group antigens and epithelial cells.
3. Evaluating the contribution of EclA to bacterial virulence using in vivo infection models.

The conceptual framework of this thesis is rooted in the principle of protein homology. While orthologous proteins often share conserved functions due to structural similarity, they can also diverge throughout evolution to acquire novel or specialized roles. The *P. aeruginosa* lectin LecA is a well-characterized virulence factor central to biofilm formation and host adhesion. As a newly discovered orthologue of LecA, EclA from *E. cloacae* was predicted to have a similar functional role, while possessing two domains with binding profiles distinct from each other and from LecA, along with structural features that differ from LecA and present new grounds for scientific investigation.

Therefore, this research was founded on the central hypothesis that EclA could act as a critical multifunctional adhesin in *E. cloacae*.

Specifically, it was hypothesized that:

1. The multivalent structure of EclA may enable it to act as a scaffolding protein, cross-linking bacterial cells to drive autoaggregation and establish the structural foundation of biofilms, mirroring LecA's role in *P. aeruginosa*.
2. EclA may have an extracellular role where its fucose-binding C-terminal domain directly mediates the adherence of *E. cloacae* to fucosylated host glycan receptors, such as the Le^a antigen, thereby promoting host colonization.
3. The deletion of the *eclA* gene may lead to a measurable attenuation of virulence, demonstrated by impaired biofilm formation in vitro and reduced pathogenicity in in vivo infection models.

This hypothesis positions EclA as a contributor to the pathophysiology of ECC species that produce it, with potential roles in both bacterial community behavior and host-pathogen interaction. The experimental work described in this thesis was designed to test these proposed functions.

3. Elucidating the Role of EclA in *E. cloacae* subsp. *dissolvens*

Section 3 introduces and analyzes the role of EclA in *E. cloacae* subsp. *dissolvens*. It opens with a scientific manuscript in Chapter 3.1, that lays the foundation by providing a comprehensive molecular and functional characterization of EclA. Building on the findings, Chapter 3.2 presents additional experiments to further elucidate EclA's role in autoaggregate formation. These include high-resolution structural analysis using scanning electron microscopy (SEM), exogenous protein complementation, and aggregation assays under shear flow. Finally, Chapter 3.3 shifts the focus to in vivo models to assess the contribution of EclA to host-pathogen interactions by establishing assays involving both zebrafish and *Galleria mellonella* larvae.

3.1. Molecular and Functional Characterization of EclA from *E. cloacae* subsp. *dissolvens*

This chapter presents the foundational research on the novel lectin EclA from *E. cloacae* subsp. *dissolvens* in the form of a scientific manuscript. The study provides a comprehensive molecular and functional characterization of EclA, starting with the hypothesis that, based on its structural orthologue LecA from *P. aeruginosa*, it may contribute to virulence in ECC. The manuscript details the generation of a targeted *eclA* deletion mutant and uses this strain to investigate the lectin's role in key virulence-associated phenotypes, such as bacterial auto-aggregation. Furthermore, it assesses the biochemical properties of recombinant EclA, including its ability to mediate hemagglutination, and explores its expression and localization within the bacterium. The findings presented would establish the primary evidence for EclA's function and serve as the basis for the subsequent investigations detailed in the following chapters of this thesis.

Molecular and Functional Characterization of the Novel Lectin EclA from the *Enterobacter cloacae* complex

Mario Fares[1,2,3], Stefanie Wagner[1,2,3], Markus Bischoff[2,4], Alexander Titz[1,2,3].

[1] Helmholtz Institute for Pharmaceutical Research Saarland (HIPS), Helmholtz Centre for Infection Research, D-66123 Saarbrücken, Germany.

[2] Deutsches Zentrum für Infektionsforschung (DZIF), Standort Hannover-Braunschweig.

[3] Department of Chemistry, PharmaScienceHub (PSH), Saarland University, D-66123 Saarbrücken, Germany.

[4] Institute for Medical Microbiology and Hygiene, Saarland University, D-66421 Homburg, Germany

Figures in this chapter are numbered independently from those in the rest of the dissertation.
All references cited in this manuscript are listed at the end of this chapter.

Introduction

Lectins are ubiquitous non-enzymatic glycan-binding proteins involved in key biological processes (Taylor et al., 2022). In bacteria, they facilitate pathogenesis by binding host or microbial glycans, promoting adhesion, biofilm formation, cytotoxicity, and immune evasion (Fares et al., 2025). These roles are especially critical in chronic infections, where biofilms drive persistent disease (Bjarnsholt, 2013).

Bacterial lectins are promising targets for antivirulence therapies, especially using glycomimetics that block lectin-glycan interactions with high affinity (Leusmann et al., 2023). This approach is increasingly relevant in light of rising antimicrobial resistance, particularly in ESKAPE pathogens, which are major drivers of hospital-acquired infections and antibiotic failure, and comprise *Enterococcus faecium*, *Staphylococcus aureu*s, *Klebsiella pneumoniae*, *Acinetobacter baumannii*, *Pseudomonas aeruginosa* and *Enterobacter* spp. (Miller & Arias, 2024; Naghavi et al., 2024; WHO, 2024). Unlike traditional antibiotics, antivirulence strategies aim to disarm rather than kill pathogens, potentially reducing resistance development, especially when used in combination with antibiotics (Gadar & McCarthy, 2023; Ogawara, 2021).

Within this context, species of the *Enterobacter cloacae* complex (ECC) have emerged as clinically significant ESKAPE pathogens. They are associated with infections such as

bacteremia, pneumonia, and urinary tract infections, particularly in hospitalized or immunocompromised patients, and are frequently capable of producing extended-spectrum β-lactamases and carbapenemases (Davin-Regli & Pagès, 2015; Ramirez & Giron, 2025). In addition to this antibiotic resistance, ECC displays notable virulence factors that are instrumental in pathogenesis and disease progression. A key factor is its outer membrane lipopolysaccharide, which plays a critical role in triggering inflammatory cascades that can progress to septic shock (Augusto et al., 2021). In addition, biofilm development and adherence to epithelial tissues are aided by the activity of a type VI secretion system, enhancing its persistence within the host (Soria-Bustos et al., 2020). Some clinical isolates also utilize a type III secretion system to inject effector proteins into host cells, leading to the destruction of phagocytes and epithelial barriers (Krzymińska et al., 2009). Furthermore, once attached to epithelial surfaces, species of ECC can release several cytotoxic agents, including α-hemolysin, enterotoxins, and thiol-activated toxins structurally related to Shiga-like toxin II, contributing to tissue damage and disease severity (Barnes et al., 1997).

Recent work by Beshr et al. (2025) has identified and structurally characterized a previously unreported lectin from *E. cloacae* subsp. *cloacae* DSM 30054 (ATCC 13047), designated EclA (*E. cloacae* lectin A, ECL_04191, GenBank: ADF63724.1). EclA is a calcium-dependent superlectin consisting of a dimer of a two-domain polypeptide which assembles in a back-to-back configuration that presents the N-terminal and C-terminal domains on opposite sides of the protein complex. The C-terminal domain of EclA (EclA-C) displays specificity for fucosylated glycans, particularly the H-antigen type II of the ABO blood group system and Lewis A from the Lewis blood group system, suggesting that *E. cloacae* may preferentially interact with individuals expressing these glycan structures (Beshr et al., 2025). The N-terminal domain of EclA (EclA-N) was revealed to be an orthologue of the galactose-binding lectins PllA from *Photorhabdus luminescens*, and the extensively characterized LecA from *Pseudomonas aeruginosa* involved in key virulence processes such as biofilm formation, and host cell binding (Beshr et al., 2017; Bruneau et al., 2023; Chemani et al., 2009; Diggle et al., 2006). With EclA-N having an amino acid sequence identity of 36.5% and 31% to PllA and LecA, respectively, its crystal structure also showed a very high overall similarity to PllA/LecA (Beshr et al., 2025). However, despite this structural resemblance, galactose was surprisingly not bound to EclA-N, making its ligand elusive to date. Bioinformatics analyses revealed that homologues of the EclA-C or EclA-N domains can also be found individually across various species, primarily in *Enterobacter ludwigii* and *Pseudomonas* species. However, both domains

are found together exclusively in *E. cloacae*, particularly within *E. cloacae* subsp. *cloacae* and subsp. *dissolvens* (Beshr et al., 2025).

Given the structural parallels between LecA and EclA through the N-terminus domain, and despite the ligand of the EclA-N remaining unidentified, we hypothesized that EclA may similarly contribute to virulence in *E. cloacae* through mechanisms involving bacterial autoaggregation and host cell adhesion.

In this study, we set out to investigate the biological role of EclA in *E. cloacae* subsp. *dissolvens*. Specifically, we analyzed EclA's expression profile using Western blot analysis to determine whether the protein is released or retained in the cell-associated fraction. We evaluated EclA's ability to mediate hemagglutination of human red blood cells as a proxy for glycan recognition and host-binding activity, and tested the inhibitory effect of methyl α-L-fucoside on this process. Furthermore, we generated a targeted deletion mutant lacking the *eclA* gene and assessed its role in bacterial autoaggregation. Through this comprehensive functional analysis, we aimed to elucidate the role of EclA in *E. cloacae* pathophysiology and explore its relevance as a novel antivirulence target.

Materials and Methods

Bacterial strains and plasmids:

Experimental work on *E. cloacae* subsp. *dissolvens* used strain DSM 16657 (ATCC 23373), selected for its genetic tractability and high EclA sequence conservation with *E. cloacae* subsp. *cloacae* DSM 30054 (ATCC 13047), from which EclA was previously characterized by Beshr et al. (2025) (SI Figure 1). The strain was obtained from the German Collection of Microorganisms and Cell Cultures (DSMZ). All other strains and plasmids along with their applications and references are represented in Table 1.

Table 1: Plasmids and bacterial strains used in this study.

Plasmid/Strain	Resistance Marker	Application	Reference
Plasmids			
pMP7605	Gentamicin	mCherry red fluorescence labeling	Lagendijk et al., (2010)
pKNG101	Streptomycin	Suicide vector facilitating double recombination events	Kaniga et al., (1991)
pKNG101_16657	Streptomycin	Suicide vector for *eclA* knockout in *E. cloacae* subsp. *dissolvens* DSM 16657	This work
Strains	**Designation**	**Application**	**Reference**
E. coli BW19610	-	pKNG101 and pKNG101_16657 cloning	Metcalf et al., (1994)
E. coli DH5α	-	pMP7605 cloning	Stock collection
E. coli BL21 (DE3) pET22b-*eclA*	-	Recombinant expression of EclA from *E. cloacae* subsp. *cloacae* DSM 30054	Beshr et al., (2025)
E. coli BL21 (DE3) pET22b-*eclA-L*	-	Recombinant expression of EclA-M14A from *E. cloacae* subsp. *cloacae* DSM 30054	Beshr et al., (2025)
E. coli BL21 (DE3) pET22b-*eclA-C*	-	Recombinant expression of EclA C-terminus from *E. cloacae* subsp. *cloacae* DSM 30054	Beshr et al., (2025)
E. coli BL21 (DE3) pET25-*pa2L*	-	Recombinant expression of LecB from *P. aeruginosa* PAO1	Mitchell et al., (2005)
E. coli HB101 pRK600	-	Helper strain in triparental mating	Boyer & Rouland-Dussoix, (1969), Keen et al., (1988)
E. cloacae subsp. *dissolvens* DSM 16657	-	*E. cloacae* subsp. *dissolvens* chosen type strain	DSMZ
E. cloacae subsp. *dissolvens* DSM 16657 Δ*eclA*	-	*E. cloacae* subsp. *dissolvens* chosen type strain with deleted *eclA*	This work
E. cloacae subsp. *dissolvens* DSM 16657 pMP7605	$S1^{WT}$	mCherry-labeled model strain for EclA-related experiments	This work
E. cloacae subsp. *dissolvens* DSM 16657 Δ*eclA* pMP7605	$S1^{\Delta}$	mCherry-labeled model strain for EclA-related experiments with *eclA* deleted	This work

EclA, EclA-M14A, EclA-C, and LecB recombinant expression and purification:

All EclA recombinant protein sequences were derived from *E. cloacae* subsp. *cloacae* DSM 30054 (NCBI RefSeq assembly GCF_000025565.1). Protein expression and purification of EclA, EclA-M14A, and EclA-C were conducted as indicated by Beshr et al. (2025) with the amino acid sequences listed in SI Table 1. EclA (the native protein from *E. cloacae* subsp. *cloacae*), EclA-M14A (a modified version of EclA in which the second start codon is mutated to alanine [M14A], resulting in a single EclA isoform upon expression and purification), and EclA-C (the C-terminus domain of EclA) were each expressed in *E. coli* BL21(DE3) strains

harboring either pET22b-*eclA*, pET22b-*eclA-L*, or pET22b-*eclA-C*, respectively. Strains were streaked onto LB agar supplemented with 100 µg/mL ampicillin. One liter of LB supplemented with ampicillin (100 µg/mL) was inoculated with a preculture of either of the strains and grown at 37 °C and 180 rpm to an OD_{600} of 0.5 - 0.6. Expression was induced by addition of IPTG (250 µM), and bacteria were then further cultured for 4 h at 30 °C and 180 rpm. The cells were harvested by centrifugation (9000 × *g*, 10 min), and the pellet was washed with TBS/Ca buffer (20 mM Tris, 137 mM NaCl, 2.6 mM KCl, pH 7.4, supplemented with 100 µM $CaCl_2$). The cells were resuspended in 40 mL of TBS/Ca with PMSF (1 mM) and lysozyme (0.4 mg/mL) and subsequently disrupted using a microfluidizer (Microfluidics, model 110P). Cell debris was removed by centrifugation (19000 × *g*, 60 min), and the supernatant was loaded onto a column containing a fucose-coupled Sepharose CL- 6B resin. The affinity resin was prepared in analogy to a previously reported procedure (Fornstedt & Porath, 1975). The column was washed with TBS/Ca buffer. All proteins were eluted by addition of 100 mM L-fucose dissolved in TBS/Ca buffer. The eluted fractions were extensively dialyzed against TBS/Ca buffer. The concentrations of EclA/-M14A/-C were determined by UV absorbance at 280 nm using a calculated molar extinction coefficient of 50420, 50420 and 27960 $M^{-1}cm^{-1}$, respectively. For the recombinant expression and purification of LecB, the same procedure was followed using the plasmid pET25-*pa2L* coding for LecB from *P. aeruginosa* PAO1 (GenBank: AAG06749.1) as previously described (Mitchell et al., 2005). Elution was performed using TBS/Ca buffer containing 100 mM D-mannose. LecB was quantified using its extinction coefficient of 6990 M^{-1} cm^{-1}.

Anti-EclA-C rabbit antibody generation:

Recombinant EclA-C in phosphate-buffered saline (PBS) (137 mM NaCl, 2.7 mM KCl, 10 mM Na_2HPO_4, 1.8 mM KH_2PO_4) supplemented with 100 µM $CaCl_2$ (PBS/Ca) was used for the generation of anti-EclA-C rabbit antibodies, a process conducted by Squarix GmbH. The antibodies were affinity purified using a column with immobilized EclA-C.

Plasmid transformations:

- Heat-shock transformations:

To prepare chemically competent *E. coli* BW19610, an overnight LB culture was subcultured and grown at 37 °C with shaking (180 rpm) until it reached an OD_{600} of 0.4-0.6. Cells were then harvested by centrifugation, washed, and resuspended in 50 mM $CaCl_2$, followed by

incubation on ice for 1 hour. After a second centrifugation step (18,000 × *g*), the pellet was resuspended in 2.5 mL of ice-cold 50 mM $CaCl_2$ containing 15% glycerol.

Aliquots (100 µL) of the resulting competent cells, which express the Π protein (pir gene product), were mixed with 500 ng of either the pKNG101_16657 or pKNG101 plasmid. Transformation was carried out via heat shock at 42 °C for 45 seconds, followed by a 2-minute incubation on ice. Cells were then recovered in SOC medium at 37 °C for 1 hour with shaking at 300 rpm on a heated shaking plate. Clone selection was done by spreading aliquots of the heat-shocked cell suspension on LB agar supplemented with 100 µg/mL of streptomycin and growing the bacteria for 24 h at 37 °C.

- Triparental mating transformations:

To an overnight culture of recipient strains in LB, an equal volume of LB was added and the mixture was incubated at 42 °C with 180 rpm agitation. The donor and helper strains were subcultured at the same time at 37 °C with 180 rpm agitation until OD_{600} reaches 0.6. An equal volume of donor and helper strains and one-third of this volume of recipient strain were added into an Eppendorf tube and centrifuged (18000 × *g*). The pellet was resuspended in 50 µL LB and spotted on LB agar followed by overnight incubation at 30 °C. The bacterial lawn was later resuspended in LB and plated on the appropriate selective medium (Table 2) and incubated at 37 °C for 48 h.

Table 2: Tri-parental mating transformations

Recipient	**Plasmid**	**Donor**	**Helper**	**Selection medium**
WT *E. cloacae.* subsp. *dissolvens*	pKNG101_16657	*E. coli* BW19610 pKNG101_16657	*E. coli* HB101 pRK600	LB + ampicillin 200 µg/mL + streptomycin 100 µg/mL
WT *E. cloacae.* subsp. *dissolvens*	pMP7605	*E. coli* DH5α pMP7605	*E. coli* HB101 pRK600	LB + ampicillin 200 µg/mL + gentamicin 60 µg/mL
Δ*eclA E. cloacae.* subsp. *dissolvens*	pMP7605	*E. coli* DH5α pMP7605	*E. coli* HB101 pRK600	LB + ampicillin 200 µg/mL + gentamicin 60 µg/mL

Deletion of *eclA* by a 2-step allelic exchange:

The suicide plasmid pKNG101_16657 was constructed by GenScript via synthesis of the fused upstream and downstream flanking regions of *eclA* from *E. cloacae* subsp. *dissolvens* (Box 1, SI Box 1), which was cloned into the pKNG101 vector (Kaniga et al., 1991) using BamHI and XbaI restriction sites.

A two-step allelic exchange was carried out as previously described (Hmelo et al., 2015) with some modifications. To initiate the allelic exchange, an overnight culture of *E. cloacae* subsp. *dissolvens* carrying the suicide plasmid pKNG101_16657 was grown in LB medium supplemented with 100 µg/mL streptomycin at 37 °C with shaking at 180 rpm. The suicide plasmid integrates into the chromosome in cis by homologous recombination (first crossover), forming a merodiploid. To promote resolution of this intermediate and select for loss of the integrated plasmid (second crossover), cultures were subcultured four times over 48 hours in LB medium containing 16% (w/v) sucrose. Cells were then streaked onto LB agar without NaCl, and single colonies were replica-plated onto LB and LB supplemented with 100 µg/mL streptomycin to identify Δ*eclA* mutants by counterselection of plasmid-bearing cells. Colonies that grew only on LB agar were selected, indicating a successful second recombination event and loss of the suicide plasmid. To confirm the *eclA* deletion, colony PCR and whole-genome sequencing was performed, along with Western blot analysis for the detection of EclA with anti-EclA-C rabbit antibodies.

Box 1: Fused upstream and downstream flanking nucleotide sequences of *eclA* in *E. cloacae* subsp. *dissolvens*, flanked by XbaI and BamHI restriction sites. The red sequences represent the restriction sites, the blue sequence corresponds to the upstream region of *eclA*, while the green sequence represents its downstream region.

TCTAGATCCCCGTCCTGAAAAAGGTACATCTGCTGGCGACCTTTGTGTTTCCAGGTGATCCGCTTACGCGGCGCGAGCTTC
ACTTTCTCTGCGACTGGCTCAAGGATCGCCGTCAGACGTTCAATGGAATGTTCAGGGCGAACAGGAGGCAATATATGCAT
GACACCACCTTTTAGCGTTGGGTACTGGCCAGTATAGACCACCGAGGTCAATGCTCAGACCGGTATGAGGGAAGGAAGG
TATATCAGGGGGCACTGCATGGGTAAAAAGATAATTTGTTTATTTTTAAACTTGACCCGCGTAACAGGTGATAAGTGTGC
CAGATTTCCTGACGTACTTACATGAATATCAATGTAAACGATGGGGAGAATAAACTATTACAAACCTGACGTATTTATCT
CCTCCCTCCTTAAGATTATTCCTATTTCGGCAATAATTATTTTATTATTTTTAAGTGATTACAAAATCGCAACCCTTAATAA
AGCGTTTCGCGTTTTGAATTGTATATACCGCCTGACTATTCTCATTCCAGCCGATAACAACCGGGTAATGAATATGAGAAG
TGTGTGCTTCTCATGAGATCATTTATTCTGATTATCAGGCGGTTAGCTGAATTGAGTGATTAAAATCACGCATTTCGTCAG
GACTATCTTTCATCTACAGAATTGTCGGTCTGCTATCCTGCGAGAATGCTGGATGGCCGTTCGATCTTCAAAAAATTGTGT
AGCGCACATGTTCAACATATGCGCTACACCAACAGGCAATAAACACACACGGCATTACTCTTTGTTATGTTGTATATCCTC
TCAATATCGGCAGCGGTTTGAAACAAGACGCGTCTTGATTAACGCCATCCAGAAACACAGCACGCTTTCGGTTAGGGGTA
CCTGAGTGGAAGCAGCACACTCATTTCATGCCAAATAAACACCAGTGGGGTAATATCGGTTCTGAATACGCATTCAGGGC
TGCATATTCACGTAATTAAAAAGATCATGGTGCCTGAAAAAGCGCACCATGGAAGAGCCACAACCTGCAATTAGCAAAG
CACATCCCTTTTTAATTAAAAGGCAACGTAATTGTACTGCCGCTATATTGTTAAACGATACAAGACCTGTCTGGTTAATTC
AGGGGTAAGCGAGAAAGTTGGTACTGACTGATTATGCCGTACACAGGAAATGTGTGCATACAAGGCTTACGCGTTATGA
GAGGCTCTCCAGCAATGGCTCAAGACAGGCTGGCTTTCAGCAAAACCACCCTCTATCGACGAAAGACCTTCTGACCCTTC
GTATTGATACTTGAGGATTCGGGGATCC

Colony PCR reactions:

Colony PCR reactions were performed to validate the *eclA* deletion in *E. cloacae* subsp. *dissolvens*. For each 50 µL reaction, 0.5 µL of Phusion® High-Fidelity DNA Polymerase (NEB, Cat. No. M0530S) was used, along with its HF Phusion® buffer at a final concentration of 1X. Primers were used at a concentration of 5 µM (Table 3), and dNTPs at 0.2 mM. As templates, a single colony was resuspended in 50 µL of H_2O and heated to 95 °C for 5 minutes. Five microliters of the lysate was used as the template in the PCR reaction. PCR cycle temperatures and times were set according to the Phusion® High-Fidelity DNA Polymerase protocol by NEB, while annealing temperatures were determined using the NEB Tm calculator.

Table 3: Primers used for the amplification of *eclA* along with flanking regions up to 150 nucleotides in *E. cloacae* subsp. *dissolvens*.

Experimental validation	Reverse primer (5'-3')	Forward primer (5'-3')
eclA knockout in *E. cloacae* subsp. *dissolvens*	MF05: GCCGATATTGAGAGGATA (128 base pairs downstream *eclA*)	MF06: CGCCTGACTATTCTCATT (146 base pairs upstream *eclA*)

Whole genome sequencing:

A single bacterial colony from either $S1^{WT}$ or $S1^{\Delta}$ was inoculated into LB medium supplemented with 60 µg/mL of gentamicin, and incubated at 37 °C with agitation at 180 rpm until mid-log phase. Bacterial cultures were adjusted to an OD_{600} of 10, the culture was pelleted by centrifugation, washed with sterile PBS, and resuspended in 0.5 mL of inactivation buffer provided by MicrobesNG, which in turn performed long-read nucleotide whole genome sequencing (WGS) using Oxford Nanopore Technology (ONT). Nucleotide reads were analyzed using Geneious Alignment (Global alignment with Needleman-Wunsch algorithm) in Geneious Prime software (version 2025.1.2)

Growth curves:

$S1^{WT}$ and $S1^{\Delta}$ were cultured in 50 mL of a minimal M63 medium composed of 15.6 g/L M63 salts (USBiological Life Sciences, #M1015) dissolved in milli-Q water, with the pH adjusted to 7.0 using 1M KOH. Complete M63 medium was prepared by supplementing M63 medium to final concentrations of 0.4% (w/v) glucose, 0.2% (w/v) casamino acids (MP Biomedicals, CAS: 91079-40-2), and 60 µg/mL gentamicin. Overnight cultures in LB supplemented with 60

μg/ml gentamicin were diluted into the supplemented M63 medium to an initial OD_{600} of 0.02. TBS/Ca was then added at 10% (v/v) of the final volume. The resulting supplemented M63 medium (including 60 μg/mL gentamicin) was referred to as $M63^{+}$. Cultures were incubated at 37 °C in non-baffled 250 mL Erlenmeyer flasks with agitation at 180 rpm and humidity at 72% for 24 hours. OD_{600} was measured hourly for the first 12 hours, followed by a final measurement at 24 hours.

Western Blot analysis for the detection of EclA:

For bacterial pellet preparation, 1 mL of a 24 h culture in $M63^{+}$, grown at 37 °C with shaking at 180 RPM, was centrifuged at 18000 × *g*; the resulting pellet was washed with PBS and resuspended in 100 μL of 1× SDS Laemmli buffer per OD_{600} = 1.

For supernatant sample preparation, 1 mL of the same culture was centrifuged, and its supernatant was collected. Proteins were precipitated by adding 110 μL of 100% (w/v) trichloroacetic acid (TCA) to the supernatant, followed by incubation on ice for 1 h. The samples were then centrifuged at 18000 × *g* for 15 min, and the supernatant was discarded. The pellet was washed with 1 mL of cold acetone (−20 °C), then air-dried. The dried pellet was resuspended in 10 μL of 1× SDS Laemmli buffer per OD_{600} = 1 and boiled at 95 °C for 5 min. Five microliters of a prestained protein ladder (Abcam, #ab116028) was used as the molecular weight marker. Protein samples were separated by SDS-PAGE on a 16% gel at 120 V, using 4.5 μL of the pellet sample and 12 μL of TCA-precipitated supernatant proteins unless stated otherwise. Proteins were transferred onto a PVDF membrane by semi-dry electroblotting at 25 V for 30 minutes**.** The membrane was blocked for 45 min in PBS containing 0.2% Tween-20 (PBS-T) and 3% bovine serum albumin (BSA). Primary antibody incubation was performed for 1 h using rabbit anti-EclA-C antibodies (2.79 ng/mL in PBS-T with 3% BSA) under gentle rocking. The membrane was washed three times with PBS-T, then incubated for 1 hour with HRP-conjugated goat anti-rabbit IgG (1:5,000 in PBS-T; Dianova, #111-035-144). Following three additional washes with PBS-T, the blot was analyzed using an enhanced chemiluminescence (ECL) substrate (1:1 mixture of solutions A and B; Solution A: 100 mM Tris-HCl pH 8.5, 0.4 mM coumaric acid, 2.5 mM luminol; Solution B: 100 mM Tris-HCl pH 8.5, 6.3 mM H_2O_2). Imaging was performed using a chemiluminescence-compatible FUSION FX7 gel documentation system and its FusionCapt Advance software (version 17.0.1.0) where exposure was set to 2 min, and high sensitivity was selected.

EclA membrane displacement assay:

$S1^{WT}$ was grown overnight in LB broth supplemented with 60 µg/mL gentamicin. 1 mL aliquots from the overnight culture were pelleted and resuspended in: (1) PBS/Ca, (2) 100 mM methyl α-L-fucoside in PBS/Ca, and (3) 100 mM methyl α-D-mannoside in PBS/Ca. After incubation at 30 °C for 20 minutes with shaking at 500 rpm, the samples were centrifuged, and the resulting supernatants were collected and subjected to TCA precipitation. Both the supernatants and corresponding pellets were analyzed by SDS-PAGE (12% gel) and Western blotting as described above, with sample volumes of 5 µL of the pellet fraction and 12.5 µL of the TCA-precipitated supernatant fraction loaded per lane. Chemiluminescence image exposure was set to 5 min.

Hemagglutination assay:

Hemagglutination assays were done as previously described (Hauck et al., 2013) with some modifications. Briefly, type O^+ human red blood cells (RBCs) (Innovative Research, Inc., #IWB3ALS40ML) from a single donor were centrifuged and washed three times with phosphate-buffered saline (PBS) at a 1:3 dilution (800 × *g*, 15 min, 4 °C). The washed RBCs were resuspended to 10% (v/v) in PBS and treated with 1% (w/v) papain and 0.1% (w/v) L-cysteine for 30 minutes at 37 °C and 50 rpm. Following enzymatic treatment, the RBCs were centrifuged and washed three times in PBS (800 × *g*, 10 min, 4 °C), then resuspended in PBS/Ca to a final concentration of 16.6% (v/v).

For hemagglutination assays, a 64.7 µM stock solution of recombinant EclA was 2-fold serially diluted in PBS/Ca across a 96-well V-bottom plate (Boettger #05-021-0100) to a final volume of 85 µL per well. Treated RBCs were added (15 µL per well), resulting in a final RBC concentration of 2.5% (v/v) in a total volume of 100 µL. Plates were incubated at 37 °C for 30 minutes and centrifuged briefly (1 min, 1000 × *g*) to visualize hemagglutination patterns.

For inhibition assays, stock solutions of methyl α-L-fucoside, and methyl α-D-mannoside, were prepared in PBS/Ca at concentrations of 1.325 M, 883 mM, 440 mM, and 88 mM. To each well, 6 µL of the appropriate inhibitor stock was mixed with 85 µL of 50 µM EclA, yielding inhibitor concentrations of 75 mM, 50 mM, 25 mM, and 5 mM, and an EclA concentration of 40 µM. After pre-incubation of the 96-well V-bottom plate at rt for 15 minutes with rocking, 15 µL of 16.6% enzyme-treated RBCs was added to each well (final RBC concentration: 2.3%). Plates were incubated at 37 °C for 30 minutes and centrifuged for 1 minute at 1000 × *g* before visual assessment of hemagglutination.

Bacterial autoaggregation assay:

An overnight culture of $S1^{WT}$ was grown in LB medium supplemented with 60 µg/mL gentamicin at 37 °C with shaking at 180 rpm. Cells were then inoculated into $M63^{+}$ medium to a final OD_{600} of 0.02. Aliquots of 1.25 mL were transferred into 24-well fluorocarbon film-bottom imaging plates (Zell-Kontakt, #3231-20), sealed with breathable foil (Greiner Bio-One, #676051), and incubated at 37 °C with 72% humidity and shaking at 180 rpm for 48-72 hours. At 48 h, whole-well fluorescence images were captured to monitor autoaggregate formation. Cultures were then resuspended to disperse autoaggregates, and OD_{600} along with fluorescence (excitation: [584] nm; emission: [620-10] nm) were measured using a FLUOstar Omega plate reader.

Fluorescence imaging and analysis:

Microscopic fluorescence images were acquired using an inverted fluorescence microscope (Leica DMi8) equipped with a 5x/0.15 DRY objective, a TXR filter cube (excitation: 540-580 nm, dichroic: 585 nm, emission: 592-668 nm), and a monochrome camera (Leica DFC7000 GT). Image acquisition was performed using Leica Application Suite X (version 3.7.4.23463), capturing the entire plate through a series of images at a single focal plane using uniform acquisition parameters. Images of each well were then merged using smooth blending mode via the LasX navigator to generate full-well views. Merged images were finally exported as TIFF files with lossless compression. Brightness and contrast of replicates b and c in the 48-h autoaggreation assay (Figure 1-A) were adjusted in Fiji by setting the maximum display value to 130 to match replicate a. For the 72-h autoaggregation assay (SI Figure 5), brightness and contrast at 48 h for replicates b and c were adjusted in Fiji by setting the maximum display value to 130 to match replicate a, and was set to 170 for all replicates at 72 h to compensate for the decrease of mCherry fluorescence.

Results:

Investigating the role of *eclA* in growth and autoaggregate formation of $S1^{WT}$

To investigate the role of EclA in bacterial growth and autoaggregation, an *eclA* deletion mutant in *E. cloacae* subsp. *dissolvens* was constructed using allelic exchange mutagenesis. The deletion was designed to precisely excise the *eclA* coding region without disrupting adjacent sequences. Following recombination, colonies were screened by PCR using primers

flanking the *eclA* locus. Agarose gel electrophoresis of the PCR products revealed a band shift in the Δ*eclA* mutant relative to the WT strain, consistent with the expected size reduction due to deletion of the *eclA* gene, indicating successful mutagenesis at the target site (SI Figure 2). To further validate the deletion, WGS was performed on both WT and Δ*eclA* strains following transformation with the mCherry-expressing plasmid pMP7605, which allows for constitutive red fluorescence labeling (Lagendijk et al., 2010). For clarity, the WT *E. cloacae* subsp. *dissolvens* harboring pMP7605 will be referred to as $S1^{WT}$, and the Δ*eclA* mutant carrying the same plasmid will be designated as $S1^{\Delta}$. Sequence alignment confirmed the precise and complete removal of the *eclA* gene in the mutant strain, with no additional mutations detected in adjacent regions (SI Figure 3).

Loss of EclA protein expression in $S1^{\Delta}$ was verified by Western blot using affinity purified anti-EclA-C antibodies. A distinct band corresponding to EclA was detected in the $S1^{WT}$ lysate but was absent in $S1^{\Delta}$, confirming the deletion at the protein level (Figure 2). These results collectively verify the successful construction of the Δ*eclA* strain, enabling further investigation of EclA's function in the physiology of *E. cloacae* subsp. *dissolvens*.

To determine whether the deletion of *eclA* affects bacterial physiology, growth kinetics of $S1^{WT}$ and $S1^{\Delta}$ were compared in $M63^{+}$ medium. Both strains exhibited comparable growth over a 24-hour period, with no significant difference in growth rates (SI Figure 4). These findings indicate that EclA does not impact the general growth capacity of *E. cloacae* subsp. *dissolvens* under the tested conditions.

To assess autoaggregate formation, both $S1^{WT}$ and $S1^{\Delta}$ were cultured for 48 h in the same medium using imaging plates with fluorocarbon film bottoms, under shaking conditions. $S1^{WT}$ formed robust, free-floating, and extensive autoaggregates, while $S1^{\Delta}$ exhibited a severely impaired aggregation phenotype (Figure 1-A). This stark contrast was maintained even after extended incubation for 72 hours (SI Figure 5).

To confirm that the observed autoaggregation defect in $S1^{\Delta}$ was not due to differences in cell density or fluorescence expression, cultures were resuspended and analyzed for OD_{600} and mCherry fluorescence intensity. No significant differences were observed between $S1^{WT}$ and $S1^{\Delta}$ in either metric (Figure 1-B), indicating that the reduced autoaggregate formation in $S1^{\Delta}$ is not attributable to growth defects or differences in mCherry expression, but rather reflects a specific role of *eclA* in autoaggregate development.

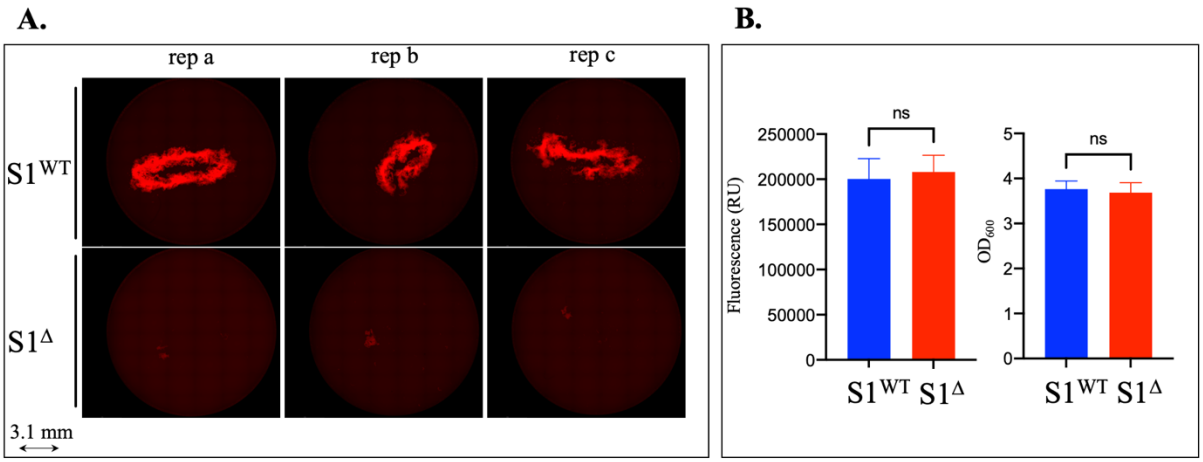

Figure 1: Autoaggregate formation assay of S1^{WT} and S1$^{\Delta}$. (A) Autoaggregate formation by S1^{WT} and S1$^{\Delta}$ was assessed 48 h after incubation under agitation at 180 rpm, 37 °C and 72% humidity. Fluorescence microscopy images show one representative well from three independent biological replicates (rep a, b, and c). **(B)** Quantification of fluorescence intensity and OD_{600} of wells from (A) using a plate reader after dispersing the bacterial autoaggregates. Statistical analysis using a two-tailed *t*-test (95% confidence interval, $P < 0.05$, N = 3) with Welch's correction for unequal variances indicated no significant (NS) difference in either fluorescence or cell density. S1^{WT}: WT *E. cloacae* subsp. *dissolvens* pMP7605. S1$^{\Delta}$: Δ*eclA E. cloacae* subsp. *dissolvens* pMP7605.

Molecular characterization of EclA in S1^{WT}

To evaluate the expression and localization of EclA, Western blot analysis were performed using rabbit-generated and affinity-purified anti-EclA-C antibodies. In 24-hour cultures of planktonic S1^{WT} grown in bacterial autoaggregation medium, EclA was detected in both the bacterial pellet and the culture supernatant, suggesting that the protein is released and is also present in the cytosol and/or associated with the cell membrane (Figure 2). Despite loading a ~26-fold higher equivalent of culture supernatant, the EclA band appeared weaker than in the pellet, indicating limited release of EclA under these conditions. To rule out cell lysis as the source of EclA in the 24-hour supernatant, a separate culture harvested during exponential phase was also analyzed and similarly showed the presence of EclA in the supernatant (SI Figure 6).

To assess whether EclA is membrane-associated via its fucose-binding domain and can be displaced from the bacterial surface, pellets from overnight cultures were incubated with methyl α-L-fucoside. Membrane association of EclA would be supported by its retention in

control pellets and specific release into the supernatant only upon treatment with methyl α-L-fucoside. However, this treatment failed to release EclA into the supernatant, as assessed by Western blot analysis (SI Figure 7). This result suggests that EclA is not surface-exposed to allow fucose-mediated displacement, or that the EclA-C terminal domain may not be involved in outer membrane binding.

The calculated molecular weights of recombinant EclA, EclA-M14A, and native EclA in *E. cloacae* subsp. *dissolvens* are nearly identical, with a high sequence similarity of 95% (SI Figure 1). Interestingly, however, the apparent molecular weight of native EclA in *E. cloacae* subsp. *dissolvens* was observed to be lower than that of the recombinant EclA-M14A (Figure 2). The specificity of the detected native EclA band is further supported by its complete absence in $S1^{\Delta}$. EclA-M14A is a modified version of EclA from *E. cloacae* subsp. *cloacae*, in which the second start codon is mutated to alanine [M14A], resulting in a single EclA isoform upon recombinant expression (SI Figure 8). Notably, WT recombinant EclA (non-M14A) produced two distinct bands, with the shorter band aligning in size with native EclA, while the longer band corresponded to the full-length protein initiated at the first start codon (SI Figure 9). This suggests that the native EclA corresponds to the shorter isoform generated by translation initiation at the second start codon, bypassing the first methionine residue.

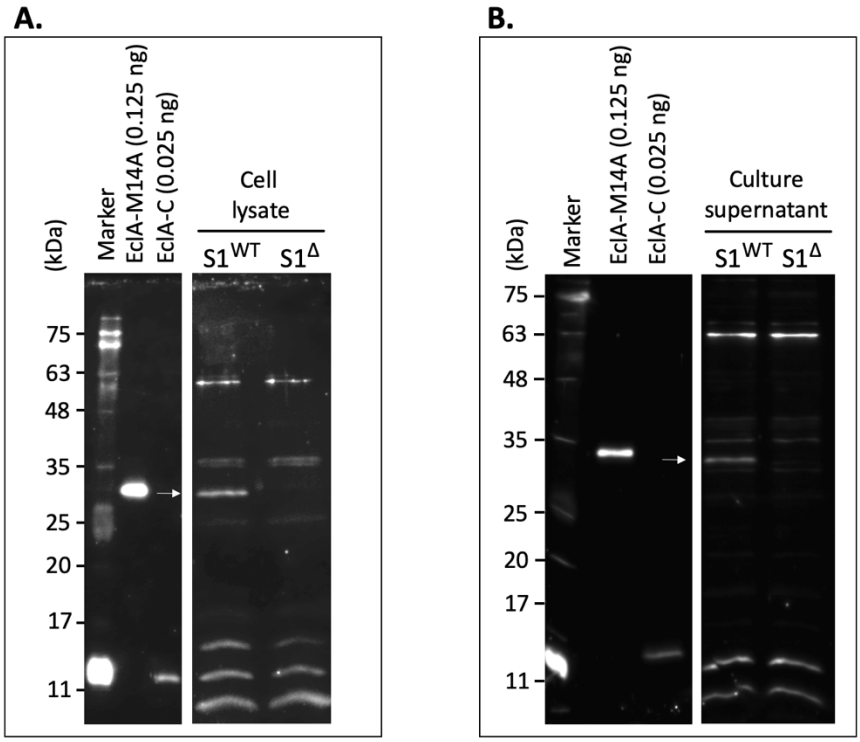

Figure 2: Western blot detection of EclA in $S1^{WT}$ using anti-EclA-C rabbit antibodies. EclA-M14A is a recombinant variant of EclA from *E. cloacae* subsp. *cloacae* with a mutation

in the second start codon, substituting methionine with alanine. EclA-C corresponds to the C-terminal domain of EclA. **(A)** Detection of EclA in the cell pellet lysate from a 24-hour culture of $S1^{WT}$ grown in $M63^{+}$ medium. **(B)** Detection of EclA from the supernatant of the same culture after TCA protein precipitation. The white arrow points at the EclA band from $S1^{WT}$ in (A) and (B). $S1^{WT}$: WT *E. cloacae* subsp. *dissolvens* pMP7605. $S1^{\Delta}$: Δ*eclA E. cloacae* subsp. *dissolvens* pMP7605.

Assessment of EclA Hemagglutination Activity and Inhibition by Fucose:

Hemagglutination assays are commonly used to assess the ability of lectins to bind and cross-link red blood cells via specific carbohydrate interactions; such interactions can often be disrupted by introducing a ligand with higher affinity, which competes for lectin binding. Recombinant EclA, derived from *E. cloacae* subsp. *cloacae* (DSM 30054), exhibited dose-dependent hemagglutination of human type O^{+} red blood cells. First signs of hemagglutination were observed at 14 µM, and full hemagglutination was seen at 55 µM (Figure 3-A). This finding suggests that EclA might interact with host cells by binding to the respective surface exposed antigens, and might mediate cross-linking of cells through its multivalent binding capacity. A positive control using recombinant lectin LecB from *P. aeruginosa* and the same batch of RBCs was included to benchmark hemagglutination efficacy. LecB induced partial hemagglutination at concentrations as low as 0.8 nM, reaching complete agglutination at 13 nM (SI Figure 10-C), indicating that LecB is a more potent hemagglutinin than EclA.

To explore the potential for EclA inhibition and assess the feasibility of developing higher-affinity glycomimetics to block its function, 40 µM EclA was preincubated with increasing concentrations of methyl α-L-fucoside. Inhibition of hemagglutination became evident at concentrations starting from 25 mM, indicating that fucose interferes with EclA-mediated red blood cell binding. In contrast, methyl α-D-mannoside failed to inhibit hemagglutination at all tested concentrations, supporting the specificity of the fucose-EclA interaction (Figure 3-B).

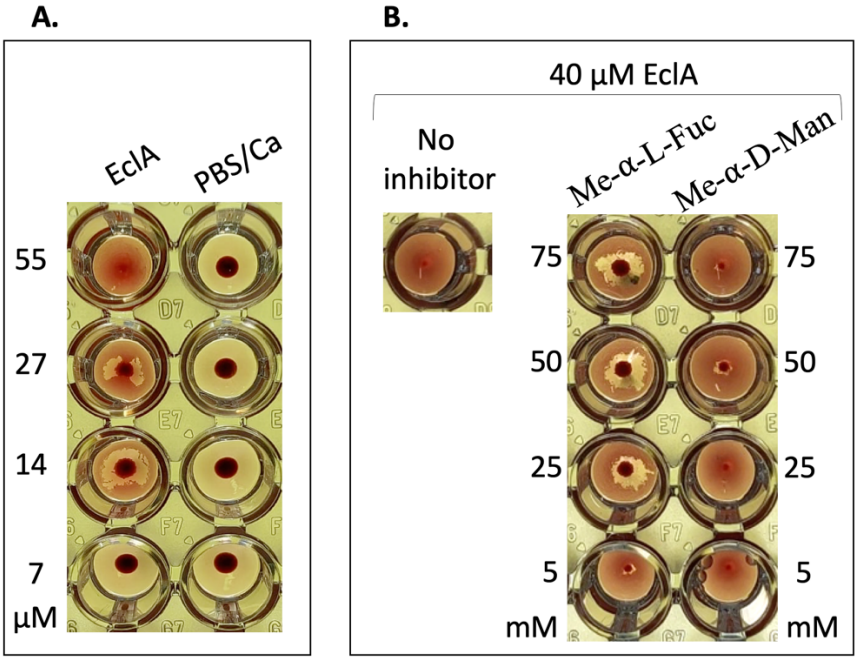

Figure 3: EclA-induced hemagglutination of human type O^+ red blood cells and its inhibition by methyl α-L-fucoside. (A) Titration of recombinant EclA from *E. cloacae* subsp. *cloacae* (DSM 30054) with human red blood cells, demonstrating dose-dependent hemagglutination. PBS/Ca and RBCs served as negative control. The image shown is a representation of one biological replicate; additional replicates are presented in SI Figure 10-A. **(B)** Inhibition of RBC hemagglutination by 40 µM recombinant EclA preincubated with different concentrations of methyl α-L-fucoside (Me-α-L-Fuc) and methyl α-D-mannoside (Me-α-D-Man). Carbohydrate concentrations refer to the amounts present during preincubation with EclA, prior to the addition of red blood cells. The assay represents one of two independent biological replicates; the second shown in SI Figure 10-B.

Discussion:

Biofilms are complex, adaptive biological structures that enable bacterial survival even in unfavorable environments (Sauer et al., 2022). These structures can adopt either surface-associated or free-floating configurations. Autoaggregation is a critical initial step in biofilm formation. A defining feature of biofilms is the production of an extracellular polymeric substance (EPS) matrix**,** which facilitates surface adhesion, environmental resistance, and structural cohesion (Di Martino, 2018; Lewis et al., 2022).

It is well established that ECC, including *E. cloacae* subsp. *dissolvens* produce EPS matrices with some being enriched in fucose (Ejaz et al., 2021; Meade et al., 1993; Nishikawa et al., 1979; Wang et al., 2013). Given the large, stable free-floating autoaggregates observed in our

experiments, even under constant mechanical stress, we conclude that these structures represent biofilms (Figure 1-A, SI Figure 5).

Indeed, *E. cloacae* subsp. *dissolvens* DSM 16657, used in this study, encodes the gene required for fucose biosynthesis, coding for GDP-L-fucose synthase (RefSeq XJE56995.1), as well as a dedicated gene cluster whose protein products are responsible for the synthesis and secretion of colanic acid (CA), a fucose-containing exopolysaccharide (SI Table 2). CA is a polyanionic heteropolysaccharide composed of repeating units of D-glucose, L-fucose, D-galactose, and D-glucuronic acid, often modified with O-acetyl and pyruvate side chains. It plays a structural role in the biofilm matrix by embedding and stabilizing its various components (Meredith et al., 2007).

Given CA's fucose-rich composition, polyanionic nature, and extracellular localization, alongside the likely presence of other fucosylated polymers synthesized by ECC, it is possible that EclA, with its positively charged N-terminal domain and fucophilic C-terminal domain, acts to crosslink colanic acid and related fucosylated polymers. This interaction could enhance matrix cohesion and contribute significantly to biofilm formation.

To investigate whether native fucosylated biopolymers such as CA serve as ligands for EclA, characterizing the EPS components of *E. cloacae* subsp. *dissolvens* could offer valuable insights into EclA's binding specificity, particularly in glycan adhesion arrays where the immobilized glycans are derived from the identified EPS constituents.

The detection of EclA in the supernatant fraction of the bacterial culture medium via Western blot supports its extracellular role in mediating cellular autoaggregation (Figure 2). Although its extracellular presence was less pronounced compared to its presence in the cell lysate, this phenomenon aligns with observations made with other lectins, such as its orthologues LecA and LecB from *P. aeruginosa,* and the lectin BambL from *Burkholderia ambifaria,* which is produced when the bacterium is grown as a biofilm but is indefinitely retained in the cytosol (Frensch et al., 2021; Glick & Garber, 1983). While the secretion mechanisms of these lectins also remain unclear, their extracellular functions, particularly in bacterial surface and host interactions, are well-documented (da Silva et al., 2019; Sych et al., 2023). Interestingly, bacterial surface-associated lectins, like the mannophilic BC2L-B and BC2L-C from *Burkholderia cenocepacia*, and the fucophilic LecB from *P. aeruginosa* could be displaced from their bacterial outer membrane into the supernatant upon treatment with their respective carbohydrate ligands (Šulák et al., 2011; Tielker et al., 2005). In contrast, EclA remained unaffected under similar conditions (SI Figure 7). This suggests that a stronger ligand than the weak binder methyl α-L-fucoside may be required for displacement, or that the fucose-binding

C-terminus of EclA does not mediate membrane attachment or is conformationally unavailable. This implies that the N-terminus could be involved in bacterial surface interaction instead.

Further investigation, such as cell fractionation studies, could help clarify whether EclA is membrane-associated or freely diffusible, particularly since, like its orthologue LecA, no signal peptide sequences or transmembrane regions were identified in its amino acid sequence based on sequence analysis software predictions. A notable observation was that native EclA from $S1^{WT}$ exhibited a lower apparent molecular weight than the recombinantly expressed EclA-M14A (Figure 2), even though both proteins have nearly identical predicted molecular weights (SI Figure 1). This discrepancy may indicate that transcription in the native context initiates from the second start codon, which was disrupted in the gene coding for EclA-M14A. Under physiological conditions, this alternative initiation may be regulated by ribosome binding site accessibility, codon context, or other translational control mechanisms. While post-translational modifications could theoretically contribute to the observed size differences, the correlation between the M14A mutation and the loss of the shorter isoform, matching the size of EclA from $S1^{WT}$, strongly implicates translation initiation as the primary factor underlying the molecular weight disparity (SI Figure 8). Purifying and characterizing the native EclA protein would further support this hypothesis and would also give new insights, which may not only explain the size difference but also potentially influence the protein's functional activity in hemagglutination, where recombinant EclA was used. Additionally, native protein analysis could provide more information on ligand interactions, particularly at the N-terminal domain, since ligand screening in previous studies were conducted using the recombinant EclA protein (Beshr et al., 2025).

To explore whether EclA undergoes cleavage into functionally distinct N- and C-terminal domains, possible cleavage products by Western blot analysis were analyzed. This hypothesis was prompted by the observation that individual EclA domains, either N-terminal or C-terminal, are found independently encoded in various *Enterobacter* species, suggesting a potential for functional modularity or post-translational cleavage (Beshr et al., 2025). However, no bands corresponding to isolated EclA-C domain was detected using the anti-EclA-C antibodies, suggesting that EclA remains intact under the conditions tested (Figure 2).

EclA demonstrated hemagglutination activity against type O^+ red blood cells, supporting its role as a lectin and its specificity toward fucosylated epitopes such as the H antigen type II (Figure 3-A). Additionally, the inhibition of hemagglutination by methyl α-L-fucoside indicates that the fucose-binding C-terminal domain of EclA mediates this activity, while the

inability of methyl α-D-mannoside to inhibit agglutination reinforces EclA's specificity for fucosylated ligands (Figure 3-B). However, both the hemagglutination and its inhibition by methyl α-L-fucoside were relatively weak. Partial hemagglutination was only observed at 14 µM, and full agglutination required concentrations as high as 55 µM. Similarly, inhibition required high concentrations of methyl α-L-fucoside (≥25 mM), and even then, inhibition was incomplete, suggesting that methyl α-L-fucoside binds with low affinity but could serve as a foundational scaffold for the design of more potent inhibitors. These observations are consistent with previously reported binding affinities, which show an IC_{50} of 1.4 mM for methyl α-L-fucoside binding to EclA, compared to an IC_{50} of 0.2-0.8 µM for the same ligand binding to LecB (Beshr et al., 2025; Sommer et al., 2016).

Another factor contributing to the weak activity of EclA is likely the number, specificities, and spatial orientation of its carbohydrate-binding domains. EclA contains two fucose-binding domains pointing to one side of the protein, whereas LecB possesses four fucose/mannose-binding domains arranged in a tetrameric structure. This configuration enables high-avidity interactions with both fucosylated and mannosylated epitopes on red blood cells, supporting hemagglutination at low nanomolar concentrations (SI Figure 10-C)(Sommer et al., 2014).

In addition, as EclA used in this assay was recombinant, it may lack structural features that enhance binding in the native context. Its altered apparent molecular weight and potentially modified folding may reduce the accessibility or orientation of the binding domains, further diminishing its functional multivalency.

Overall, these findings suggest that while EclA could play a role in host-pathogen interaction by adhesion and cross-linking cells, its low valency and modest binding affinity in hemagglutination may reflect a biological role in mediating more transient, rather than strong cell-cell adhesion. In addition, as the absence of EclA did not impact the general growth capacity of $S1^{WT}$ under the tested conditions, its role could support such processes rather than core bacterial fitness (SI Figure 4). As an example, Lewis A antigens are highly expressed especially in neonates, raising important questions about EclA's involvement in infections, particularly in neonatal intensive care unit settings, where *Enterobacter* species have been implicated in outbreaks (Arcilla & Sturgeon, 1971; Girlich et al., 2021). The affinity of EclA for Lewis A suggests that ECC strains expressing *eclA* may preferentially target individuals with this antigen. Future studies should investigate whether EclA mediates adherence to fucosylated host targets, including Lewis A, and whether this interaction can be disrupted. Identifying high-affinity glycomimetics that target both the C- and N-terminal domains of EclA, alongside elucidating the function and ligands of the latter, could open new avenues for

understanding and preventing *E. cloacae*-mediated infections. Such a dual-targeting strategy, aimed at simultaneously blocking both domains, may provide a more effective means of suppressing EclA activity and disrupting its role in host interaction and biofilm formation.

References

Adegbola, R. A., & Old, D. C. (1983). Fimbrial Haemagglutinins in Enterobacter Species. *Microbiology*, *129*(7), 2175-2180. https://doi.org/10.1099/00221287-129-7-2175

Ahmed, T., Lundgren, A., Arifuzzaman, M., Qadri, F., Teneberg, S., & Svennerholm, A.-M. (2009). Children with the Le(a+b−) Blood Group Have Increased Susceptibility to Diarrhea Caused by Enterotoxigenic *Escherichia coli* Expressing Colonization Factor I Group Fimbriae. *Infection and Immunity*, *77*(5), 2059-2064. https://doi.org/10.1128/IAI.01571-08

Akbari, M., Bakhshi, B., & Najar Peerayeh, S. (2016). Particular Distribution of Enterobacter cloacae Strains Isolated from Urinary Tract Infection within Clonal Complexes. *Iranian Biomedical Journal*, *20*(1), 49-55. https://doi.org/10.7508/ibj.2016.01.007

Anantharaman, V., Iyer, L. M., & Aravind, L. (2012). Ter-dependent stress response systems: novel pathways related to metal sensing, production of a nucleoside-like metabolite, and DNA-processing. *Molecular BioSystems*, *8*(12), 3142. https://doi.org/10.1039/c2mb25239b

Anderson, A. J. G., Morrell, B., Lopez Campos, G., & Valvano, M. A. (2023). Distribution and diversity of type VI secretion system clusters in Enterobacter bugandensis and Enterobacter cloacae. *Microbial Genomics*, *9*(12). https://doi.org/10.1099/mgen.0.001148

Annavajhala, M. K., Gomez-Simmonds, A., & Uhlemann, A.-C. (2019). Multidrug-Resistant Enterobacter cloacae Complex Emerging as a Global, Diversifying Threat. *Frontiers in Microbiology*, *10*. https://doi.org/10.3389/fmicb.2019.00044

Arcilla, M. B., & Sturgeon, P. (1971). Perinatal expression of the Lewis and secretor blood group systems. *Pediatric Research*, *5*(8), 422-423. https://doi.org/10.1203/00006450-197108000-00215

Augusto, L. A., Bourgeois-Nicolaos, N., Breton, A., Barreault, S., Alonso, E. H., Gera, S., Faraut-Derouin, V., Semaan, N., De Luca, D., Chaby, R., Doucet-Populaire, F., & Tissières, P. (2021). Presence of 2-hydroxymyristate on endotoxins is associated with death in neonates with *Enterobacter cloacae* complex septic shock. *IScience*, *24*(8), 102916. https://doi.org/10.1016/j.isci.2021.102916

Barnes, A. I., Ortiz, C., Paraje, M. G., Balanzino, L. E., & Albesa, I. (1997). Purification and characterization of a cytotoxin from *Enterobacter cloacae*. *Canadian Journal of Microbiology*, *43*(8), 729-733. https://doi.org/10.1139/m97-105

Beshr, G., Sikandar, A., Gläser, J., Fares, M., Sommer, R., Wagner, S., Köhnke, J., & Titz, A. (2025). A fucose-binding superlectin from *Enterobacter cloacae* with high Lewis and ABO blood group antigen specificity. *Journal of Biological Chemistry*, *301*(2), 108151. https://doi.org/10.1016/j.jbc.2024.108151

Beshr, G., Sikandar, A., Jemiller, E.-M., Klymiuk, N., Hauck, D., Wagner, S., Wolf, E., Koehnke, J., & Titz, A. (2017). Photorhabdus luminescens lectin A (PllA): A new probe for detecting α-galactoside-terminating glycoconjugates. *Journal of Biological Chemistry*, *292*(48), 19935-19951. https://doi.org/10.1074/jbc.M117.812792

Bhar, S., Edelmann, M. J., & Jones, M. K. (2021). Characterization and proteomic analysis of outer membrane vesicles from a commensal microbe, Enterobacter cloacae. *Journal of Proteomics*, *231*, 103994. https://doi.org/10.1016/j.jprot.2020.103994

Bjarnsholt, T. (2013). The role of bacterial biofilms in chronic infections. *APMIS*, *121*(s136), 1-58. https://doi.org/10.1111/apm.12099

Boman, H. G., & Hultmark, D. (1987). Cell-Free Immunity in Insects. *Annual Review of Microbiology*, *41*(1), 103-126. https://doi.org/10.1146/annurev.mi.41.100187.000535

Boyer, H. W., & Roulland-dussoix, D. (1969). A complementation analysis of the restriction and modification of DNA in Escherichia coli. *Journal of Molecular Biology*, *41*(3), 459-472. https://doi.org/10.1016/0022-2836(69)90288-5

Brenner, D. J., McWhorter, A. C., Kai, A., Steigerwalt, A. G., & Farmer, J. J. (1986). Enterobacter asburiae sp. nov., a new species found in clinical specimens, and reassignment of Erwinia dissolvens and Erwinia nimipressuralis to the genus Enterobacter as Enterobacter dissolvens comb. nov. and Enterobacter nimipressuralis comb. nov. *Journal of Clinical Microbiology*, *23*(6), 1114-1120. https://doi.org/10.1128/jcm.23.6.1114-1120.1986

Bruneau, A., Gillon, E., Furiga, A., Brachet, E., Alami, M., Roques, C., Varrot, A., Imberty, A., & Messaoudi, S. (2023). Discovery of potent 1,1-diarylthiogalactoside glycomimetic inhibitors of *Pseudomonas aeruginosa* LecA with antibiofilm properties. *European Journal of Medicinal Chemistry*, *247*, 115025. https://doi.org/10.1016/j.ejmech.2022.115025

Chang, C.-Y., Huang, P.-H., & Lu, P.-L. (2022). The Resistance Mechanisms and Clinical Impact of Resistance to the Third Generation Cephalosporins in Species of Enterobacter cloacae Complex in Taiwan. *Antibiotics*, *11*(9), 1153. https://doi.org/10.3390/antibiotics11091153

Chemani, C., Imberty, A., de Bentzmann, S., Pierre, M., Wimmerová, M., Guery, B. P., & Faure, K. (2009). Role of LecA and LecB Lectins in *Pseudomonas aeruginosa* -Induced Lung Injury and Effect of Carbohydrate Ligands. *Infection and Immunity*, *77*(5), 2065-2075. https://doi.org/10.1128/IAI.01204-08

da Silva, D. P., Matwichuk, M. L., Townsend, D. O., Reichhardt, C., Lamba, D., Wozniak, D. J., & Parsek, M. R. (2019). The Pseudomonas aeruginosa lectin LecB binds to the exopolysaccharide Psl and stabilizes the biofilm matrix. *Nature Communications*, *10*(1), 2183. https://doi.org/10.1038/s41467-019-10201-4

Davin-Regli, A., Lavigne, J.-P., & Pagès, J.-M. (2019). *Enterobacter* spp.: Update on Taxonomy, Clinical Aspects, and Emerging Antimicrobial Resistance. *Clinical Microbiology Reviews*, *32*(4). https://doi.org/10.1128/CMR.00002-19

Davin-Regli, A., & Pagès, J.-M. (2015). *Enterobacter aerogenes* and *Enterobacter cloacae*; versatile bacterial pathogens confronting antibiotic treatment. *Frontiers in Microbiology*, *6*. https://doi.org/10.3389/fmicb.2015.00392

de Oliveira, I. A., & Corvelo, T. C. de O. (2021). ABH and Lewis blood group systems and their relation to diagnosis and risk of Helicobacter pylori infection. *Microbial Pathogenesis*, *152*, 104653. https://doi.org/10.1016/j.micpath.2020.104653

Debroy, R., & Ramaiah, S. (2023). Translational protein RpsE as an alternative target for novel nucleoside analogues to treat MDR Enterobacter cloacae ATCC 13047: network analysis and molecular dynamics study. *World Journal of Microbiology and Biotechnology*, *39*(7), 187. https://doi.org/10.1007/s11274-023-03634-z

Di Martino, P. (2018). Extracellular polymeric substances, a key element in understanding biofilm phenotype. *AIMS Microbiology*, *4*(2), 274-288. https://doi.org/10.3934/microbiol.2018.2.274

Díaz-Pascual, F., Ortíz-Severín, J., Varas, M. A., Allende, M. L., & Chávez, F. P. (2017). In vivo Host-Pathogen Interaction as Revealed by Global Proteomic Profiling of Zebrafish Larvae. *Frontiers in Cellular and Infection Microbiology*, *7*. https://doi.org/10.3389/fcimb.2017.00334

Diggle, S. P., Stacey, R. E., Dodd, C., Cámara, M., Williams, P., & Winzer, K. (2006). The galactophilic lectin, LecA, contributes to biofilm development in *Pseudomonas aeruginosa*. *Environmental Microbiology*, *8*(6), 1095-1104. https://doi.org/10.1111/j.1462-2920.2006.001001.x

Ejaz, M., Zhao, B., Wang, X., Bashir, S., Haider, F. U., Aslam, Z., Khan, M. I., Shabaan, M., Naveed, M., & Mustafa, A. (2021). Isolation and Characterization of Oil-Degrading Enterobacter sp. from Naturally Hydrocarbon-Contaminated Soils and Their Potential Use against the Bioremediation of Crude Oil. *Applied Sciences*, *11*(8), 3504. https://doi.org/10.3390/app11083504

Fares, M., Imberty, A., & Titz, A. (2025). Bacterial lectins: multifunctional tools in pathogenesis and possible drug targets. *Trends in Microbiology*. https://doi.org/10.1016/j.tim.2025.03.007

Farfour, E., Dortet, L., Guillard, T., Chatelain, N., Poisson, A., Mizrahi, A., Fournier, D., Bonnin, R. A., Degand, N., Morand, P., Janvier, F., Fihman, V., Corvec, S., Broutin, L., Le Brun, C., Yin, N., Héry-Arnaud, G., Grillon, A., Bille, E., … Vasse, M. (2022). Antimicrobial Resistance in Enterobacterales Recovered from Urinary Tract Infections in France. *Pathogens*, *11*(3), 356. https://doi.org/10.3390/pathogens11030356

Farsiani, H., Salimiyan Rizi, K., & Ghazvini, K. (2019). Published by: Mashhad University of Medical Sciences Salimiyan Rizi K, Ghazvini K, Farsiani H. Clinical and pathogenesis overview of Enterobacter infections. In *Clinical Medicine Rev Clin Med* (Vol. 6, Issue 4). http://rcm.mums.ac.ir

Ferry, A., Plaisant, F., Ginevra, C., Dumont, Y., Grando, J., Claris, O., Vandenesch, F., & Butin, M. (2020). Enterobacter cloacae colonisation and infection in a neonatal intensive care unit: retrospective investigation of preventive measures implemented after a multiclonal outbreak. *BMC Infectious Diseases*, *20*(1), 682. https://doi.org/10.1186/s12879-020-05406-8

Flores, E., Dutta, S., Bosserman, R., van Hoof, A., & Krachler, A.-M. (2023). Colonization of larval zebrafish (*Danio rerio*) with adherent-invasive *Escherichia coli* prevents recovery of the intestinal mucosa from drug-induced enterocolitis. *MSphere*, *8*(6). https://doi.org/10.1128/msphere.00512-23

Fornstedt, N., & Porath, J. (1975). Characterization studies on a new lectin found in seeds of Vicia ervilia. *FEBS Letters*, *57*(2), 187-191. https://doi.org/10.1016/0014-5793(75)80713-7

Frensch, M., Jäger, C., Müller, P. F., Tadić, A., Wilhelm, I., Wehrum, S., Diedrich, B., Fischer, B., Meléndez, A. V., Dengjel, J., Eibel, H., & Römer, W. (2021). Bacterial lectin BambL acts as a B cell superantigen. *Cellular and Molecular Life Sciences*, *78*(24), 8165-8186. https://doi.org/10.1007/s00018-021-04009-z

Frutos-Grilo, E., Kreling, V., Hensel, A., & Campoy, S. (2023). Host-pathogen interaction: Enterobacter cloacae exerts different adhesion and invasion capacities against different host cell types. *PLOS ONE*, *18*(10), e0289334. https://doi.org/10.1371/journal.pone.0289334

Gadar, K., & McCarthy, R. R. (2023). Using next generation antimicrobials to target the mechanisms of infection. *Npj Antimicrobials and Resistance*, *1*(1), 11. https://doi.org/10.1038/s44259-023-00011-6

Gan, Y., Zhao, G., Wang, Z., Zhang, X., Wu, M. X., & Lu, M. (2023). Bacterial Membrane Vesicles: Physiological Roles, Infection Immunology, and Applications. *Advanced Science*, *10*(25). https://doi.org/10.1002/advs.202301357

Ganbold, M., Seo, J., Wi, Y. M., Kwon, K. T., & Ko, K. S. (2023). Species identification, antibiotic resistance, and virulence in Enterobacter cloacae complex clinical isolates from South Korea. *Frontiers in Microbiology*, *14*. https://doi.org/10.3389/fmicb.2023.1122691

Garinet, S., Fihman, V., Jacquier, H., Corvec, S., Le Monnier, A., Guillard, T., Cattoir, V., Zahar, J.-R., Woerther, P.-L., Carbonnelle, E., Wargnier, A., Kernéis, S., & Morand, P. C. (2018). Elective distribution of resistance to beta-lactams among Enterobacter cloacae genetic clusters. *Journal of Infection*, *77*(3), 178-182. https://doi.org/10.1016/j.jinf.2018.05.005

Gasteiger, E., Hoogland, C., Gattiker, A., Duvaud, S., Wilkins, M. R., Appel, R. D., & Bairoch, A. (2005). Protein Identification and Analysis Tools on the Expasy Server. In J. M. Walker (Ed.), *The Proteomics Protocols Handbook* (1st ed., pp. 571-607). Humana Press. https://doi.org/10.1385/1592598900

Girlich, D., Ouzani, S., Emeraud, C., Gauthier, L., Bonnin, R. A., Le Sache, N., Mokhtari, M., Langlois, I., Begasse, C., Arangia, N., Fournier, S., Fortineau, N., Naas, T., & Dortet, L. (2021). Uncovering the novel Enterobacter cloacae complex species responsible for septic shock deaths in newborns: a cohort study. *The Lancet Microbe*, *2*(10), e536-e544. https://doi.org/10.1016/S2666-5247(21)00098-7

Glick, J., & Garber, N. (1983). The Intracellular Localization of Pseudomonas aeruginosa Lectins. *Microbiology*, *129*(10), 3085-3090. https://doi.org/10.1099/00221287-129-10-3085

Grimont, F., & Grimont, P. A. D. (2006). The Genus Enterobacter. In M. Dworkin, S. Falkow, E. Rosenberg, K. Schleifer, & E. Stackebrandt (Eds.), *The Prokaryotes* (pp. 197-214). Springer New York. https://doi.org/10.1007/0-387-30746-X_9

Guerrero-Mandujano, A., Hernández-Cortez, C., Ibarra, J. A., & Castro-Escarpulli, G. (2017). The outer membrane vesicles: Secretion system type zero. *Traffic*, *18*(7), 425-432. https://doi.org/10.1111/tra.12488

Hauck, D., Joachim, I., Frommeyer, B., Varrot, A., Philipp, B., Möller, H. M., Imberty, A., Exner, T. E., & Titz, A. (2013). Discovery of Two Classes of Potent Glycomimetic Inhibitors of *Pseudomonas aeruginosa* LecB with Distinct Binding Modes. *ACS Chemical Biology*, *8*(8), 1775-1784. https://doi.org/10.1021/cb400371r

Hennigs, J. K., Baumann, H. J., Schmiedel, S., Tennstedt, P., Sobottka, I., Bokemeyer, C., Kluge, S., & Klose, H. (2011). Characterization of Enterobacter cloacae Pneumonia: A Single-Center Retrospective Analysis. *Lung*, *189*(6), 475-483. https://doi.org/10.1007/s00408-011-9323-2

Hernandez-Alonso, E., Bourgeois-Nicolaos, N., Lepainteur, M., Derouin, V., Barreault, S., Waalkes, A., Augusto, L. A., Gera, S., Gleizes, O., Tissieres, P., Salipante, S. J., de Luca, D., & Doucet-Populaire, F. (2022). Contaminated Incubators: Source of a Multispecies Enterobacter Outbreak of Neonatal Sepsis. *Microbiology Spectrum*, *10*(4). https://doi.org/10.1128/spectrum.00964-22

Hmelo, L. R., Borlee, B. R., Almblad, H., Love, M. E., Randall, T. E., Tseng, B. S., Lin, C., Irie, Y., Storek, K. M., Yang, J. J., Siehnel, R. J., Howell, P. L., Singh, P. K., Tolker-Nielsen, T., Parsek, M. R., Schweizer, H. P., & Harrison, J. J. (2015). Precision-engineering the Pseudomonas aeruginosa genome with two-step allelic exchange. *Nature Protocols*, *10*(11), 1820-1841. https://doi.org/10.1038/nprot.2015.115

Hoffmann, H., & Roggenkamp, A. (2003). Population Genetics of the Nomenspecies *Enterobacter cloacae*. *Applied and Environmental Microbiology*, *69*(9), 5306-5318. https://doi.org/10.1128/AEM.69.9.5306-5318.2003

Hoffmann, H., Stindl, S., Ludwig, W., Stumpf, A., Mehlen, A., Heesemann, J., Monget, D., Schleifer, K. H., & Roggenkamp, A. (2005). Reassignment of Enterobacter dissolvens to Enterobacter cloacae as E. cloacae subspecies dissolvens comb. nov. and emended description of Enterobacter asburiae and Enterobacter kobei. *Systematic and Applied Microbiology*, *28*(3), 196-205. https://doi.org/10.1016/j.syapm.2004.12.010

Howe, K., Clark, M. D., Torroja, C. F., Torrance, J., Berthelot, C., Muffato, M., Collins, J. E., Humphray, S., McLaren, K., Matthews, L., McLaren, S., Sealy, I., Caccamo, M., Churcher, C., Scott, C., Barrett, J. C., Koch, R., Rauch, G.-J., White, S., … Stemple, D. L. (2013). The zebrafish reference genome sequence and its relationship to the human genome. *Nature*, *496*(7446), 498-503. https://doi.org/10.1038/nature12111

Kaniga, K., Delor, I., & Cornelis, G. R. (1991). A wide-host-range suicide vector for improving reverse genetics in Gram-negative bacteria: inactivation of the blaA gene of Yersinia enterocolitica. *Gene*, *109*(1), 137-141. https://doi.org/10.1016/0378-1119(91)90599-7

Keen, N. T., Tamaki, S., Kobayashi, D., & Trollinger, D. (1988). Improved broad-host-range plasmids for DNA cloning in Gram-negative bacteria. *Gene*, *70*(1), 191-197. https://doi.org/10.1016/0378-1119(88)90117-5

Keller, R., Pedroso, M. Z., Ritchmann, R., & Silva, R. M. (1998). Occurrence of Virulence-Associated Properties in *Enterobacter cloacae*. *Infection and Immunity*, *66*(2), 645-649. https://doi.org/10.1128/IAI.66.2.645-649.1998

Kim, S.-M., Lee, H.-W., Choi, Y.-W., Kim, S.-H., Lee, J.-C., Lee, Y.-C., Seol, S.-Y., Cho, D.-T., & Kim, J. (2012). Involvement of curli fimbriae in the biofilm formation of Enterobacter cloacae. *The Journal of Microbiology*, *50*(1), 175-178. https://doi.org/10.1007/s12275-012-2044-2

Kimmel, C. B., Ballard, W. W., Kimmel, S. R., Ullmann, B., & Schilling, T. F. (1995). Stages of embryonic development of the zebrafish. *Developmental Dynamics*, *203*(3), 253-310. https://doi.org/10.1002/aja.1002030302

Kremer, A., & Hoffmann, H. (2012). Prevalences of the Enterobacter cloacae complex and its phylogenetic derivatives in the nosocomial environment. *European Journal of Clinical Microbiology & Infectious Diseases*, *31*(11), 2951-2955. https://doi.org/10.1007/s10096-012-1646-2

Krzymińska, S., Koczura, R., Mokracka, J., Puton, T., & Kaznowski, A. (2010). Isolates of the Enterobacter cloacae complex induce apoptosis of human intestinal epithelial cells. *Microbial Pathogenesis*, *49*(3), 83-89. https://doi.org/10.1016/j.micpath.2010.04.003

Krzymińska, S., Mokracka, J., Koczura, R., & Kaznowski, A. (2009). Cytotoxic activity of *Enterobacter cloacae* human isolates. *FEMS Immunology & Medical Microbiology*, *56*(3), 248-252. https://doi.org/10.1111/j.1574-695X.2009.00572.x

Lagendijk, E. L., Validov, S., Lamers, G. E. M., De Weert, S., & Bloemberg, G. V. (2010). Genetic tools for tagging Gram-negative bacteria with mCherry for visualization in vitro and in natural habitats, biofilm and pathogenicity studies. *FEMS Microbiology Letters*, *305*(1), 81-90. https://doi.org/10.1111/j.1574-6968.2010.01916.x

Leslie, J. L., Weddle, E., Yum, L. K., Lin, Y., Jenior, M. L., Lee, B., Ma, J. Z., Kirkpatrick, B. D., Nayak, U., Platts-Mills, J. A., Agaisse, H. F., Haque, R., & Petri, W. A. (2021). Lewis Blood-group Antigens Are Associated With Altered Susceptibility to Shigellosis. *Clinical Infectious Diseases : An Official Publication of the Infectious Diseases Society of America*, *72*(11), e868-e871. https://doi.org/10.1093/cid/ciaa1409

Leusmann, S., Ménová, P., Shanin, E., Titz, A., & Rademacher, C. (2023). Glycomimetics for the inhibition and modulation of lectins. *Chemical Society Reviews*, *52*(11), 3663-3740. https://doi.org/10.1039/D2CS00954D

Lewis, A. L., Szymanski, C. M., Schnaar, R. L., & Aebi, M. (2022). Bacterial and Viral Infections. In Varki A, Cummings RD, & Esko JD (Eds.), *Essentials of Glycobiology* (4th edn) (pp. 555-568). Cold Spring Harbor Laboratory Press.

Lindh, E., & Ursing, J. (1991). Genomic groups and biochemical profiles of clinical isolates of *Enterobacter cloacae*. *APMIS*, *99*(1-6), 507-514. https://doi.org/10.1111/j.1699-0463.1991.tb05183.x

Liu, H. Y., Prentice, E. L., & Webber, M. A. (2024). Mechanisms of antimicrobial resistance in biofilms. *Npj Antimicrobials and Resistance*, *2*(1), 27. https://doi.org/10.1038/s44259-024-00046-3

Liu, S., Chen, L., Wang, L., Zhou, B., Ye, D., Zheng, X., Lin, Y., Zeng, W., Zhou, T., & Ye, J. (2022). Cluster Differences in Antibiotic Resistance, Biofilm Formation, Mobility, and Virulence of Clinical Enterobacter cloacae Complex. *Frontiers in Microbiology*, *13*. https://doi.org/10.3389/fmicb.2022.814831

Lopez-Baez, J. C., Simpson, D. J., LLeras Forero, L., Zeng, Z., Brunsdon, H., Salzano, A., Brombin, A., Wyatt, C., Rybski, W., Huitema, L. F. A., Dale, R. M., Kawakami, K., Englert, C., Chandra, T., Schulte-Merker, S., Hastie, N. D., & Patton, E. E. (2018). Wilms Tumor 1b defines a wound-specific sheath cell subpopulation associated with notochord repair. *ELife*, *7*. https://doi.org/10.7554/eLife.30657

Maheswari, U., Palvai, S., Anuradha, P., & Kammili, N. (2013). Hemagglutination and biofilm formation as virulence markers of uropathogenic Escherichia coli in acute urinary tract infections and urolithiasis. *Indian Journal of Urology*, *29*(4), 277. https://doi.org/10.4103/0970-1591.120093

Marsh, E. K., & May, R. C. (2012). Caenorhabditis elegans, a Model Organism for Investigating Immunity. *Applied and Environmental Microbiology*, *78*(7), 2075-2081. https://doi.org/10.1128/AEM.07486-11

Meade, M. J., Nakas, J. P., & Tanenbaum, S. W. (1993). Highly viscous polysaccharide produced by an Enterobacter isolate on a hemicellulose hydrolysate. *Biotechnology Letters*, *15*(4), 389-392. https://doi.org/10.1007/BF00128282

Ménard, G., Rouillon, A., Cattoir, V., & Donnio, P.-Y. (2021). Galleria mellonella as a Suitable Model of Bacterial Infection: Past, Present and Future. *Frontiers in Cellular and Infection Microbiology*, *11*. https://doi.org/10.3389/fcimb.2021.782733

Meredith, T. C., Mamat, U., Kaczynski, Z., Lindner, B., Holst, O., & Woodard, R. W. (2007). Modification of Lipopolysaccharide with Colanic Acid (M-antigen) Repeats in Escherichia coli. *Journal of Biological Chemistry*, *282*(11), 7790-7798. https://doi.org/10.1074/jbc.M611034200

Merhi, G., Amayri, S., Bitar, I., Araj, G. F., & Tokajian, S. (2023). Whole Genome-Based Characterization of Multidrug Resistant Enterobacter and Klebsiella aerogenes Isolates from Lebanon. *Microbiology Spectrum*, *11*(1). https://doi.org/10.1128/spectrum.02917-22

Mezzatesta, M. L., Gona, F., & Stefani, S. (2012). *Enterobacter cloacae* Complex: Clinical Impact and Emerging Antibiotic Resistance. *Future Microbiology*, *7*(7), 887-902. https://doi.org/10.2217/fmb.12.61

Mikkelsen, H., McMullan, R., & Filloux, A. (2011). The Pseudomonas aeruginosa Reference Strain PA14 Displays Increased Virulence Due to a Mutation in ladS. *PLoS ONE*, *6*(12), e29113. https://doi.org/10.1371/journal.pone.0029113

Miller, W. R., & Arias, C. A. (2024). ESKAPE pathogens: antimicrobial resistance, epidemiology, clinical impact and therapeutics. *Nature Reviews Microbiology*, *22*(10), 598-616. https://doi.org/10.1038/s41579-024-01054-w

Mitchell, E. P., Sabin, C., Šnajdrová, L., Pokorná, M., Perret, S., Gautier, C., Hofr, C., Gilboa-Garber, N., Koča, J., Wimmerová, M., & Imberty, A. (2005). High affinity fucose binding of *Pseudomonas aeruginosa* lectin PA-IIL: 1.0 Å resolution crystal structure of the complex combined with thermodynamics and computational chemistry approaches. *Proteins: Structure, Function, and Bioinformatics*, *58*(3), 735-746. https://doi.org/10.1002/prot.20330

Moore, W. E. C., Stackebrandt, E., Kandler, O., Colwell, R. R., Krichevsky, M. I., Truper, H. G., Murray, R. G. E., Wayne, L. G., Grimont, P. A. D., Brenner, D. J., Starr, M. P., & Moore, L. H. (1987). Report of the Ad Hoc Committee on Reconciliation of Approaches to Bacterial Systematics. *International Journal of Systematic and Evolutionary Microbiology*, *37*(4), 463-464. https://doi.org/10.1099/00207713-37-4-463

Morand, P. C., Billoet, A., Rottman, M., Sivadon-Tardy, V., Eyrolle, L., Jeanne, L., Tazi, A., Anract, P., Courpied, J.-P., Poyart, C., & Dumaine, V. (2009). Specific Distribution within the *Enterobacter cloacae* Complex of Strains Isolated from Infected Orthopedic Implants. *Journal of Clinical Microbiology*, *47*(8), 2489-2495. https://doi.org/10.1128/JCM.00290-09

Mustafa, A., Ibrahim, M., Rasheed, M. A., Kanwal, S., Hussain, A., Sami, A., Ahmed, R., & Bo, Z. (2020). Genome-wide Analysis of Four Enterobacter cloacae complex type strains: Insights into Virulence and Niche Adaptation. *Scientific Reports*, *10*(1), 8150. https://doi.org/10.1038/s41598-020-65001-4

Naghavi, M., Vollset, S. E., Ikuta, K. S., Swetschinski, L. R., Gray, A. P., Wool, E. E., Robles Aguilar, G., Mestrovic, T., Smith, G., Han, C., Hsu, R. L., Chalek, J., Araki, D. T., Chung, E., Raggi, C., Gershberg Hayoon, A., Davis Weaver, N., Lindstedt, P. A., Smith, A. E., … Murray, C. J. L. (2024). Global burden of bacterial antimicrobial resistance 1990-2021: a systematic analysis with forecasts to 2050. *The Lancet*. https://doi.org/10.1016/S0140-6736(24)01867-1

Neu, T. R., Swerhone, G. D. W., & Lawrence, J. R. (2001). Assessment of lectin-binding analysis for in situ detection of glycoconjugates in biofilm systems. *Microbiology*, *147*(2), 299-313. https://doi.org/10.1099/00221287-147-2-299

Nishikawa, K., Oi, S., & Yamamoto, T. (1979). Induced Production of Acidic Polysaccharide by Benzalkonium Chloride in a Bacterium and Some Properties of the Acidic Polysaccharide Produced. *Agricultural and Biological Chemistry*, *43*(11), 2305-2310. https://doi.org/10.1080/00021369.1979.10863803

Nogaret, P., El Garah, F., & Blanc-Potard, A.-B. (2021). A Novel Infection Protocol in Zebrafish Embryo to Assess Pseudomonas aeruginosa Virulence and Validate Efficacy of a Quorum Sensing Inhibitor In Vivo. *Pathogens*, *10*(4), 401. https://doi.org/10.3390/pathogens10040401

Ogawara, H. (2021). Possible drugs for the treatment of bacterial infections in the future: anti-virulence drugs. *The Journal of Antibiotics*, *74*(1), 24-41. https://doi.org/10.1038/s41429-020-0344-z

Ostadfar, A. (2016). Fluid Mechanics and Biofluids Principles. In *Biofluid Mechanics* (pp. 1-60). Elsevier. https://doi.org/10.1016/B978-0-12-802408-9.00001-6

Ponnusamy, D., & Clinkenbeard, K. D. (2015). Role of Tellurite Resistance Operon in Filamentous Growth of Yersinia pestis in Macrophages. *PLOS ONE*, *10*(11), e0141984. https://doi.org/10.1371/journal.pone.0141984

Pont, S., & Blanc-Potard, A.-B. (2021). Zebrafish Embryo Infection Model to Investigate Pseudomonas aeruginosa Interaction With Innate Immunity and Validate New

Therapeutics. *Frontiers in Cellular and Infection Microbiology*, *11*. https://doi.org/10.3389/fcimb.2021.745851

Poplimont, H., Georgantzoglou, A., Boulch, M., Walker, H. A., Coombs, C., Papaleonidopoulou, F., & Sarris, M. (2020). Neutrophil Swarming in Damaged Tissue Is Orchestrated by Connexins and Cooperative Calcium Alarm Signals. *Current Biology*, *30*(14), 2761-2776.e7. https://doi.org/10.1016/j.cub.2020.05.030

Rahal, A., Andreo, A., Le Gallou, F., Bourigault, C., Bouchand, C., Ferriot, C., Corvec, S., Guillouzouic, A., Gras-Leguen, C., Launay, E., Flamant, C., & Lepelletier, D. (2021). Enterobacter cloacae complex outbreak in a neonatal intensive care unit: multifaceted investigations and preventive measures are needed. *Journal of Hospital Infection*, *116*, 87-90. https://doi.org/10.1016/j.jhin.2021.07.012

Ramesh, A., Sharma, S. K., Sharma, M. P., Yadav, N., & Joshi, O. P. (2014). Plant Growth-Promoting Traits in Enterobacter cloacae subsp. dissolvens MDSR9 Isolated from Soybean Rhizosphere and its Impact on Growth and Nutrition of Soybean and Wheat Upon Inoculation. *Agricultural Research*, *3*(1), 53-66. https://doi.org/10.1007/s40003-014-0100-3

Ramirez, D., & Giron, M. (2025). Enterobacter Infections. In *StatPearls*. StatPearls Publishing. https://www.ncbi.nlm.nih.gov/books/NBK559296/

Rayner, C. R., Ioannides-Demos, L. L., Brien, J.-A. E., Liolios, L. L., & Spicer, W. J. (1998). Initial Concentration-Time Profile of Gentamicin Determines Efficacy against *Enterobacter cloacae* ATCC 13047. *Antimicrobial Agents and Chemotherapy*, *42*(6), 1370-1374. https://doi.org/10.1128/AAC.42.6.1370

Ren, Y., Ren, Y., Zhou, Z., Guo, X., Li, Y., Feng, L., & Wang, L. (2010). Complete Genome Sequence of *Enterobacter cloacae* subsp. *cloacae* Type Strain ATCC 13047. *Journal of Bacteriology*, *192*(9), 2463-2464. https://doi.org/10.1128/JB.00067-10

Rosen H.R. (1922). The bacterial pathogen of corn stalk rot. *Phytopathology*, *12*, 497-499.

Roy, P., Horswill, A. R., & Fey, P. D. (2021). Glycan-Dependent Corneocyte Adherence of Staphylococcus epidermidis Mediated by the Lectin Subdomain of Aap. *MBio*, *12*(4), e02908-20. https://doi.org/10.1128/mBio.02908-20

Sartorio, M. G., Pardue, E. J., Feldman, M. F., & Haurat, M. F. (2021). Bacterial Outer Membrane Vesicles: From Discovery to Applications. *Annual Review of Microbiology*, *75*, 609-630. https://doi.org/10.1146/annurev-micro-052821-031444

Sauer, K., Stoodley, P., Goeres, D. M., Hall-Stoodley, L., Burmølle, M., Stewart, P. S., & Bjarnsholt, T. (2022). The biofilm life cycle: expanding the conceptual model of biofilm formation. *Nature Reviews Microbiology*, *20*(10), 608-620. https://doi.org/10.1038/s41579-022-00767-0

Schenkel-Brunner, H. (2007). Blood Group Antigens. In H. Kamerling (Ed.), *Comprehensive Glycoscience* (pp. 343-372). Elsevier. https://doi.org/10.1016/B978-044451967-2/00039-8

Schmitz, D. A., Wechsler, T., Li, H. B., Menze, B. H., & Kümmerli, R. (2024). A new protocol for multispecies bacterial infections in zebrafish and their monitoring through automated image analysis. *PLOS ONE*, *19*(8), e0304827. https://doi.org/10.1371/journal.pone.0304827

Scott, C. A., Carney, T. J., & Amaya, E. (2022). Aerobic glycolysis is important for zebrafish larval wound closure and tail regeneration. *Wound Repair and Regeneration*, *30*(6), 665-680. https://doi.org/10.1111/wrr.13050

Sommer, R., Exner, T. E., & Titz, A. (2014). A Biophysical Study with Carbohydrate Derivatives Explains the Molecular Basis of Monosaccharide Selectivity of the Pseudomonas aeruginosa Lectin LecB. *PLoS ONE*, *9*(11), e112822. https://doi.org/10.1371/journal.pone.0112822

Sommer, R., Wagner, S., Varrot, A., Nycholat, C. M., Khaledi, A., Häussler, S., Paulson, J. C., Imberty, A., & Titz, A. (2016). The virulence factor LecB varies in clinical isolates: consequences for ligand binding and drug discovery. *Chemical Science*, *7*(8), 4990-5001. https://doi.org/10.1039/C6SC00696E

Soria-Bustos, J., Ares, M. A., Gómez-Aldapa, C. A., González-y-Merchand, J. A., Girón, J. A., & De la Cruz, M. A. (2020). Two Type VI Secretion Systems of Enterobacter cloacae Are Required for Bacterial Competition, Cell Adherence, and Intestinal Colonization. *Frontiers in Microbiology*, *11*. https://doi.org/10.3389/fmicb.2020.560488

Stowell, C. P., & Stowell, S. R. (2019). Biologic roles of the <scp>ABH</scp> and Lewis histo-blood group antigens Part I: infection and immunity. *Vox Sanguinis*, *114*(5), 426-442. https://doi.org/10.1111/vox.12787

Šulák, O., Cioci, G., Lameignère, E., Balloy, V., Round, A., Gutsche, I., Malinovská, L., Chignard, M., Kosma, P., Aubert, D. F., Marolda, C. L., Valvano, M. A., Wimmerová, M., & Imberty, A. (2011). Burkholderia cenocepacia BC2L-C Is a Super Lectin with Dual Specificity and Proinflammatory Activity. *PLoS Pathogens*, *7*(9), e1002238. https://doi.org/10.1371/journal.ppat.1002238

Sutton, G. G., Brinkac, L. M., Clarke, T. H., & Fouts, D. E. (2018). Enterobacter hormaechei subsp. hoffmannii subsp. nov., Enterobacter hormaechei subsp. xiangfangensis comb. nov., Enterobacter roggenkampii sp. nov., and Enterobacter muelleri is a later heterotypic synonym of Enterobacter asburiae based on computational analysis of sequenced Enterobacter genomes. *F1000Research*, *7*, 521. https://doi.org/10.12688/f1000research.14566.2

Sych, T., Omidvar, R., Ostmann, R., Schubert, T., Brandel, A., Richert, L., Mely, Y., Madl, J., & Römer, W. (2023). The bacterial lectin LecA from P. aeruginosa alters membrane organization by dispersing ordered domains. *Communications Physics*, *6*(1), 153. https://doi.org/10.1038/s42005-023-01272-3

Taylor, M. E., Drickamer, K., Imberty, A., van Kooyk, Y., Schnaar, R. L., Etzler, M. E., & Varki, A. (2022). Discovery and Classification of Glycan-Binding Proteins. In A. Varki, R. Cummings, & J. Esko (Eds.), *Essentials of Glycobiology* (4th edn) (pp. 375-386). Cold Spring Harbor Laboratory Press.

Tielker, D., Hacker, S., Loris, R., Strathmann, M., Wingender, J., Wilhelm, S., Rosenau, F., & Jaeger, K.-E. (2005). Pseudomonas aeruginosa lectin LecB is located in the outer membrane and is involved in biofilm formation. *Microbiology*, *151*(5), 1313-1323. https://doi.org/10.1099/mic.0.27701-0

Toptchieva, A., Sisson, G., Bryden, L. J., Taylor, D. E., & Hoffman, P. S. (2003). An inducible tellurite-resistance operon in Proteus mirabilis. *Microbiology*, *149*(5), 1285-1295. https://doi.org/10.1099/mic.0.25981-0

Van der Vaart, M., Spaink, H. P., & Meijer, A. H. (2012). Pathogen Recognition and Activation of the Innate Immune Response in Zebrafish. *Advances in Hematology*, *2012*, 1-19. https://doi.org/10.1155/2012/159807

Varas, M., Fariña, A., Díaz-Pascual, F., Ortíz-Severín, J., Marcoleta, A. E., Allende, M. L., Santiviago, C. A., & Chávez, F. P. (2017). Live-cell imaging of Salmonella Typhimurium interaction with zebrafish larvae after injection and immersion delivery methods. *Journal of Microbiological Methods*, *135*, 20-25. https://doi.org/10.1016/j.mimet.2017.01.020

Vávrová, S., Grones, J., Šoltys, K., Celec, P., & Turňa, J. (2024). The tellurite resistance gene cluster of pathogenic bacteria and its effect on oxidative stress response. *Folia Microbiologica*, *69*(2), 433-444. https://doi.org/10.1007/s12223-024-01133-8

Wang, F., Yang, H., & Wang, Y. (2013). Structure characterization of a fucose-containing exopolysaccharide produced by Enterobacter cloacae Z0206. *Carbohydrate Polymers*, *92*(1), 503-509. https://doi.org/10.1016/j.carbpol.2012.10.014

WHO. (2024). *2023 Antibacterial agents in clinical and preclinical development: an overview and analysis*.

Yang, H.-F., Pan, A.-J., Hu, L.-F., Liu, Y.-Y., Cheng, J., Ye, Y., & Li, J.-B. (2017). Galleria mellonella as an in vivo model for assessing the efficacy of antimicrobial agents against Enterobacter cloacae infection. *Journal of Microbiology, Immunology and Infection*, *50*(1), 55-61. https://doi.org/10.1016/j.jmii.2014.11.011

Yang, R., Han, S., Yu, Y., Li, H., Helmann, J. D., Schaufler, K., Johnson, M. D. L., Yang, Q. E., & Rensing, C. (2025). The *Klebsiella pneumoniae* tellurium resistance gene *terC* contributes to both tellurite and zinc resistance. *Microbiology Spectrum*, *13*(5). https://doi.org/10.1128/spectrum.02634-24

Zahorska, E., Denig, L. M., Lienenklaus, S., Kuhaudomlarp, S., Tschernig, T., Lipp, P., Munder, A., Gillon, E., Minervini, S., Verkhova, V., Imberty, A., Wagner, S., & Titz, A. (2024). High-Affinity Lectin Ligands Enable the Detection of Pathogenic *Pseudomonas aeruginosa* Biofilms: Implications for Diagnostics and Therapy. *JACS Au*. https://doi.org/10.1021/jacsau.4c00670

Supplementary material:

Open reading frame of *eclA* and its flanking regions in *E. cloacae* subsp. *dissolvens*:

1

TCCCCGTCCTGAAAAAGGTACATCTGCTGGCGACCTTTGTGTTTCCAGGTGATCCGCTTACGCGGCGCGAGCTTCACTTTCTCTGCGA
CTGGCTCAAGGATCGCCGTCAGACGTTCAATGGAATGTTCAGGGCGAACAGGAGGCAATATATGCATGACACCACCTTTTAGCGTTG
GGTACTGGCCAGTATAGACCACCGAGGTCAATGCTCAGACCGGTATGAGGGAAGGAAGGTATATCAGGGGGCACTGCATGGGTAAA
AAGATAATTTGTTTATTTTTAAACTTGACCCGCGTAACAGGTGATAAGTGTGCCAGATTTCCTGACGTACTTACATGAATATCAATGT
AAACGATGGGGAGAATAAACTATTACAAACCTGACGTATTTATCTCCTCCCTCCTTAAGATTATTCCTATTTCGGCAATAATTATTTT
ATTATTTTTAAGTGATTACAAAATCGCAACCCTTAATAAAGCGTTTCGCGTTTTGAATTGTATATACCGCCTGACTATTCTCATTCCAG
CCGATAACAACCGGGTAATGAATATGAGAAGTGTGTGCTTCTCATGAGATCATTTATTCTGATTATCAGGCGGTTAGCTGAATTGAG

650

TGATTAAAATCACGCATTTCGTCAGGACTATCTTTCAATGGCGAATGTATTCGCCACGCTGTCACAGGAGTCAGACATGAGCGATAA
TTTAATCTGGTCGGGAAAAGTTGACGCTAAAAATACCGAAGGAACAAATACAGGGATATCCCTCAAAGCGGGAGAGATAATTACCA
TTCTGGCCAGTGGTTGGGCCAGGAATGGAAGTGAAAATTTTGCCCTTACCGCACCACAGGGACGTATTCCCAGAGAGGGCGAAACG
CTAGCCTTACGCAATCCTTCGCTTCAGGCACGCATTGGTAACGAAAATTATCCGGTAGGTAATCATAAATACCGCTGGTCGGTTCCTG
CTGAAGGAACGCTAACGCTGATTTTTGCCGACGGCAAAGACCAGTACAAAGACAACGCCGGTGAATTCAGCGTTGAAGTCTATCGC
GAGGCGGATATTTCCGCCGAGGCTGCAGTACCGTTTGAAGATTTCACCAACTTTGAGCGTGATAACTGGAATAGCTGGCAGGCAGGA
CCTGCCGGGCACGATCTGTACCTGGTTGACGCCAGCGCGCGGGCCGTCGAGTTTATTACCAACCCCAATAAAAATCATGCCGGCGAA
ATCCTCAAAAAGACGCTGACAGGTCTGACTGCCGGGCATGAATATACCTGGACGGTGAAAGCGGCACGCATTATAGGAAAATATGA
GGCGCCAAAAATATCACTCCGTGCGGATGGCAAAGACATTTCCGCCCCCCTGGAACTGAAGCAGGCGAATGAATGGGTAACCCTGA
GTGGAAAATTCAAAGCCGCGGGTAATCAGGCTGAACTCGCGGTAGTCAGCCATGTTGCAGCGAGTATGGGGAATGATTTCCGCATC

1053

AAAGAGCTCAGGATAAAGGGTTAATCTACAGAATTGTCGGTCTGCTATCCTGCGAGAATGCTGGATGGCCGTTCGATCTTCAAAAAA
TTGTGTAGCGCACATGTTCAACATATGCGCTACACCAACAGGCAATAAACACACACGGCATTACTCTTTGTTATGTTGTATATCCTCT
CAATATCGGCAGCGGTTTGAAACAAGACGCGTCTTGATTAACGCCATCCAGAAACACAGCACGCTTTCGGTTAGGGGTACCTGAGTG
GAAGCAGCACACTCATTTCATGCCAAATAAACACCAGTGGGGTAATATCGGTTCTGAATACGCATTCAGGGCTGCATATTCACGTAA
TTAAAAAGATCATGGTGCCTGAAAAAGCGCACCATGGAAGAGCCACAACCTGCAATTAGCAAAGCACATCCCTTTTTAATTAAAAG
GCAACGTAATTGTACTGCCGCTATATTGTTAAACGATACAAGACCTGTCTGGTTAATTCAGGGGTAAGCGAGAAAGTTGGTACTGAC
TGATTATGCCGTACACAGGAAATGTGTGCATACAAGGCTTACGCGTTATGAGAGGCTCTCCAGCAATGGCTCAAGACAGGCTGGCTT
TCAGCAAAACCACCCTCTATCGACGAAAGACCTTCTGACCCTTCGTATTGATACTTGAGGATTCGG

2152

SI Box 1: Nucleotide sequence from *E. cloacae* subsp. *dissolvens* of *eclA* open reading frame (ORF) and flanking sequences used in homologous recombination with nucleotide positions indicated. The ORF (shown in black), which corresponds to the region deleted during homologous recombination, is flanked by upstream (blue) and downstream (green) sequences used in the recombination process.

Size and amino acid sequence comparison of EclA variants from *E. cloacae* subsp. *cloacae* and *E. cloacae* subsp. *dissolvens*:

The amino acid sequence of EclA from *E. cloacae* subsp. *dissolvens* was obtained by performing a tBLASTn of the EclA sequence from *E. cloacae* subsp. *cloacae* (GenBank: ADF63724.1) against the genome of *E. cloacae* subsp. *dissolvens* DSM 16657 (ASM966045v1). The EclA-M14A variant corresponds to the *E. cloacae* subsp. *cloacae* EclA sequence carrying a methionine-to-alanine substitution at position 14 (M14A).

Sequence alignment and percentage similarity were calculated in Geneious using global alignment with free end gaps, with the BLOSUM90 substitution matrix and a similarity threshold of 1. The molecular weights of all three protein sequences were determined using the ProtParam tool (Gasteiger et al., 2005).

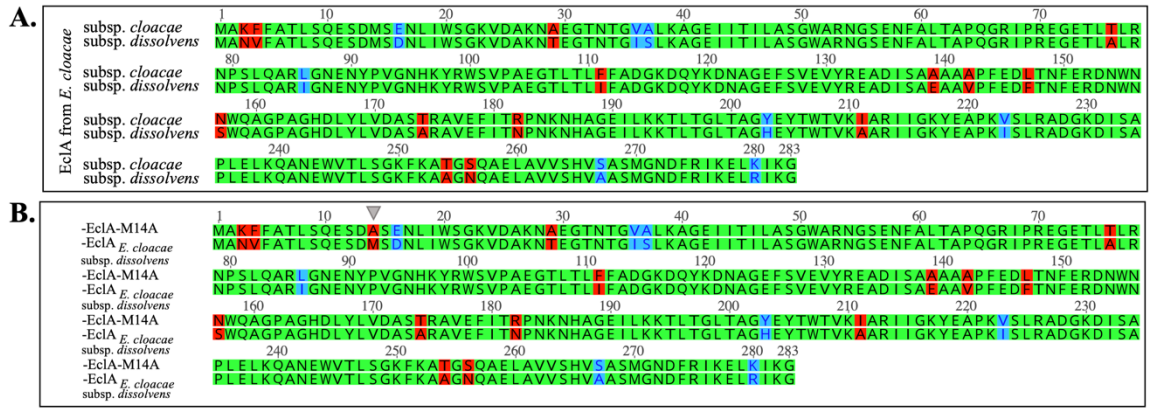

C.

Alignment	Identities	Similarity
A	260/283 (91.9%)	94.7%
B	261/283 (92.2%)	95.1%

D.

Protein	Amino acids	Molecular weight (Da)
EclA *E. cloacae* subsp. *cloacae* DSM 30054	283	30960.73
EclA-M14A *E. cloacae* subsp. *cloacae* DSM 30054	283	30900.61
EclA *E. cloacae* subsp. *dissolvens* DSM 16657	283	30856.49

SI Figure 1: Comparative sequence analysis of EclA variants from *E. cloacae* subsp. *cloacae* and *E. cloacae* subsp. *dissolvens*. **(A)** Amino acid sequence alignment of EclA from *E. cloacae* subsp. *cloacae* and *E. cloacae* subsp. *dissolvens*. **(B)** Sequence alignment of recombinant EclA-M14A (Beshr et al., 2025) with native EclA from *E. cloacae* subsp. *dissolvens*. Residues are color-coded: green for identical (100%), blue for similar (60-80%), and red for non-identical. The engineered M14A mutation is indicated by a grey triangle. **(C)** Percentage identity and similarity from alignments shown in panels A and B. **(D)** Comparison of the predicted molecular weights of the EclA variants.

Amino acid sequences of recombinant EclA:

SI Table 1: Amino acid sequences of recombinantly expressed EclA and its derivatives in *E. coli* from Beshr et al. (2025).

Recombinant protein	Number of amino acids	Amino acid sequence	MW (Da)
EclA *E. cloacae* subsp. *cloacae* DSM 30054	283	MAKFFATLSQESDMSENLIWSGKVDAKNAEGTNTGVALKAGEIITILASGWARNGSE NFALTAPQGRIPREGETLTLRNPSLQARLGNENYPVGNHKYRWSVPAEGTLTLFFAD GKDQYKDNAGEFSVEVYREADISAAAAAPFEDLTNFERDNWNNWQAGPAGHDLYL VDASTRAVEFITRPNKNHAGEILKKTLTGLTAGYEYTWTVKIARIIGKYEAPKVSLRA DGKDISAPLELKQANEWVTLSGKFKATGSQAELAVVSHVSASMGNDFRIKELKIKG	30960
EclA-M14A	283	MAKFFATLSQESDASENLIWSGKVDAKNAEGTNTGVALKAGEIITILASGWARNGSE NFALTAPQGRIPREGETLTLRNPSLQARLGNENYPVGNHKYRWSVPAEGTLTLFFAD GKDQYKDNAGEFSVEVYREADISAAAAAPFEDLTNFERDNWNNWQAGPAGHDLYL VDASTRAVEFITRPNKNHAGEILKKTLTGLTAGYEYTWTVKIARIIGKYEAPKVSLRA DGKDISAPLELKQANEWVTLSGKFKATGSQAELAVVSHVSASMGNDFRIKELKIKG	30900
EclA-C *E. cloacae* subsp. *cloacae* DSM 30054	144	MAAPFEDLTNFERDNWNNWQAGPAGHDLYLVDASTRAVEFITRPNKNHAGEILKKT LTGLTAGYEYTWTVKIARIIGKYEAPKVSLRADGKDISAPLELKQANEWVTLSGKFK ATGSQAELAVVSHVSASMGNDFRIKELKIKG	15908

Colony PCR of the *eclA* locus in WT vs Δ*eclA E. cloacae* subsp. *dissolvens*:

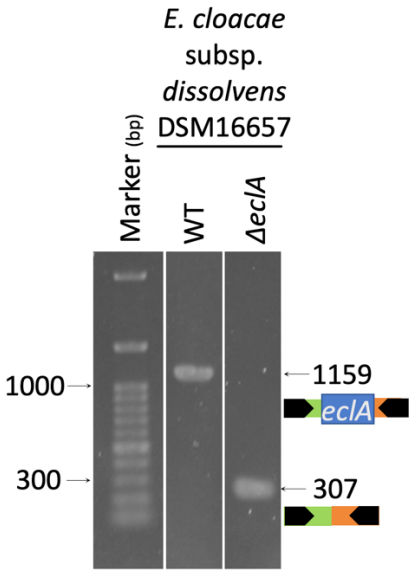

SI Figure 2: Confirmation of *eclA* deletion by colony PCR. 1% agarose gel showing colony PCR products amplified using primers flanking the *eclA* locus. The WT strain exhibits a larger amplicon corresponding to the intact *eclA* region, while the Δ*eclA* strain displays a smaller amplicon consistent with deletion of the *eclA* coding sequence. On the right, the expected base pair sizes of the PCR products are indicated, alongside schematic representations of the *eclA* genomic locus. The blue box represents the upstream sequence, the green box represents the downstream sequence, and the black arrows indicate the positions of the forward and reverse primers.

Sequence alignment of *eclA* locus in S1^{WT} compared to S1$^{\Delta}$:

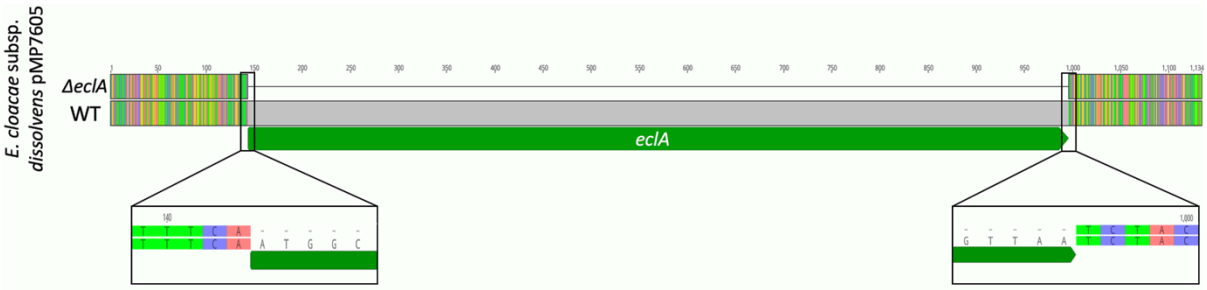

SI Figure 3: Sequence alignment of the *eclA* gene and its flanking regions in S1^{WT} compared to S1$^{\Delta}$. Colored bars indicate regions of nucleotide identity in the flanking sequences. The green arrow denotes the coding DNA sequence (CDS) of *eclA*. The grey box highlights the *eclA* nucleotide sequence present only in S1^{WT}. Sequencing was performed on genomic DNA by MicrobesNG using Oxford Nanopore technology. Sequences were aligned using Geneious Alignment (Global alignment with Needleman-Wunsch algorithm) in Geneious Prime software (version 2025.1.2).

Growth curves of S1^{WT} compared to S1$^{\Delta}$:

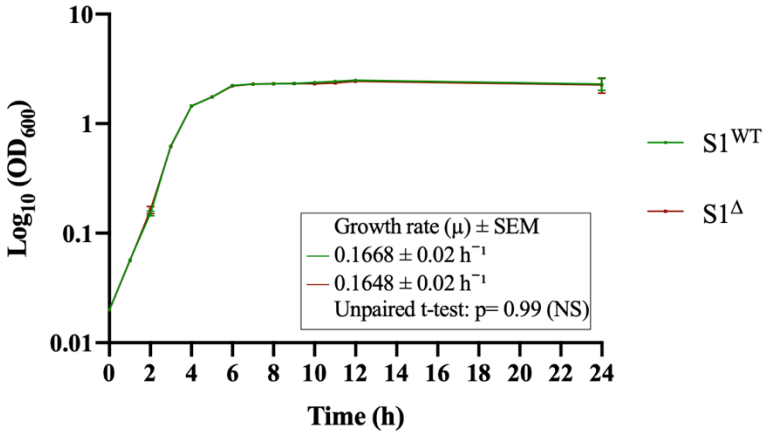

SI Figure 4: 24-hour growth curve of S1^{WT} and S1$^{\Delta}$ in M63^{+} medium. Data points represent the average of two technical replicates (n = 2) from three independent biological replicates (N = 3). Growth rates were determined using the slope of a simple linear regression curve between t = 3-7 h. An unpaired t-test with Welch's correction was performed to determine statistical significance (p-value). S1^{WT}: WT *E. cloacae* subsp. *dissolvens* pMP7605. S1$^{\Delta}$: Δ*eclA E. cloacae* subsp. *dissolvens* pMP7605.

Autoaggregate formation assay over 72 h

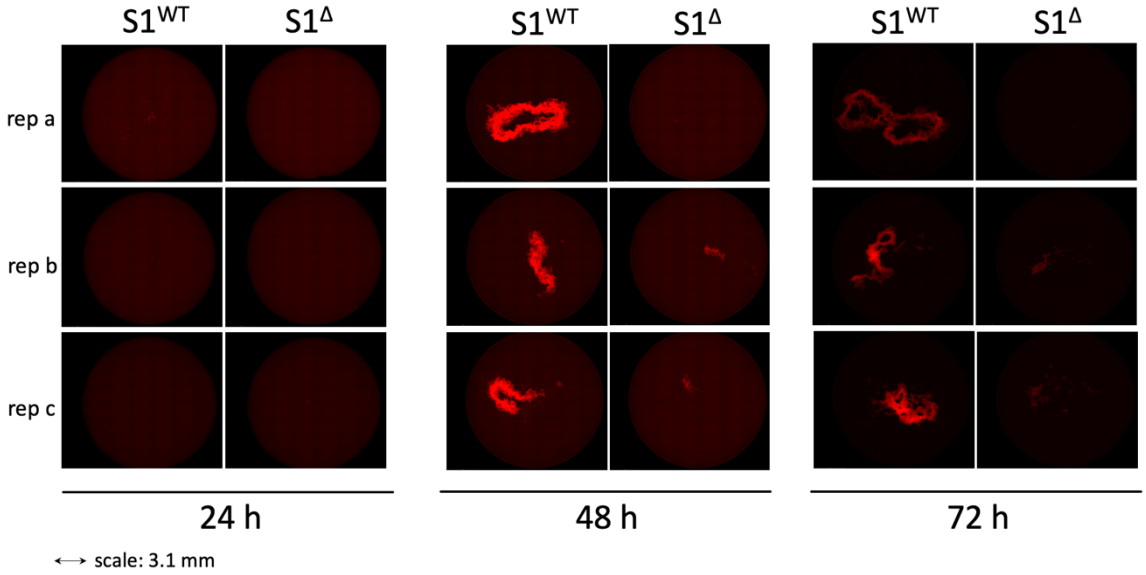

SI Figure 5: Autoaggregate formation assay of $S1^{WT}$ and $S1^{\Delta}$ over 72 hours. Images show one well of each strain from three independent biological replicates (rep a, b, c). Autoaggregate formation was assessed 72 h after incubation under agitation at 180 rpm, 37 °C and 72% humidity. Fluorescence microscopy images show one representative well from three independent biological replicates (rep a, b, and c). $S1^{WT}$: WT *E. cloacae* subsp. *dissolvens* pMP7605. $S1^{\Delta}$: Δ*eclA E. cloacae* subsp. *dissolvens* pMP7605.

EclA release during the exponential growth phase of $S1^{WT}$:

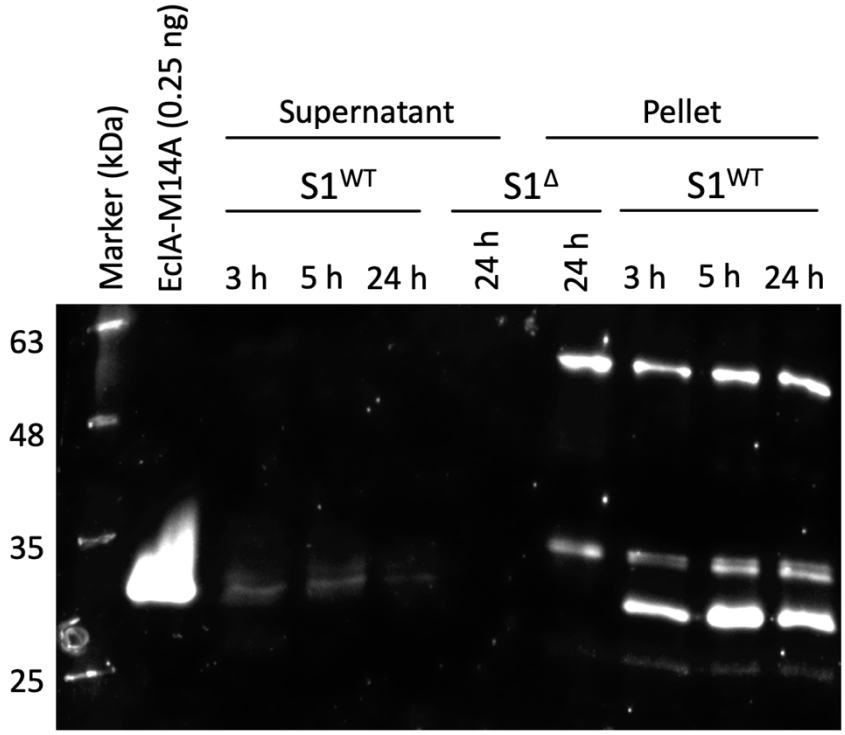

SI Figure 6: Western blot analysis of EclA expression in pellet and supernatant fractions during early and late exponential phases of $S1^{WT}$ growth in $M63^{+}$. Growth conditions matched those used in the growth curve experiment. Supernatant and pellet fractions were loaded at 20 µL and 5 µL, respectively. Samples were normalized by optical density: pellet samples were prepared by resuspending OD_{600} = 1 in 150 µL Laemmli buffer; supernatant proteins were TCA-precipitated and resuspended in 15 µL Laemmli buffer per OD_{600} = 1 of culture. Samples were resolved on a 12% SDS-PAGE gel. Additional Western blot details are provided in the Materials and Methods section. The final image was adjusted for brightness and contrast in FIJI (maximum B&C value set to 8961). $S1^{WT}$: WT *E. cloacae* subsp. *dissolvens* pMP7605. $S1^{\Delta}$: Δ*eclA E. cloacae* subsp. *dissolvens* pMP7605.

Membrane displacement attempt of EclA in S1^{WT}:

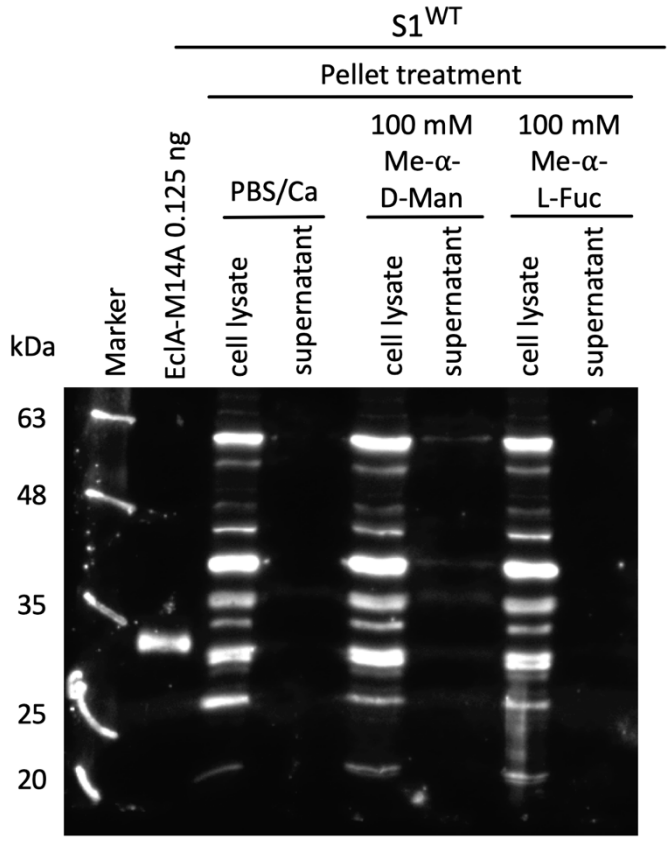

SI Figure 7: Western blot analysis investigating potential carbohydrate-mediated displacement of EclA from the cell fraction of S1^{WT}. Bacterial pellets were treated with 100 mM methyl α-D-mannoside (Me-α-D-Man), methyl α-L-fucoside (Me-α-L-Fuc), or PBS as a negative control. Proteins were separated on a 12% gel and detected using anti-EclA-C antibodies. Additional Western blot details are provided in the Materials and Methods section. S1^{WT}: WT *E. cloacae* subsp. *dissolvens* pMP7605.

Comparison between EclA and EclA-M14A:

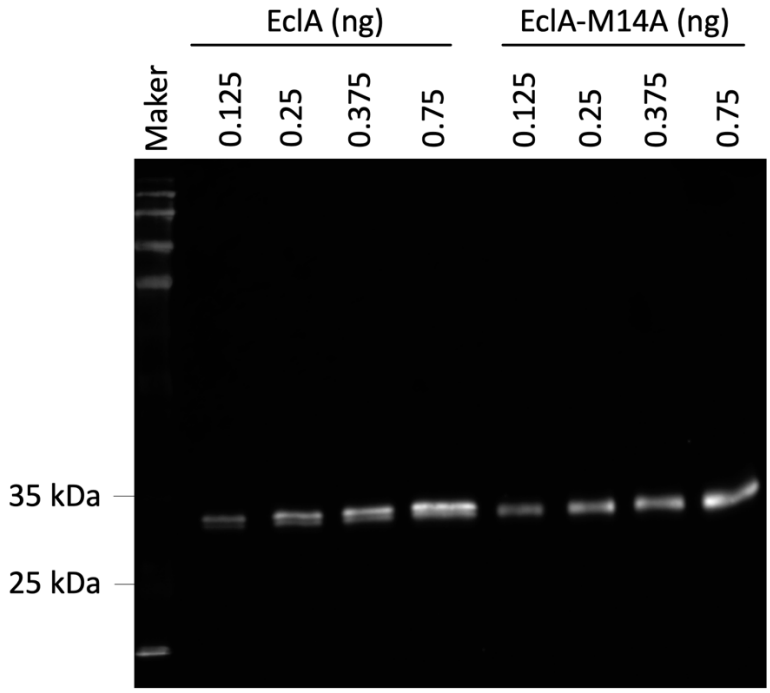

SI Figure 8: Western blot analysis of recombinant EclA and its EclA-M14A derivative. Both proteins were heterologously expressed in *E. coli* and analyzed by Western blot using a 12% SDS-PAGE gel (additional details provided in the Materials and Methods section). Two isoforms of EclA are observed due to the presence of two start codons, separated by 12 nucleotides (SI Figure 1). The M14A mutation effectively abolishes expression of the shorter EclA isoform.

Comparison between recombinant EclA from *E. cloacae* subsp. *cloacae* and native EclA from S1^{WT}:

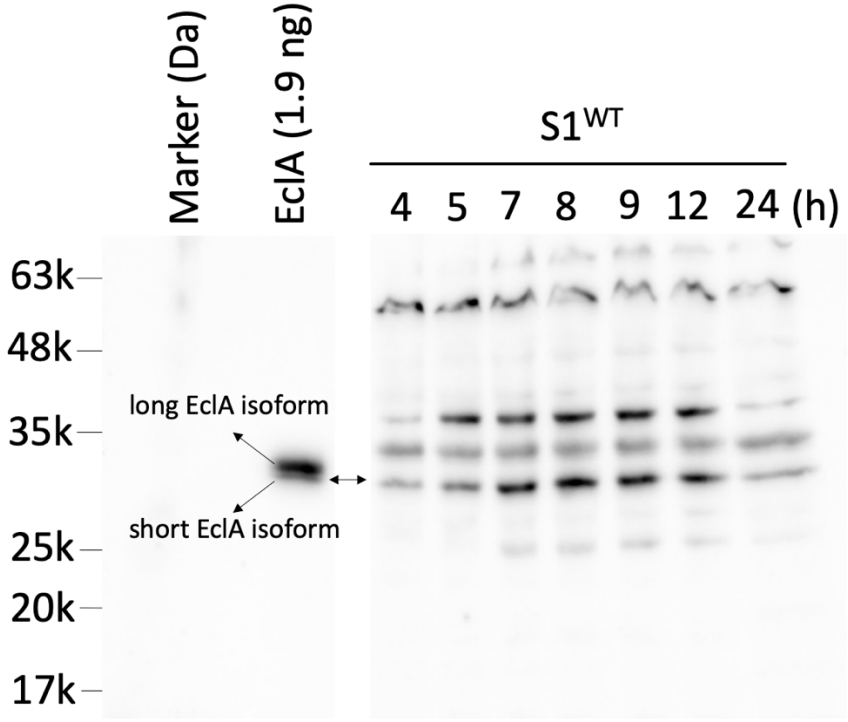

SI Figure 9: Western blot analysis of recombinant EclA from *E. cloacae* subsp. *cloacae* and native EclA from S1^{WT}. Pellet samples from a 24-hour culture of S1^{WT} in M63^{+} medium, under the same conditions as used in the growth curve experiment, were collected at various time points. Samples were normalized by optical density: pellets corresponding to $OD_{600} = 1$ were resuspended in 150 µL of Laemmli buffer. These were compared to recombinant EclA expressed from *E. cloacae* subsp. *cloacae*. All samples were separated on a 12% SDS-PAGE gel and analyzed by Western blot as described in the Materials and Methods section. Colors were inverted to enhance band visibility. The shorter EclA isoform corresponds to the native protein expressed in S1^{WT}. S1^{WT}: WT *E. cloacae* subsp. *dissolvens* pMP7605.

Hemagglutination assay replicates and hemagglutination with LecB:

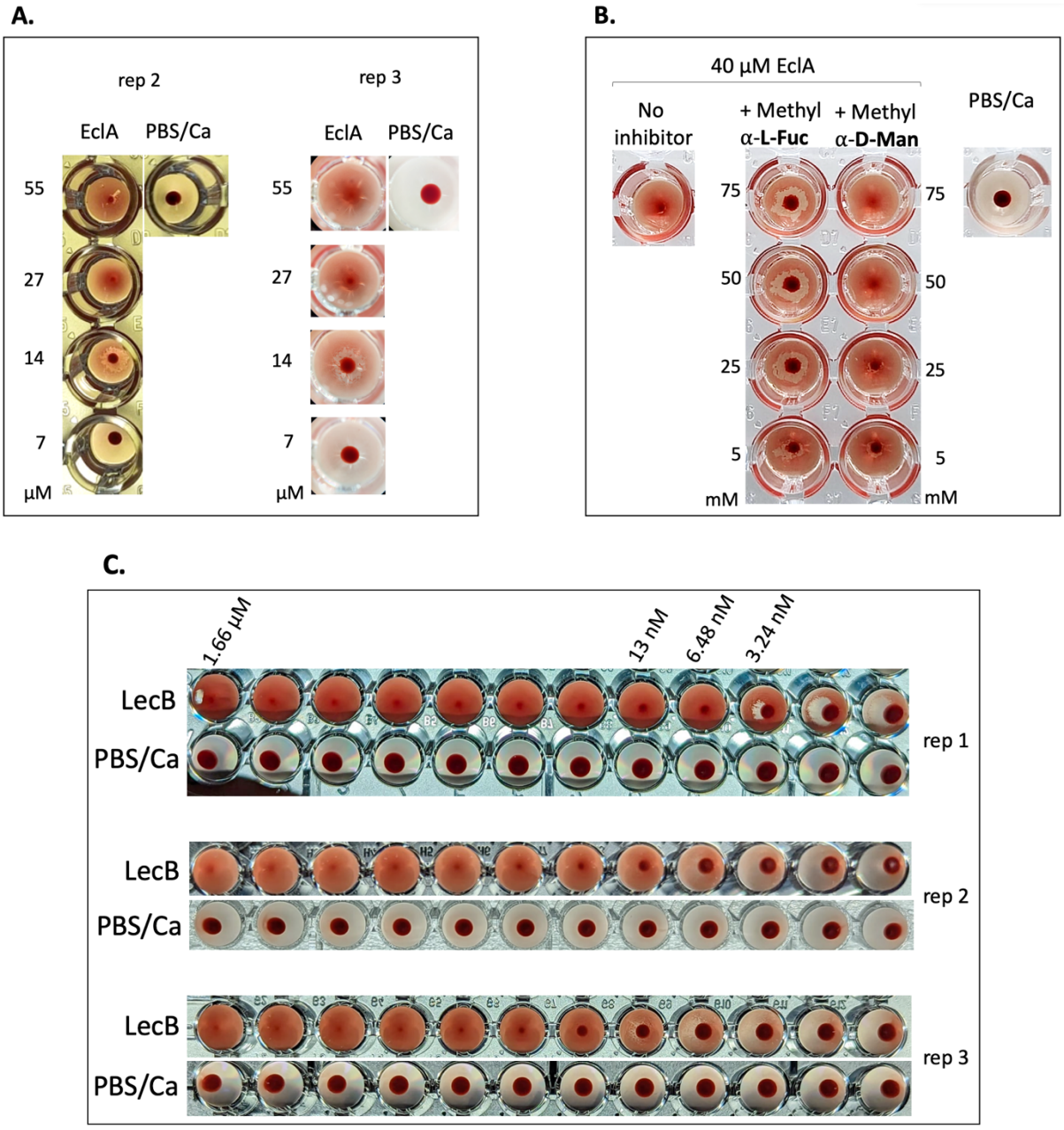

SI Figure 10: Hemagglutination of human type O^+ red blood cells by recombinant LecB and EclA, and inhibition of EclA-induced agglutination by methyl α-L-fucoside. (A) Second and third biological replicate for the hemagglutination of human type O^+ red blood cells by recombinant EclA from *E. cloacae* subsp. *cloacae.* Red blood cells used in replicate 2 (rep 2) and Figure 3-A were obtained from the same donor, while replicate 3 (rep 3) used a separate donor batch. **(B)** Second replicate for the inhibition of EclA-induced hemagglutination by preincubating 40 µM EclA with increasing concentrations of methyl α-L-fucoside or methyl α-D-mannoside. Red blood cells used here matched those from Figure 3-B. Carbohydrate

concentrations refer to the amounts present during preincubation with EclA, prior to the addition of red blood cells. **(C)** Titration of recombinant LecB from *P. aeruginosa* to assess dose-dependent agglutination of human type O^+ red blood cells. Results from three independent biological replicates are shown. Replicate 1 (rep 1) used a different blood batch than replicates 2 (rep 2) and 3 (rep 3), which shared the same batch as in Figure 3-A and Figure 3-B. PBS/Ca wells served as a negative control.

Colanic acid genetic cluster:

SI Table 2: Components of the colanic acid genetic cluster found in *E. cloacae* subsp. *dissolvens* DSM 16657.

Genes	Base pairs	NCBI RefSeq
cpsB	1437	NP_310881.1
cpsG	1371	WP_017383277.1
GDP-mannose mannosyl hydrolase	480	NP_416555.2
gmd	1122	WP_005128297.1
MOP flippase family protein	1479	WP_014170812.1
NAD-dependent epimerase/dehydratase family protein	966	NP_310884.1
wza Polysaccharide export protein	1140	NP_461063.1
wcaA	843	WP_010431930.1
wcaB	492	WP_004386763.1
wcaC	1218	NP_310889.1
wcaD	1221	WP_014832621.1
wcaE	747	WP_014170821.1
wcaF	549	NP_416558.1
wcaI	1224	NP_310882.1
wcaJ	1395	NP_461048.1
wcaK	1281	NP_310877.1
wcaL	1221	NP_416548.1
wcaM	1392	WP_010431967.1
wzb	444	NP_461062.1
wzc	2163	NP_416564.4

3.2. The Role of EclA in Autoaggregate Formation of *E. cloacae* subsp. *dissolvens*

Building upon the findings of the manuscript presented in Chapter 3.1, which established that EclA is essential for the formation of autoaggregates in *E. cloacae* subsp. *dissolvens*, this chapter presents additional experiments aimed at further elucidating its role. To provide a more detailed perspective on EclA's function in autoaggregate development, three complementary approaches were employed. First, SEM was used to conduct a structural examination of the autoaggregates. Second, an exogenous complementation experiment was performed to test whether the aggregation-deficient phenotype of the Δ*eclA* mutant could be restored by adding recombinant EclA. Finally, autoaggregation was analyzed under dynamic shear flow using a continuous flow chamber system to assess autoaggregate formation in a more physiologically relevant setting. The following strain designations will be used throughout this chapter; $S1^{WT}$: WT *E. cloacae* subsp. *dissolvens* pMP7605; $S1^{\Delta}$: Δ*eclA E. cloacae* subsp. *dissolvens* pMP7605.

3.2.1. Scanning Electron Microscopy of Autoaggregates

To further examine the autoaggregates formed by $S1^{WT}$ and $S1^{\Delta}$, autoaggregation assays were performed as outlined in Chapter 3.1. The resulting aggregates were collected, processed, and fixed onto 0.2 µm filter membranes. Samples were then imaged at various magnifications using SEM, following the procedure detailed in Chapter 7.1.

While less aggregates were found in $S1^{\Delta}$ compared to $S1^{WT}$, scanning electron microscopy revealed that both strains exhibited uniform bacterial morphology with rough surfaces, with no discernible structural differences between their autoaggregates (Figure 1). This suggests that EclA does not play a role in cell shape or surface architecture. Notably, discrete, approximately spherical, electron-dense structures were consistently observed at the polar regions of cells in both strains. The origin of these structures remains undefined; while they could represent biological features, preparation-induced artifacts like dehydration effects cannot be excluded.

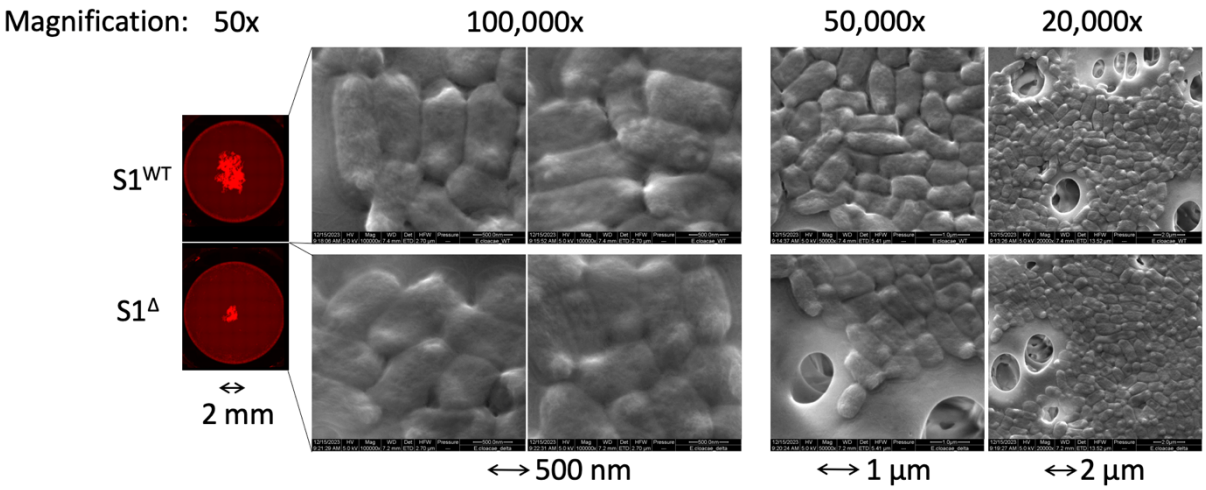

Figure 1: SEM images of autoaggregates formed by S1^{WT} and S1$^{\Delta}$. Autoaggregates were collected from an autoaggregation assay following 72 hours of incubation at 37 °C and 180 rpm in M63+ medium, starting from an OD_{600} of 0.02. Samples were fixed with 0.2% glutaraldehyde, washed, and dried on 0.2 µm filter membranes using sterile milli-Q water. SEM images were taken at various magnifications. The 50× image represents a fluorescence microscopy overview captured prior to autoaggregate collection and processing for SEM. S1^{WT}: WT *E. cloacae* subsp. *dissolvens* pMP7605. S1$^{\Delta}$: Δ*eclA E. cloacae* subsp. *dissolvens* pMP7605. Images were acquired from one biological experiment (N = 1).

3.2.2. Autoaggregation Rescue by Exogenous Recombinant EclA and Structural Comparison with Native EclA from *E. cloacae* subsp. *dissolvens*

In Chapter 3.1, S1$^{\Delta}$ showed a significant decrease in autoaggregation compared to the WT strain. To determine whether the S1$^{\Delta}$ phenotype could be restored to the WT level, the experiment was repeated with the addition of exogenous recombinant EclA or EclA-M14A. Each protein, diluted in TBS/Ca, was introduced into the M63^{+} autoaggregation medium as detailed in Chapter 7.1, and their ability to rescue autoaggregation was assessed.

Neither recombinant EclA nor EclA-M14A restored autoaggregation in S1$^{\Delta}$, despite the portrayed role of *eclA* in autoaggregate formation (Figure 2). This was evident from the large aggregates observed in the WT strain, which were absent in the Δ*eclA* mutant under all conditions. This suggests that EclA's role in autoaggregation may depend on its native expression context, as the recombinant proteins expressed in *E. coli* and derived from a different subspecies (*cloacae* rather than *dissolvens*), were insufficient to rescue the phenotype when added exogenously.

In figure 2-B, supplementing with 100 µM EclA required a higher volume of TBS/Ca, which diluted the M63+ medium and delayed cell growth. Consequently, imaging was performed at 72 hours instead of 48 hours.

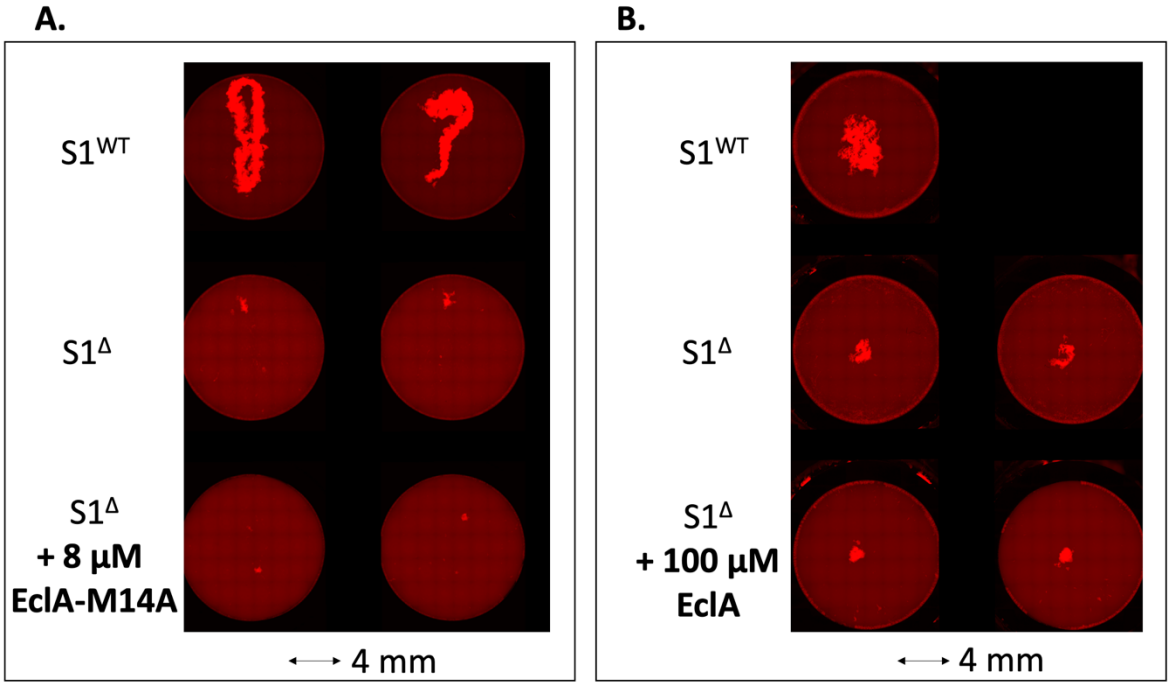

Figure 2: Autoaggregation of S1$^{\Delta}$ with exogenous complementation of recombinant EclA. Fluorescence imaging of whole wells in two separate autoaggregation assays: **(A)** Complementation of S1$^{\Delta}$ with EclA-M14A. **(B)** Complementation of S1$^{\Delta}$ with EclA. Overnight cultures of S1^{WT} *and* S1$^{\Delta}$ were grown in LB medium supplemented with 60 µg/mL gentamicin at 37 °C with shaking at 180 rpm. Cultures were diluted into M63^{+} medium to a final OD_{600} of 0.02. Prior to aliquoting, recombinant EclA or the mutant variant EclA-M14A was added to a final concentration of 100 µM or 8 µM, respectively. The same volume of buffer was added to S1^{WT} and S1$^{\Delta}$ controls. Fluorescence imaging was performed after 48 hours for (A) and after 72 hours for (B). S1^{WT}: WT *E. cloacae* subsp. *dissolvens* pMP7605. S1$^{\Delta}$: Δ*eclA E. cloacae* subsp. *dissolvens* pMP7605. For both panels, N = 1.

The native EclA structure of *E. cloacae* subsp. *dissolvens* was predicted using the protein modeling and analysis server Phyre2.2, as described in Chapter 7.1, with the experimental crystal structures of the N- and C-terminal domains of EclA from *E. cloacae* subsp. *cloacae* DSM 30054 serving as templates (Figure 3). The predicted N-terminal (Figure 3-A) and C-terminal (Figure 3-B) domains both adopt backbones consistent with their corresponding experimental structures (PDB 6YGQ and PDB 6YF6). No amino acid differences were

observed near the carbohydrate-binding site of the N-terminus where the Ca^{2+} ion involved in ligand binding is located, indicating conservation of this region. In contrast, the C-terminus exhibited a single amino acid variation, an arginine (R) in the experimental structure replaced by an asparagine (N) in *E. cloacae* subsp. *dissolvens* (R181N according to the numbering of crystal structure PDB 6YF6), within 4 Å of the methyl α-L-selenofucoside ligand in the binding site (Figure 3-C). Although neither residue forms direct hydrogen bonds with the ligand, the presence of this substitution near the binding site could influence interactions with other native ligands specific to *E. cloacae* subsp. *dissolvens*, potentially explaining the inability of EclA to rescue the $S1^{\Delta}$ phenotype.

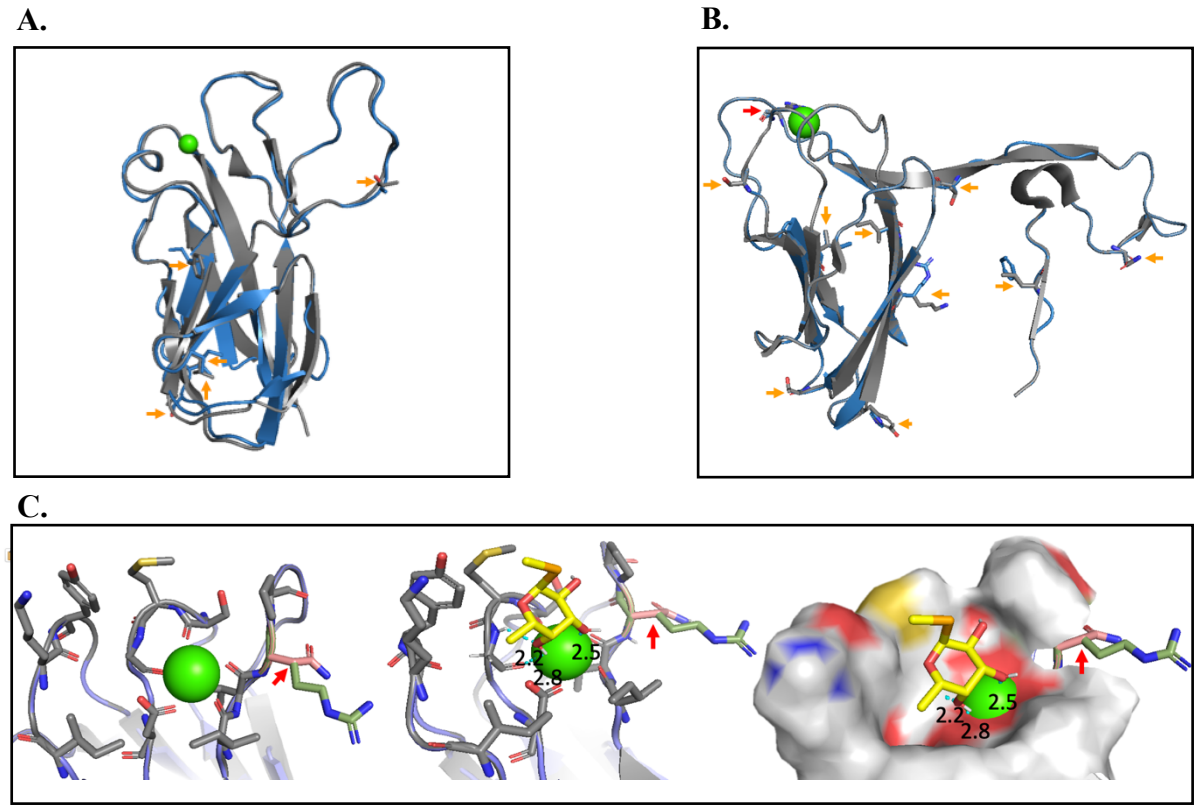

Figure 3: Predicted native structure of EclA domains from *E. cloacae* subsp. *dissolvens* based on experimental EclA crystal structures from *E. cloacae* subsp. *cloacae*. The native EclA structure from *E. cloacae* subsp. *dissolvens* (blue) was predicted using the Phyre2.2 modeling server and visualized in PyMOL, with the experimental crystal structures of the N- and C-terminal domains from *E. cloacae* subsp. *cloacae* DSM 30054 (gray; PDB 6YGQ and PDB 6YF6) serving as templates. Green spheres represent Ca^{2+} ions involved in ligand binding at both termini. **(A)** Predicted N-terminal domain (blue) aligned with the experimental crystal structure of the N-terminal domain from *E. cloacae* subsp. *cloacae* (gray; PDB 6YGQ). **(B)** Predicted C-terminal domain (blue) aligned with the experimental crystal structure of the

C-terminal domain (gray; PDB 6YF6). In both (A) and (B), orange arrows indicate amino acid variations between the two sequences; blue sticks represent residues from *E. cloacae* subsp. *dissolvens* and gray sticks from *E. cloacae* subsp. *cloacae*. The red arrow in (B-C) marks the R181N residue substitution located within 4 Å of the calcium ion within the ligand-binding site. **(C)** Different close-ups of the C-terminal binding pocket showing all residues within 4 Å of the ligand methyl α-L-selenofucoside (yellow sticks). All residues (gray) are conserved except for the substitution R181N of arginine (green stick; *E. cloacae* subsp. *cloacae*) with asparagine (salmon stick; *E. cloacae* subsp. *dissolvens*). Cyan dashed lines indicate hydrogen bonds, and numbers denote bond distances (Å).

3.2.3. Autoaggregate formation under flow conditions

To assess bacterial autoaggregation and surface attachment under dynamic conditions, $S1^{WT}$ and $S1^{\Delta}$ were analyzed using a continuous flow chamber system that enables autoaggregation under shear flow. Bacterial suspensions were introduced into flow chambers, allowed to settle, and then exposed to a constant flow of nutrient medium at 30 °C as indicated in Chapter 7.1. Aggregation patterns from three experimental conditions, with 2 technical replicates each, were assessed by brightfield and fluorescence microscopy to evaluate the extent of autoaggregate formation (Figure 4).

In panel A and C, visual inspection of both $S1^{WT}$ and $S1^{\Delta}$ showed comparable levels of aggregate formation. The aggregates were well attached to the channel surface and appeared as evenly dispersed clusters of cells across the channel, with no clear morphological or quantitative differences between the two strains.

In contrast, in panel B, $S1^{\Delta}$ exhibited a noticeably higher number of small aggregates compared to $S1^{WT}$, which formed fewer but seemingly larger clusters. All aggregates were also visibly attached to the surface of the channels. The increased frequency of smaller aggregates in $S1^{\Delta}$ suggests a potential decrease in cell attachment to the flow cell channels where EclA could be involved, and also shows a role of EclA in autoaggregate maturation. This phenotype was consistently observed across both technical replicates.

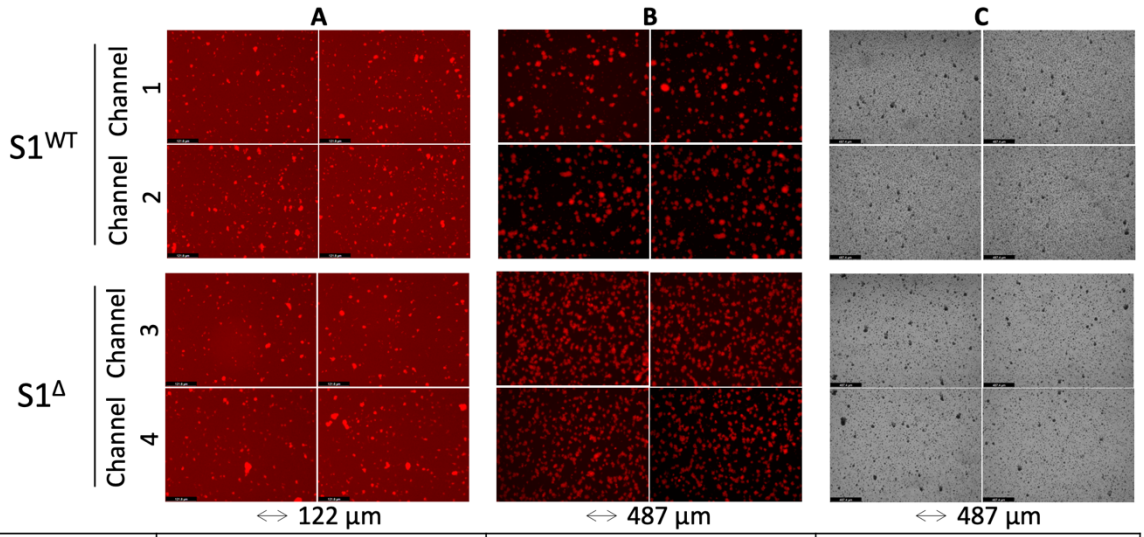

Inoculum	0.075 OD_{600} from an exponential phase of a subculture	0.02 OD_{600} from an overnight culture	0.02 OD_{600} from an overnight culture
Settling time	15 min	5 min	15 min
Medium	M63*	M63**	M63***
Incubation time	16 h	16 h	7 h
Objective	5x	20x	20x

Figure 4: Autoaggregation assay of $S1^{WT}$ and $S1^{\Delta}$ under three conditions. Panels A-C show microscopy images comparing $S1^{WT}$ and $S1^{\Delta}$, with two technical replicates per strain (in separate channels). **(A)** Fluorescence microscopy using a 5× objective. **(B)** Fluorescence microscopy using a 20× objective. **(C)** Brightfield microscopy using a 20× objective. The specific condition tested in each panel is indicated beneath the corresponding images. * M63 medium supplemented with 0.4% (w/v) glucose, 0.2% (w/v) casamino acids, gentamicin (60 µg/mL), and $MgCl_2$ (1 mM). ** M63 medium supplemented with 0.16% (w/v) glucose, 0.08% (w/v) casamino acids, gentamicin (60 µg/mL), and $MgCl_2$ (1 mM). *** M63 medium supplemented with 0.4% (w/v) glucose, 0.2% (w/v) casamino acids, gentamicin (60 µg/mL), $MgCl_2$ (1 mM), and $CaCl_2$ (100 µM). $S1^{WT}$: WT *E. cloacae* subsp. *dissolvens* pMP7605. $S1^{\Delta}$: Δ*eclA E. cloacae* subsp. *dissolvens* pMP7605. For all conditions, N = 1.

Discussion, Chapter 3.2: The role of EclA in autoaggregate formation of *E. cloacae* subsp. *dissolvens*

The involvement of EclA in autoaggregation of $S1^{WT}$ was evaluated using a combination of structural imaging, complementation assays, and flow cell experiments. These approaches provided complementary perspectives on how EclA contributes to bacterial autoaggregation. In Subchapter 3.2.1, $S1^{\Delta}$ showed reduced number of autoaggregates compared to $S1^{WT}$. Nevertheless, SEM revealed no apparent structural differences between both strains (Figure 1). Both strain aggregates were composed of morphologically uniform cells with rough surfaces, likely indicating the presence of exopolysaccharides. This finding suggests that EclA does not contribute to alterations in cell shape or surface. The discrete, electron-dense spherical structures could be the result of capillary forces during drying, which might have drawn cell surface components toward the poles, which would be a limitation of using conventional SEM in this experiment. Techniques such as live-cell SEM or cryo-SEM may be better suited to resolve the native architecture of these aggregates and role of EclA.

Subchapter 3.2.2 investigated whether the autoaggregation-deficient phenotype of $S1^{\Delta}$ could be rescued by the addition of exogenous recombinant EclA or its M14A variant (Figure 2). Neither protein was successful in restoring autoaggregation, as evidenced by the absence of large, dense aggregates in $S1^{\Delta}$ under all tested conditions, in contrast to $S1^{WT}$. This outcome suggests that EclA function may depend on native expression.

A potential explanation for the failed complementation lies in the origin and structure of the recombinant protein. The recombinant EclA-M14A used in this study was produced in *E. coli* and derived from *E. cloacae* subsp. *cloacae*, whereas the tested strain belongs to subsp. *dissolvens*. This phylogenetic difference may influence protein compatibility or proper folding within the cellular environment, potentially affecting its functional performance. In fact, protein homology results showed that, based on the predicted structure of native EclA from *E. cloacae* subsp. *dissolvens*, a single amino acid substitution (R181N) occurs within 4 Å of the calcium ion involved in ligand binding of the C-terminal binding pocket (Figure 3). While neither residue appears to directly contribute to methyl α-L-selenofucoside binding, the substitution could alter the local chemical environment of the pocket, potentially accommodating different ligands that are native to *E. cloacae* subsp. *dissolvens*. These native ligands might include components of its exopolysaccharide matrix or other carbohydrates specific to this subspecies.

Moreover, as discussed in Chapter 3.1, the native *eclA* gene in *E. cloacae* subsp. *cloacae* may initiate transcription from a downstream start codon, resulting in a truncated version of the protein. The recombinant EclA used here includes an additional 13 N-terminal amino acids, which could alter its structural conformation or interaction interface, thereby impairing its function in autoaggregation. Given these challenges, a more reliable approach for functional complementation would involve a chromosomal knock-in of *eclA*, ensuring that the gene is expressed from its native genomic context. This strategy would avoid the need for plasmid-based overexpression and allow EclA to be processed, localized, and regulated in a physiologically relevant manner.

It is also important to note that complementation failure is not uncommon in biofilm studies. For example, a study on *P. aeruginosa* reported that while LecB complementation restored WT biofilm architecture, complementation with its CdrA lectin failed to do so, despite the presence of its ligand Psl in the biofilm matrix (da Silva et al., 2019). The inability to restore biofilm structure was hypothesized to result from differences in protein stability or environmental sensitivity, or the absence of yet unidentified co-factors or matrix proteins required for full functionality. Similarly, in the case of EclA, simple exogenous addition may be insufficient to replicate the complex requirements for aggregation, particularly if its activity relies on native regulatory components that are not elucidated to date.

In Subchapter 3.2.3, autoaggregation under flow conditions was assessed, simulating more physiologically relevant settings (Figure 4). While some conditions displayed no differences between $S1^{WT}$ and $S1^{\Delta}$, one condition (Figure 4-B) showed that $S1^{\Delta}$ produced a greater number but smaller aggregates compared to the $S1^{WT}$. This phenotype suggests a role for EclA in the maturation of aggregates rather than in their initial formation. It is plausible that the presence of EclA redirects bacterial behavior away from simple surface attachment and towards intercellular aggregation, promoting the development of larger, more mature structures. However, the qualitative nature of the observations and variability between conditions limit the strength of this conclusion. More replicates are necessary to confirm the observed trends.

In addition, optimizing experimental conditions to prevent aggregate detachment is critical for improving the reliability of autoaggregation assays. This includes refining parameters such as incubation time, bacterial settling duration, and growth media composition to enhance the stability of aggregates for accurate visualization and quantification. The current conditions tested (Figure 4) supported the initial formation and stable attachment of aggregates to the channel surfaces. However, with extended incubation, aggregate detachment was consistently observed across all conditions (data not shown). This detachment complicates quantitative

comparisons and underscores the importance of optimizing assay conditions to maintain aggregate integrity throughout the experiment. Additionally, while standard fluorescence and brightfield microscopy provided a useful means for rapid assessment and condition screening, higher-resolution imaging techniques such as confocal microscopy or 3D fluorescence imaging are necessary to quantify biofilm biomass and enable a more robust comparison between strains. These methods would allow for the evaluation of aggregate volume and density, offering deeper insights into the role of EclA in autoaggregate formation.

In summary, this chapter expanded on the findings from Chapter 3.1 by introducing additional experiments to investigate the role of EclA in autoaggregation. These analyses provided key insights into the complexity of EclA's function. The failure of exogenous complementation, for example, suggests that EclA's activity is dependent on its native expression context or requires subspecies-specific compatibility. Furthermore, preliminary data from flow-cell assays hinted at a potential role for EclA in aggregate maturation; however, these findings remain inconclusive due to the qualitative nature of the experiments and the absence of biological replicates. Therefore, this section underscores the need for further investigation using more robust methods, such as chromosomal knock-in for definitive genetic proof, more extensive screening of flow-cell conditions, and advanced microscopy for quantitative analysis, to fully clarify the mechanistic role of EclA in autoaggregate formation.

3.3. The Role of EclA in Virulence and Host Survival

Having established a correlation between *eclA* and in vitro autoaggregation in Chapter 3.1, this chapter transitions to an in vivo setting to investigate whether this phenotype translates to a measurable impact on host survival. The primary aim was to assess the contribution of *eclA* to the virulence of *E. cloacae* subsp. *dissolvens*. To this end, two distinct infection models were sequentially employed. Initially, the zebrafish larva (*Danio rerio*) was selected as a vertebrate model to assess infection outcomes via immersion, with and without physical injury. Following the challenges encountered with this system, the investigation pivoted to the wax moth larva (*Galleria mellonella*) model, a well-established system for studying the virulence of *Enterobacter* species. This chapter describes the results from both models, with a focus on establishing a viable infection system. The following strain designations will be used throughout this chapter; $S1^{WT}$: WT *E. cloacae* subsp. *dissolvens* pMP7605; $S1^{\Delta}$: Δ*eclA E. cloacae* subsp. *dissolvens* pMP7605.

3.3.1. *Danio rerio* Infection Model

To assess the impact of *eclA* on host survival, an immersion-based zebrafish larva (*Danio rerio*) infection model was employed using *E. cloacae* subsp. *dissolvens* pMP7605 strains as detailed in Chapter 7.2. AB line zebrafish larvae were exposed to bacterial suspensions containing either $S1^{WT}$ or $S1^{\Delta}$ at varying concentrations, and larval survivability was monitored for 72 hours post-infection (hpi). Two experimental designs were used: larvae at 24 hours post-fertilization (hpf) were immersed without prior manipulation, while larvae at 48 hpf underwent a post-caudal vein tail amputation immediately before immersion. This injury severed the caudal vein, including the fin fold epithelium and underlying mesenchyme, providing an additional route of entry for bacteria as indicated by previous studies (Nogaret et al., 2021; Scott et al., 2022). This approach allowed the assessment of EclA's role in host survivability under both intact and compromised tissue conditions.

Results showed a 100% larval survivability in all experimental groups, regardless of the presence or absence of *eclA*, the applied bacterial concentration (10^6, 10^7, and 10^8 CFU/mL), or whether larvae were subjected to caudal injury (Figure 5). Neither $S1^{WT}$ nor $S1^{\Delta}$ strains caused any observable mortality over the 72-hour infection period in either the amputated (Figure 5-A) or unamputated (Figure 5-B) groups. These findings suggest that, under the tested conditions, *E. cloacae* subsp. *dissolvens* does not establish a lethal infection in zebrafish larvae via immersion, and that the deletion of *eclA* does not impact host survival in this model.

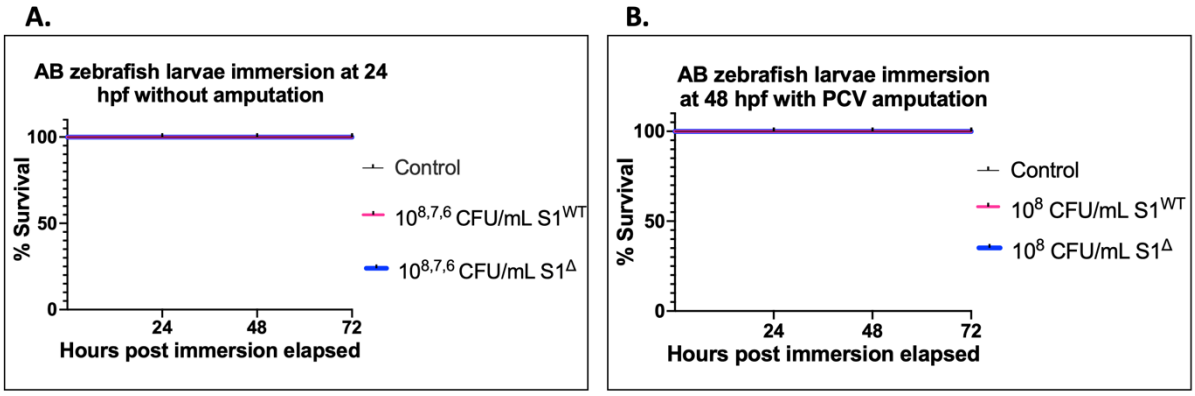

Figure 5: Kaplan-Meier survival curves of *Danio rerio* AB line larvae immersed in $S1^{WT}$ or $S1^{\Delta}$. **(A)** Survival of larvae (n = 12 larvae per group) immersed at 24 hpf in bacterial suspensions of $S1^{WT}$ or $S1^{\Delta}$ at concentrations of 10^6, 10^7, and 10^8 CFU/mL, with N = 1. **(B)** Survival of larvae immersed at 48 hpf following post-caudal vein (PCV) tail amputation. Larvae (n = 24 larvae per group) were exposed to the same bacterial strains in (A) at 10^8 CFU/mL, with N = 1. For both panels, larvae were monitored for 72 hpi and maintained at 28 °C. Bacterial suspensions were prepared from exponential-phase subcultures (OD_{600} = 0.7-0.8) grown in LB supplemented with 60 µg/mL gentamicin, derived from overnight cultures in the same medium. The suspensions were then adjusted to OD_{600} = 1 in 0.3× Danieau's medium (without methylene blue) prior to immersion. Control groups consisted of larvae immersed in 0.3× Danieau's medium (without methylene blue). $S1^{WT}$: WT *E. cloacae* subsp. *dissolvens* pMP7605; $S1^{\Delta}$: Δ*eclA E. cloacae* subsp. *dissolvens* pMP7605.

Since no larval mortality was observed following immersion with either $S1^{WT}$ and $S1^{\Delta}$, *P. aeruginosa* was employed to test for larval killing. Both PAO1 and the more virulent PA14 strains were tested alongside their respective Δ*lecA*Δ*lecB* double mutants, which lack the lectins LecA and LecB known to contribute to biofilm formation and virulence (Fares et al., 2025; Mikkelsen et al., 2011). For PA14 infections, *Danio rerio* larvae of the Casper line were used. Larvae at 24 hpf were immersed in 10^8 CFU/mL suspensions of either the WT PA14 or its Δ*lecA*Δ*lecB* mutant both carrying pMP7605 without prior manipulation. Another experiment was conducted at 48 hpf using larvae that underwent PCV tail amputation immediately prior to immersion in the same bacterial suspensions. Similarly, PAO1 infections were performed using AB line zebrafish larvae under identical conditions. At 24 hpf, uninjured larvae were immersed in 10^8 CFU/mL of either WT PAO1 or its Δ*lecA*Δ*lecB* mutant both carrying pMP7605. At 48 hpf, larvae underwent PCV amputation prior to immersion. These infection setups were designed to replicate conditions reported in previous studies, where

P. aeruginosa exposure, with or without injury, resulted in significant larval mortality, thereby validating their use as positive controls to benchmark the infection model (Pont & Blanc-Potard, 2021).

However, no larval mortality was observed in any of the conditions tested with either PA14 or PAO1 strains harboring pMP7605 (Figure 6). Across all experimental groups, whether infected with WT or Δ*lecA*Δ*lecB* double mutants, and regardless of whether larvae were uninjured (24 hpf) or received PCV tail amputations (48 hpf), survivability remained at 100% throughout the 72-hour post-immersion period. This was consistent across both Casper and AB zebrafish lines. These results suggest that, under the tested conditions, immersion with *P. aeruginosa* at 10^8 CFU/mL does not induce larval death, even with tail injury intended to facilitate bacterial entry. This resistance in the zebrafish larvae lines used in the experimental setup highlights the robustness of the zebrafish innate immune barrier and suggests that a higher bacterial load or more invasive delivery routes may be necessary to induce infection-related mortality in this model.

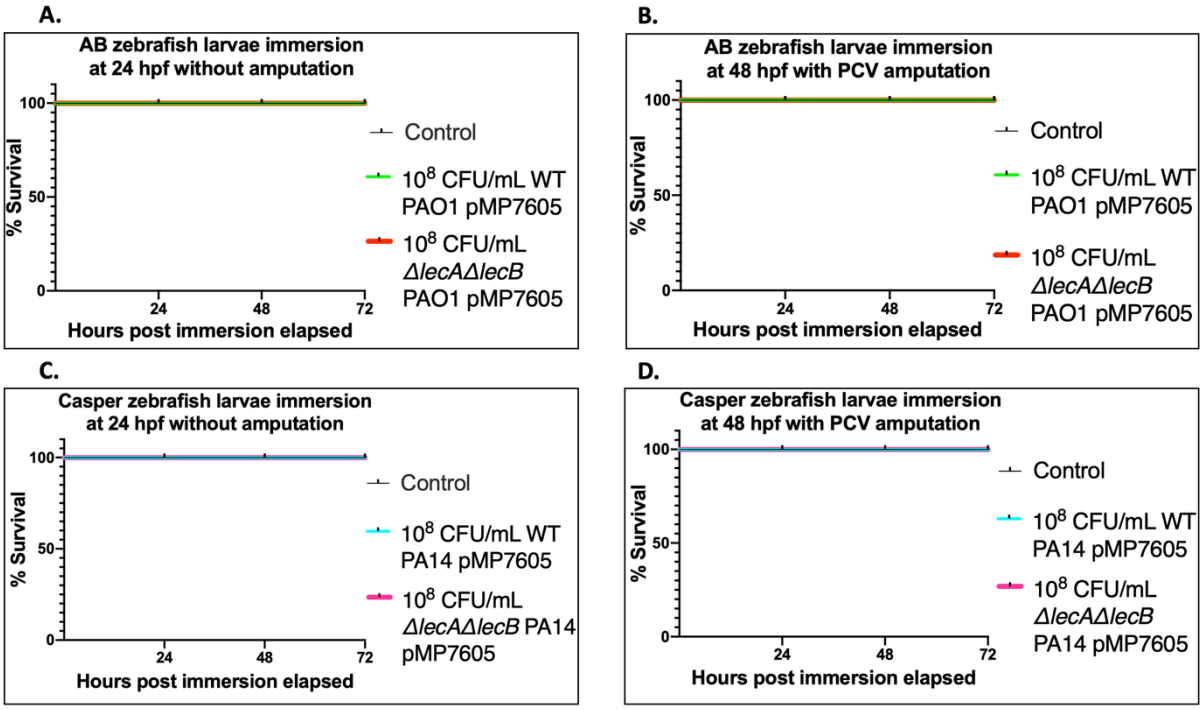

Figure 6: Kaplan-Meier survival curves of zebrafish larvae following immersion in *P. aeruginosa* PAO1 and PA14 strains and their Δ*lecA*Δ*lecB* double mutants. AB and Casper line zebrafish larvae were immersed in bacterial suspensions of either WT or Δ*lecA*Δ*lecB P. aeruginosa* (PAO1 or PA14) both carrying pMP7605 at 10^8 CFU/mL. Bacterial suspensions were prepared from exponential-phase subcultures (OD_{600} = 0.7-0.8) grown in LB supplemented with 60 µg/mL gentamicin, derived from overnight cultures in the same medium.

The suspensions were then adjusted to OD_{600} = 1 in 0.3× Danieau's medium (without methylene blue) prior to immersion. Control groups consisted of larvae immersed in 0.3× Danieau's medium (without methylene blue). **(A)** AB larvae (n = 24 per group) were immersed at 24 hpf in PAO1 suspensions, without tail amputation. **(B)** AB larvae (n = 15 per group) underwent PCV tail amputation at 48 hpf prior to immersion in the same PAO1 suspensions. **(C)** Casper larvae (N = 24 per group) were immersed at 24 hpf in PA14 suspensions, without amputation. **(D)** Casper larvae (n = 10 per group) underwent PCV amputation at 48 hpf immediately before immersion in the same PA14 suspensions. All larvae were incubated at 28 °C for 72 hpi. For all panels, N = 1.

3.3.2. *Galleria mellonella* Infection Model

Since an immersion-based zebrafish model, despite tail amputation, did not yield an infection phenotype, an alternative invertebrate host model using the wax moth larva *Galleria mellonella* was explored as described in Chapter 7.2 to evaluate the role of EclA in host survival during ECC infections. As a first step, the ability of *E. cloacae* subsp. *dissolvens* to cause infection was assessed and compared to *E. cloacae* subsp. *cloacae*, previously introduced in Subchapter 1.3.3. Both strains, harboring the plasmid pMP7605, were injected into *G. mellonella* at varying concentrations to evaluate their virulence, and validate the usage of *G. mellonella* as a suitable infection model for these strains. The following strain designations will be used throughout this subchapter; $S1^{WT}$: WT *E. cloacae* subsp. *dissolvens* pMP7605; $S1^{\Delta}$: Δ*eclA E. cloacae* subsp. *dissolvens* pMP7605. $S2^{WT\text{-}HS0}$: WT *E. cloacae* subsp. *cloacae* pMP7605.

To establish the assay, it was first necessary to evaluate the fitness of the provided larvae, and ensure that mortality could be attributed specifically to infection rather than handling. This included assessing survival in uninjected larvae, in larvae injected with buffer alone (PBS + 20% glycerol), and in groups injected with non-pathogenic bacteria (*E. coli* DH5α) or heat-killed cells. These controls were essential to determine whether any bacterial exposure could trigger mortality, or if larval death might occur simply due to physical injection trauma or bacterial overload. Kaplan-Meier survival curves from Figure 7-A showed that the uninjected group showed a survivability of 93%, indicating that a small proportion of larvae died due to unrelated, background causes. Larvae injected with PBS + 20% glycerol (resuspension buffer) exhibited a survival rate of 86%. A control group injected with 10^4 CFU of *E. coli* DH5α pMP7605 showed a similar survival of 80%, suggesting that injection of a non-pathogenic strain does not significantly impact larval viability. Additionally, larvae injected with heat-

killed preparations of 10^5 CFU of $S1^{WT}$ or $S2^{WT\text{-}HS0}$ demonstrated survivals of 93% and 86%, respectively. Statistical comparison of all survival curves using the Log-rank (Mantel-Cox) test revealed no significant differences between groups ($p = 0.77$). These data indicate that injection alone does not cause mortality, and that virulence observed in subsequent experiments can be attributed to viable *E. cloacae* strains rather than to injection trauma, bacterial overload, or innate immune activation by heat-stable components such as lipopolysaccharide (LPS).

Figure 7-B shows the survival curves of larvae injected with 10^5 CFU of viable $S1^{WT}$ or $S2^{WT\text{-}HS0}$. Larvae infected with $S1^{WT}$ exhibited a survival rate of 46% at 64 hours post-injection, while those infected with $S2^{WT\text{-}HS0}$ showed a higher survival of 73%. In contrast, the negative control group injected with buffer maintained a survival of 86%. Statistical analysis using the Log-rank (Mantel-Cox) test showed no significant difference between the $S2^{WT\text{-}HS0}$-infected group and the negative control. However, the difference in survival between the negative control and the $S1^{WT}$-infected group was statistically significant ($p = 0.02$).

A dose-response analysis of larval mortality following injection with different doses (10^5, 10^3, and 10 CFU) of $S1^{WT}$ and $S2^{WT\text{-}HS0}$ was also established (Figure 7-C). This experiment aimed to evaluate the ability of each strain to induce lethality across different bacterial loads. The results demonstrated a more consistent dose-dependent response for $S1^{WT}$ with a clear decrease in larval survival as the bacterial dose increased. In contrast, larvae infected with 10^3 and 10 CFU of $S2^{WT\text{-}HS0}$ exhibited nearly identical survival rates, indicating limited or no killing at these lower concentrations. This suggests that the bacterial load used for subsp. *cloacae* may have been below the effective threshold required to establish infection, and that higher doses might be necessary to observe a clearer dose-response trend. These findings suggest that *E. cloacae* subsp. *dissolvens* exhibits higher virulence in *G. mellonella* compared to subsp. *cloacae* under the tested conditions, reinforcing its utility as a model for studying pathogenicity factors such as EclA.

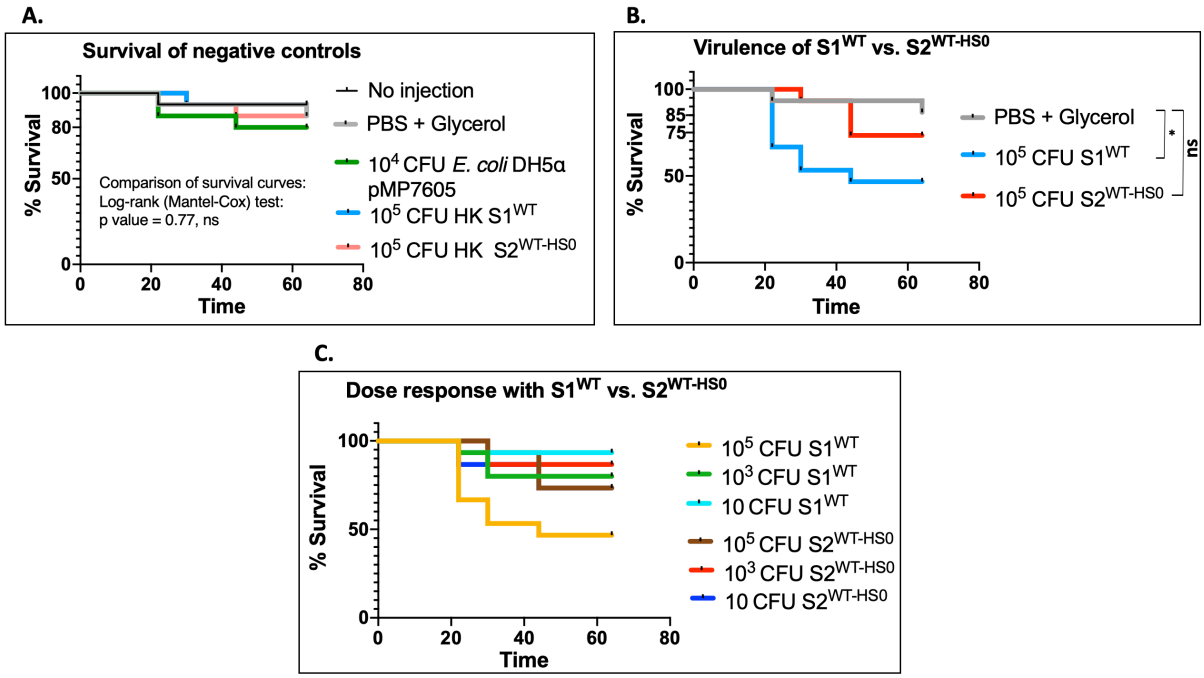

Figure 7: Survival of *Galleria mellonella* larvae following injection with $S1^{WT}$ or $S2^{WT\text{-}HS0}$. All data presented in this figure were obtained from a single experiment (N = 1). Larvae were injected with 5 µL of bacterial suspensions stored at -80 °C in PBS supplemented with glycerol. Post-injection, larvae were incubated at 37 °C for 64 hours, and survival was monitored based on the absence of response to mechanical stimulation. Viable CFUs were confirmed by plating 5 µL of each injected dose. 15 larvae were used per any given group. **(A)** Survival probability of control groups with a statistical significance test using Log-rank (ns: no significant difference) (HK: heat-killed). **(B)** Survival of larvae injected with WT *E. cloacae* subsp. *dissolvens* or subsp. *cloacae* with a statistical significance test using Log-rank (* = $p < 0.05$ = significant difference). **(C)** Dose-response survival curves for larvae injected with different concentrations of $S1^{WT}$ or $S2^{WT\text{-}HS0}$. $S1^{WT}$: WT *E. cloacae* subsp. *dissolvens* pMP7605; $S2^{WT\text{-}HS0}$: WT *E. cloacae* subsp. *cloacae* pMP7605.

Discussion, <u>Chapter 3.3</u>: The role of EclA in virulence and host survival

This chapter aimed to investigate the role of *eclA* in host survival following exposure to *E. cloacae* using two in vivo models. Zebrafish larvae (*Danio rerio*) were first used to assess the effect of EclA on host survival; however, as no mortality was observed in this model, wax moth larvae (*Galleria mellonella*) were subsequently employed to evaluate their suitability as an alternative infection model.

In Subchapter 3.3.1, zebrafish larvae were selected as an initial infection model due to numerous advantages. The optical transparency of zebrafish enables microscopy, making it possible to visualize fluorescently labeled *E. cloacae* expressing mCherry, immersion infection experiments are relatively easy to handle, and the availability and ease of receiving zebrafish embryos were an added advantage. An important aspect of studying the infection on zebrafish is their genome which shares considerable homology with humans, where over 80% of human disease-associated genes are conserved in zebrafish (Howe et al., 2013). Most importantly, zebrafish develop a functional innate immune system as early as 1 dpf, including macrophages, neutrophils, pattern recognition receptors, cytokines, chemokines, and complement components, many of which mirror their mammalian counterparts (Van der Vaart et al., 2012). Zebrafish larvae infection models are well-established in studying Enterobacteriaceae and ESKAPE pathogen virulence, including *Acinetobacter baumanni*, *Salmonella*, *E. coli*, *Klebsiella pneumoniae*, and *P. aeruginosa* (Flores et al., 2023; Schmitz et al., 2024; Varas et al., 2017). Therefore, an attempt to establish a zebrafish infection model using *E. cloacae* was a relevant extension even though it had not been previously explored.

Despite previous reports demonstrating zebrafish susceptibility to *P. aeruginosa* via immersion (Díaz-Pascual et al., 2017), and particularly when coupled with tail injury (Nogaret et al., 2021), no significant larval mortality was observed in any condition tested with either $S1^{WT}$ or *P. aeruginosa* strains carrying pMP7605 (Figure 5, 6). This was true across different zebrafish lines (AB and Casper), developmental stages (24 hpf and 48 hpf), and bacterial loads (up to 10^8 CFU/mL). Even PCV amputation, intended to breach tissue barriers and provide a route for bacterial entry, failed to produce lethality (Figure 5, 6). These results suggest that zebrafish larvae are highly resistant to infection by immersion under the tested conditions, and that $S1^{WT}$ does not exhibit virulence in this host system via natural or injury exposure.

Several explanations may account for this resistance. Zebrafish larvae at early developmental stages have robust innate immune barriers and limited oral uptake, especially before mouth opening (< 72 hpf), which may reduce infection efficiency during immersion (Kimmel et al., 1995). Alternatively, a microinjection-based approach although laborious, could be better in establishing lethal infections, either local or systemic, depending on the injection route. In addition to delivering the bacterial load immediately inside the zebrafish, injection avoids effects related to injury-induced immune responses. Notably, tissue damage in zebrafish larvae caused by amputation or wounding can trigger rapid neutrophil swarming, which effectively seals off breached barriers within 20 minutes post-injury, thereby limiting bacterial entry and dissemination (Poplimont et al., 2020). This rapid immune response may help explain the

absence of zebrafish mortality observed in the experiments, even following tail amputation. Additionally, while 28 °C is optimal for zebrafish development, it may not support optimal expression of *E. cloacae* virulence genes, which would be induced at 37 °C in a human infection setting.

Subchapter 3.3.2 aimed at overcoming the limitations of the zebrafish model by employing *G. mellonella* larvae as an alternative host system. This invertebrate model has proven utility for studying the virulence of different species in ECC and other human pathogenic bacteria (Ganbold et al., 2023; Girlich et al., 2021; Ménard et al., 2021). Furthermore, the model offers compatibility with 37 °C, a temperature that more closely mimics human infection conditions, and where *E. cloacae* thrive at. Importantly, *G. mellonella* possesses an innate immune system with functional similarities to that of mammals. Hemocytes, its primary immune cells, resemble mammalian neutrophils and are involved in key defense mechanisms such as phagocytosis, nodulation, encapsulation, lysozyme production, and the secretion of antimicrobial peptides and opsonins (Boman & Hultmark, 1987).

In this subchapter, both $S1^{WT}$ and $S2^{WT\text{-}HS0}$ were injected into the hemocoel of *G. mellonella* larvae at various doses to assess their pathogenic potential and to establish an infection model suitable for elucidating in future experiments the role of EclA in host survival following *E. cloacae* infection. Heat-killed bacteria, and non-pathogenic *E. coli* DH5α did not cause significant mortality, confirming that killing was species-specific and due to active infection rather than injection trauma or immune overactivation (Figure 7-A).

$S1^{WT}$ induced substantial mortality at 10^5 CFUs injected (46% survival at 64 hpi), while $S2^{WT\text{-}HS0}$ caused less killing (73% survival) at the same injected dose, a number that had no significant difference after statistical analysis compared to larvae injected with buffer (Figure 7-B). A dose-response analysis further showed that $S1^{WT}$ exhibited a clear gradient of lethality from 10 to 10^5 CFUs injected, while $S2^{WT\text{-}HS0}$ showed limited killing at lower doses, suggesting it has a higher infectious threshold (Figure 7-C). The outcome of the results aligns with previous studies assessing the virulence of various ECC species in the *G. mellonella* model. Notably, at the same dose of 10^5 CFU, $S1^{WT}$ demonstrated greater virulence than the highly virulent *E. hormaechei* and *E. xiangfangensis*, two species commonly implicated in hospital-associated infections (Girlich et al., 2021). Among tested ECC members, only *E. bugandensis* exhibited higher virulence, with survival dropping to 20% at 64 hpi. These comparisons highlight the pathogenic potential of $S1^{WT}$ in the *G. mellonella* model and support its relevance for further infection experiments. Similarly, in another study using *E. cloacae* clinical isolates, injection of 10^5 CFU resulted in 25% larval survival at 64 hpi, while increasing the dose to 10^6

CFU led to complete mortality by 48 hpi (H.-F. Yang et al., 2017). Additionally, very few larval deaths occurred with doses at or below 10^4 CFU, consistent with the current experiment conducted.

These data suggest that a higher inoculum of $S2^{WT\text{-}HS0}$ in the present study could result in stronger virulence and more larval killing. Additionally, although CFU counts were confirmed after thawing, the use of frozen bacterial stocks may have influenced gene expression and decreased virulence. Therefore, utilizing freshly cultured bacteria could improve the consistency of the dose-response relationship in $S2^{WT\text{-}HS0}$ and enhance the overall virulence expression of both *E. cloacae* strains used in this model. In the same study cited, infection assays performed at reduced incubation temperatures (30 °C and 25 °C instead of 37 °C) resulted in significantly increased larval survival at a given bacterial dose, underscoring the importance of temperature in virulence expression (H.-F. Yang et al., 2017). This finding may help explain the lack of mortality observed in the zebrafish model, which was conducted at 28 °C. These results further support the use of *G. mellonella* as a more suitable model for studying *E. cloacae* virulence compared to temperature-limited hosts such as *Caenorhabditis elegans* (20-25 °C) (Marsh & May, 2012) or zebrafish larvae (28 °C). It is important to note that the *Galleria* infection data were derived from a single experiment which constitutes a limitation in this subchapter. Attempts to repeat the experiment using newly sourced larvae failed due to poor larval fitness reflected by high background mortality in uninjected controls (data not shown). Future work should ensure rigorous sourcing of research-grade larvae that are fit, healthy and at the same developmental stage.

In summary, while *E. cloacae* subsp. *dissolvens* failed to induce infection in zebrafish larvae via immersion, it displayed virulence in the *G. mellonella* model, surpassing that of the model organism *E. cloacae* subsp. *cloacae*. Although the results originated from one experimental assay, compatible literature findings and appropriate controls validated the results. Future experiments should build on these insights by confirming these results across biological replicates and expanding into the functional elucidation of EclA, specifically, by comparing the virulence of the Δ*eclA* mutant with that of the WT strain in the established *Galleria* infection model.

Closing Section 3: Elucidating the role of EclA in *E. cloacae* subsp. *dissolvens*

This section investigated the molecular and functional characterization of the novel lectin EclA in *E. cloacae* subsp. *dissolvens* by generating a Δ*eclA* mutant and conducting in vitro phenotypic assays, structural analyses, and in vivo infection experiments.

EclA as a determinant of autoaggregation

Chapter 3.1 demonstrated that deletion of *eclA* results in a loss of autoaggregation by $S1^{WT}$ in an in vitro autoaggregation assay under shaking conditions. Despite no detectable effect on planktonic growth, the Δ*eclA* mutant formed no visible aggregates, in contrast to the WT strain, which developed large, free-floating ones. This phenotype was not attributable to differences in fluorescence or cell density, affirming a specific role of EclA in bacterial cohesion.

Biochemical analyses indicated that EclA is both cell-associated and released in small amounts, reminiscent of other bacterial lectins such as LecA and LecB in *P. aeruginosa*. Interestingly, fucose competition assays failed to displace EclA from bacterial pellets, suggesting that its membrane association is either not mediated by the fucose-binding C-terminal domain or involves stronger or structurally obstructed interactions. The observed lower apparent molecular weight of native EclA relative to recombinant forms supports the hypothesis that it is naturally translated from a downstream start codon, producing a shorter, potentially functionally distinct isoform.

Functionally, recombinant EclA exhibited fucose-sensitive hemagglutination, albeit with markedly lower potency than LecB. This difference likely reflects the higher fucose-binding affinity of LecB compared to EclA, as discussed, as well as differences in the number, specificity, and spatial arrangement of their carbohydrate-binding domains. EclA possesses two fucose-binding domains oriented on the same side of the protein, whereas LecB forms a tetramer with four fucose/mannose-binding sites arranged on opposing faces, enabling multivalent binding to red blood cells. This relatively modest affinity of EclA to fucose could mean that it functions as a weak cross-linker supporting autoaggregation, rather than mediating strong, static interactions, assuming the C-terminus is indeed responsible for the observed autoaggregation phenotype.

Chapter 3.2 extended this functional analysis by exploring whether the aggregation phenotype could be complemented with exogenous recombinant EclA. The failure of both full-length and M14A variants to restore aggregation supports the notion that EclA's function is regulated by

its native cellular context, possibly because the native EclA from *E. cloacae* subsp. *dissolvens* carries an R181N amino acid substitution within 4Å of its C-terminal binding site compared to the recombinant protein from *E. cloacae* subsp. *cloacae*.

Together, these data highlight EclA as a key biofilm component, potentially functioning as a structural linker within an EPS matrix enriched in fucose-containing polymers like colanic acid. While exogenous complementation was unsuccessful, future chromosomal knock-in strategies may more accurately recapitulate native EclA function.

No virulence in zebrafish, stronger potential in *Galleria mellonella*

In Chapter 3.3, the role of EclA and the infectious potential of $S1^{WT}$, $S1^{\Delta}$, and $S2^{WT\text{-}HS0}$ were explored in the context of host interaction using two infection models. In the zebrafish larvae (*Danio rerio*) model, neither $S1^{WT}$ or $S1^{\Delta}$ caused mortality via immersion, even following tail amputation, a strategy used to breach tissue barriers. Surprisingly, even virulent *P. aeruginosa* strains (PAO1 and PA14) failed to induce killing, suggesting that the zebrafish model, under the tested conditions, does not support infection at the bacterial loads examined, contrary to what has been reported in the literature.

Multiple factors likely contribute to this resistance: zebrafish innate immunity is active by 1 dpf, tail injury triggers rapid neutrophil swarming that restricts pathogen entry, and the experimental temperature of 28 °C may suppress *E. cloacae* virulence gene expression.

To circumvent these limitations, the *G. mellonella* infection model was employed. This system offers the advantages of temperature compatibility with mammalian pathogens, and an innate immune system that resembles to key components of vertebrate responses. Injection-based infection allowed controlled delivery of bacterial loads directly into the hemocoel.

With that model, *E. cloacae* subsp. *dissolvens* induced significant larval mortality at 10^5 CFU, outperforming *E. cloacae* subsp. *cloacae* under identical conditions. A dose-response experiment further confirmed the higher virulence potential of subsp. *dissolvens*, which showed clear lethality trends across decreasing CFUs. In contrast, subsp. *cloacae* only showed virulence at the highest dose, and even then, with weak effect.

The data indicate that *E. cloacae* subsp. *dissolvens* can cause mortality in this model, suggesting its potential utility for investigating the contribution of pathogenicity determinants such as EclA. Notably, the 46% mortality at 10^5 CFU aligns with virulence reported for clinical ECC strains, suggesting that *dissolvens*, despite its classification as a plant pathogen, can act as a pathogen in animal hosts.

However, these conclusions are limited by the fact that only a single successful *G. mellonella* infection experiment was performed. Subsequent trials were hindered by poor larval fitness and restricted availability, highlighting the importance of sourcing high-quality larvae for reproducible infection experiments.

Future directions and functional elucidation of EclA

Two key results from this chapter are the strong impact of EclA in bacterial autoaggregation, and the hemagglutination of human red blood cells by its recombinant form. While immersion-based infection in zebrafish proved ineffective, the successful establishment of a *Galleria* infection model sets the stage for future virulence comparisons between WT and Δ*eclA* strains. Further validation of EclA's contribution to pathogenicity will require:

- **Chromosomal complementation** to definitively establish causality of EclA in bacterial autoaggregation
- **High-resolution biofilm imaging** such as confocal microscopy, to quantify aggregate morphology and density in flow-cell assays
- **Ligand-binding characterization** beyond fucose, particularly regarding the N-terminal domain of EclA. Functional analysis of EPS composition could help with the identification
- **Structure-function relationship** studies to investigate the impact of the R181N substitution in the C-terminal domain by generating point mutants or by expressing the native EclA from *E. cloacae* subsp. *dissolvens*, to assess how these structural differences influence ligand binding and the ability to complement the $S1^{\Delta}$ phenotype.
- **Larval survival assays with Δ*eclA* mutants** in *G. mellonella* to link EclA function to host outcomes
- **Adhesion assays using human cells**, such as urinary tract or lung cell lines, to test whether WT *E. cloacae* subsp. *dissolvens* binds more robustly than the Δ*eclA* mutant
- **Surface localization studies**, cell fractionation experiments can help determine whether EclA is bacterial surface-associated. If confirmed, it would support a dual-binding mechanism in which one domain binds to bacterial exopolysaccharides while the other engages host glycans.

Ultimately, the findings support a model in which EclA functions as a fucose-specific scaffolding lectin that facilitates biofilm formation through low-avidity interactions with fucosylated EPS. Its potential surface localization, combined with multiple carbohydrate-

binding domains and its demonstrated ability to cross-link red blood cells, suggests that EclA may also act as a bridging adhesin, linking *E. cloacae* subsp. *dissolvens* to host tissues and thereby promoting colonization.

4. Elucidating the Role of EclA in *E. cloacae* subsp. *cloacae*

The *eclA* gene is also present in *E. cloacae* subsp. *cloacae*, a widely used model organism for studying infections within the *E. cloacae* species, in part because its genome was the first to be fully sequenced in ECC (Ren et al., 2010). This section explores the functional characteristics of EclA in subsp. *cloacae*, comparing them to those previously established for EclA in subsp. *dissolvens*. Specifically, it investigates whether EclA exhibits conserved roles in release, localization, and autoaggregate formation across the two subspecies. As outlined in Subchapter 1.3.3, *E. cloacae* subsp. *cloacae* is more frequently isolated from clinical infections than subsp. *dissolvens*, highlighting the medical relevance of studying EclA's function in this context and its potential role in human pathogenesis (Chang et al., 2022; Garinet et al., 2018; S. Liu et al., 2022).

4.1. Generation of an *eclA* Knockout Mutant

To investigate the role of EclA in *E. cloacae* subsp. *cloacae*, a knockout mutant was generated using allelic exchange mutagenesis as was done in Chapter 3.1 for *E. cloacae* subsp. *dissolvens*.

4.1.1. Construction of a Compatible Mutator Plasmid

Following the successful use of the suicide vector pKNG101_16657 for *eclA* deletion via two-step allelic exchange in *E. cloacae* subsp. *dissolvens* (Chapter 3.1), a parallel strategy was employed to delete *eclA* in *E. cloacae* subsp. *cloacae*. For this, a new construct, pKNG101_30054, was generated by cloning the fused nucleotide sequences flanking the *eclA* gene from subsp. *cloacae* (SI Table 1) into the pKNG101 backbone.

However, a major limitation emerged: pKNG101 carries a streptomycin resistance marker, and *E. cloacae* subsp. *cloacae* exhibits inherent resistance to streptomycin, rendering this selection ineffective. To address this, a gentamicin resistance (GmR) cassette containing the GmR gene, which encodes gentamicin-3-acetyltransferase (GenBank: AAB06696.1), was amplified by PCR from plasmid pMP7605 (Figure 8-A). This gene originates from the parent plasmid of

pMP7605, the cloning vector pBBR1MCS-5 (GenBank: U25061.1), and was amplified along with approximately 300 bp of flanking sequence using the primers listed in (SI Table 3), as described in Chapter 7.3. The cassette was then inserted into pKNG101_30054 following successful single-site SpeI digestion and ligation (Figure 8-B) resulting in the construct pKNG101_30054_GmR as indicated in Chapter 7.3. The ligation product was then used to transform various *E. coli* strains.

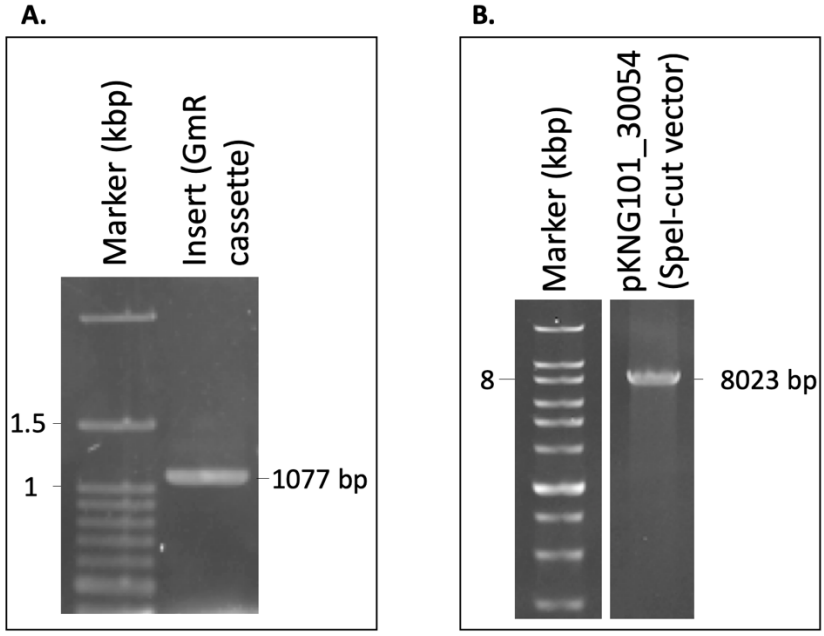

Figure 8: Analytical gel electrophoresis confirming insert amplification and vector digestion for the construction of pKNG101_30054_GmR. (A) PCR amplification of the gentamicin resistance (GmR) cassette from plasmid pMP7605. The gel shows a distinct band at the expected size (1077 bp), confirming successful amplification of the insert intended for ligation. **(B)** Restriction digestion of the suicide vector pKNG101_30054 with SpeI, producing linearized vector DNA for subsequent ligation with the GmR cassette. The band at 8023 bp confirms successful digestion.

Notably, only electrocompetent TransforMax™ EC100D™ pir-116 cells yielded clones on gentamicin LB agar. In contrast, although *E. coli* BW19610 and SM10 λpir successfully supported cloning of pKNG101, pKNG101_16657 and pKNG101_30054, transformation with pKNG101_30054_GmR was unsuccessful for unknown reasons.

To verify the successful construction of pKNG101_30054_GmR and assess its expected plasmid size, miniprepped DNA from seven colonies was subjected to SpeI restriction digestion. Unexpectedly, none of the samples produced digestion patterns corresponding to the

expected plasmid size (Figure 9-A). To investigate this further, PCR was performed on three plasmids to amplify the GmR cassette along with the adjacent *eclA* flanking sequences. All three plasmids yielded the expected amplicon size (Figure 9-B), confirming the presence of the gentamicin resistance insert, despite the puzzling restriction results.

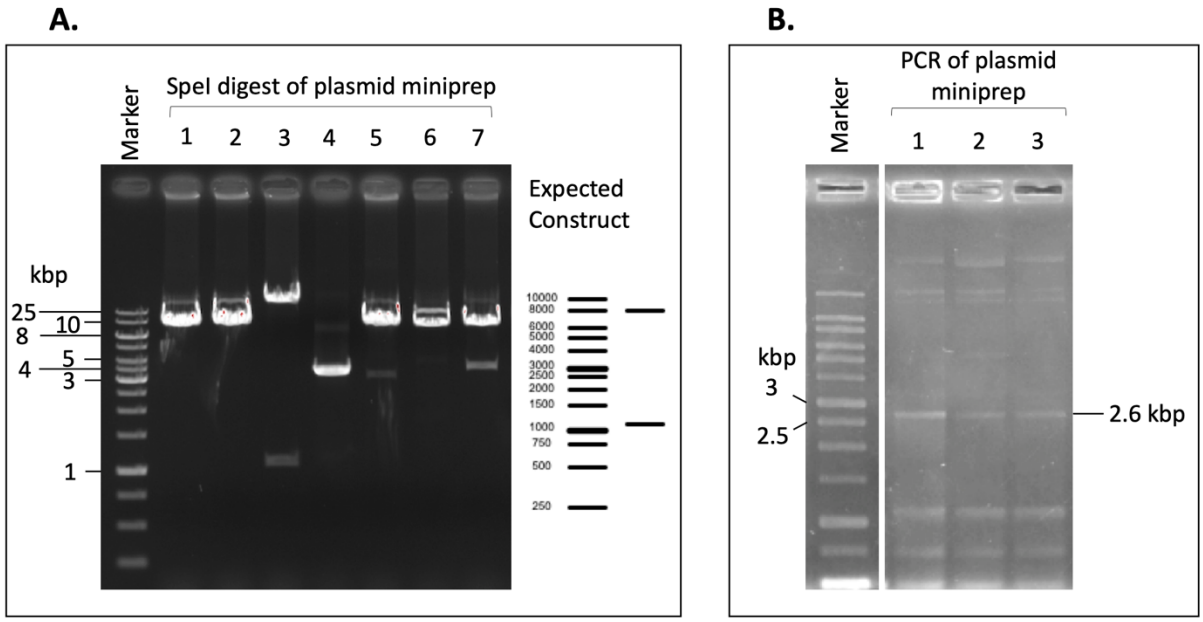

Figure 9: Verification of plasmid construct pKNG101_30054_GmR by restriction digestion and PCR amplification. (A) Analytical gel electrophoresis of SpeI-digested plasmid DNA miniprepped from seven positive colonies (1-7) following ligation and transformation of the GmR cassette into pKNG101_30054. The expected restriction fragment sizes based on the theoretical map of the construct are shown on the right of the gel, serving as a reference for comparison. **(B)** PCR amplification of the gentamicin resistance gene and adjacent fused *eclA* flanking sequences from miniprepped plasmids of colonies 1-3 using primer pair #1001 and MF 18.1. The band at ~2.6 kb was observed in all three samples, confirming the correct insertion of the GmR cassette adjacent to the fused flanking regions of *eclA* from *E. cloacae* subsp. *cloacae*.

To investigate the unexpected restriction digest pattern, plasmid DNA from colony 2 (Figure 9) was sequenced. The results confirmed that the plasmid contained the fused upstream and downstream *eclA* flanking sequences, with the GmR gene correctly positioned immediately downstream of the fusion site, as intended (Figure 10-C). The SpeI site used for insert ligation was restored as expected, while the second anticipated SpeI site (illustrated in Figure 10-B) appeared to be mutated (Figure 10-C).

Interestingly, only a very short (36 bp) sequence of the original streptomycin resistance (SmR) locus remained, and a rearranged sequence architecture was observed in its place (Figure 10-C). This rearrangement comprised duplicated or partially duplicated segments originating from internal regions of the native pKNG101_30054 plasmid (represented in Figure 10-A). Among these features represented in Figure 10-C, was a non-canonical insertion of an R6K origin of replication (New Ori), flanked by an unassigned DNA fragment (Part of UN seq.) derived from a larger native region within pKNG101_30054 (UN seq.), and the same residual nucleotide sequence from the original SmR locus (SmR seq. remaining). This was followed by a segment corresponding to part of the reverse primer used to amplify the GmR cassette (originally only present in the insert), a second unmutated SpeI site (likely the one intended to form during ligation), and again, the same residual SmR sequence replicated. Collectively, these findings suggest an internal rearrangement or partial duplication rather than the insertion of entirely foreign DNA.

Downstream of this rearranged region, the plasmid resumed with the canonical R6K origin and a large unannotated sequence (UN seq.), both of which were fully (R6K) or partially (unannotated region) duplicated in the upstream architectural rearrangement Figure 10-C. Other essential plasmid features also remained intact, including the *sacB* gene for counter-selection, its upstream promoter, and the oriT and traJ elements necessary for conjugative transfer of pKNG101_30054_GmR into *E. cloacae* subsp. *cloacae* Figure 10-C.

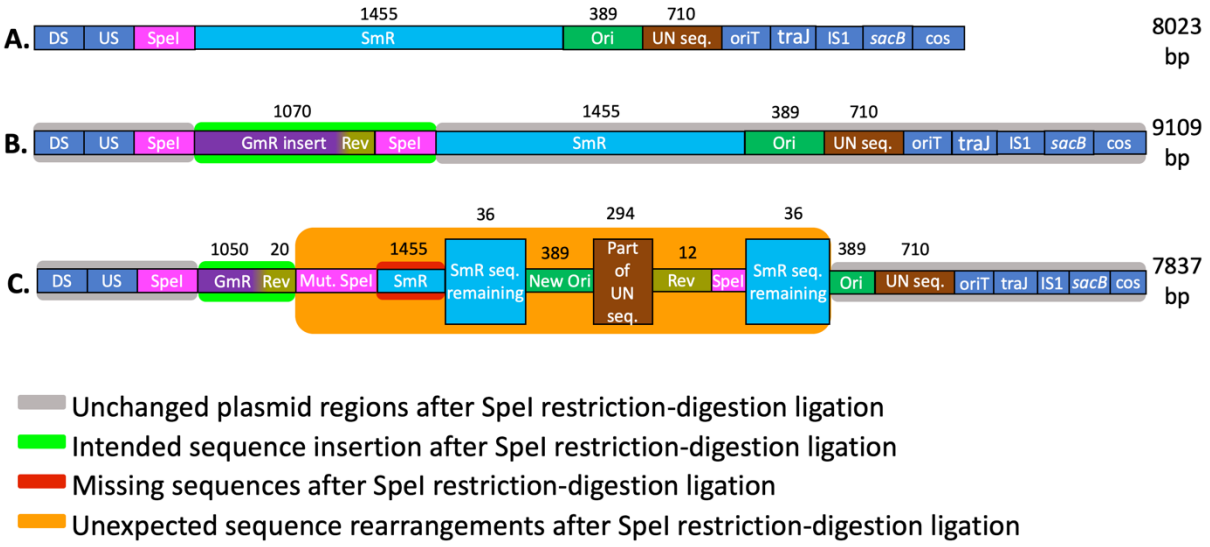

Figure 10: Schematic representation of plasmid structures from whole-plasmid sequencing. Panels A-C depict the architecture of pKNG101_30054 and pKNG101_30054_GmR, with rectangles representing key genetic components or restriction

sites derived from sequencing data. **(A)** Native pKNG101_30054 plasmid showing intact structure prior to insertion. **(B)** Theoretical structure of pKNG101_30054_GmR after insertion of the 1,077 bp gentamicin resistance cassette at the SpeI site via restriction digestion-ligation. **(C)** Final structure of pKNG101_30054_GmR based on ONT sequencing. Sharp-edged rectangles represent genes or restriction sites. Gray, round-edged rectangles represent unchanged plasmid regions. Green, round-edged rectangles represent the intended sequence insertion. Red, round-edged rectangles indicate deleted sequences. Orange, round-edged rectangles indicate unexpected sequences observed post-ligation. Plasmid lengths (in bp) are shown to the right of each map. Numbers above genes indicate their length in base pairs. Matching gene colors from different panels, or within the same panel (with exception to dark blue), denote 100% sequence identity unless otherwise specified. DS: DNA sequence downstream *eclA* in *E. cloacae* subsp. *cloacae*. US: DNA sequence upstream of *eclA* in *E. cloacae* subsp. *cloacae*.

4.1.2. A 2-step Allelic Exchange for the Deletion of *eclA*

As pKNG101_30054_GmR carried the fused *eclA* flanks, GmR, *sacB*, oriT, and traJ, all of which facilitate homologous recombination, the plasmid was used to perform the *eclA* deletion, despite its unexpected rearrangements. Similarly to the 2-step allelic exchange strategy used for *eclA* deletion in *E. cloacae* subsp. *dissolvens* (Chapter 3.1), *eclA* in subsp. *cloacae* was precisely excised without disrupting adjacent sequences or introducing genetic scars as detailed in Chapter 7.3. Following recombination, PCR using primers flanking the *eclA* locus was performed as indicated in Chapter 7.3. A band shift consistent with the expected size reduction confirmed successful deletion and generation of the Δ*eclA* mutant (Figure 11A). Both WT strain and its Δ*eclA* derivative were further transformed with pMP7605 for the purpose of subsequent experiments, as indicated in Chapter 7.3. These transformants are designated $S2^{WT\text{-}HS0}$ and $S2^{\Delta\text{-}HS3}$, respectively, as later introduced in Subchapter 4.4.1. In addition, WGS of these transformed strains confirmed the precise deletion of *eclA* without affecting adjacent regions (Figure 11-B).

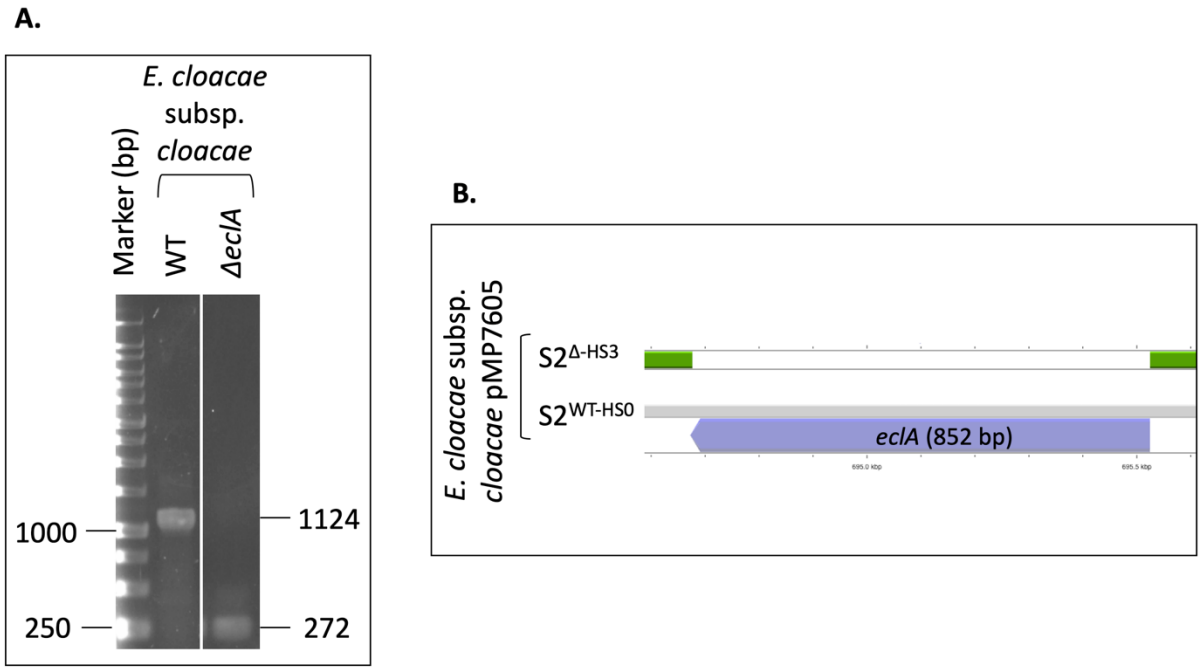

Figure 11: Validation of *eclA* deletion in *E. cloacae* subsp. *cloacae* using colony PCR and whole-genome sequencing. (A) Analytical agarose gel electrophoresis of colony PCR products amplifying the *eclA* locus from WT and Δ*eclA* colonies. Expected band lengths of amplicons (in bp) are indicated to the right of the gel image. **(B)** Schematic representation of the *eclA* locus based on WGS analysis, generated using the web-based platform Proksee. Both $S2^{WT\text{-}HS0}$ and $S2^{\Delta\text{-}HS3}$ are pMP7605-transformed using the same WT and Δ*eclA* *E. cloacae* subsp. *cloacae* backgrounds shown in (A), with the transformed WT strain designated as $S2^{WT\text{-}HS0}$ and the transformed Δ*eclA* strain as $S2^{\Delta\text{-}HS3}$ (introduced in Subchapter 4.4.1). The native *eclA* locus is shown in gray, with the coding DNA sequence (CDS) marked by a blue arrow. In $S2^{\Delta\text{-}HS3}$, the corresponding region is shown in green, representing nucleotide sequences with 100% identity to the WT locus outside the deleted *eclA* gene.

Discussion, Chapter 4.1: Generation of an *eclA* knockout mutant in *E. cloacae* subsp. *cloacae*

This chapter aimed to expand on previous work in *E. cloacae* subsp. *dissolvens*, by generating a corresponding Δ*eclA* mutant in *E. cloacae* subsp. *cloacae*, the frequently employed model organism of ECC, using allelic exchange. The suicide vector pKNG101 was again employed, but its native streptomycin resistance marker was not compatible with this strain due to intrinsic resistance. To overcome this limitation, the gentamicin resistance gene from pMP7605 was PCR-amplified and successfully inserted into pKNG101_30054, a derivative of pKNG101 harboring the flanking sequences of *eclA*. This was done via single-site SpeI digestion and

ligation to generate pKNG101_30054_GmR (Figure 8). While initial transformations into *E. coli* strains BW19610 and SM10 λpir were unsuccessful, raising the possibility of a failed ligation, subsequent transformation using TransforMax™ EC100D™ pir-116 cells confirmed successful plasmid ligation. However, unexpected outcomes were observed during downstream validation.

Restriction digestion of plasmid DNA from multiple colonies did not produce the expected fragment sizes (Figure 9-A). However, PCR targeting the gentamicin cassette and adjacent *eclA* flanking regions confirmed the presence of the correct insert (Figure 9-B), indicating that the ligation had at least partially succeeded.

Subsequent plasmid sequencing revealed an unexpected and complex rearrangement in the construct (Figure 10-C). Notably, while the correct fused *eclA* flanking regions and gentamicin resistance gene were present in the expected configuration, the streptomycin resistance cassette from the original vector was lost and replaced by a rearranged sequence architecture. This rearrangement included partial duplication of internal sequences from the native pKNG101_30054 backbone, including a non-canonical R6K origin of replication, segments derived from a reverse primer used during insert amplification, and residual nucleotide fragments from the original streptomycin locus.

This rearrangement likely arose during the transformation process, since the PCR insert and the pKNG101_30054 vector were of expected size and sequence. Unknown in vivo recombination events could have driven this process. Further analysis of this recombination is outside the scope of this work, but despite these unexpected findings, the essential functional components of the plasmid, including the fused flanking sequences, gentamicin marker, *sacB* gene for counter-selection, and mobilization elements, remained intact. This allowed successful conjugation of pKNG101_30054_GmR into *E. cloacae* subsp. *cloacae*, enabling two-step allelic exchange.

Using this construct, *eclA* was successfully deleted in *E. cloacae* subsp. *cloacae* without disrupting adjacent regions. PCR across the flanking regions showed a band shift consistent with *eclA* deletion (Figure 11-A), and whole-genome sequencing confirmed that the gene was precisely excised (Figure 11-B). This validated that, despite the rearranged plasmid architecture, the core function of the mutator construct was preserved.

In summary, while the construction of pKNG101_30054_GmR encountered unexpected recombination events, the strategy remained effective in generating a scarless Δ*eclA* mutant in *E. cloacae* subsp. *cloacae,* which would provide the foundation for comparative EclA functional studies described in the following chapters.

4.2. Growth Comparison: WT vs. Δ*eclA E. cloacae* subsp. *cloacae*

To assess whether *eclA* influences the general physiology of *E. cloacae* subsp. *cloacae* strains harboring pMP7605, which were used in subsequent experiments, growth kinetics of pMP7605-transformed WT and Δ*eclA E. cloacae* subsp. *cloacae* strains, designated as $S2^{WT\text{-}HS0}$ and $S2^{\Delta\text{-}HS3}$, were monitored in liquid culture over a 24-hour period as described in Chapter 7.4. The results revealed no significant differences ($p = 0.94$) in growth dynamics between the two strains under the tested conditions (Figure 12), indicating that deletion of *eclA* does not impair the overall growth capacity of *E. cloacae* subsp. *cloacae*. This suggests that EclA is not required for essential cellular functions or metabolic fitness in standard culture conditions.

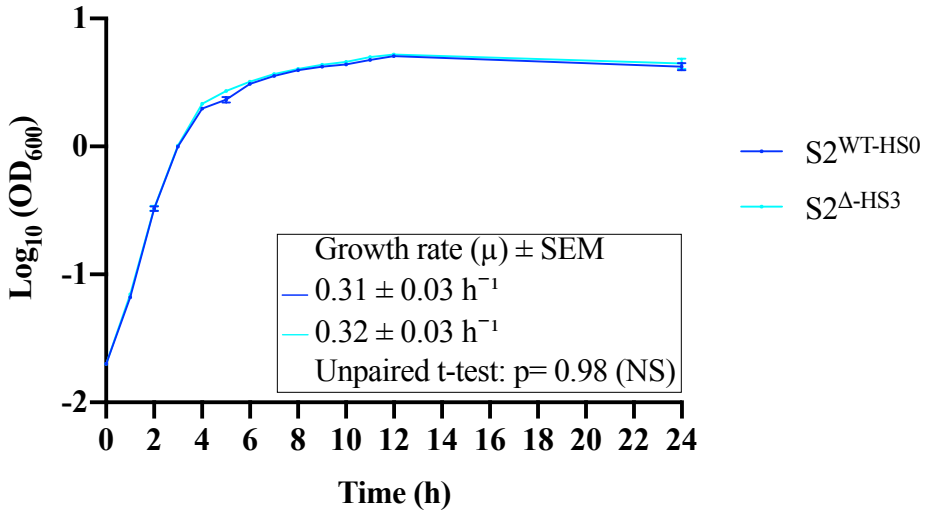

Figure 12: Growth kinetics of pMP7605-transformed WT and Δ*eclA* strains of *E. cloacae* subsp. *cloacae* over 24 hours. Growth curves of $S2^{WT\text{-}HS0}$ and $S2^{\Delta\text{-}HS3}$ were monitored in LB medium at 37 °C with shaking over 24 hours. OD_{600} was recorded at regular intervals and log_{10}-transformed for display. Each curve represents the mean ± SD of three biological replicates, each with two technical replicates. Growth rates (μ) were calculated from the slope of the natural logarithm (ln)-transformed OD_{600} values during the exponential phase (1-3 hours). An unpaired t-test with Welch's correction was used to assess statistical significance; $p > 0.05$ was considered not significant (NS). $S2^{WT\text{-}HS0}$: WT *E. cloacae* subsp. *cloacae* pMP7605; $S2^{\Delta\text{-}HS3}$: Δ*eclA E. cloacae* subsp. *cloacae* pMP7605.

The observation that deletion of *eclA* in $S2^{\Delta\text{-}HS3}$ had no significant impact on growth dynamics in Figure 12, is consistent with findings reported for *E. cloacae* subsp. *dissolvens* in Chapter 3.1. In each case, the growth curves of the Δ*eclA* mutants paralleled those of their respective WT strains, indicating that EclA is not required for bacterial replication or metabolic fitness under the tested conditions. Rather, its role may be more specialized, potentially linked to host interactions, adhesion, or biofilm formation, functions that are showed to be supported in Chapter 3.1.

The media used, LB for subsp. *cloacae* and $M63^{+}$ for subsp. *dissolvens,* were specifically chosen based on their ability to support biofilm formation in microtiter plate assays for each subspecies. While these media are suitable for biofilm growth in 24-well plates, only planktonic growth was assessed here in Erlenmeyer flasks. All strains analyzed carried the pMP7605 plasmid, as they were used in biofilm assays, making the comparison of growth kinetics more directly relevant to the subsequent phenotypic studies.

4.3. Molecular Characterization of EclA Expression and Localization

Similarly as indicated in Chapter 3.1, EclA synthesis and localization in *E. cloacae* subsp. *cloacae* were evaluated by Western blot analysis as indicated in Chapter 7.5 using the rabbit-generated affinity-purified anti-EclA-C antibodies, previously used to detect EclA in subsp. *dissolvens*. Overnight cultures of WT *E. cloacae* subsp. *cloacae* pMP7605 and Δ*eclA* *E. cloacae* subsp. *cloacae* pMP7605, designated as $S2^{WT\text{-}HS0}$ and $S2^{\Delta\text{-}HS3}$, respectively, were grown in LB medium, the same medium used for subsequent autoaggregation experiments, to ensure that EclA was expressed under comparable conditions.

The results were compared to those of WT *E. cloacae* subsp. *dissolvens* pMP7605 ($S1^{WT}$) in Chapter 3.1, to identify any discrepancies, particularly given that native EclA from subsp. *dissolvens* appeared shorter than the recombinant EclA expressed in *E. coli* having the sequence from subsp. *cloacae*. This comparison aimed to determine whether the observed size difference reflects transcription in *E. cloacae* initiating from a downstream start codon, thereby generating a shorter EclA isoform (Chapter 3.1 SI Table 1).

As observed in $S1^{WT}$, EclA was also detected in both the pellet and the culture supernatant of $S2^{WT\text{-}HS0}$, confirming its production and release (Figure 13-A, C). Despite loading a ~26-fold higher equivalent of culture supernatant, the EclA band appeared weaker than in the pellet, indicating that release under these conditions is minimal. To confirm that EclA's presence in

the supernatant was due to active release rather than cell lysis, a time-course subculture starting at OD_{600} = 0.02 was monitored. EclA became detectable in the supernatant only after 2 hours of incubation (Figure 13-B), supporting the hypothesis of active release. Notably, the EclA band was absent in $S2^{\Delta\text{-HS3}}$ in both fractions, further confirming successful deletion of the gene. Although bands at the level corresponding to EclA-C were detected in both the supernatant and pellet fractions of $S2^{\text{WT-HS0}}$, similar bands were also present in $S2^{\Delta\text{-HS3}}$. The absence of any additional lower-molecular-weight bands unique to $S2^{\text{WT-HS0}}$ indicates that no detectable C-terminal cleavage or proteolytic processing occurred (Figure 13-B).

Finally, direct comparison with recombinant EclA produced in *E. coli* revealed that native EclA from both subspecies migrates at a lower molecular weight (Figure 13-C, Chapter 3.1 SI Figure 9). This suggests that in *E. cloacae*, transcription likely initiates from a second downstream start codon, producing a shorter isoform, a phenomenon investigated in Chapter 3.1.

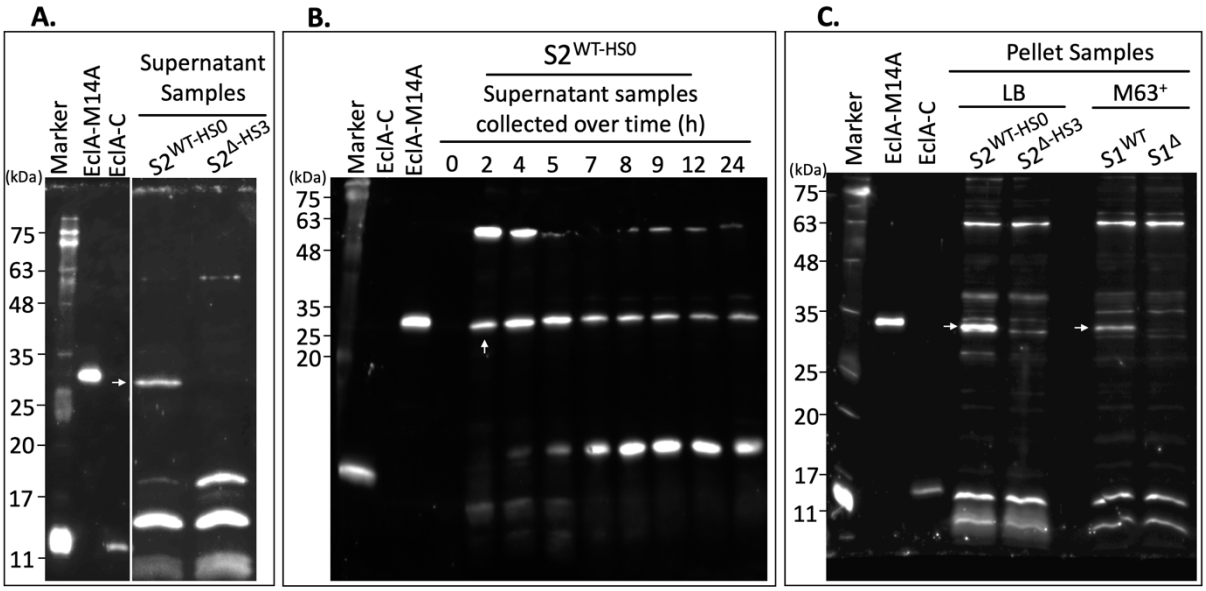

Figure 13: **Western blot analysis of EclA expression and extracellular release in $S2^{\text{WT-HS0}}$.** EclA was detected using affinity-purified anti-EclA-C antibodies. Recombinant EclA-M14A and EclA-C were used as protein standards with a mass of 0.125 ng and 0.025 ng, respectively. Sample preparation and gel conditions are as described in Chapter 3.1 unless otherwise stated. (**A**) Western blot analysis of TCA-precipitated supernatant samples from overnight LB-grown cultures of $S2^{\text{WT-HS0}}$ and $S2^{\Delta\text{-HS3}}$. (**B**) Time-course analysis of EclA release. Supernatants from subcultures initiated at OD_{600} = 0.02 were harvested at the indicated time points and analyzed by Western blot. A 12% SDS-PAGE gel was used, and the blot was imaged after 10 minutes of exposure. (**C**) Comparison of EclA in $S2^{\text{WT-HS0}}$ and $S2^{\Delta\text{-HS3}}$ pellet samples with those from $S1^{\text{WT}}$ (Chapter 3.1, Figure 2), alongside recombinant EclA expressed in *E. coli*. $S2^{\text{WT-HS0}}$: WT

E. cloacae subsp. *cloacae* pMP7605; $S2^{\Delta\text{-}HS3}$: Δ*eclA E. cloacae* subsp. *cloacae* pMP7605; $S1^{WT}$: WT *E. cloacae* subsp. *dissolvens* pMP7605; $S1^{\Delta}$: Δ*eclA E. cloacae* subsp. *dissolvens* pMP7605.

Membrane displacement attempts were also conducted to investigate whether EclA in $S2^{WT\text{-}HS0}$ is membrane-associated, as previously performed for $S1^{WT}$ in Chapter 3.1. Following the protocol described in Chapter 7.5, bacterial pellets from overnight cultures were resuspended in PBS containing methyl α-L-fucoside, a ligand intended to displace proteins bound via fucose-mediated interactions, aiming to displace EclA into the supernatant if associated to the cell membrane through a fucosylated antigen. However, as shown in Figure 14, EclA levels in the supernatant after treatment remained unchanged and were comparable to the treatment with PBS/Ca (negative control), indicating no detectable displacement. A similar outcome was previously observed in $S1^{WT}$ under comparable conditions. These results suggest that either the C-terminal fucose-binding domain of EclA does not mediate membrane attachment, is sterically inaccessible, requires a stronger ligand for effective displacement, or that EclA is not associated with the outer cell membrane. This also raises the possibility that the N-terminal domain may instead mediate surface interaction, assuming EclA is indeed associated with the outer membrane.

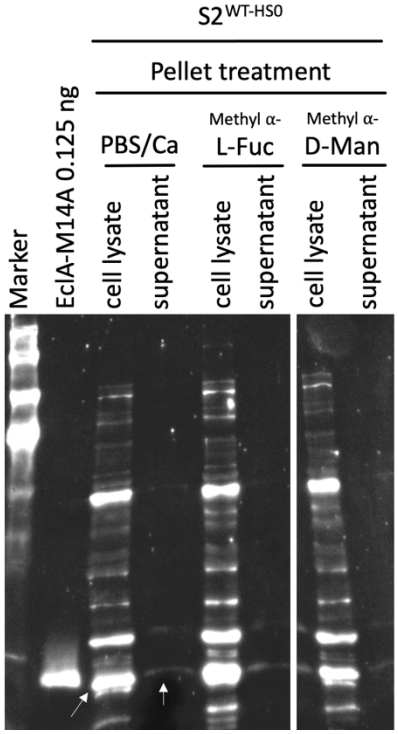

Figure 14: Western blot analysis investigating potential carbohydrate-mediated displacement of EclA from the cell fraction of $S2^{WT\text{-}HS0}$. $S2^{WT\text{-}HS0}$ pellets obtained from

overnight LB cultures supplemented with gentamicin (60 µg/mL) were treated with either 100 mM methyl α-D-mannoside (methyl α-D-Man), methyl α-L-fucoside (methyl α-L-Fuc), or PBS/Ca as a negative control. Proteins released into the supernatant were TCA-precipitated, while cell-associated proteins were extracted by lysis with Laemmli buffer. Protein samples were separated by 12% SDS-PAGE, and EclA was detected using anti-EclA-C antibodies. Additional details on sample preparation are provided in Chapter 7.5. White arrows point at EclA bands from PBS/Ca control pellet treatment. $S2^{WT\text{-}HS0}$: WT *E. cloacae* subsp. *cloacae* pMP7605.

The molecular characterization of EclA in *E. cloacae* subsp. *cloacae* reinforces and extends the findings obtained in subsp. *dissolvens*, suggesting that the expression, release patterns, and resistance to outer membrane displacement are conserved across both subspecies (Figure 13, 14; Chapter 3.1 Figure 2, SI Figure 7). The relatively weak signal in the supernatant despite concentrated sample loading indicates that EclA is only released in small amounts, which may indicate that its release is tightly regulated or context-dependent (Figure 13-A). While the detection of EclA in the supernatant of early-phase subcultures provided evidence for active release (Figure 13-B), this method does not definitively rule out cell lysis. To obtain more conclusive proof, future experiments should include rigorous controls to assess cell integrity. For instance, performing a lactate dehydrogenase (LDH) release assay on the culture supernatant would quantify any potential cell death. Alternatively, a Western blot for a known cytoplasmic protein, such as the plasmid-encoded mCherry, would serve as a robust control to confirm that the presence of extracellular EclA is not an artifact of cell lysis. No lower-molecular-weight bands corresponding to potential C-terminal cleavage products were observed, ruling out detectable proteolytic processing and supporting the idea that EclA is released in its full-length form.

The consistent size difference observed between native and recombinant EclA proteins across both subspecies further suggests that *E. cloacae* utilize a downstream start codon for *eclA* translation, leading to the expression of a shorter isoform than that produced recombinantly in *E. coli*. This implies that the native coding sequence may begin 13 bp downstream of the originally annotated start codon (Beshr et al., 2025). Future studies involving mass spectrometry analysis of native purified EclA would help clarify whether this size difference is purely due to translational start site selection or involves post-translational modifications. Overall, these findings provide important insight into the endogenous expression profile of EclA and validate the Δ*eclA* mutant at the protein level. In addition, studies such as cell

fractionation and identification of the EclA N-terminal ligand are needed to conclusively determine its localization and mode of surface attachment, especially following the unsuccessful attempts to displace EclA from the *E. cloacae* outer membrane using methyl α-L-fucoside.

4.4. Discovery of an Autoaggregation-Enhanced *E. cloacae* subsp. *cloacae* Variant

To investigate the role of EclA in biofilm formation, autoaggregation assays were conducted to replicate the approach used in Chapter 3.1. During the course of the experiments, a spontaneous *E. cloacae* subsp. *cloacae* variant harboring pMP7605, transformed via heat shock, was identified. This variant, designated $S2^{WT\text{-}HS0}$ (where "HS" denotes heat shock), exhibited a markedly enhanced biofilm phenotype compared to other transformants. This unanticipated observation shifted part of the study's focus toward characterizing this variant. The following subchapters present a detailed analysis of $S2^{WT\text{-}HS0}$, including its autoaggregate formation capacity, autoaggregate disruption behavior, genomic profile via WGS, and surface morphology examined by SEM.

4.4.1. Autoaggregate Formation and Disruption Assays

Two assays revealed the superiority of the autoaggregate-enhanced variant $S2^{WT\text{-}HS0}$ in both autoaggregate formation and retention. These were: an autoaggregate formation assay and an autoaggregate disruption assay, both described in Chapter 7.6.

For the autoaggregate formation assay, an overnight LB supplemented with gentamicin (60 µg/mL) culture of *E. cloacae* subsp. *cloacae* harboring pMP7605 was subcultured into fresh LB at a starting OD_{600} of 0.02 in 24-well plates. Gentamicin was added where indicated to maintain plasmid selection. Cultures were incubated under shaking conditions (180 rpm) at 37 °C for 48 hours.

The autoaggregate disruption assay followed the same protocol, with the exception that cultures were incubated statically for 48 hours to allow aggregate maturation. After this, mechanical disruption was applied by placing the plates in a shaking incubator at 180 rpm for 3 minutes to assess the robustness of the formed autoaggregates.

To investigate the phenotype of the $S2^{WT\text{-}HS0}$ variant, three independent colonies each of WT and Δ*eclA E. cloacae* subsp. *cloacae* transformed with pMP7605 by heat shock were isolated and designated $S2^{WT\text{-}HS1\text{-}3}$ and $S2^{\Delta\text{-}HS1\text{-}3}$, respectively. In the autoaggregate disruption assay

(Figure 15-A), only $S2^{WT\text{-}HS0}$ retained visible aggregates after mechanical disruption, whereas all other transformed clones, as well as the parental WT and Δ*eclA* strains lacking pMP7605 and not exposed to gentamicin, failed to maintain autoaggregates. This indicated a unique robustness in $S2^{WT\text{-}HS0}$ not attributable to the presence or absence of *eclA*. In the autoaggregate formation assay (Figure 15-B), $S2^{WT\text{-}HS0}$ again displayed a distinct phenotype, maintaining strong aggregation, while $S2^{WT\text{-}HS1\text{-}3}$ and $S2^{\Delta\text{-}HS1\text{-}3}$ lost this ability. Notably, the parental strains formed autoaggregates to a similar extent of $S2^{WT\text{-}HS0}$, regardless of *eclA* status, suggesting that neither the gene nor its deletion affects autoaggregate formation under these conditions. The complete loss of aggregation in $S2^{WT\text{-}HS1\text{-}3}$ and $S2^{\Delta\text{-}HS1\text{-}3}$ in the presence of pMP7605 and gentamicin implies that one or both of these factors may interfere with aggregate formation. However, $S2^{WT\text{-}HS0}$ appears resistant to this interference, pointing to a unique adaptation or mutation that enables the expression of a robust autoaggregative phenotype.

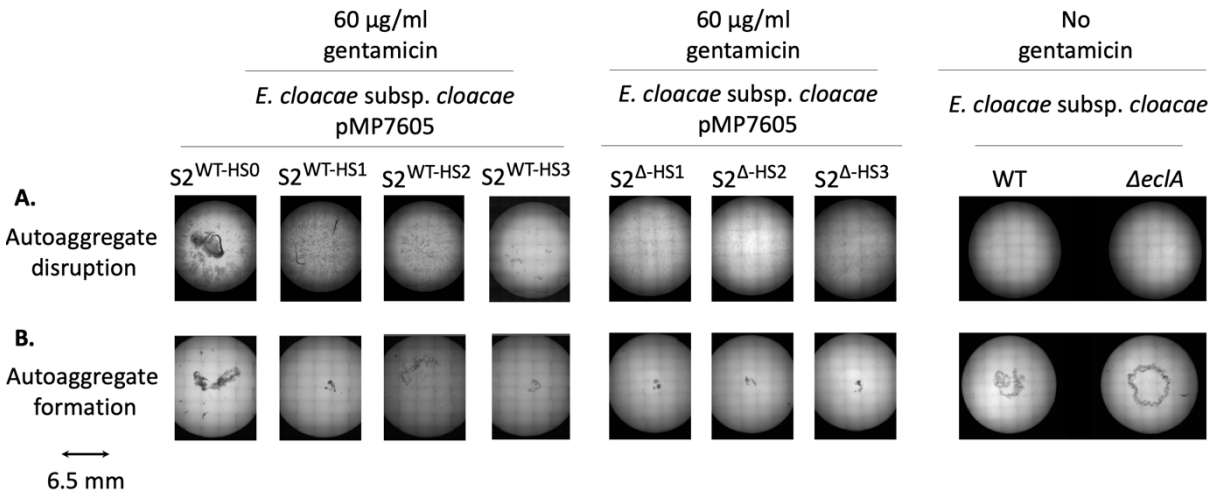

Figure 15: Autoaggregation phenotypes of parental (untransformed) and pMP7605-transformed *E. cloacae* subsp. *cloacae* WT and Δ*eclA* strains. The figure represents one biological replicate for each panel. **(A)** Autoaggregate disruption assay. Cultures of WT and Δ*eclA* strains, either untransformed or transformed via heat shock with pMP7605, were initiated at OD_{600} = 0.02 in 24-well plates and incubated statically to form autoaggregates at 37 °C for 48 hours in LB with or without gentamicin (60 µg/mL), as indicated. After mechanical disruption of autoaggregates (180 rpm, 3 minutes), brightfield images of whole wells were captured with uniform settings at 5× magnification. **(B)** Autoaggregate formation assay. Cultures were prepared as in (A) but incubated under shaking conditions (180 rpm) at 37 °C for 48 hours to assess autoaggregate formation. Brightfield images were taken as in (A). $S2^{WT\text{-}HS0\text{-}3}$: WT *E. cloacae* subsp. *cloacae* transformed with pMP7605 by heat shock (isolates

HS0-HS3); $S2^{\Delta\text{-HS1-3}}$: Δ*eclA E. cloacae* subsp. *cloacae* transformed with pMP7605 by heat shock (isolates HS1-HS3).

4.4.2. The Role of Gentamicin and pMP7605 in Modulating Autoaggregation

To further investigate the role of gentamicin in modulating autoaggregate formation, untransformed parental WT and Δ*eclA* strains of *E. cloacae* subsp. *cloacae*, being gentamicin-sensitive due to the absence of pMP7605, were subjected to the same autoaggregation assays under subinhibitory gentamicin concentrations.

In the autoaggregate disruption assay (Figure 16-A), neither WT nor Δ*eclA* retained their aggregates across any of the gentamicin titrations tested, mirroring their behavior in the absence of gentamicin (Figure 15-A). Thus, gentamicin had no observable effect on aggregate retention in these conditions.

In contrast, the autoaggregate formation assay (Figure 16-B) revealed that both WT and Δ*eclA* strains lose their ability to form autoaggregates in the presence of even the lowest gentamicin concentration (1 μg/mL) compared to when it was not added (Figure 15-B). This indicates that gentamicin interferes with aggregate formation during shaking incubation.

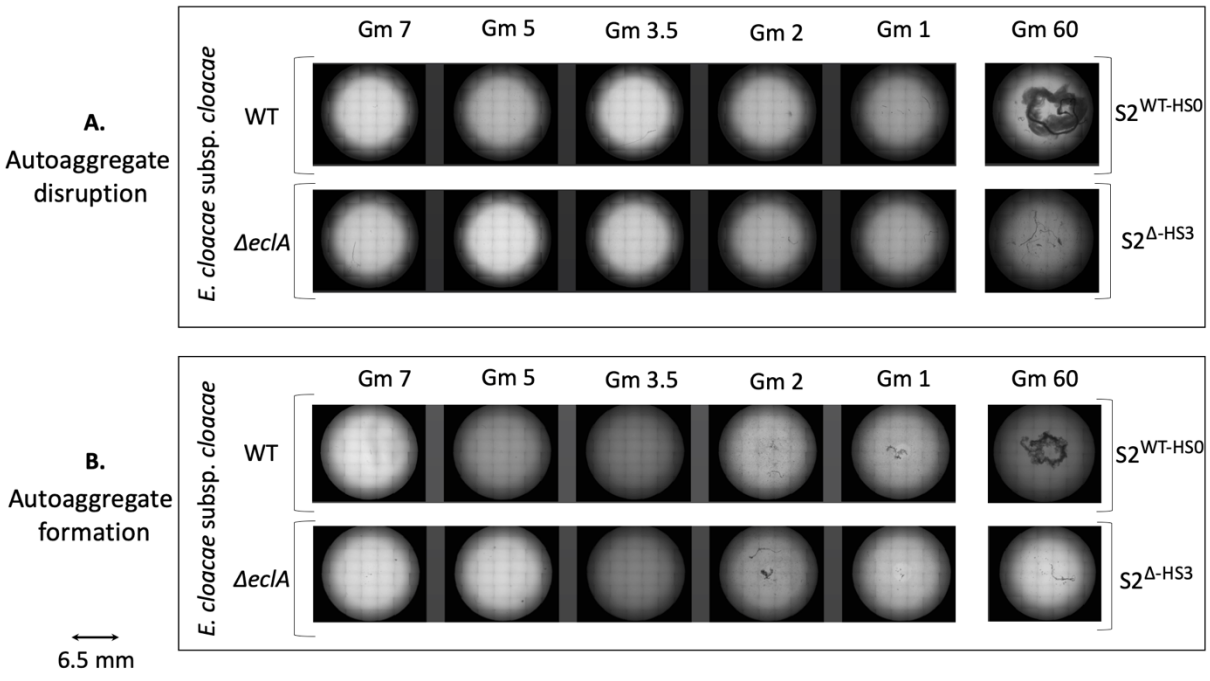

Figure 16: The effect of subinhibitory concentrations of gentamicin on the autoaggregation of untransformed WT and Δ*eclA E. cloacae* subsp. *cloacae* strains. The figure represents one biological replicate for each panel. **(A)** Autoaggregate disruption assay.

Untransformed parental WT and Δ*eclA* cultures were initiated at OD_{600} = 0.02 and incubated statically to form autoaggregates in LB medium supplemented with gentamicin (Gm; 1, 2, 3.5, 5, or 7 µg/mL) in 24-well plates for 72 hours at 37 °C. Wells were then mechanically agitated to disrupt autoaggregates (180 rpm, 3 minutes), and brightfield images were captured at 5× magnification using uniform settings. **(B)** Autoaggregate formation assay. Cultures were prepared as in (A) but incubated under shaking conditions (180 rpm) at 37 °C for 48 hours to assess autoaggregate formation. Brightfield images were taken as in (A). $S2^{WT\text{-}HS0}$: WT *E. cloacae* subsp. *cloacae* pMP7605 isolate HS0; $S2^{\Delta\text{-}HS3}$: Δ*eclA E. cloacae* subsp. *cloacae* pMP7605 isolate HS3.

Taken together, these findings further highlighted the unique phenotype of $S2^{WT\text{-}HS0}$. Unlike all other tested strains, $S2^{WT\text{-}HS0}$ consistently resisted aggregate disruption and retained the ability to form aggregates in the presence of gentamicin, underscoring a distinct behavior. Notably, the resistance to mechanical disruption was only observed under gentamicin exposure and was not present in its absence (Figure 17-A), suggesting that pMP7605 is not responsible for that phenotype. Aggregate formation by $S2^{WT\text{-}HS0}$ remained unaffected by gentamicin (Figure 17-B), unlike the parental WT and Δ*eclA* strains, which lost this ability under the same conditions (Figure 16-B). Importantly, the fact that $S2^{\Delta\text{-}HS3}$, lost its ability to form aggregates only upon gentamicin exposure confirms that the inhibitory effect on aggregate formation is due to gentamicin itself, not the presence of the plasmid.

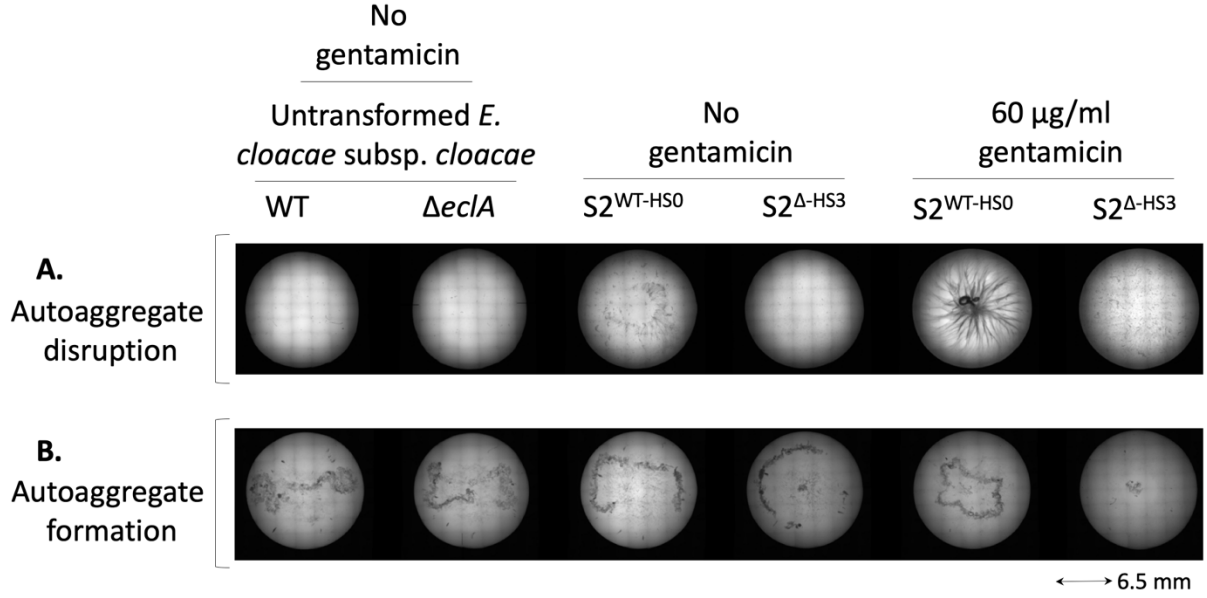

Figure 17: Autoaggregation behavior of $S2^{WT\text{-}HS0}$ and $S2^{\Delta\text{-}HS3}$ strains in the presence or absence of gentamicin. The figure represents one biological replicate for each panel.

(A) Autoaggregate disruption assay. Cultures of $S2^{WT\text{-}HS0}$ and $S2^{\Delta\text{-}HS3}$ were initiated at OD_{600} = 0.02 in 24-well plates and incubated statically to form autoaggregates at 37 °C for 48 hours in LB with or without gentamicin (60 µg/mL), as indicated. After mechanical disruption of autoaggregates (180 rpm, 3 minutes), brightfield images of whole wells were captured with uniform settings at 5× magnification. **(B)** Autoaggregate formation assay. Cultures were prepared as in (A) but incubated under shaking conditions (180 rpm) at 37 °C for 48 hours to assess autoaggregate formation. Brightfield images were taken as in (A). $S2^{WT\text{-}HS0}$: WT *E. cloacae* subsp. *cloacae* pMP7605 isolate HS0; $S2^{\Delta\text{-}HS3}$: Δ*eclA E. cloacae* subsp. *cloacae* pMP7605 isolate HS3.

4.4.3. The Effect of Exogenous EclA Complementation on Autoaggregation

To better clarify the role of EclA in autoaggregate formation and stability, a complementation assay was performed by supplementing Δ*eclA E. cloacae* subsp. *cloacae* strains with recombinant EclA, as indicated in Chapter 7.6. This approach aimed to distinguish the influence of EclA from other variables affecting the phenotype in earlier assays in this chapter. In the autoaggregate disruption assay (Figure 18-A), $S2^{WT\text{-}HS0}$ remained the only one able to retain visible aggregates following mechanical agitation, confirming its consistent robust phenotype seen in Figure 15-A and Figure 17-A. Additional strains transformed with pMP7605 by electroporation ($S2^{WT\text{-}EP}$ and $S2^{\Delta\text{-}EP}$) displayed no autoaggregate retention (Figure 18-A), behaving similarly to $S2^{WT\text{-}HS1\text{-}3}$ and $S2^{\Delta\text{-}HS1\text{-}3}$ as seen in the previous assays (Figure 15-A), indicating that the transformation method had no impact on this phenotype. Parental WT and Δ*eclA* strains (lacking pMP7605 and grown without gentamicin) could equally not retain aggregates (Figure 18-A), consistent with earlier observations (Figure 15-A). Importantly, the addition of 10 µM recombinant EclA to $S2^{\Delta\text{-}EP}$ did not induce aggregate retention (Figure 18-A), suggesting that EclA is not involved in stabilizing aggregates under these specific disruption conditions.

In contrast, results from the autoaggregate formation assay (Figure 18-B) revealed that parental WT and Δ*eclA* strains (lacking pMP7605 and grown without gentamicin) could both form aggregates efficiently, consistent with earlier observations (Figure 15-B). $S2^{WT\text{-}EP}$ and $S2^{\Delta\text{-}EP}$ failed to form aggregates in the presence of gentamicin, similarly to $S2^{WT\text{-}HS1\text{-}3}$ and $S2^{\Delta\text{-}HS1\text{-}3}$, with the exception of $S2^{WT\text{-}HS0}$, as seen in previous assays (Figure 15-B and Figure 17-B). This reinforces the role of gentamicin in inhibiting autoaggregate formation as was seen in (Figure

16). Notably, the addition of recombinant EclA to $S2^{\Delta\text{-EP}}$ induced aggregate formation despite gentamicin exposure. This indicates that EclA, when present in excess compared to its presence in $S2^{\text{WT-EP}}$, may help counteract the aggregate-inhibiting effects of gentamicin in this condition. In contrast to *E. cloacae* subsp. *dissolvens*, where EclA supplementation had no effect in aggregate formation (Chapter 3.2.2), this result suggests that EclA's role in aggregation may be subspecies-specific, as the EclA sequence was derived from *E. cloacae* subsp. *cloacae*.

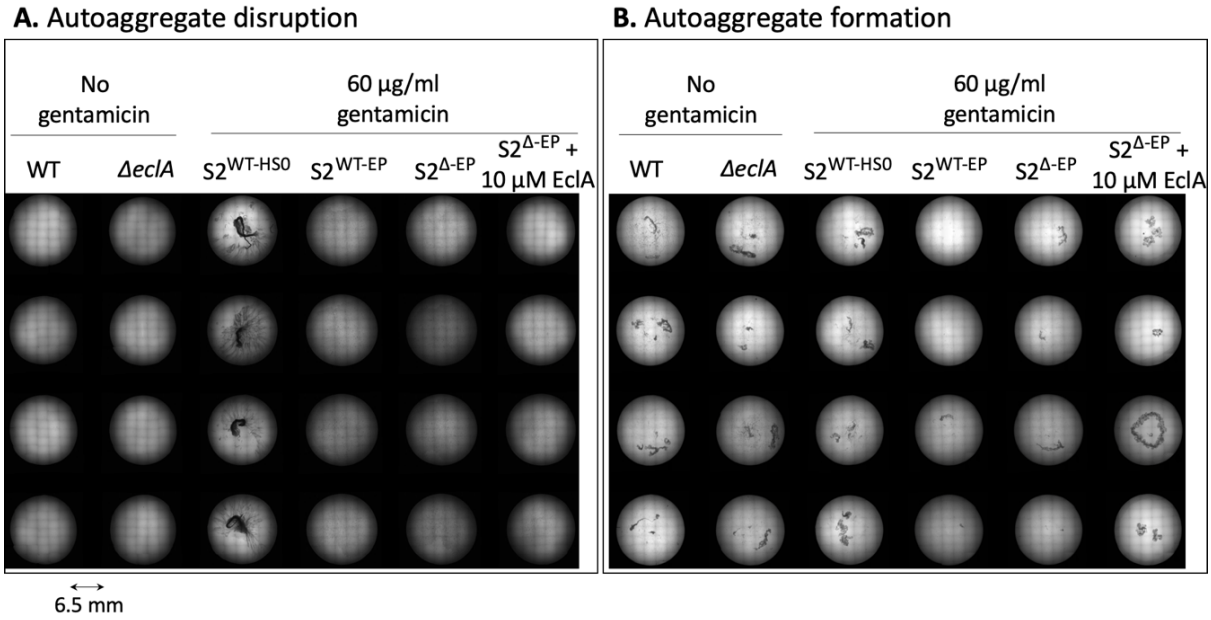

Figure 18: Effect of exogenous recombinant EclA on autoaggregation in *E. cloacae* subsp. *cloacae*. The figure represents one biological replicate for each panel. **(A)** Autoaggregate disruption assay. Parental WT and Δ*eclA* strains of *E. cloacae* subsp. *cloacae* and their derivatives carrying pMP7605, either obtained by heat shock ($S2^{\text{WT-HS0}}$) or electroporation ($S2^{\text{WT-EP}}$ and $S2^{\Delta\text{-EP}}$), were subcultured from an LB (with or without gentamicin added) overnight culture starting at OD_{600} = 0.02 in 24-well plates and incubated statically to form autoaggregates at 37 °C for 48 hours in LB with or without gentamicin (60 µg/mL), as indicated. Recombinant EclA (10 µM) was added to $S2^{\Delta\text{-EP}}$ cultures to assess complementation. After mechanical disruption (180 rpm, 3 minutes), brightfield images of whole wells were captured with uniform settings at 5x magnification. **(B)** Autoaggregate formation assay. The same strains and conditions as in (A) were used, except cultures were incubated with shaking at 180 rpm to assess aggregate formation over 48 hours. Brightfield images were taken as in (A). $S2^{\text{WT-HS0}}$: WT *E. cloacae* subsp. *cloacae* transformed with pMP7605 by heat shock (isolate 0); $S2^{\text{WT-EP}}$: WT *E. cloacae* subsp. *cloacae* transformed with pMP7605 by electroporation; $S2^{\Delta\text{-EP}}$: Δ*eclA E. cloacae* subsp. *cloacae* transformed with pMP7605 transformed by electroporation.

4.4.4. Whole-Genome Sequencing and Identification of Genomic Regions Deleted in the Autoaggregate-Enhanced variant

Given the unique and stable autoaggregation phenotype of $S2^{WT\text{-}HS0}$, WGS was performed to investigate potential genetic elements underlying its enhanced autoaggregation. Since $S2^{WT\text{-}HS1\text{-}3}$ displayed a completely different phenotype, failing to retain autoaggregates and losing aggregate formation under gentamicin exposure, a genetic alteration in $S2^{WT\text{-}HS0}$ was suspected.

WGS and genome assembly was carried out by MicrobesNG using ONT and their bioinformatics pipeline on $S2^{WT\text{-}HS0}$, $S2^{WT\text{-}HS2}$, and $S2^{\Delta\text{-}HS3}$ as described in Chapter 7.6. While ONT sequencing has lower base-calling accuracy, it provides long reads and complete genome assemblies, making it well suited for identifying large deletions or structural variations.

Alignment of $S2^{WT\text{-}HS2}$ genome against $S2^{WT\text{-}HS0}$ using the BLAST tool within the Proksee platform revealed two distinct genomic regions, referred to as locus 1 and locus 2, that were absent in $S2^{WT\text{-}HS0}$ but present in $S2^{WT\text{-}HS2}$ (Figure 19-A). These loci were located on pECl_A (NCBI accession number CP001919), a native plasmid found in *E. cloacae* subsp. *cloacae*, independent of its main circular chromosome.

Importantly, both loci were also detected in WGS-sequenced $S2^{\Delta\text{-}HS3}$ (Figure 19-B, C), indicating that their absence is specific to $S2^{WT\text{-}HS0}$ and likely the result of a deletion event specific to this isolate. This suggests a possible link between the loss of these plasmid-encoded regions and the autoaggregation-enhanced phenotype of $S2^{WT\text{-}HS0}$.

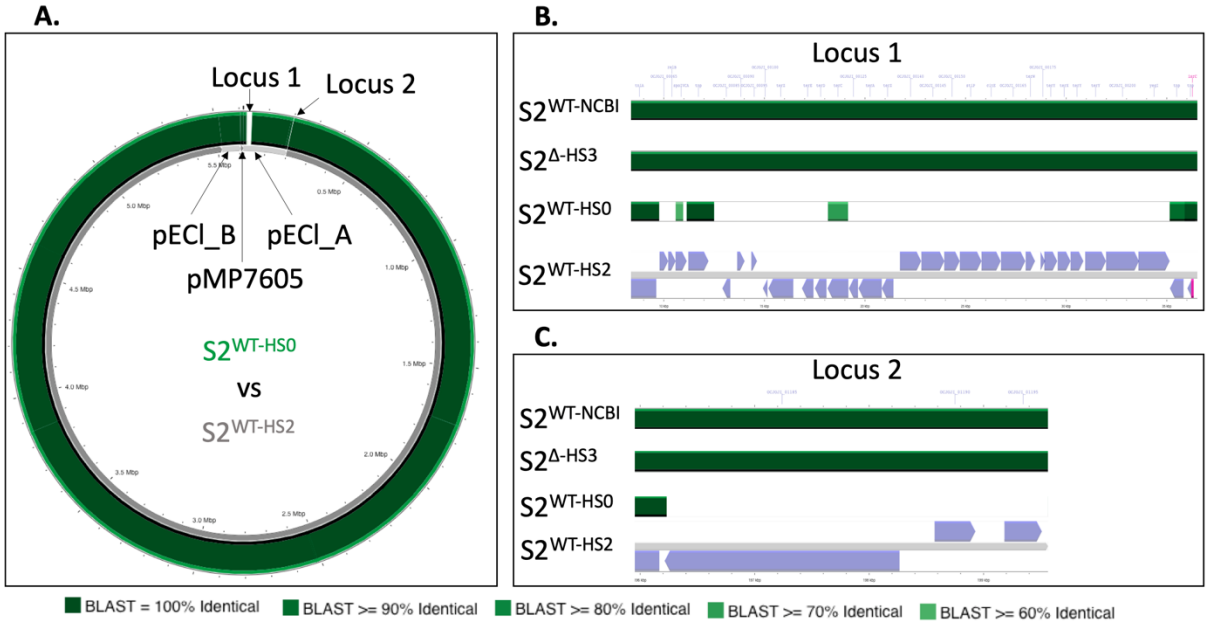

Figure 19: Whole-genome comparison revealing deleted loci in the autoaggregation-enhanced variant S2^{WT-HS0}. (A) Proksee BLAST alignment of the S2^{WT-HS0} query genome (green) against the S2^{WT-HS0} reference (gray; light gray for plasmids, dark gray for chromosome). **(B, C)** BLAST alignment of locus 1 and locus 2, respectively, with S2^{WT-HS2} as subject (gray), and S2^{WT-HS0}, S2$^{\Delta-HS3}$, and *E. cloacae* subsp. *cloacae* DSM 30054 (NCBI RefSeq assembly GCF_000025565.1) designated as S2$^{WT-NCBI}$ as queries. Blue arrows indicate coding DNA sequences in these loci. For all panels, green shadings indicate sequence identity, as illustrated by the BLAST sequence identity scale at the bottom of the figure. S2^{WT-HS0}: WT *E. cloacae* subsp. *cloacae* pMP7605 isolate HS0; S2^{WT-HS2}: WT *E. cloacae* subsp. *cloacae* pMP7605 isolate HS2; S2$^{\Delta-HS3}$: Δ*eclA E. cloacae* subsp. *cloacae* pMP7605 isolate HS3.

To assess the relevance of the deleted loci to the distinct autoaggregation phenotype observed in S2^{WT-HS0}, the coding DNA sequences (CDS) absent in this variant were analyzed using NCBI database annotations. A total of 29 CDS were identified as deleted in S2^{WT-HS0} compared to S2^{WT-HS2} (Table 2). Of these, nearly half (14 CDS) belonged to the tellurite resistance (TeR) gene cluster. The remaining deletions included one unannotated CDS, seven hypothetical proteins, and six miscellaneous CDS encoding enzymes such as transposases, aldolases, and phosphatases that could potentially contribute to tellurite resistance (Anantharaman et al., 2012), as well as proteins of unknown function. Beyond its established role in tellurite detoxification, the TeR cluster has also been implicated in broader bacterial defense responses against xenobiotics (Anantharaman et al., 2012). The absence of this cluster in S2^{WT-HS0} suggests a compromised capacity to enable such defenses. This may explain its unique

phenotype observed, which is only displayed in the presence of gentamicin. One possible interpretation is that, lacking the TeR-associated protective mechanisms, $S2^{WT\text{-}HS0}$ experiences elevated stress upon gentamicin exposure and compensates by activating an alternative stress-response involving autoaggregation. In contrast, other strains retaining the TeR cluster may not perceive gentamicin as a comparable stressor and therefore do not initiate this aggregative response.

Table 2: Missing coding DNA sequences from $S2^{WT\text{-}HS0}$ compared to $S2^{WT\text{-}HS2}$

#	**CDS**	**NCBI annotation**
1	unannotated	unannotated
2	WP_000301242.1	TeR-associated proteins
3	WP_001053338.1	
4	WP_000116677.1	
5	WP_000007448.1	
6	WP_001054787.1	
7	WP_000254136.1	
8	WP_001035171.1	
9	WP_001282603.1	
10	WP_001182415.1	
11	WP_001176767.1	
12	WP_001388628.1	
13	WP_000116681.1	
14	WP_013087240.1	
15	WP_013087239.1	
16	WP_003100853.1	Hypothetical proteins
17	WP_000341066.1	
18	WP_001151575.1	
19	WP_000077926.1	
20	WP_000374059.1	
21	WP_001040062.1	
22	ADF64886.1	
23	WP_003100858.1	
24	WP_000797363.1	HpcH/HpaI aldolase/citrate lyase family protein
25	WP_000506888.1	Uncharacterized T3SS apparatus domain with an unknown function
26	WP_013087238.1	Ser/Thr phosphatase
27	CAM4001861.1	Helix-hairpin containing protein
28	ADF64928.1	Tn3-family transposase
29	WP_003465043.1	Uncharacterized cupin domain-containing protein

4.4.5. Scanning Electron Microscopy of Autoaggregates

To further examine the phenotypic differences between WT and Δ*eclA* strains of *E. cloacae* subsp. *cloacae*, SEM was employed to visualize the surface architecture of autoaggregates formed by $S2^{WT\text{-}HS0}$ and $S2^{\Delta\text{-}HS3}$. While a direct comparison between these strains is complicated by their differing genotypes, $S2^{WT\text{-}HS0}$ retains *eclA* but lacks the TeR cluster, while Δ*eclA*^{HS3} has the TeR cluster but lacks *eclA*, both strains were included in the analysis. At the time of the experiment, the genetic differences in $S2^{WT\text{-}HS0}$ were not yet elucidated, justifying its inclusion.

SEM was performed on glutaraldehyde-fixed, air-dried autoaggregate samples harvested from either an autoaggregate disruption assay, or an exponential-phase culture as indicated in Chapter 7.6. The same methodology used in Subchapter 3.2.1 to compare WT and Δ*eclA E. cloacae* subsp. *dissolvens* was used, allowing additional evaluation of strain-specific architectural features.

In Figure 20-A, SEM analysis of autoaggregates collected from autoaggregate disruption assays revealed no observable morphological differences between $S2^{WT\text{-}HS0}$ and $S2^{\Delta\text{-}HS3}$ strains under the tested conditions. Bacterial cells in these samples appeared notably flattened, possibly due to sample processing, and were extensively covered by outer membrane vesicles (OMVs). This vesicle abundance, coupled with potential artifacts from the preparation method, likely obscured surface details, making it difficult to evaluate any structural influence of EclA or the TeR cluster.

To circumvent these limitations, SEM was performed on cells harvested from exponential-phase subcultures (OD_{600} = 2), a condition expected to reduce vesicle production and extracellular artifacts. As shown in Figure 20-B, both $S2^{WT\text{-}HS0}$ and $S2^{\Delta\text{-}HS3}$ displayed smooth and morphologically indistinguishable surfaces. These observations suggest that, under the tested growth phase and processing conditions, neither the presence nor absence of EclA or the TeR cluster results in detectable differences in cell surface architecture.

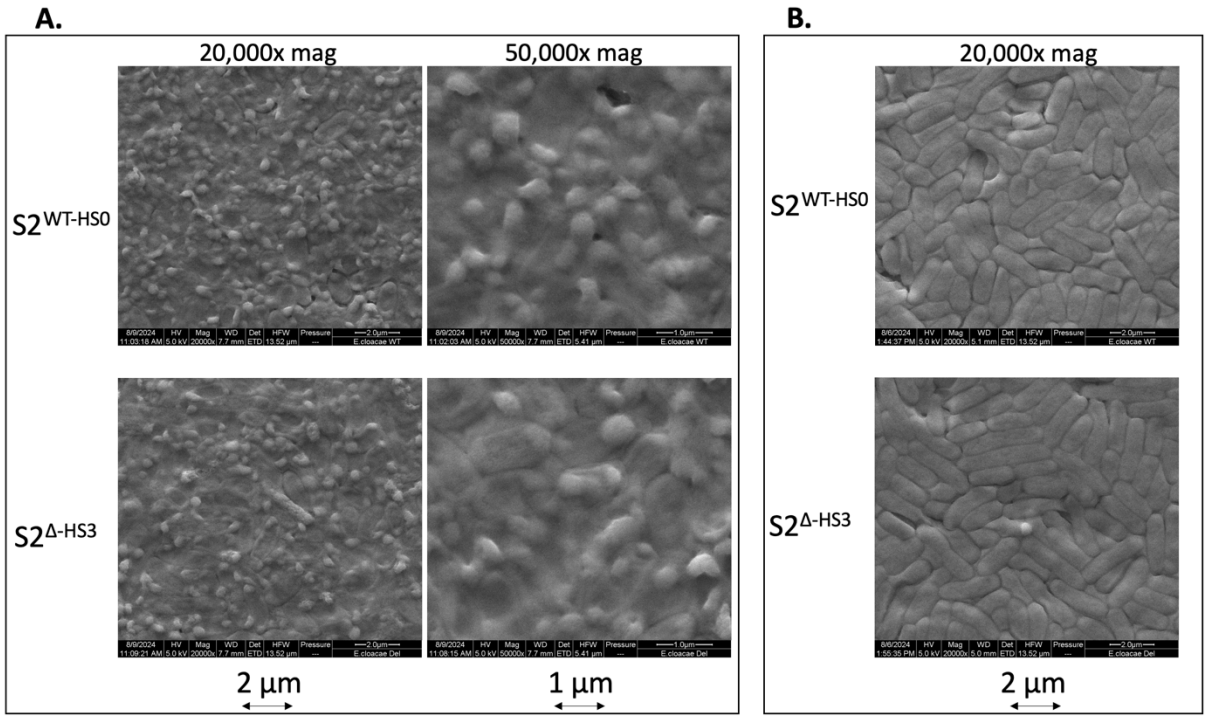

Figure 20: Scanning electron microscopy of autoaggregates from *E. cloacae* subsp. *cloacae*. (A) SEM images of glutaraldehyde-fixed, dried autoaggregates obtained from autoaggregate disruption assays of $S2^{WT\text{-}HS0}$ and $S2^{\Delta\text{-}HS3}$. For $S2^{\Delta\text{-}HS3}$, in the absence of visible autoaggregates, cells were collected directly from the liquid culture. **(B)** SEM images of glutaraldehyde-fixed, dried samples of $S2^{WT\text{-}HS0}$ and $S2^{\Delta\text{-}HS3}$ obtained from exponential-phase subcultures grown at 37 °C and 180 rpm (until $OD_{600} = 2$) in LB supplemented with 60 µg/mL gentamicin. $S2^{WT\text{-}HS0}$: WT *E. cloacae* subsp. *cloacae* pMP7605 isolate HS0; $S2^{\Delta\text{-}HS3}$: Δ*eclA* *E. cloacae* subsp. *cloacae* pMP7605 isolate HS3.

Discussion, Chapter 4.4: Discovery of an autoaggregation-enhanced *E. cloacae* subsp. *cloacae* variant

The unexpected identification of the $S2^{WT\text{-}HS0}$ variant, which displays a markedly enhanced autoaggregation phenotype, prompted a shift in the study's trajectory, from evaluating the role of EclA alone to dissecting a novel and genetically distinct behavioral variant of *E. cloacae* subsp. *cloacae*. This chapter explored the emergence, phenotype, genetic basis, and morphological features of $S2^{WT\text{-}HS0}$ using different experimental approaches.

$S2^{WT\text{-}HS0}$ consistently was superior to all other tested strains in both autoaggregate formation and retention, distinguishing itself from other heat shock transformants ($S2^{WT\text{-}HS1\text{-}3}$ and $S2^{\Delta\text{-}HS1\text{-}3}$) and the unstransformed parental WT and Δ*eclA* strains. The stability of this phenotype across assays, strongly suggested a genetic change. Interestingly, the unique

phenotype only manifested under gentamicin exposure, suggesting a stress-induced mechanism was at play. Subinhibitory concentrations of gentamicin abolished autoaggregation in parental strains, confirming gentamicin as the inhibitory agent and ruling out the plasmid pMP7605 as a contributing factor. The resilience of $S2^{WT\text{-}HS0}$ in this context therefore reflected a compensatory mechanism to gentamicin-induced stress.

The complementation experiments further clarified the involvement of EclA. While exogenous recombinant EclA induced aggregate formation in $S2^{\Delta\text{-}EP}$ exposed to gentamicin, it did not cause aggregate retention following mechanical disruption. This implies that EclA may play a role in the early stages of aggregate formation, possibly by mediating intercellular adherence, but not necessarily in structural stabilization. Importantly, this effect was not observed in *E. cloacae* subsp. *dissolvens* (Chapter 3.2.2), where the same recombinant EclA (derived from subsp. *cloacae*) had no impact, suggesting a possible subspecies-specific sequence compatibility requirement for functional complementation. However, the current finding is based on a single biological replicate and should be interpreted cautiously. Additional replicates are needed to validate the apparent induction of aggregation by EclA under gentamicin stress. Nevertheless, this is a significant finding: despite gentamicin being sufficient to disrupt autoaggregation in all other strains, the addition of excess exogenous EclA in micromolar concentrations, likely exceeding the amount present in the WT context, was able to override this inhibition. This suggests that EclA plays a compensatory role in mitigating stress-mediated aggregation loss.

WGS of $S2^{WT\text{-}HS0}$ revealed two large deletions in the native plasmid, pECl_A, affecting 29 coding sequences, 14 of which belong to the TeR cluster. Although historically associated with resistance to tellurite, a rare and toxic metalloid, the functions of the TeR cluster are increasingly recognized to extend far beyond this narrow role. TeR genes have been implicated in protection against oxidative stress, DNA damage, and bacteriophage attack, as well as in broader xenobiotic defense pathways (Anantharaman et al., 2012; Vávrová et al., 2024). Furthermore, the cluster is thought to influence virulence, membrane signaling, RNA metabolism, and filamentous cell morphology in various Gram-negative human pathogens, including *Yersinia pestis*, *E. coli*, *Proteus mirabilis*, and *Klebsiella pneumoniae* (Ponnusamy & Clinkenbeard, 2015; Toptchieva et al., 2003; R. Yang et al., 2025).

The presence of the TeR cluster in all other tested strains but not in $S2^{WT\text{-}HS0}$ strongly suggests that its absence sensitizes $S2^{WT\text{-}HS0}$ to gentamicin exposure. In this sensitized state, $S2^{WT\text{-}HS0}$ appears to activate autoaggregation as an alternative survival mechanism. This is consistent with growing evidence that bacterial aggregation and biofilm formation act as protective

adaptations to environmental stress and antibiotic challenge (H. Y. Liu et al., 2024). Interestingly, while no growth defect under gentamicin exposure was observed in $S2^{WT\text{-}HS0}$ compared to $S2^{\Delta\text{-}HS3}$, the aggregation phenotype may represent a stress response that is not reflected in growth rates.

Further supporting the functional relevance of the TeR deletion, several of the missing CDSs encode proteins with potential roles in stress mitigation, such as phosphatases, lyases, and aldolases, which could be integral components of the TeR-associated response network (Anantharaman et al., 2012). The loss of these genes may impair the ability of $S2^{WT\text{-}HS0}$ to manage gentamicin-induced intracellular stress through conventional pathways, prompting a switch to physical aggregation as a compensatory survival strategy.

The presence of the TeR cluster on plasmids in various human pathogens, including *E. coli*, *K. pneumoniae*, *P. mirabilis*, as discussed, further underlines its adaptive value beyond tellurite resistance, as tellurite is completely absent in human infection settings. Thus, the findings from $S2^{WT\text{-}HS0}$ add to the growing understanding of TeR's diverse and emerging functions, with autoaggregation identified here as a novel phenotype associated with its absence while under antibiotic stress.

SEM imaging aimed to reveal whether morphological differences could be attributed to either EclA loss or TeR cluster deletion. However, flattened bacteria, likely due to sample treatment in aggregate-disruption samples, and heavy OMV coverage made structural interpretation difficult. Such OMV production is consistent with previous reports on *E. cloacae* subsp. *cloacae* DSM 30054 (Bhar et al., 2021). OMVs are membrane-enclosed spherical structures bulging from the bacterial outer membrane and range from 20-300 nm. They contain a plethora of bacterial proteins, toxins, and metabolites, and are often released by the bacteria, prompting them to be studied as a distinct secretion system (Guerrero-Mandujano et al., 2017). OMVs are known to mediate bacterial stress responses, virulence, nutrient acquisition, quorum sensing, biofilm formation, and immune modulation (Gan et al., 2023). They can also serve as vehicles for horizontal gene transfer and antibiotic resistance (Sartorio et al., 2021). Proteomic analysis done on OMVs from *E. cloacae* subsp. *cloacae* DSM 30054 by Bhar et al., (2021) shows membrane-bound proteins involved in transport, signaling, cell interactions and biofilm formation. By downloading the data of the mapped proteins identified in the *E. cloacae* OMVs from the article's supplementary information, the accession number of the *eclA* gene (ECL_04191 or ECL_RS20915) and protein (ADF63724.1) were not found in the excel sheet enumerating the findings, despite finding multiple proteins having a molecular weight of 30

kDa and composed of 283 amino acids similarly to EclA (Bhar et al., 2021). This may suggest that EclA is not OMV-associated, which keeps its secretion pattern elusive to date.

When exponential-phase cells were examined to reduce vesicle and artifact interference, both $S2^{WT\text{-}HS0}$ and $S2^{\Delta\text{-}HS3}$ appeared morphologically similar, with smooth surfaces and no obvious structural differences. This indicates that, at least under these specific growth conditions and preparation methods, neither *eclA* deletion nor TeR absence causes changes in observable cell surface architecture.

In summary, this chapter describes the emergence of an *E. cloacae* subsp. *cloacae* variant ($S2^{WT\text{-}HS0}$) with a unique autoaggregative phenotype likely linked to the deletion of the TeR cluster on the native plasmid pECl_A. The loss of TeR may increase the bacterium's sensitivity to antibiotics (gentamicin), leading to a distinct adaptive strategy in the form of robust autoaggregation. Importantly, this adds a new characteristic to the still-evolving understanding of TeR function, suggesting its involvement in regulating responses to aminoglycoside stress. While tellurium is scarce in nature, the prevalence of TeR clusters in clinically relevant pathogens indicates they may be co-opted for other survival advantages, such as metal ion homeostasis, virulence, oxidative stress management, with their absence now possibly leading to a novel phenotype identified as autoaggregation while under antibiotic stress.

Closing Section 4: Elucidating the Role of EclA in *E. cloacae* subsp. *cloacae*

This section of the thesis extended the investigation of EclA from *E. cloacae* subsp. *dissolvens* to the commonly used model organism, *E. cloacae* subsp. *cloacae* DSM 30054. The primary objectives were to generate a corresponding Δ*eclA* mutant, characterize the molecular properties of EclA in this new context, and evaluate its role in autoaggregate formation, allowing for a direct comparison of the role of EclA between the two subspecies. While the section achieved its core goal of creating a functional knockout mutant, the investigation also led to the discovery of a hyper-aggregative variant, $S2^{WT\text{-}HS0}$, shifting the focus towards understanding a complex interplay between antibiotic stress, genetic background, and autoaggregate formation.

Generation of a Δ*eclA* mutant and the conserved molecular profile of EclA

In Chapter 4.1, the initial step of designing the mutator plasmid required significant technical adaptation and troubleshooting. The suicide vector pKNG101, used successfully in subsp. *dissolvens*, was ineffective because of the intrinsic streptomycin resistance of subsp. *cloacae*.

This challenge was overcome by engineering the mutator plasmid to carry a gentamicin resistance marker, creating pKNG101_30054_GmR. Although subsequent sequencing revealed a complex and unexpected plasmid rearrangement had occurred, the essential components for allelic exchange remained intact. This enabled the successful generation of a precise, scarless Δ*eclA* mutant in *E. cloacae* subsp. *cloacae*, which was validated by both PCR and whole-genome sequencing.

Molecular characterization in Chapter 4.2 and 4.3 revealed that the fundamental properties of EclA are conserved across both subsp. *cloacae* and subsp. *dissolvens*.

- No impact on planktonic growth: The deletion of *eclA* had no effect on the growth kinetics of subsp. *cloacae* in planktonic culture. This mirrors the exact same observation made in subsp. *dissolvens*, confirming that EclA is a non-essential gene for metabolic fitness and replication under standard laboratory conditions in both subspecies.
- Identical localization and release pattern: Western blot analysis showed that EclA in subsp. *cloacae* is present in both the cell-associated pellet and, to a lesser extent, the culture supernatant. This dual localization is identical to that observed in subsp. *dissolvens*. In both cases, release appears to be minimal.
- Conserved native isoform: The native EclA from subsp. *cloacae* migrates at a lower apparent molecular weight than the recombinant protein, perfectly aligning with the native EclA from subsp. *dissolvens*. This provides strong, cross-subspecies evidence for the hypothesis first raised in Chapter 3.1 that *E. cloacae* natively translates *eclA* from a second, downstream start codon, producing a shorter isoform than the one predicted from the annotated gene sequence used for recombinant expression.
- Resistance to membrane displacement: Attempts to displace EclA from the surface of subsp. *cloacae* using its ligand methyl α-L-fucoside were unsuccessful. This failure to displace the protein recapitulates the results from subsp. *dissolvens*, suggesting that if EclA is surface-associated, its attachment is not mediated by a simple, accessible interaction via its fucose-binding C-terminal domain in either subspecies.

The unexpected emergence of the S2$^{WT\text{-}HS0}$ variant

The most significant discovery in this section was the identification of the S2$^{WT\text{-}HS0}$ variant, a heat shock-transformed *E. cloacae* subsp. *cloacae* with pMP7605, which exhibited a uniquely robust autoaggregation phenotype that was both resistant to mechanical disruption and inhibition of autoaggregate formation, both, only in the presence of gentamicin. While

gentamicin acted as an inhibitor of aggregation in parental strains, $S2^{WT\text{-}HS0}$ required it for its autoaggregation state. This observation in Chapter 4.4 pointed towards a genetic adaptation that alters the bacterium's response to antibiotic-induced stress.

WSG provided the genetic basis for this unique behavior, revealing two large deletions on the *E. cloacae* subsp. *cloacae* native plasmid pECl_A in $S2^{WT\text{-}HS0}$, most notably eliminating the TeR gene cluster. The absence of this cluster in $S2^{WT\text{-}HS0}$, while present in all other tested strains and the reference genome, strongly suggests a causal link. The central hypothesis is that the loss of the TeR cluster, which is implicated in broad xenobiotic and oxidative stress defense pathways, sensitizes $S2^{WT\text{-}HS0}$ to gentamicin. In response to this elevated stress, $S2^{WT\text{-}HS0}$ appears to activate a compensatory survival strategy: robust autoaggregation. This finding contributes a novel phenotype to the expanding functions of the TeR cluster, whose role in clinically relevant pathogens is increasingly understood to extend far beyond tellurite detoxification.

Contrasting outcomes of EclA complementation across subspecies

The addition of exogenous recombinant EclA in Subchapter 4.4.3 induced aggregate formation in $S2^{\Delta\text{-}EP}$ that was inhibited by gentamicin (and the presence of the TeR cluster). This result is significant for two reasons. First, it demonstrates that EclA can play a role in mitigating stress-induced aggregation loss. Second, it stands in strong contrast to the findings in Chapter 3.2.2, where the same recombinant EclA failed to restore the aggregation defect in Δ*eclA* from subsp. *dissolvens,* even when EclA was added at 10 times the concentration. Since the recombinant EclA was derived from the subsp. *cloacae* sequence, it was likely compatible with its native background but not in subsp. *dissolvens*, where the R181N amino acid substitution could have contributed to this failure in rescuing the $S1^{\Delta}$ phenotype. This highlights that the minor sequence variations between orthologs could have significant functional consequences. However, since the current finding is based on a single biological replicate, additional replicates are needed to validate the apparent induction of aggregation by EclA under gentamicin stress.

Morphological analysis and EclA's elusive release mechanism

SEM analysis in Subchapter 4.4.5 revealed no significant morphological differences between $S2^{WT\text{-}HS0}$ and $S2^{\Delta\text{-}HS3}$, suggesting that neither the deletion of the TeR cluster nor the absence of EclA alters cell surface architecture in the tested conditions. However, interpretation was

limited by extensive OMV production, a known feature of *E. cloacae* subsp. *cloacae*, as well as possible bacterial flattening possibly from the sample preparation method used. In this study, SEM preparation involved fixation with 2% glutaraldehyde, filtration through a 0.2 µm membrane, and a single wash with milli-Q water. In contrast, Bhar et al. (2021) employed a more thorough protocol: fixation with 2% paraformaldehyde, adherence to poly-L-lysine-treated membranes, additional fixation with osmium tetroxide and Trump's fixative, buffer washes, graded ethanol dehydration, and critical point drying. This more rigorous approach likely preserved native surface features, minimized the artifacts observed in the samples, and allowed for better sample analysis. In contrast to the SEM images from *E. cloacae* subsp. *cloacae*, SEM images of *E. cloacae* subsp. *dissolvens* showed no visible OMVs; while few bulges were observed, they were likely preparation artifacts that didn't resemble OMVs. Interestingly, EclA was not detected in a published proteomic analysis of OMVs from *E. cloacae* subsp. *cloacae*, suggesting that its release remains unclear in both subspecies and warrants further investigation.

Conclusion and future directions

In conclusion, Section 4 successfully generated the necessary Δ*eclA* mutant in *E. cloacae* subsp. *cloacae* and established that the lectin's fundamental molecular characteristics are conserved. The unanticipated discovery of the TeR-deleted $S2^{WT\text{-}HS0}$ variant, however, uncovered a novel link between a plasmid-encoded stress response cluster (TeR) and antibiotic-induced autoaggregation. This work identifies a potential function for EclA in counteracting this stress.

This section lays the groundwork for several critical future experiments:

- Validate the EclA complementation finding in subsp. *cloacae* with further biological replicates to confirm its role in overcoming gentamicin-induced stress.
- Directly test the TeR cluster's role by complementing it back into $S2^{WT\text{-}HS0}$ to see if the phenotype is reversed, and by deleting it in the parental WT strain.
- Find a condition similar to the autoaggregation experiment with *E. cloacae* subsp. *dissolvens* where the role of EclA in autoaggregation is clearly highlighted.

5. The Role of EclA in *E. cloacae* Adhesion

As most lectins also function as adhesins (Fares et al., 2025), this section investigates the hypothesis that EclA also functions as a surface-associated adhesin for host-cell interactions. To explore this potential role, three distinct in vitro adhesion experiments were employed. The section details experiments assessing the attachment of *E. cloacae* to human red blood cells (RBCs), A549 lung epithelial cells, and immobilized Lewis blood group antigens. The collective goal is to determine if EclA directly contributes to bacterial adherence and to gain deeper mechanistic insights into its function as a lectin.

5.1. Human Red Blood Cell Hemagglutination with *E. cloacae*, and Mechanistic Insights into EclA-Red Blood Cell interactions

Expanding on the findings in Chapter 3.1 that recombinant EclA can mediate hemagglutination, this chapter delves deeper into its role in adhesion to human red blood cells. The investigation comprises 2 parts. First, it assesses whether native EclA functions as a surface-associated adhesin by comparing the hemagglutination capabilities of WT and Δ*eclA* strains from both *E. cloacae* subsp. *dissolvens* and subsp. *cloacae*, harboring pMP7605. Second, it explores the molecular mechanisms underlying the EclA-RBC interaction by evaluating the activity of isolated recombinant EclA domains and its "long" isoform EclA-M14A. Together, these experiments aim to clarify the function of EclA as a bacterial adhesin and define the structural requirements for its activity.

5.1.1. Human Red Blood Cell Hemagglutination by WT and Δ*eclA E. cloacae* Strains and their Supernatants

This subchapter investigates whether EclA functions as a surface-associated adhesin on the bacterium itself. The primary objective is to determine if native, potentially cell-surface associated EclA can bridge *E. cloacae* to RBCs, thereby causing hemagglutination and providing evidence for its localization on the outer membrane.

For hemagglutination to occur with live bacteria, EclA must be surface-exposed. One possible mechanism is that the two N-terminal domains bind to their yet-unknown ligands on the *E. cloacae* EPS or LPS, leaving the two fucose-binding C-terminal domains exposed to fucosylated RBC ligands (Figure 21-A1). Alternatively, the opposite orientation is also

plausible: the C-terminal domains may interact with fucosylated antigens on *E. cloacae*, while the N-terminal domains bind to yet-unidentified ligands on RBCs (Figure 21-A2). Both orientations could also occur simultaneously (Figure 21-A3). In this model, hemagglutination arises from multiple EclA molecules on the bacterial surface collectively mediating cross-linking between RBCs, with the bacterium itself acting as the bridge. Because both binding sites in each of the N- and C-terminal domains are oriented in one direction, each EclA molecule would likely bind one single RBC. This is due both to the large size of the RBC, having a thickness of 2.8-0.5 µm, a central thickness of 0.8-1 µm, and a length of 7.7-7.0 µm (Figure 21-B)(Ostadfar, 2016), and to the short distance between the two binding sites within each domain, which are separated by only 30.7 Å in the N-terminus and 42.2 Å in the C-terminus (Figure 21-C).

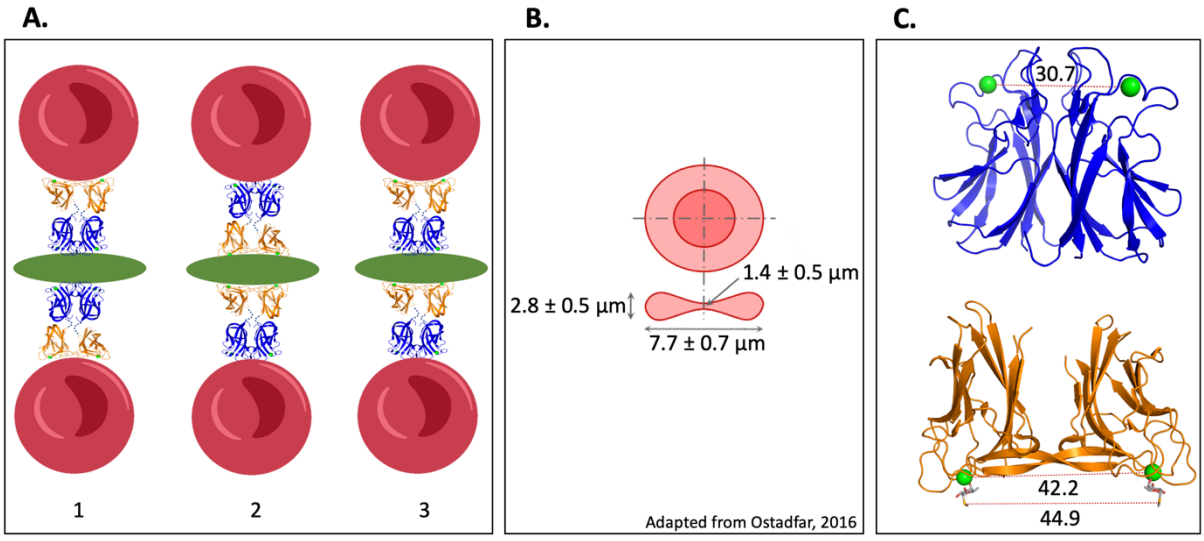

Figure 21: Model of EclA-mediated hemagglutination between live *E. cloacae* and human RBCs. (A) Possible orientations of full-length EclA from Beshr et al. (2025), shown with the C-terminal domain in orange (PDB 6YFC), and the N-terminus in blue (PDB 6YGQ), illustrating how the protein may interact with *E. cloacae* (dark green ovals) and human RBCs (red spheres) to promote hemagglutination. **(B)** Schematic representation and dimensions of a human RBC adapted from Ostadfar, (2016). **(C)** Spatial arrangement of the EclA binding sites in the N-terminal (blue - PDB 6YGQ) and C-terminal (orange - PDB 6YFC) domains. Green spheres indicate calcium ions involved in ligand binding. Distances were measured (red dotted lines) between calcium ions in PyMOL, and all values are given in Å. For the C-terminal domain, the distances between the two methyl α-L-selenofucoside ligands were also measured from the selenium atom.

Hemagglutination assays were performed as described in Chapter 7.7. Briefly, overnight cultures of *E. cloacae* subsp. *dissolvens* WT and Δ*eclA* strains, both carrying pMP7605 (designated $S1^{WT}$ and $S1^{\Delta}$, respectively), and *E. cloacae* subsp. *cloacae* strains (designated $S2^{WT\text{-}HS0}$ and $S2^{\Delta\text{-}HS3}$), were grown in LB medium supplemented with 60 µg/mL gentamicin. Cultures were then washed with PBS/Ca, adjusted to the designated OD_{600} using the same buffer, and mixed with human type O^+ RBCs. In parallel, the filter-sterilized supernatants of the overnight cultures were also incubated with human RBCs. A result whereby the WT strain agglutinates RBCs while the Δ*eclA* mutant does not, would provide evidence for EclA's role as a surface-exposed adhesin. Although a direct comparison between these two strains is complicated by the unforseen genomic deletions identified in $S2^{WT\text{-}HS0}$ (discussed in Subchapter 4.4.4), this assay was initially performed before such deletions were known.

Neither $S1^{WT}$ nor $S1^{\Delta}$ exhibited hemagglutination at any tested cell density Figure 22, suggesting that under these conditions, EclA is either not sufficiently surface-exposed or not surface-exposed at all.

Conversely, strong hemagglutination was observed for both $S2^{WT\text{-}HS0}$ and $S2^{\Delta\text{-}HS3}$, even at the lowest tested OD_{600} of 0.5. The identical hemagglutination phenotype observed in both strains suggests that EclA is not responsible for the observed RBC agglutination in subsp. *cloacae*. Instead, it indicates the presence of one or more additional surface-associated adhesins capable of mediating hemagglutination independently of EclA. Furthermore, the absence of hemagglutination activity in the supernatants from both subspecies, despite prior evidence demonstrating the release of EclA into the medium (Chapter 3.1 and Chapter 4.3), suggests that the released quantities of EclA alone are insufficient for detectable hemagglutination, or that the binding sites of EclA are occupied by other ligands. This interpretation is further supported by the second biological replicate (Rep 2) in Figure 22, in which the $S2^{\Delta\text{-}HS3}$ strain had not yet been generated. Instead, $S2^{WT\text{-}HS0}$ was used with the addition of 100 mM L-fucose to create a functional knockout of the *eclA* gene, and no hemagglutination inhibition was observed under these conditions.

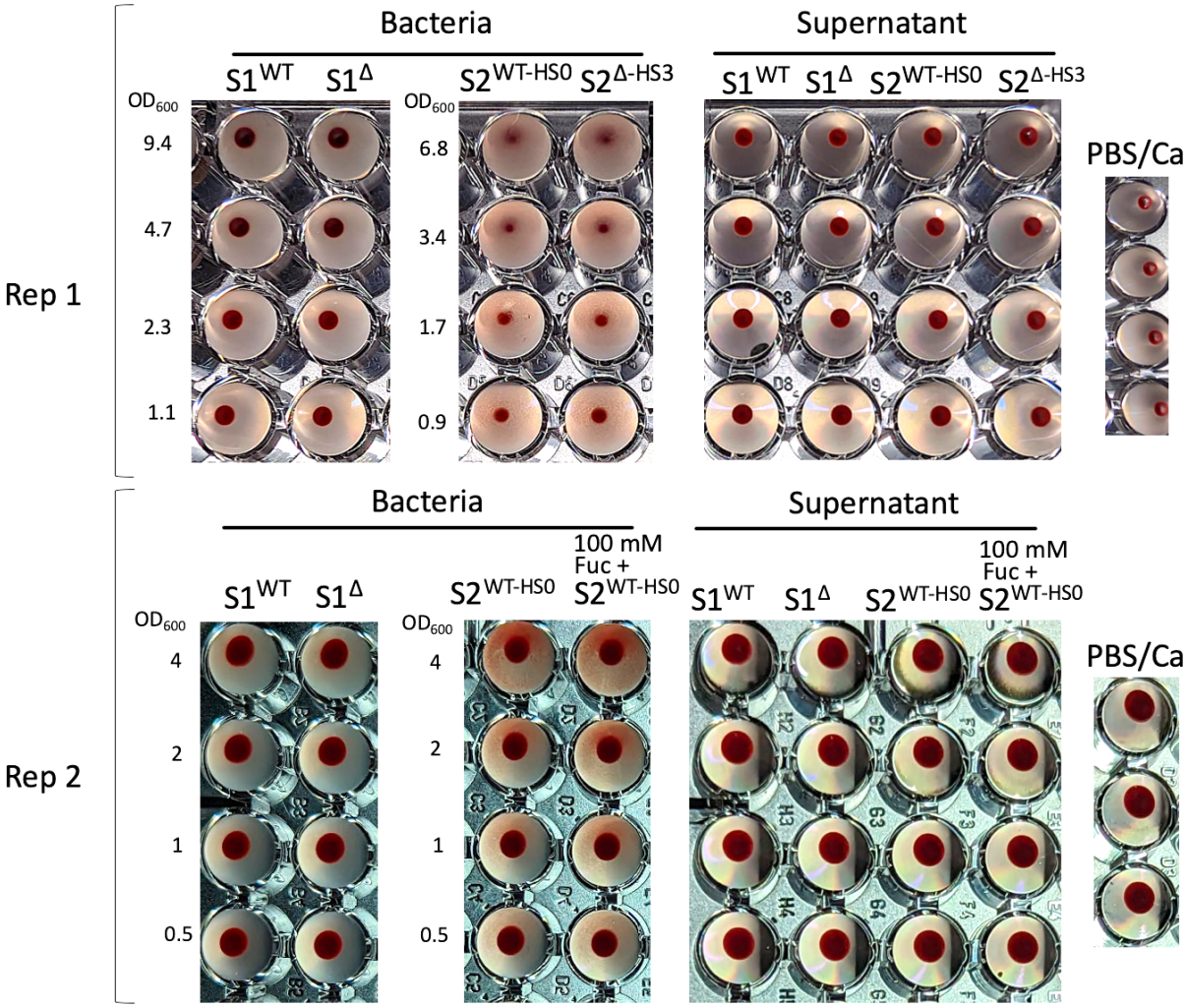

Figure 22: Hemagglutination assay of human type O^+ red blood cells with *E. cloacae* species and their culture supernatants. Rep 1 and Rep 2 indicate 2 biological replicates in which blood samples from different individuals were used (N = 2). Overnight bacterial cultures grown in LB supplemented with 60 µg/mL gentamicin were harvested, washed, and adjusted to specified optical densities, followed by two-fold serial dilution in V-shaped 96-well plates to a final volume of 50 µL per well. Culture supernatants were filter-sterilized and similarly dispensed (undiluted) into plates. Washed and prepared human type O^+ RBCs were added to each well, reaching a final RBC concentration of 2.5% and a total volume of 100 µL. PBS/Ca served as a negative control for hemagglutination. Fuc: L-Fucose. Numbers to the left of each plate image represent bacterial OD_{600} values. Images show the 96-well plates from below. $S1^{WT}$: WT *E. cloacae* subsp. *dissolvens* pMP7605; $S1^{\Delta}$: Δ*eclA E. cloacae* subsp. *dissolvens* pMP7605. $S2^{WT\text{-}HS0}$: WT *E. cloacae* subsp. *cloacae* pMP7605 isolate HS0; $S2^{\Delta\text{-}HS3}$: Δ*eclA E. cloacae* subsp. *cloacae* pMP7605 isolate HS3.

5.1.2. Mechanistic Insights into EclA-Red Blood Cell Interactions

Further experiments utilizing recombinant EclA-M14A and the isolated recombinant EclA domains (EclA-C, and EclA-N, the His-tagged N-terminal domain) where carried out to clarify the hemagglutination mechanism of EclA as indicated in Chapter 7.7. For hemagglutination to occur, both the N- and C-terminal domains must participate in RBC binding, as each domain alone is theoretically incapable of engaging more than one RBC due to size constraints (Figure 21-B, C). Figure 23 demonstrates that the isolated C-terminal domain of recombinant EclA, previously implicated in hemagglutination in Chapter 3.1 due to its inhibition by methyl α-L-fucose, failed to induce hemagglutination even at double the concentration tested previously. This suggests that the hemagglutination activity EclA-C requires the presence of the full-length EclA protein. Similarly, the EclA-N alone did not cause hemagglutination, indicating that both domains are interdependent for hemagglutination to take place.

The EclA-M14A variant, representing the longer isoform of EclA lacking the methionine at position 14, showed weak hemagglutination activity. This finding suggests that the shorter EclA isoform, which lacks the first 13 amino acids due to transcription initiation at the second start codon, may have higher hemagglutination efficiency. Indeed, recombinant EclA comprising a mixture of both isoforms demonstrated complete hemagglutination at half the protein concentration used here, as shown previously in Chapter 3.1. The reduced hemagglutination observed for EclA-M14A even at higher concentrations highlights a potential functional difference between the two isoforms. Furthermore, mixing equimolar amounts of EclA-C and EclA-N did not restore hemagglutination, confirming that covalent linkage between these domains within a single polypeptide chain is necessary for effective hemagglutination.

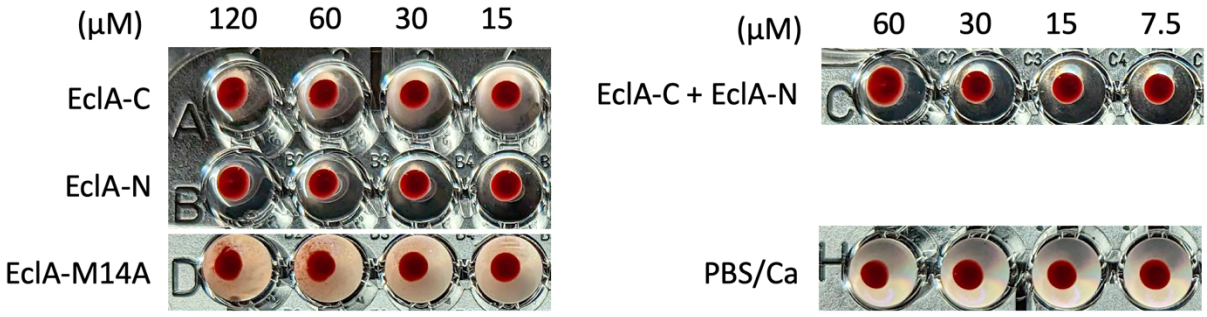

Figure 23: Hemagglutination assay of human red blood cells with recombinant EclA domains and the EclA-M14A variant. Recombinant proteins tested include the isolated EclA

N-terminal domain (EclA-N), C-terminal domain (EclA-C), the full-length variant EclA-M14A, and a combination of EclA-N and EclA-C mixed at equimolar concentrations. Proteins were diluted in two-fold serial dilutions in V-shaped 96-well plates, reaching a final volume of 50 µL per well. EclA-M14A was prepared in TBS/Ca buffer, while EclA-C and EclA-N were in PBS/Ca buffer. Subsequently, washed human type O^+ red blood cells were added to each well, achieving a final concentration of 2.5% RBC in a total volume of 100 µL per well. PBS/Ca alone served as a negative control. Numbers above wells indicate the final protein concentration (µM). Images show the 96-well plates from below.

Discussion, Chapter 5.1: Human red blood cell hemagglutination by *E. cloacae*, and mechanistic insights into EclA-red blood cell interactions

This chapter explored the role of native EclA in mediating the hemagglutination of human RBCs by *E. cloacae*, building upon earlier findings that the recombinant EclA protein could independently hemagglutinate RBCs (Chapter 3.1). The investigation sought to determine if EclA functions as a surface-exposed adhesin capable of bridging bacterial cells to RBCs, considering two plausible mechanisms dependent on the protein's orientation. The findings revealed subspecies-specific hemagglutination and provided critical insights into the structural requirements for EclA's function.

E. cloacae subspecies exhibited distinct hemagglutination phenotypes. The subsp. *cloacae* strain showed hemagglutination activity; however, this activity was independent of EclA. Specifically, the $S2^{\Delta\text{-HS3}}$ mutant retained the full hemagglutinating capacity of $S2^{\text{WT-HS0}}$, and the latter strain also failed to exhibited hemagglutination inhibition in the presence of 100 mM fucose. This contrasts with EclA-mediated hemagglutination, which was inhibited by methyl α-L-fucoside (Chapter 3.1 Figure 3). This strongly suggests the presence of at least one additional, lectin in this subspecies that primarily mediates the observed hemagglutination phenotype, effectively masking any contribution from EclA. Previous studies have shown that most *E. cloacae* hospital isolates exhibit MSHA (hemagglutination inhibited by D-mannose) (Keller et al., 1998). Notably, *E. cloacae* subsp. *cloacae* DSM 30054 expresses the gene coding for the mannose-binding lectin FimH, which plays a key role in adhesion to various mannosylated urinary tract cells and is also capable of MSHA (Frutos-Grilo et al., 2023; Maheswari et al., 2013). Therefore, it is plausible that FimH or another lectin is responsible for the hemagglutination phenotype observed in this subspecies.

Hemagglutination by *E. cloacae* subsp. *dissolvens* was absent, even though $S1^{WT}$ was shown to synthesize and release EclA (Chapter 3.1 Figure 2). This suggests that on the native subsp. *dissolvens* surface, EclA is insufficiently expressed to mediate cell cross-linking. Furthermore, the lack of activity in bacterial culture supernatants in all subspecies and strains, despite confirmed EclA release in the cases of WT strains, indicates that the quantity of released protein is below the threshold needed to induce visible hemagglutination. Furthermore, subsp. *dissolvens* also encodes *fimH* (Genomic location: NZ_WJWQ01000005.1:100133-101137, based on the shotgun genome assembly of *E. cloacae* subsp. *dissolvens* ATCC 23373, ASM966045v1), which corresponds to the protein WP_153907835.1. While this does not definitively rule out the involvement of *fimH* in the subsp. *cloacae* strain, since the difference in expression profiles of *fimH* in both strains is unknown, characterizing the lectin responsible for the observed hemagglutination phenotype remains of interest.

Mechanistic insights into the role of EclA domains and isoforms further revealed the complexity of EclA-RBC interactions. EclA-C and EclA-N each failed to induce hemagglutination when tested independently. In both domains, the two binding sites are closely spaced and oriented in the same direction, preventing either domain from bridging two RBCs on its own. While EclA-C can bind a fucosylated ligand on one RBC, hemagglutination also requires the N-terminal domain to engage an additional, yet unidentified ligand on a second RBC, and vice versa. Therefore, the N- and C-terminal domains must be connected within the full-length EclA for the protein to bridge two RBCs and induce hemagglutination, since an equimolar mixture of isolated N- and C-terminal domains failed to do so. Consequently, the two binding sites on each domain likely serve to increase the binding affinity to one target through avidity, rather than to enable interactions with multiple separate ligands.

Furthermore, it could also be that each individual domain depends on the full length EclA for proper conformation and functional activity. This observation aligns with findings from other lectins, for instance, the accumulation-associated protein (Aap) from *S. epidermidis* requires both its A and B domains for functional glycan binding. In Aap, the A domain mediates adhesion to corneocytes via lectin binding to glucosamines, while the B domain serves as a fibrillar scaffold anchoring the protein to the cell wall. Although the B domain does not directly contribute to adhesion, its absence impairs the A domain's glycan-binding function (Roy et al., 2021).

These experiments also underscored a potential functional difference in hemagglutination between the two EclA isoforms. The EclA-M14A variant, representing the "long" isoform, displayed only weak hemagglutination. This result contrasts with the potent activity of the

previously used recombinant EclA, which comprised a mixture of both isoforms and caused complete hemagglutination at lower concentrations. This observation suggests that the "short" isoform, lacking the initial 13 amino acids and likely representing the native form, exhibits higher hemagglutination efficiency. Furthermore, it implies that if only the short isoform were expressed, hemagglutination might be even stronger, since the presence of the less active long isoform in the mixed preparation currently reduces the effective concentration of the potent short isoform. Variation in blood group antigens among individual donors may have influenced the hemagglutination phenotype of the recombinant EclA variants, and the His-tag on the N-terminal domain may have also affected hemagglutination, adding an additional variable to consider when interpreting these findings.

5.2. Adhesion of *E. cloacae* subsp. *cloacae* to A549 Human Lung Cells

Given that EclA is an ortholog of LecA, a known adhesin facilitating *P. aeruginosa* attachment to human lung cells (Chemani et al., 2009), and considering the documented capacity of *E. cloacae* to cause lung infections and attach to A549 human lung epithelial cells (Frutos-Grilo et al., 2023; Hennigs et al., 2011; Ramirez & Giron, 2025), adhesion was assessed using A549 cells. This experiment aimed to investigate whether EclA contributes to the cell attachment capabilities of *E. cloacae* subsp. *cloacae* strains $S2^{WT\text{-}HS0}$ (WT, isolate HS0, transformed with pMP7605) and $S2^{\Delta\text{-}HS3}$(Δ*eclA*, isolate HS3, transformed with pMP7605). Although a direct comparison between these two strains is complicated by the unforseen genomic deletions identified in $S2^{WT\text{-}HS0}$ (discussed in Subchapter 4.4.4), this assay was initially performed before such deletions were known. As such, the current results serve primarily as a preliminary investigation, laying the groundwork for future experiments.

The adhesion assay followed the protocol described in Chapter 7.8. A549 cells were cultured to confluency in 96-well plates and incubated with bacteria pre-stained with the green fluorescent dye SYTO™ 9 at a defined optical density. A short incubation period of 15 min was employed, as lectin-mediated attachment typically occurs rapidly (Neu et al., 2001). Fluorescence microscopy was subsequently utilized to quantify bacterial adhesion, with fluorescent cell counting providing an initial measure of the binding efficiency of *E. cloacae* subsp. *cloacae* to the host epithelial cells.

Figure 24 shows the results of the bacterial adhesion assay using $S2^{WT\text{-}HS0}$ and $S2^{\Delta\text{-}HS3}$. No substantial difference in adhesion to A549 lung epithelial cells was observed between the two

strains. However, at an OD_{600} of 0.2, $S2^{WT\text{-}HS0}$ appeared to display slightly reduced bacterial attachment compared to $S2^{\Delta\text{-}HS3}$ based on visual inspection. The quantification of fluorescence was limited by two main factors: the strong background autofluorescence of A549 cells and the small size of bacteria under 63× magnification, making individual bacteria difficult to accurately discern.

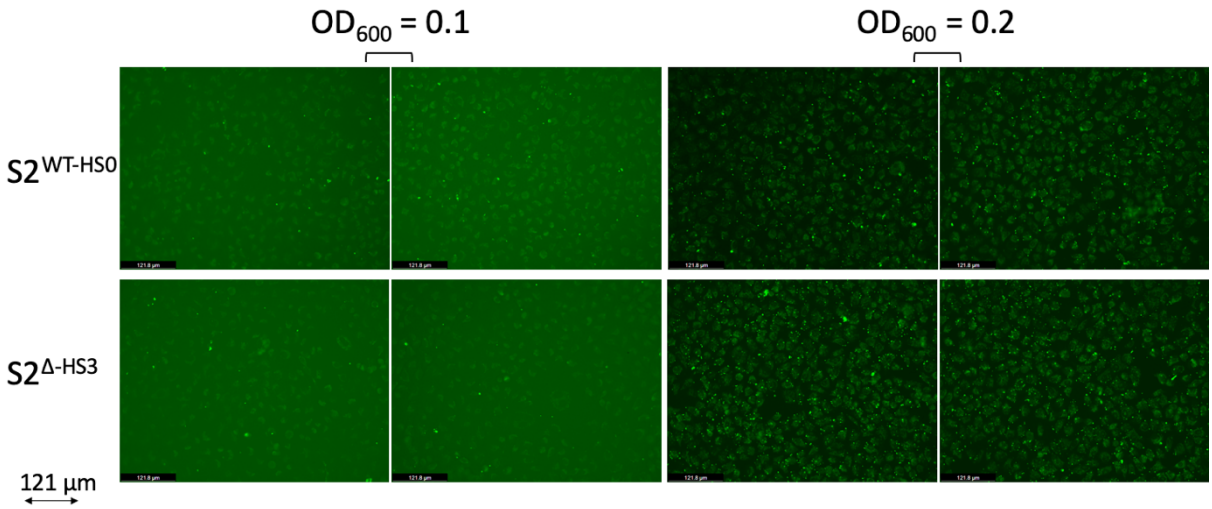

Figure 24: Adhesion of *E. cloacae* subsp. *cloacae* to A549 human lung epithelial cells. $S2^{WT\text{-}HS0}$ and $S2^{\Delta\text{-}HS3}$ were grown overnight in LB + 60 µg/mL gentamicin, washed, stained with 1 µM SYTO™ 9, blocked with 3% BSA in PBS/Ca, and adjusted to OD_{600} 0.1 or 0.2. A549 cells were cultured in 96-well plates until confluence (72 h) and incubated with 50 µL of prestained bacteria per well. Plates where either immediately incubated for 15 minutes (in the case of assays with OD_{600} 0.1) or centrifuged at 1000 × *g* for 5 min before incubation (in the case of assays with OD_{600} 0.2). After five PBS/Ca washes to remove non-adherent bacteria, bacterial adhesion was assessed using an inverted fluorescence microscope with a 63× objective and FITC filter. Identical imaging settings were used for all samples. $S2^{WT\text{-}HS0}$: WT *E. cloacae* subsp. *cloacae* pMP7605 isolate HS0; $S2^{\Delta\text{-}HS3}$: Δ*eclA E. cloacae* subsp. *cloacae* pMP7605 isolate HS3.

The A549 adhesion assay was conducted to evaluate whether EclA contributes to *E. cloacae* attachment to human lung epithelial cells similarly to its orthologue LecA in *P. aeruginosa*. Under the conditions tested, both $S2^{WT\text{-}HS0}$ and $S2^{\Delta\text{-}HS3}$ exhibited similar levels of binding to A549 cells, implying that EclA is not the principal adhesin mediating this interaction, or that the assay conditions did not highlight its role. Interpretation is further complicated by the additional genomic deletions present in $S2^{WT\text{-}HS0}$, addressed in Subchapter 4.4.4, including the loss of the TeR cluster and other coding sequences that may influence attachment behavior. A

more precise comparison using the $S2^{WT\text{-}HS2}$ strain, which differs from $S2^{\Delta\text{-}HS3}$ only by the absence of *eclA*, would more directly isolate the specific contribution of EclA to cell attachment.

Previous work demonstrated that *E. cloacae* adhesion to A549 cells is highly sensitive to the bacteria-to-cell ratio (BCR), with optimal binding observed at a 100:1 ratio and no attachment at 10:1 (Frutos-Grilo et al., 2023). In this study, an OD_{600} of 0.2 was used, which corresponds to approximately 5.86×10^7 CFU/mL for $S2^{WT\text{-}HS0}$ (as established in SI Figure 1). Since 50 µL of this bacterial suspension was added per well, a total of 2.93×10^6 CFU were introduced. Given that confluent A549 cells reach a density of approximately 9×10^4 cells/cm², and the well surface area is 2.88 cm², the estimated number of A549 cells per well would be ~2.59×10^5 cells. This yields an estimated BCR of 113:1. Thus, the experimental conditions aligned with the literature.

Despite this, microscopy-based quantification failed. Significant autofluorescence from A549 cells, combined with the small size of bacteria using the 63× objective lens, made individual bacteria difficult to visualize and count. Additionally, incubating bacteria in PBS/Ca supplemented with 3% BSA was crucial to prevent nonspecific binding to the well surface (data not shown), but may have influenced interaction dynamics with epithelial cells.

To address these limitations, future experiments could utilize CFU-based adhesion assays, which offer direct counts of attached bacteria without reliance on fluorescence and are less prone to host-cell autofluorescence. Higher-magnification imaging or alternative fluorescent labels such as fluorescein isothiocyanate (FITC) may enhance bacterial detection (Frutos-Grilo et al., 2023). Flow cytometry represents another possible approach, enabling quantification of bacterial attachment per host cell while also assessing host-cell viability and count (Frutos-Grilo et al., 2023).

In conclusion, the preliminary adhesion assay suggests that EclA might be dispensable for *E. cloacae* attachment to A549 cells under the tested conditions. However, technical challenges and the complex genetic background of $S2^{WT\text{-}HS0}$ limit interpretation. Employing a genetically matched pair ($S2^{WT\text{-}HS2}$ and $S2^{\Delta\text{-}HS3}$), refining the incubation time and visualization techniques, and adopting complementary quantification methods will be essential to definitively determine EclA's role in epithelial cell adhesion.

5.3. Adhesion of *E. cloacae* subsp. *dissolvens* to Lewis Blood Group Antigens

Lewis antigens are histo-blood group antigens expressed in humans across various tissues, including lymphocytes, platelets, vascular endothelium, and epithelial surfaces of the kidney, genitourinary, and gastrointestinal tracts. They are also present in most body fluids, except the cerebrospinal fluid. Notably, Lewis antigens are not synthesized by red blood cells themselves but are instead passively adsorbed from circulating serum glycoproteins onto the RBC membrane (de Oliveira & Corvelo, 2021).

Lewis antigens are key mediators of cell adhesion and recognition in both physiological and pathological contexts. They contribute to critical biological processes such as embryonic development, lymphocyte homing to secondary lymphoid organs, and acute inflammatory responses (Schenkel-Brunner, 2007). The expression of Lewis antigens on host cell surfaces has been linked to varying susceptibility to microbial infections, as many pathogens, such as Enterotoxigenic *E. coli*, *Shigella flexneri*, *H. pylori*, and the Norovirus, exploit these glycoconjugates as adhesion receptors (Ahmed et al., 2009; de Oliveira & Corvelo, 2021; Leslie et al., 2021; Stowell & Stowell, 2019).

Previous work demonstrated that EclA specifically binds to the Lewis A (Le^a) antigen (Beshr et al., 2025). Given that nearly 90% of infants are Le^a-positive during the first two years of life (Arcilla & Sturgeon, 1971), this interaction may have particular relevance in neonatal infections, especially considering that ECC species are prevalent pathogens in neonatal intensive care units (Ferry et al., 2020; Girlich et al., 2021; Hernandez-Alonso et al., 2022; Rahal et al., 2021).

To investigate whether EclA promotes the adhesion of *E. cloacae* to Lewis antigen-coated abiotic surfaces, an in vitro adhesion assay was performed as described in Chapter 7.9. Wells of a 96-well plate were coated with different polyacrylamide-conjugated Lewis antigens and incubated with acridine orange-labeled *E. cloacae* subsp. *dissolvens* $S1^{WT}$ (WT) and $S1^{\Delta}$ (Δ*eclA*) strains harboring pMP7605. Following incubation and washing steps, bacterial attachment was quantified using a fluorescence plate reader.

Both $S1^{WT}$ and $S1^{\Delta}$ bound to all wells, including uncoated controls, despite prior blocking with 3% BSA Figure 25-A. This nonspecific binding complicates interpretation and suggests that the bacterial strains intrinsically adhere to the plastic surface, regardless of Lewis antigen coating. Despite this, the positive control with 1 µM EclA-M14A-FITC confirmed successful coating and assay functionality. Strong, specific binding was observed to the Le^a-coated wells,

validating previous findings. Interestingly, low but detectable binding was also observed for Le^{b}-coated wells.

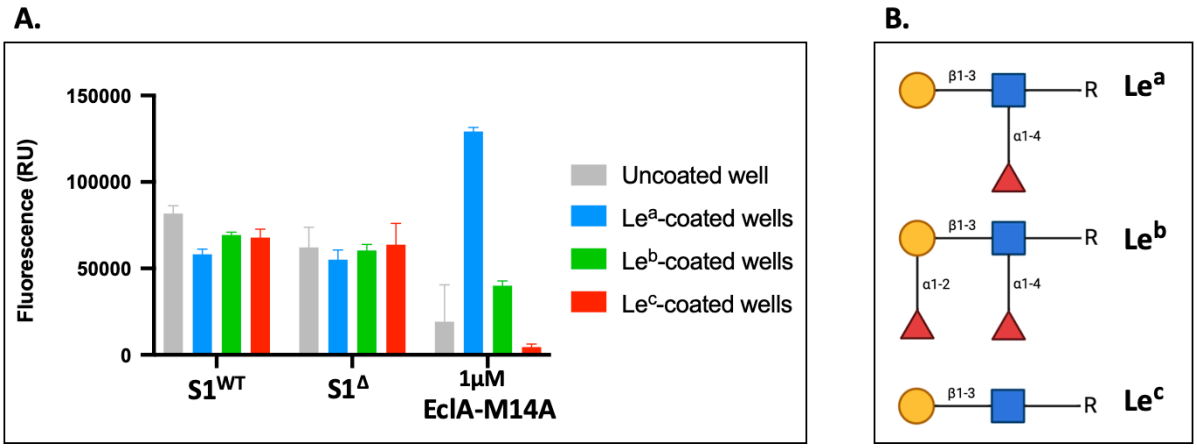

Figure 25: Adhesion of *E. cloacae* subsp. *dissolvens* to polyacrylamide-conjugated Lewis antigens. **(A)** Fluorescence-based adhesion assay measuring the binding of S1^{WT} and S1$^{\Delta}$ strains of *E. cloacae* subsp. *dissolvens* to Lewis antigens Le^{a}, Le^{b}, and Le^{c} coated as polyacrylamide polymers on 96-well plates. Bacteria were stained with acridine orange (1 µg/mL, 10 min), washed, and adjusted to OD_{600} = 2 in PBS. 100 µL of each bacterial suspension was added to antigen-coated or uncoated wells and incubated for 10 min at 37 °C with shaking (80 rpm). After washing the wells 3 times with PBS, fluorescence intensity (Ex/Em: 485/520 nm) was measured using a FLUOstar Omega plate reader. As a positive control, 1 µM of recombinant EclA-M14A-FITC was added under identical conditions. Bars represent mean fluorescence values of two technical replicates from one biological experiment. Error bars indicate standard deviation. **(B)** Represents the structure of the Lewis antigens used in (A) with the yellow circle as galactose, blue square as N-acetylglucosamine, and red triangle as fucose. R represents the poly[N-(2-hydroxyethyl) acrylamide] conjugate. S1^{WT}: WT *E. cloacae* subsp. *dissolvens* pMP7605; S1$^{\Delta}$: Δ*eclA E. cloacae* subsp. *dissolvens* pMP7605.

The prominent binding of EclA-M14A-FITC to Le^{a}-coated wells confirms prior findings (Beshr et al., 2025) and validates the integrity of the Lewis antigen coating used in the assay. However, the pervasive binding of both S1^{WT} and S1$^{\Delta}$ to uncoated wells, and the similar fluorescence signals observed for Le^{a}-coated wells across both strains indicate that the assay conditions were not well-suited to evaluate EclA-dependent adhesion at the whole-cell level due to substantial nonspecific binding. Although the wells were blocked with BSA, the bacterial cells themselves were not pre-incubated in BSA. Notably, results from the A549 adhesion assay (Chapter 5.2) demonstrated that bacterial pre-treatment with 3% BSA

significantly reduces nonspecific attachment to plastic surfaces. Including this pre-incubation step in future assays may therefore help reduce background noise and enhance the specificity of bacterial adhesion signals.

Importantly, the PBS used during washing steps and bacterial OD_{600} adjustment lacked calcium, a factor known to be essential for EclA-binding activity based on its predicted calcium-binding motifs. Future assays should include calcium in all buffers to preserve potential lectin-glycan interactions.

It's also worth noting that the medium and incubation conditions used here are similar to those in shaking biofilm assays, where the EclA-dependent autoaggregate formation phenotype was observed. However, the bacterial supernatant, which contains low amounts of EclA, as established in Chapter 3.1, was removed during acridine orange staining and not reintroduced. This step may have excluded released EclA that could have contributed to Le^a recognition. However, A549 adhesion assays (Chapter 5.2) showed no EclA-dependent adhesion when stained and washed cells were resuspended in their filter-sterilized culture medium, suggesting that released EclA concentration in the medium is too low to have an effect. The switch to acridine orange staining was necessary due to insufficient fluorescence signal from mCherry-expressing strains under these conditions (data not shown). In future protocols, retaining the supernatant for resuspension post-staining could help preserve released EclA or other extracellular factors that may play a role in its activity.

The low-level signal observed for Le^b was not seen in earlier studies and may be explained by differences in assay conditions, especially by the multivalent surface in the assay conducted. Structurally, both Le^a and Le^b antigens share fucosylated motifs, but Le^b carries an additional α1-2-linked fucose on the galactose residue, which may introduce steric hindrance to EclA binding (Figure 25-B). EclA may favor Le^a due to its more accessible configuration with only one α1-4-linked fucose. The emergence of detectable Le^b binding in this experiment is likely due to the high antigen coating concentration of 100 µg/mL. Supporting this interpretation, SI Figure 2 shows that when Le^b was coated at 15 µg/mL, no measurable EclA-M14A-FITC binding was detected, consistent with earlier results reported by Beshr et al., (2025).

In summary, while these results do not refute the hypothesis that EclA mediates *E. cloacae* binding to Le^a, they highlight limitations in the current assay and underscore the need for improved experimental conditions to assess this interaction reliably.

Closing Section 5: The Role of EclA in *E. cloacae* Adhesion:

This chapter sought to determine if EclA functions as a surface-associated adhesin in *E. cloacae*, bridging the gap between its known biochemical properties and its potential role in host-cell interactions. The investigation utilized three distinct models of adhesion: hemagglutination of human RBCs, attachment to A549 human lung epithelial cells, and binding to immobilized Lewis blood group antigens. While these experiments provided significant mechanistic insights into the structural requirements for EclA's function, they consistently suggested that EclA is not a primary surface adhesin under the tested conditions. Instead, the findings point towards a more complex, context-dependent role for EclA.

The difference between recombinant protein activity and whole-cell function

A central theme emerging from this section is the contrast between the strong activity of recombinant EclA and the absence of a clear activity in whole-cell assays under the tested conditions. The conducted studies confirmed that recombinant EclA is capable of crosslinking glycans on human RBCs and that this activity depends on its structural integrity. Covalent linkage between the N- and C-terminal domains is essential for crosslinking, and the "short" isoform, likely representing the native form of the protein, appears to be the more potent configuration for mediating hemagglutination. Despite this inherent biochemical activity of hemagglutination, EclA's function as a cell-surface adhesin was not observed under the tested conditions. *E. cloacae* subsp. *dissolvens* cells failed to agglutinate RBCs or specifically bind to Le^a-coated surfaces. This discrepancy suggests that while EclA can function as an adhesin, its native role on the bacterial surface may be minimal, regulated, masked by other effectors or dependent on experimental conditions and bacterial cell states.

A plausible explanation for this observation may be found by drawing a parallel to the well-studied lectins LecA and LecB in *P. aeruginosa*. An early, study demonstrated that only slight lectin activity was detected on the surface of intact *P. aeruginosa* cells, while significantly higher activities were found in the periplasmic space and more internal cellular compartments (Glick & Garber, 1983). It is therefore conceivable that EclA, being an orthologue of the adhesin LecA, may also function within the periplasm or other internal compartments of *E. cloacae*, rather than as a prominent surface-exposed adhesin. Such a role could be related to cell wall homeostasis or the proper folding and presentation of other surface factors, which could indirectly affect phenotypes like biofilm formation.

However, this potential internal function does not rule out an external one. Evidence from earlier experiment clearly shows that EclA is also released into the extracellular medium (Chapter 3.1, 4,3).

Therefore, a more comprehensive model is that EclA, much like its orthologue LecA, likely has a context-dependent, dual function. A pool of EclA may reside periplasmically, while another portion is released to act externally. Its ultimate role, whether in biofilm matrix cross-linking or direct cell adhesion, is likely dependent on specific environmental cues, the presence of its ligands, and growth conditions.

The broader adhesion landscape and future directions

The findings from this chapter also show a strong, EclA-independent hemagglutination exhibited by *E. cloacae* subsp. *cloacae*. Given that many hospital isolates of *E. cloacae* are known to exhibit mannose-sensitive hemagglutination (Keller et al., 1998), it is possible this phenotype is mediated by a yet-uncharacterized mannose-binding lectin. Although FimH was suspected to be responsible for this activity, its presence in subsp. *dissolvens* did not result in a comparable hemagglutination pattern. While differential fimH expression between the two subspecies, potentially influenced by growth conditions or physiological states, cannot be excluded, a future approach would involve performing a mannose-based pull-down assay to isolate and identify the lectin responsible from *E. cloacae* subsp. *cloacae* extracts, thereby determining whether it is indeed FimH or another mannose-binding lectin.

To definitively clarify EclA's role, future adhesion studies must be refined as discussed. The A549 adhesion assay was complicated by the use of the $S2^{WT\text{-}HS0}$ strain with its genomic deletions. Future experiments should utilize the genetically matched pair, $S2^{WT\text{-}HS2}$ and $S2^{\Delta\text{-}HS3}$, to provide a clean comparison. Crucially, these assays must also be performed with *E. cloacae* subsp. *dissolvens*, as the difference in its EclA-dependent biofilm phenotype suggests its adhesion mechanisms may differ from subsp. *cloacae*.

Finally, the biochemical characterization of EclA itself should continue. Purifying and testing the "short" isoform of recombinant EclA is necessary to confirm its superior activity in functional assays; if confirmed, it should be adopted for all future studies. Furthermore, the discovery of the EclA-N ligand remains a critical objective that could unlock a deeper understanding of where and how EclA functions. Together, these refined experimental approaches will be essential to fully elucidate the complex and multifaceted role of EclA in *E. cloacae* pathophysiology.

6. Concluding Remarks

This thesis embarked on an investigation to elucidate the biological functions of EclA, a novel two-domain lectin from *E. cloacae*. The research was driven by the central hypothesis that EclA, as a structural orthologue of the well-characterized *P. aeruginosa* virulence factor LecA, would function similarly, mediating both biofilm formation and host-cell interactions. Through a series of genetic, biochemical, and phenotypic analyses across two subspecies, *E. cloacae* subsp. *dissolvens* and subsp. *cloacae*, this work has revealed a far more nuanced and context-dependent role for EclA than initially predicted. The findings confirm EclA's importance in bacterial community behavior, but could not provide proof for its proposed function as a primary host adhesin under the tested conditions.

6.1. Synthesis of Key Findings

The functional characterization of EclA yielded several key insights. The lectin's molecular profile was conserved across both subspecies: it was found to be both cell-associated and released in small quantities, and native expression likely initiates from a downstream start codon, contrary to what was previously thought, producing a shorter, potentially more active isoform.

The investigation into EclA's role in biofilm formation produced the most compelling, albeit complex, results. In *E. cloacae* subsp. *dissolvens*, the deletion of *eclA* led to a complete loss of the robust autoaggregation phenotype observed in $S1^{\Delta}$ under specific in vitro conditions (growth with plasmid pMP7605 and gentamicin exposure). This provided the strongest initial evidence for EclA's role as a key structural component in biofilms. In contrast, the investigation in *E. cloacae* subsp. *cloacae* was inconclusive. The role of EclA was not immediately apparent, having been overshadowed by the unexpected discovery of the hyper-aggregative $S2^{WT\text{-}HS0}$ variant, which maintains autoaggregates and continues autoaggregate formation even under gentamicin exposure, an exposure that was shown to disperse autoaggregates and prevent their formation in other isolated WT colonies harboring pMP7605. Whole-genome sequencing linked this unique phenotype to the spontaneous deletion of a plasmid-borne tellurite resistance gene cluster, suggesting that robust autoaggregation in this context was a stress response to gentamicin, to which $S2^{WT\text{-}HS0}$ was sensitized.

Conversely, the hypothesis that EclA acts as a primary surface adhesin for host cells was not supported by the experimental data. While recombinant EclA effectively mediated hemagglutination and bound specifically to its known ligand, the Lewis A antigen, this activity

did not translate to a whole-cell phenotype in vitro. *E. cloacae* subsp. *dissolvens* failed to cause hemagglutination, while *E. cloacae* subsp. *cloacae* exhibited strong, but EclA-independent, hemagglutination. These findings collectively suggest that EclA's primary adhesive function under the tested conditions is directed towards the bacterial community, rather than directly mediating attachment to host tissues.

Finally, the in vivo studies successfully established the *G. mellonella* larva as a viable infection model for assessing the virulence of *E. cloacae*, particularly for subsp. *dissolvens*, which demonstrated notable pathogenic potential. The failure of the zebrafish immersion model highlighted the importance of host- and condition-specific factors in virulence studies and pointed towards the robust resistance of zebrafish to exogenous bacteria, even when exposure occurred through a direct wound.

6.2. Revisiting the Initial Hypothesis

In light of these findings, the initial hypotheses can be critically evaluated:

1. **Hypothesis 1:** EclA acts as a scaffolding protein for autoaggregation and biofilm formation. This hypothesis is partially confirmed, with significant context dependency. The phenotype observed in *E. cloacae* subsp. *dissolvens* strongly supports this role under the specific conditions tested. In contrast, its function in *E. cloacae* subsp. *cloacae* was not evident, likely due to the absence of conditions that reveal its activity. Therefore, while EclA has been shown to be a biofilm determinant, its functional expression appears to be condition-dependent.
2. **Hypothesis 2:** EclA has an extracellular role in mediating adherence to host glycan receptors. While EclA is released and biochemically capable of binding host glycans, such as those on human red blood cells, it does not appear to act as a primary adhesin on the bacterial surface in the limited conditions examined. Instead, its adhesive properties seem to be directed inward, toward the autoaggregate matrix. However, further investigation under a broader range of conditions and cell types is necessary before this hypothesis can be definitively ruled out.
3. **Hypothesis 3**: Deletion of *eclA* would lead to attenuated virulence. This hypothesis remains an open but well-supported question. While a direct link between EclA and in vivo virulence was not established in this work, its demonstrated role in biofilm formation, a cornerstone of chronic infection and immune evasion, strongly implies a

contribution to pathogenicity. The establishment of the *G. mellonella* model provides a platform to directly test this prediction in future studies.

6.3. Limitations and Future Perspectives

A key consideration arising from this work is the condition-dependent nature of the EclA phenotype, particularly regarding the autoaggregation assay in *E. cloacae* subsp. *dissolvens*. It is acknowledged that this definitive phenotype was observed in the presence of the pMP7605 plasmid and gentamicin, and was not tested in their absence. As the work in *E. cloacae* subsp. *cloacae* demonstrated, these factors can induce stress and influence aggregation independently of the lectin. Therefore, a future experiment that could be done is to repeat the autoaggregation assay using the parental *E. cloacae* subsp. *dissolvens* strains with no plasmid or antibiotic pressure.

However, even if the phenotype were to disappear under these conditions, it would not invalidate the conclusion that EclA is involved in autoaggregate formation. Rather, it would reinforce the finding that EclA's function is most critical under conditions of cellular stress, a scenario highly relevant during infection. This interpretation is strongly supported by the fact that whole-genome sequencing confirmed that $S1^{WT}$ and $S1^{\Delta}$ were genetically identical aside from the *eclA* locus, allowing for a direct causal link to be drawn, a clarity not afforded in $S2^{WT\text{-}HS0}$ and $S2^{\Delta\text{-}HS3}$ comparison due to the confounding TeR cluster deletion. Notably, this TeR cluster is absent in *E. cloacae* subsp. *dissolvens*, eliminating it as a potential variable in that background. To definitively establish causality, the gold-standard experiment would be the chromosomal knock-in of the *eclA* gene into the $S1^{\Delta}$ to demonstrate full restoration of the phenotype.

Building on the foundation of this thesis, several exciting avenues for future research emerge:

- **Virulence testing:** Directly compare the virulence of the $S1^{WT}$ and $S1^{\Delta}$, and $S2^{WT\text{-}HS2}$ and $S2^{\Delta\text{-}HS3}$ in the established *G. mellonella* model.
- **Ligand identification:** Elucidate the unknown ligand for the N-terminal domain of EclA, which is critical for a complete understanding of its binding mechanism and function.
- **Mechanistic dissection:** Investigate the role of the TeR cluster in the stress-induced aggregation of *E. cloacae* subsp. *cloacae* through targeted deletion and complementation experiments.
- **Biochemical characterization:** Purify and functionally test the native "short" isoform of EclA to confirm its potentially enhanced activity.

- **Identification of other adhesins:** Characterize the potent, EclA-independent hemagglutinin in *E. cloacae* subsp. *cloacae*.

In conclusion, this thesis defines the role of EclA as a nuanced, context-dependent lectin whose primary function appears to be the maintenance of bacterial community integrity, especially under antibiotic stress. By providing a deep functional characterization and establishing critical experimental models, this research lays the essential groundwork for future investigations into EclA's role in pathogenicity and its potential as a target for novel anti-virulence therapies.

7. Materials and Methods

7.1. Supplementary Information for Chapter 3.2

Scanning electron microscopy

Autoaggregates of $S1^{WT}$ and $S1^{\Delta}$ were grown as indicated in the materials and methods section of Chapter 3.1. Aliquots of aggregates (200 µL) were fixed with 2% glutaraldehyde for 30 minutes, deposited onto 0.2 µm pore-size filters, washed under vacuum with 500 µL milli-Q water to remove salts, and air-dried. Fixed samples were transferred to the Leibniz Institute for New Materials (Saarbrücken) for imaging. Samples were sputter-coated with Au-Pd, and imaged under high vacuum using a field-emission SEM at different magnifications with an Everhart-Thornley Detector (ETD), and 5.0 kV accelerating voltage.

Autoaggregation assay with exogenous recombinant EclA complementation

An overnight culture of $S1^{\Delta}$ was grown in LB medium supplemented with 60 µg/mL gentamicin at 37 °C with shaking at 180 rpm. Cells were diluted into $M63^{+}$ medium to a final OD_{600} of 0.02. Prior to aliquoting, recombinant EclA or the EclA-M14A variant (in TBS/Ca) was added to the culture to final concentrations of 100 µM (EclA), or 8 µM (EclA-M14A), respectively. The same volume of TBS/Ca only was added to $S1^{WT}$ and $S1^{\Delta}$ controls.

Aliquots of 1.25 mL were transferred into 24-well fluorocarbon film-bottom imaging plates (Zell-Kontakt, #3231-20), sealed with breathable foil (Greiner Bio-One, #676051), and incubated at 37 °C with 72% relative humidity and shaking at 180 rpm for 48 hours. After incubation, whole-well fluorescence images were acquired with uniform acquisition parameters as described in the materials and methods section of Chapter 3.1.

Homology protein modeling and structural analysis

The EclA protein sequence from *E. cloacae* subsp. *dissolvens* DSM 16657 was retrieved by performing a BLAST search against the NCBI protein database using the EclA sequence (ECL_04191) from *E. cloacae* subsp. *cloacae* DSM 30054 as the query. The corresponding EclA homolog from DSM 16657 was then obtained for further analysis. Based on the domain boundaries reported by Beshr et al., (2025) for EclA from *E. cloacae* subsp. *cloacae* DSM 30054, the N- and C-terminal domains to be modeled for *E. cloacae* subsp. *dissolvens* were extracted from the full-length DSM 16657 sequence. The N-terminal domain sequence was: MANVFATLSQESDMSDNLIWSGKVDAKNTEGTNTGISLKAGEIITILASGWARNGSE

NFALTAPQGRIPREGETLALRNPSLQARIGNENYPVGNHKYRWSVPAEGTLTLIFAD GKDQYKDNAGEFSVEVYREAD. The C-terminal domain sequence was: AAVPFEDF TNFERDNWNSWQAGPAGHDLYLVDASARAVEFITNPNKNHAGEILKKTLTGLTAGH EYTWTVKAARIIGKYEAPKISLRADGKDISAPLELKQANEWVTLSGKFKAAGNQAEL AVVSHVAASMGNDFRIKELRIKG.

Structural models of both domains were generated using the Phyre2.2 server (http://www.sbg.bio.ic.ac.uk/phyre2) in normal modeling mode, with the experimental EclA structures from *E. cloacae* subsp. *cloacae* DSM 30054 (PDB 6YGQ for the N-terminal domain and PDB 6YF6 for the C-terminal domain) serving as templates. Predicted structures were visualized and aligned with their respective template structures using PyMOL (Schrödinger, LLC). Structural superimpositions were performed to evaluate backbone alignment. Residues within 4 Å of the methyl α-L-selenofucoside ligand in the C-terminal domain were identified for further structural annotation. Hydrogen bond interactions, calcium coordination sites, and amino acid variations were annotated in the models for subsequent analysis.

Autoaggregation assay under shear flow

The autoaggregation assay under flow conditions was performed as previously described, using a continuous flow system composed of a medium reservoir (inlet), a peristaltic pump, a flow chamber for bacterial growth analysis, and an outlet connected to a waste container (Zahorska et al., 2024). The medium used in the system consisted of: M63 medium supplemented with 0.4% (w/v) glucose, 0.2% (w/v) casamino acids, gentamicin (60 µg/mL), and $MgCl_2$ (1 mM); M63 medium supplemented with 0.16% (w/v) glucose, 0.08% (w/v) casamino acids, gentamicin (60 µg/mL); and $MgCl_2$ (1 mM), and M63 medium supplemented with 0.4% (w/v) glucose, 0.2% (w/v) casamino acids, gentamicin (60 µg/mL), $MgCl_2$ (1 mM), and $CaCl_2$ (100 µM).

The medium was transported from the reservoir to the peristaltic pump (Watson-Marlow Fluid Technology Solutions) through 1.6 mm silicone tubing (ibidi, Germany). Stopper hoses (Carl Roth) placed in the pump were connected to the silicone tubing using standard connectors (ibidi, Germany). The flow was directed through bubble traps (provided by Claus Sternberg, DTU Copenhagen) via 0.8 mm silicone tubing (ibidi, Germany) to eliminate air from the system. Downstream of the bubble traps, the medium entered the flow cell (µ-Slide VI^0.4

ibiTreat, ibidi, Germany), which was connected using 1.6 mm silicone tubing. The outlet led from the flow cell to a waste container.

To inoculate the flow cell, the silicone tubing downstream of the chamber was clamped to temporarily stop the flow. Suspensions of *E. cloacae* subsp. *dissolvens* pMP7605 strains, prepared from either overnight cultures or subcultures grown in LB at 37 °C with shaking (180 rpm) to an OD_{600} of 0.4-0.6, were washed with PBS and adjusted to an OD_{600} of 0.075 or 0.02 in LB. These suspensions were then injected into the tubing upstream of the flow chamber using a 0.30 × 12 mm cannula (Sterican), followed by immediate clamping of the upstream tubing. The injection site was sealed with silicone glue. After a settling phase of 15 or 30 minutes, the clamps were removed and the medium flow was resumed at 1.66 µL/s. The temperature of the flow chamber was maintained at either 25 °C or 30 °C using a dedicated heating system (ibidi, Germany).

Brightfield and fluorescence microscopy (TXR filter cube excitation: 540-580 nm; dichroic: 585 nm; emission: 592-668 nm) were performed using an inverted fluorescence microscope (Leica DMi8) equipped with a Leica DFC7000 GT monochrome camera, and a 5× and 20× objective lens (HC PL APO CS2 20×/0.75 IMM UV). Imaging was conducted under uniform acquisition settings.

7.2. Supplementary Information for Chapter 3.3

Danio rerio zebrafish larvae immersion infection model

Embryos of Casper or AB zebrafish (sourced from the European Zebrafish Resource Center at the Karlsruhe Institute of Technology) were used for all experiments prior to reaching 120 hpf, in accordance with EU Directive 2010/63/EU, which does not classify such early developmental stages as animal experiments. All husbandry practices were conducted in compliance with the German Animal Welfare Act (§11 Abs. 1 TierSchG). Euthanasia was performed by immersion in ice water for at least 12 hours. Embryos and larvae were maintained at 28 °C in 0.3× Danieau's solution (17.4 mM NaCl, 0.21 mM KCl, 0.12 mM $MgSO_4$, 0.18 mM $Ca(NO_2)_2$, 1.5 mM HEPES, 1.2 µM methylene blue, pH 7.1-7.3) with the medium refreshed three times daily. For dechorionation, 28 hpf embryos were incubated for 5 minutes in 1 mg/mL pronase (Sigma-Aldrich, #P5147) prepared in 0.3× Danieau's, followed by three washes with 0.3× Danieau's (without methylene blue). During tail amputations, embryos were

anesthetized by immersion in 945 µM tricaine (Sigma-Aldrich, #E10521) diluted in 0.3× Danieau's, from a 4 mg/mL stock solution prepared in 1% Na_2HPO_4 (pH 7.0-7.5).

P. aeruginosa strains PA14, PAO1, and their Δ*lecA*Δ*lecB* double mutant, as well as $S1^{WT}$ and $S1^{\Delta}$, were streaked onto LB agar plates supplemented with 60 µg/mL gentamicin. Overnight cultures were grown in LB + 60 µg/mL gentamicin at 37 °C with shaking at 180 rpm. The following day, cultures were diluted in fresh LB + 60 µg/mL gentamicin to an OD_{600} of 0.02 and grown to mid-log phase (OD_{600} = 0.7-0.8). Cells were harvested by centrifugation (18,000 × *g*, 5 min), washed twice with 0.3× Danieau's medium without methylene blue, and resuspended to OD_{600} = 1, corresponding to approximately 4×10^8 CFU/mL. A 1:10 serial dilution series was performed to generate bacterial suspensions ranging from 10^8 to 10^6 CFU/mL in a flat transparent 96-well plate (Greiner bio-one, #655101) with 200 µL of bacterial suspension per well. Aliquots were taken for viable cell count analysis.

Zebrafish infections by immersion were conducted at either 1- or 2-dpf. At 1 dpf, following dechorionation, individual larvae were transferred into separate wells of a 96-well plate (one larva per well), with 12-24 larvae per experimental group. At 2 dpf, immersion infection was performed following tail amputation. After dechorionation, larvae were anesthetized in tricaine, and a tail transection was made just past the tip of the caudal vein as described by (Lopez-Baez et al., 2018). Amputated larvae were then washed with 0.3× Danieau's medium (without methylene blue) and similarly distributed into 96-well plates. Control wells received only 0.3× Danieau's medium (without methylene blue). In all cases, larvae were monitored once a day for a duration of 72 hours while incubated at 28 °C. Survival data of larvae were displayed in a Kaplan-Meier curve, and statistical analysis for significance was done using log-rank (Mantel-Cox) test.

Galleria mellonella infection model

The *Galleria mellonella* infection model was adapted as previously indicated, with some modifications (H.-F. Yang et al., 2017). Larvae were commercially sourced from Valomolia (Strasbourg, France) and selected for uniformity in size (15 per group) and absence of melanization. Bacterial suspensions were prepared as follows: Strains were streaked onto LB agar then grown overnight in LB at 37 °C (media were supplemented with 60 µg/mL gentamicin for strains carrying the plasmid pMP7605). A subculture in LB (with 60 µg/mL gentamicin supplementation for strains carrying the plasmid pMP7605) was inoculated at an initial OD_{600} of 0.02 and incubated at 37 °C (180 rpm) until reaching OD_{600} 0.6-0.8. Cells were

pelleted, washed twice in PBS, and resuspended to a final OD_{600} of 4.3 (corresponding to ~1 × 10^9 colony-forming units CFU/mL) in PBS supplemented with a final concentration of 20% (w/w) glycerol. Aliquots were stored at -80 °C, thawed, and cultured on LB agar overnight at 37 °C to confirm bacterial viability and concentration. Serial dilutions of the suspensions were performed prior to use from thawed stocks to achieve the desired inoculum for injection.

For infection, larvae were immobilized ventral side up using thumb and forefinger, and 5 µL of bacterial suspension was injected into the last left proleg proximal to the anal proleg using a 30G Sterican® insulin needle (B. Braun, Article 4656300) affixed to a 1 mL syringe and microinjector (NE-1000X single pump system). Post-injection, 5 µL of the inoculum was plated to verify delivered CFU. Larvae were incubated at 37 °C for 64 hours. Death was defined as the absence of movement upon mechanical stimulation.

7.3. Supplementary Information for Chapter 4.1

Construction of the mutator plasmid pKNG101_30054_GmR

The suicide plasmid pKNG101_30054, carrying the fused upstream and downstream flanking regions of *eclA* from *E. cloacae* subsp. *cloacae*, was constructed by GenScript using BamHI and XbaI restriction sites to clone the fused fragment (SI Table 1) into the pKNG101 vector from Kaniga *et al.* (1991).

To provide a compatible antibiotic selection marker for *E. cloacae* subsp. *cloacae*, which exhibits intrinsic resistance to streptomycin (the original pKNG101 selection marker), a gentamicin resistance cassette was amplified from pMP7605 using primers MF17.1 and MF18.1 (SI Table 3). This cassette was subsequently inserted into pKNG101_30054 by restriction digestion and ligation cloning, using an NEB kit and protocol for SpeI digestion and T4 DNA ligase-mediated ligation, resulting in the construction of pKNG101_30054_GmR. For restriction digestion, 50 µL reactions were prepared containing 3 µg of DNA, 1 µL of SpeI-HF (NEB, R3133), 5 µL of 10× rCutSmart buffer, and milli-Q water to a final volume of 50 µL. The reactions were incubated at 37 °C for 2 hours. Digested DNA was subsequently purified by agarose gel electrophoresis, followed by DNA extraction using GenElute™, Sigma Life Science's gel extraction kit (#NA1111-1KT). Ligation was performed using a T4 DNA Ligase Kit (NEB, M0202). Each 20 µL ligation reaction contained 2 µL of 10× T4 DNA ligase buffer, an insert-to-vector molar ratio of 3:1, 1 µL of T4 DNA ligase, and nuclease-free water to 20 µL. Ligation reactions were incubated overnight at 16 °C. The ligation reaction was

transformed into electrocompetent *E. coli* TransforMax™ EC100D™ pir-116, *E. coli* SM10 λpir, and chemically competent *E. coli* BW19610 cells.

Following miniprep of pKNG101_30054_GmR from *E. coli* TransforMax™ EC100D™ pir-116 selected clones, the plasmid was subjected to whole-plasmid sequencing using Oxford Nanopore Technology performed by Eurofins Genomics.

SI Table 1: Fused flanking regions of *eclA* from *E. cloacae* subsp. *cloacae* used for 2-step allelic exchange. The nucleotides in blue and green represent the downstream and upstream sequences, respectively. BamHI and XbaI restriction sites are designated in red.

Fused flanking nucleotide sequences of *eclA* in *E. cloacae.* subsp. *cloacae*	GATCCCCAGGAAATTACAGCAATTCTACTCAGGCCGGAAATTAAGGGCTGGCATTTTCCTAATAAGTTGCCGTTCGGGCTCAAAAGC GAAATGTCACGACAATGGATTCATGAACATTTCGGAGAGCCGCTAAGAAGTTCACCACCTAAAACTATTATGAGGCGTGCCTTGGG ATGGGTAGATCTTTTTGATGCCGCAACTGGAGACATCCCAGTGAGTATGCAGATTGATTATGACGTAATGGACAATGCTTTATCTGT AACATTTATGCCAACCTCAGAGCATCGCTGGTAGTGTTCAATATAAGCCCCGGTAGGGGCTTTTTGCAGTGTTGCATACTACGATTC GCAGTACGAACGATAGCCTTAATGCGGAGGCTGCTAACAGAATGACTGTCTGGCCCGCCCATACCCTTATCGACAGGCTTTGTGTTG TTTGTATTTATTTATCCAGTTCTGATCTCACTATTCCTTTGAATTAACCATAACCAGACAGGTCTTGTATCGTTTAGCGATATAGCAG CGCACAATAACCTTGCCCACTGGTGTTTATTACCTGTTGGTGTAGCGCATATGTTGAACATGTGCGCTACACAATTTTGAACATCGC ACTGCCATTCAGCATTCCCGCTAAATAGCAGCCCGACTATTTGACGTGAAAGATAGTCCTTACGAAATGCGTGATTTAAGTCACTCA GTTCTGCTAACCGCCTGATAATTTGAATAAATAAAATCCTGAGAAGCACGAACTTCTCATCATCATTACCCGGTTGTTATCGGCAGG AATGAGAATAGTCAGGTGGTATATACAATTCAAAACGCTAAAAGCTTTATTAAGGGTTGCGATTTTGTAATTAATTAAAAATAATAA AATAATTATCGCTGAATTAGGAATAATCTTAAGCAATATGAGGGTGAGTGCAGGGTTTTTAAATCGTTTATTCTCCCCATTGTTTACG TTGATAATCATGTAAGCACTTCAGGAAATCGGGCATACTTATCACGTGTCACGCAGGTAAAGTTCAAAAATAAACAAATTATCTTTT TACGCATGCAGCGACCTCTGATATACCTTCCTTCCCTCATACCAGTCTGAGTGATGACCGCTGTGGTCTATACTGGCCATTATCGAAT ACCCAAAGGTGGTGTCATGCATATATTGCCTCCTGTTCGCCCTGAACACTCCATTGAACGTCTGACGGCGGTACTTGAACCCATTGC GGAAAAAGTGAAGCTTGCGCCGCGTAAGCGGATTACCTGGAAACATAAAGGCCGCCAGCAAATGTATCTTTTTCAGGAAGGAGAGT CTAGA

Transformation by electroporation

E. coli TransforMax™ EC100D™ pir-116 cells, SM10 λpir and *E. cloacae* subsp. *cloacae* were made electrocompetent by growing them overnight in LB medium at 37 °C with shaking at 180 rpm, followed by washing with milli-Q water and resuspension in 10% glycerol. Fifty microliters of the prepared electrocompetent cells were mixed with 100 ng of plasmid pKNG101_30054_GmR or pMP7605 in the case of *E. cloacae* subsp. *cloacae*, and electroporated using a 1.6 kV pulse for 6 ms. Immediately after electroporation, LB medium was added, and the cells were incubated at 37 °C with shaking at 300 rpm for 1 hour to allow recovery. Transformants were selected on LB agar plates supplemented with gentamicin (60 µg/mL).

Transformations by heat shock

Transformations of WT and Δ*eclA* *E. cloacae* subsp. *cloacae* strains, and *E. coli* BW19610/SM10 λpir were carried out by preparing chemically competent cells followed by heat shock, as described in the materials and methods section of Chapter 3.1. Transformed cells

were selected after incubation for 24 hours at 37 °C on LB agar plates supplemented with 60 µg/mL gentamicin to isolate clones harboring either pKNG101_30054_GmR or pMP7605.

Transformations by triparental mating

Triparental mating was performed as described in the materials and methods section of Chapter 3.1, using the recipient, donor, and helper strains, along with the corresponding selection medium, as detailed in SI Table 2.

SI Table 2: Tri-parental mating transformations

Recipient	**Plasmid**	**Donor**	**Helper**	**Selection medium**
E. cloacae. subsp. *cloacae* DSM 30054	pKNG101_30054_GmR	*E. coli* TransforMax™ EC100D™ pir-116 pKNG101_30054_GmR	*E. coli* HB101 pRK600	LB + ampicillin 200 µg/mL + gentamicin 60 µg/mL

Deletion of *eclA* in *E. cloacae* subsp. *cloacae* by 2-step allelic exchange

The 2-step allelic exchange was performed according to Hmelo *et al.,* (2015) with some modifications. Briefly, 10 µL of *E. cloacae* subsp. cloacae harboring pKNG101_30054_GmR was taken from an overnight LB culture supplemented with 16% (w/v) sucrose and streaked on LB agar (without salt) to isolate single colonies. Single colonies were replica-plated on both LB agar, and LB agar supplemented with 60 µg/mL gentamicin, for the counter selection of *E. cloacae* subsp. *cloacae*. Colonies only growing on LB were selected, indicating the occurrence of the second recombination event and the loss of pKNG101_30054_GmR. To validate the deletion of *eclA* colony PCR and whole-genome sequencing was conducted.

Polymerase chain reactions and plasmid purifications

PCR reactions were conducted to validate transformations and gene deletions. The gentamicin resistance cassette, intended as an insert in pKNG101_30054*,* was also amplified by PCR from pMP7605.

Generally, for each 50 µL PCR reaction, 0.5 µL of Phusion® High-Fidelity DNA Polymerase (NEB, Cat. No. M0530S) was used, with its HF Phusion® buffer adjusted to a final concentration of 1X. Primer concentrations were at 5 µM, and dNTPs at 0.2 mM.

As templates:

-For colony PCR, a single colony is resuspended in 50 µL H2O and heated to 95 °C for 5 min. Five microliter of the lysate is used as template in the PCR reaction.

-For plasmid templates, plasmids were purified using the GenElute™ Plasmid Miniprep Kit (Sigma-Aldrich, Cat. No. PLN350-1KT) and following its protocol. Plasmid concentrations were measured by using a NanoDrop spectrophotometer (Thermo Scientific, NanoDrop 2000c) and measuring absorbance at 260 nm and applying Beer's law with 50 ng/µL cm^{-1} as the mass extinction coefficient for dsDNA. To each PCR reaction, 250 ng of plasmid was added.

The volume of the reaction was finally adjusted to 50 µL with milli-Q water.

PCR cycling conditions followed a standard protocol: an initial denaturation step at 95 °C for 1 minute, followed by 30 cycles of denaturation at 95 °C for 10 seconds, annealing at a temperature based on primer melting temperature (T_m) values calculated using the NEB T_m calculator, and extension at 72 °C for 30 seconds per kilobase of the expected amplicon. A final extension was performed at 72 °C for 10 minutes.

SI Table 3: PCR reactions listing the DNA templates and their respective primer pairs used for amplification.

Experimental validation	**Template**	**Forward primer (5'-3')**	**Reverse primer (5'-3')**
2nd recombination event: *eclA* knockout from *E. cloacae* subsp. *cloacae*	Single colony	MF07: gatgatgagaagttcgtg	MF08: cagacaggtcttgtatcg
Transformation of pKNG101_30054_GmR into *E. coli* TransforMax™ EC100D™ pir-116	Single colony	MF17.1: aaaaaactagtccgcatgatgaacctgaatcgc	MF18.1: aaaaaactagtccttgaatcggatatgcaggc
Insertion of GmR into pKNG101_30054_GmR	Single colony	#1001: tattaattgatctgcatcaacttaacg	MF18.1: aaaaaactagtccttgaatcggatatgcaggc

Insert Generation	Template	Forward primer (5'-3')	Reverse primer (5'-3')
Amplifying the gentamicin resistance cassette from pMP7605 with SpeI overhangs	pMP7605	MF17.1: aaaaaactagtccgcatgatgaacctgaatcgc	MF18.1: aaaaaactagtccttgaatcggatatgcaggc

Whole genome sequencing of WT and Δ*eclA E. cloacae* subsp. *cloacae*

Whole genome sequencing of all *E. cloacae* subsp. *cloacae* derivatives harboring pMP7605 was done by MicrobesNG as described in the materials and methods section of Chapter 3.1.

7.4. Supplementary Information for Chapter 4.2

Growth curves of WT vs Δ*eclA E. cloacae* subsp. *cloacae*

$S2^{WT\text{-}HS0}$ and $S2^{\Delta\text{-}HS3}$ were grown in 50 mL of LB broth supplemented with 60 µg/mL gentamicin in non-baffled 250 mL Erlenmeyer flasks. Cultures were incubated at 37 °C with shaking at 180 rpm and maintained at 72% relative humidity. Bacterial growth was monitored by measuring the OD_{600} using a spectrophotometer. Measurements were taken every hour for the first 12 hours, with a final measurement taken at 24 hours. In parallel with the OD_{600} measurements, samples were withdrawn at the same selected time points to determine the viable cell count. To achieve this, samples were serially diluted in sterile PBS, and aliquots were plated onto LB agar. Following incubation at 37 °C for 24 hours, colonies were counted to calculate the concentration in CFU/mL. A standard curve was then established by plotting the OD_{600} values against their corresponding CFU/mL. The resulting slope, represented in SI Figure 1, was subsequently used to estimate bacterial concentrations for all relevant experiments.

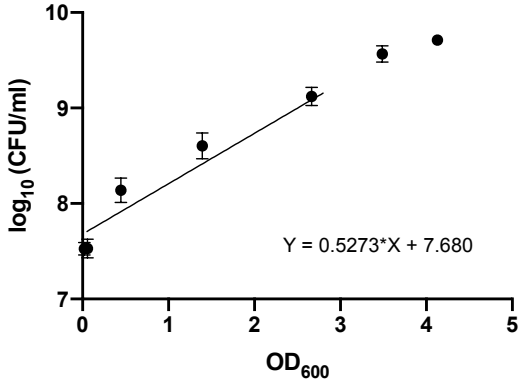

SI Figure 1: Correlation between optical density and viable cell count for *E. cloacae* subsp. *cloacae* pMP7605 ($S2^{WT\text{-}HS0}$). Data points represent the mean ± standard deviation of

two independent biological replicates. For each biological replicate, the CFU/mL and OD_{600} values were determined from the average of three technical replicates. The line represents the linear regression fit to the data points within the exponential growth phase.

7.5. Supplementary Information for Chapter 4.3

Western blot analysis for the detection of EclA in *E. cloacae* subsp. *cloacae*

Both pellet and supernatant fractions were collected from an overnight culture of $S2^{WT\text{-}HS0}$ and $S2^{\Delta\text{-}HS3}$ in LB supplemented with 60 µg/mL of gentamicin at 37 °C with shaking at 180 rpm. SDS sample preparation, SDS-PAGE, and Western blotting using anti-EclA-C as the primary antibody and HRP conjugated goat anti-rabbit as the secondary antibody, were done as described in the materials and methods section of Chapter 3.1 unless otherwise stated.

EclA membrane displacement assay in *E. cloacae* subsp. *cloacae*

Pellet fractions from $S2^{WT\text{-}HS0}$ grown in LB supplemented with 60 µg /mL gentamicin overnight at 37 °C and 180 rpm were treated with one of the following solutions: (1) PBS/Ca, (2) 100 mM methyl α-L-fucoside in PBS/Ca, or (3) 100 mM methyl α-D-mannoside in PBS/Ca. These treatments and EclA Western Blot analysis were conducted as described in the materials and methods section of Chapter 3.1.

7.6. Supplementary Information for Chapter 4.4

Autoaggregation formation assay for *E. cloacae* subsp. *cloacae*

An overnight culture of *E. cloacae* subsp. *cloacae* was grown in LB medium (supplemented with 60 µg/mL gentamicin if the strains were carrying pMP7605) at 37 °C with shaking at 180 rpm. Cells were then inoculated into LB medium (supplemented with 60 µg/mL gentamicin if the strains were carrying pMP7605) to a final OD_{600} of 0.02. Aliquots of 1.25 mL were transferred into 24-well coverglass-bottom imaging plates (Zell-Kontakt, #5231-20), sealed with breathable foil (Greiner Bio-One, #676051), and incubated at 37 °C with 72% humidity and shaking at 180 rpm for 48 h. For exogenous EclA supplementation assays, a final concentration of 10 µM recombinant EclA was added to the LB medium prior to aliquoting the cultures onto the plates. Following incubation, whole-well brightfield images were acquired using the same procedure described in the materials and methods section of Chapter 3.1 for fluorescence microscopy.

Autoaggregate disruption assay, brightfield, and SEM for *E. cloacae* subsp. *cloacae*

E. cloacae subsp. *cloacae* strains were cultured under identical medium and conditions as described for the autoaggregate formation assay, with the following modifications: Biofilms were grown under static conditions in 24-well coverglass-bottom imaging plates (Zell-Kontakt, #5231-20) at 37 °C with 72% relative humidity for 48 hours. For exogenous EclA supplementation assays, a final concentration of 10 µM recombinant EclA was added to the LB medium prior to aliquoting the cultures onto the plates. Initial brightfield images were captured to document pre-disruption biofilm architecture using the same procedure described in the materials and methods section of Chapter 3.1 for fluorescence microscopy.

To assess autoaggregate stability, plates were subsequently agitated at 180 rpm for 3 minutes in a shaker incubator. Post-disruption brightfield images were then acquired using the same approach.

For SEM analysis of *E. cloacae* subsp. *cloacae* autoaggregates, 200 µL aliquots were collected from cultures following mechanical autoaggregate disruption (autoaggregates were included if present). Samples were fixed with glutaraldehyde (2% final concentration) in Eppendorf tubes and incubated at room temperature for 30 minutes. Fixed samples were then spotted onto 0.2 µm pore-size filter membranes under vacuum suction. Membranes were washed with 500 µL sterile distilled water to remove residual salts and medium components, then air-dried at room temperature. Fixed samples were transferred to the Leibniz Institute for New Materials (Saarbrücken) for imaging. Samples were sputter-coated with Au-Pd, and imaged under high vacuum using a field-emission SEM. Images were acquired at different magnifications with an Everhart-Thornley Detector (ETD), and 5.0 kV accelerating voltage.

Whole genome sequencing, assembly, and analysis of *E. cloacae* subsp. *cloacae* strains

WGS of all *E. cloacae* subsp. *cloacae* derivatives harboring pMP7605 was done using ONT by MicrobesNG as described in the materials and methods section of Chapter 3.1. Genomic assembly was also provided by MicrobesNG through their bioinformatics pipeline. Data analysis and visualization was done using the web-based software Proksee where .gbk files of complete genome assemblies were uploaded. Genome alignment between assemblies from different strains was done using the BLAST tool within Proksee by uploading the query assembly after choosing to filter low complexity sequences and skip enclosed lower-scored

features. The BLAST formatter was used to generate % identity and display the results by color matching.

7.7. Supplementary Information for Chapter 5.1

EclA N-terminus recombinant expression and purification:

The His-tagged N-terminal domain of EclA (EclA-N), derived from *E. cloacae* subsp. *cloacae* DSM 30054 (NCBI RefSeq assembly GCF_000025565.1), was recombinantly expressed and purified. The corresponding protein sequence is shown in SI Table 4. Expression and purification followed the protocol previously described by Beshr et al. (2025) for other recombinant proteins (Chapter 3.1). Briefly, *E. coli* BL21(DE3) harboring the plasmid pET22b-*eclA-N-tag* was used for expression. Following induction and cell lysis, the supernatant was loaded onto a HiTrap affinity column (GE Healthcare), washed with TBS/Ca buffer containing 20 mM imidazole, and eluted with TBS/Ca supplemented with 250 mM imidazole. The eluted protein was then dialyzed against TBS/Ca buffer, and the concentration of EclA-N was calculated using a molar extinction coefficient of 27,960 M^{-1} cm^{-1}.

SI Table 4: Amino acid sequence of His-tagged N-terminus of EclA derived from *E. cloacae* subsp. *cloacae*

EclA-N amino acid sequence	MHHHHHHAKFFATLSQESDASENLIWSGKVDAKNAE GTNTGVALKAGEIITILASGWARNGSENFALTAPQGRI PREGETLTLRNPSLQARLGNENYPVGNHKYRWSVPAE GTLTLFFADGKDQYKDNAGEFSVEVYREADISAAA

Hemagglutination of human red blood cells with *E. cloacae*, EclA-M14A, and the individual C- and N-terminal domains of EclA and their combination

Hemagglutination assays were performed as previously described in the materials and methods section of Chapter 3.1, with the following modifications. The final red blood cell concentration used in the assay was 5% (v/v).

For protein-based hemagglutination, the following recombinant proteins were prepared at a stock concentration of 240 µM in PBS/Ca: EclA-M14A, EclA-C, and EclA-N. A 1:1 mixture of EclA-C and EclA-N was prepared by combining equal volumes of their 240 µM stocks, resulting in a final concentration of 120 µM for each protein. All samples were two-fold serially

diluted in PBS/Ca across 96-well V-bottom plates (Boettger, #05-021-0100) to a final volume of 50 µL per well.

For bacterial hemagglutination, *E. cloacae* subsp. *cloacae* and *E. cloacae* subsp. *dissolvens* strains carrying plasmid pMP7605 were pelleted, washed three times with PBS, and adjusted to a similar OD_{600} for each subspecies and serially diluted. Bacterial samples were similarly two-fold serially diluted in PBS/Ca to a final volume of 50 µL per well.

Treated RBCs (50 µL per well) were added, yielding a final RBC concentration of 2.5% (v/v) in a total volume of 100 µL. Plates were incubated at 37 °C for 30 minutes and centrifuged briefly (1 min at 1000 × g) to visualize hemagglutination patterns.

7.8. Supplementary Information for Chapter 5.2

Adhesion to A549 cells by *E. cloacae* subsp. *cloacae*

A549 human alveolar epithelial cells were cultured in DMEM (Sigma-Aldrich) supplemented with 10% FBS (Sigma-Aldrich), 1% penicillin and 1% streptomycin, and maintained at 37 °C in a humidified 5% CO_2 incubator. For subculturing, cells were washed with PBS, detached using trypsin, and resuspended in fresh medium following centrifugation. Cell viability and concentration were assessed using trypan blue exclusion and only cultures with >95% viability were seeded into a black 96-well plate (Zell kontakt, #3241-20) at a density of 4×10^5 cells/mL followed by incubation for 72 h to reach confluence.

Overnight cultures of *E. cloacae* subsp. *cloacae* $S2^{WT\text{-}HS0}$ and $S2^{\Delta\text{-}HS3}$ strains were grown in LB supplemented with 60 µg/mL gentamicin. Bacterial cultures were washed with PBS/Ca stained with 1 µM SYTO™ 9 (Invitrogen) at rt for 15 min, then washed twice and incubated in PBS/Ca containing 3% BSA for 15 min. OD_{600} was adjusted to 0.1 or 0.2 with filtered LB medium of the same overnight culture, and 50 µL of the suspension was added to each A549-seeded well. Plates were either immediately incubated for 15 min or centrifuged at 1000 × *g* for 5 min as indicated, followed by a 15 min incubation at 37 °C and 5% CO_2. Non-adherent bacteria were removed by five washes with 100 µL PBS/Ca and wells. Bacterial attachment was assessed using an inverted fluorescence microscope (Leica DMi8) equipped with a 63× objective (HC PL APO CS2 63×/0.75 IMM UV), an FITC filter cube (Ex: 460-500 nm, DC: 505 nm, Em: 512-542 nm), and a monochrome camera (Leica DFC7000 GT). Identical imaging settings were applied across all conditions.

7.9. Supplementary Information for Chapter 5.3

Labeling of EclA-M14A with fluorescein isothiocyanate

FITC labeling of EclA-M14A was performed by mixing 1 mL of 60 µM EclA-M14A, dissolved in 500 mM sodium carbonate buffer (Na_2CO_3, pH 9.3), with 47.1 µL of freshly prepared 3 mg/mL FITC (dissolved in the same Na_2CO_3 buffer). The reaction mixture was incubated at 25 °C for 1 hour with shaking at 500 rpm. To remove unreacted FITC and exchange the buffer, the mixture was centrifuged through a 5 kDa molecular weight cutoff Vivaspin column and washed four times with PBS/Ca.

In Vitro Lewis antigen adhesion of *E. cloacae* subsp. *dissolvens*

The adhesion of *E. cloacae* subsp. *dissolvens* $S1^{WT}$ and $S1^{\Delta}$ strains to polyacrylamide-conjugated Lewis antigens (PAA-Le^a, Le^b, Le^c; GlycoNZ) was evaluated using a modified fluorescence-based assay (Hauck et al., 2013). PAA-glycans were diluted to 100 µg/mL in carbonate buffer (pH 9.5; 15.9 mM Na_2CO_3, 30 mM $NaHCO_3$), and 100 µL/well was coated onto a 96-well high-binding black microtiter plate (GreinerBioOne Germany, #655077). After brief centrifugation (1000 × *g*, 30 s) plates were dried overnight at 40 °C. Wells were washed three times with 120 µL PBS containing 0.05% Tween-20 (PBS-T), blocked with 5% BSA in PBS (120 µL/well, 2 h, 37 °C), and washed again three times with PBS-T (150 µL/well).
Bacteria were grown in $M63^+$ medium for 48 h at 37 °C. For fluorescence detection, cultures were washed in PBS, stained with acridine orange (1 µg/mL final concentration, 10 min shaking), and washed twice before resuspension in PBS to OD_{600} = 2. Bacterial suspensions (100 µL) or 100 µL of FITC-labeled EclA-M14A (1 µM) were added to coated/uncoated wells, incubated (10 min, 37 °C, 80 rpm), and wells were subsequently washed 3 times with PBS. Fluorescence was measured (Ex/Em: 485/520 nm) with a FLUOstar Omega plate reader. SI Figure 2 shows the validation of the Lewis antigen coating by using 1 µM of EclA-M14A-FITC.

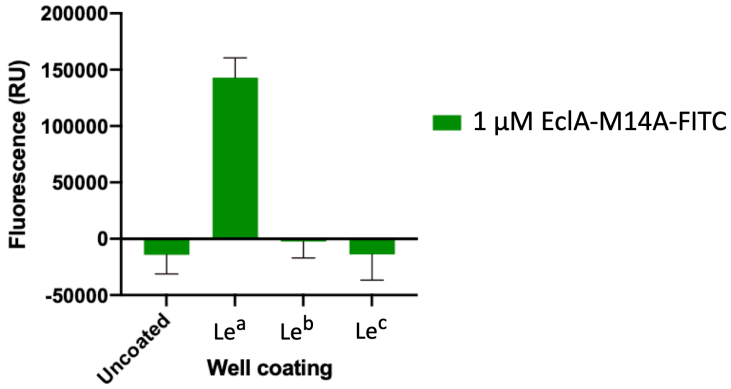

SI Figure 2: Validation of polyacrylamide-conjugated Lewis antigen coating to wells by EclA-M14A-FITC adhesion. The coating procedure was conducted as described above, with the modification of PAA-Lewis antigen concentration used (15 µg/mL).

7.10. Strains, Plasmids and Primers

SI Table 5: *E. cloacae* subsp. *dissolvens* strains used.

***E. cloacae* subsp. *dissolvens* strains**	**Thesis designation**	**Note**	**Lab/other designation**	**Reference**	**CBCH Stock Collection Code**
***E. cloacae* subsp. *dissolvens* DSM 16657**	-	-	-	DSMZ	M13
E. cloacae* subsp. *dissolvens* DSM 16657 Δ*eclA	-	- M13 with deleted *eclA* via allelic exchange	-	This work	M18
***E. cloacae* subsp. *dissolvens* DSM 16657 pMP7605**	$S1^{WT}$	- M13 conjugated via triparental mating with pMP7605 - ONT-sequenced as 289632L_WTS1pMP7605	-WT EclS1 -WT S1	This work	M16
***E. cloacae* subsp. *dissolvens* DSM 16657 Δ*eclA* pMP7605**	$S1^{\Delta}$	- M18 conjugated via triparental mating with pMP7605 -Δ*eclA* - ONT sequenced as 289633L_DelS1pMP7605	-ΔEclS1 -Del S1	This work	M19

SI Table 6: *E. cloacae* subsp. *cloacae* strains used.

***E. cloacae* subsp. *cloacae* strains**	**Thesis designation**	**Note**	**Lab/other designation**	**Reference**	**CBCH Stock Collection Code**
***E. cloacae* subsp. *cloacae* DSM 30054**	-	-	-	DSMZ	M12
E. *cloacae* subsp. *cloacae* DSM 30054 Δ*teR* pMP7605	$S2^{WT\text{-}HS0}$	- M12 heat shock with pMP7605 - Δ*teR* - Autoaggregate enhanced variant - ONT-sequenced as 289634L_WTS2pMP7605HSori	WT HSori	This work	M14
***E. cloacae* subsp. *cloacae* DSM 30054 pMP7605**	$S2^{WT\text{-}HS1}$	- M12 heat shock with pMP7605 - WT control strain	WT HS1	This work	M32
***E. cloacae* subsp. *cloacae* DSM 30054 pMP7605**	$S2^{WT\text{-}HS2}$	- M12 heat shock with pMP7605 - ONT-sequenced as 289635L_WTS2pMP7605HS2 - WT control strain	WT HS2	This work	M33
***E. cloacae* subsp. *cloacae* DSM 30054 pMP7605**	$S2^{WT\text{-}HS3}$	- M12 heat shock with pMP7605 - WT control strain	WT HS3	This work	M34
***E. cloacae* subsp. *cloacae* DSM 30054 pMP7605**	$S2^{WT\text{-}EP}$	- M12 electroporated with pMP7605 - WT control strain	WTEP	This work	M25
E. cloacae* subsp. *cloacae* DSM 30054 Δ*eclA	-	- M12 with deleted *eclA* by allelic exchange	ΔEclS2	This work	M22
***E. cloacae* subsp. *cloacae* DSM 30054 Δ*eclA* pMP7605**	$S2^{\Delta\text{-}HS1}$	- M22 heat shock with pMP7605 - Δ*eclA* control strain	ΔHS1	This work	M27

***E. cloacae* subsp. *cloacae* DSM 30054 Δ*eclA* pMP7605**	$S2^{\Delta\text{-HS2}}$	- M22 heat shock with pMP7605 - Δ*eclA* control strain	ΔHS2	This work	M28
***E. cloacae* subsp. *cloacae* DSM 30054 Δ*eclA* pMP7605**	$S2^{\Delta\text{-HS3}}$	- M22 heat shock with pMP7605 - ONT-sequenced as 289636L_DelS2pMP7605HS3 - Δ*eclA* control strain	ΔHS3	This work	M23
***E. cloacae* subsp. *cloacae* DSM 30054 Δ*eclA* pMP7605**	$S2^{\Delta\text{-EP}}$	- M22 electroporated with pMP7605 -Δ*eclA* control strain	ΔEP	This work	M26

SI Table 7: *P. aeruginosa* strains used.

***P. aeruginosa* strains**	**Thesis designation**	**Note**	**Lab/other designation**	**Reference**	**CBCH Stock Collection Code**
***P. aeruginosa* PAO1 pMP7605**	-	- Used for in vivo zebrafish larvae immersion experiments	WT PAO1	Stock collection	PA13
***P. aeruginosa* PAO1 Δ*lecA*Δ*lecB* pMP7605**	-	- Used for in vivo zebrafish larvae immersion experiments	ΔΔ PAO1	Stock collection	PA34
***P. aeruginosa* PA14 pMP7605**	-	- Used for in vivo zebrafish larvae immersion experiments	WT PA14	Stock collection	PA14
***P. aeruginosa* PA14 Δ*lecA*Δ*lecB* pMP7605**	-	- Used for in vivo zebrafish larvae immersion experiments	ΔΔ PA14	Stock collection	PA42

SI Table 8: Recombinant protein expression strains used.

Recombinant protein expression strains	Note	Reference	CBCH Stock Collection Code
E. coli* BL21 (DE3) pET22b-*eclA	- Recombinant expression of EclA-WT (short + long) from *E. cloacae* subsp. *cloacae* DSM 30054	Beshr et al., (2025)	EC74
E. coli* BL21 (DE3) pET22b-*eclA-L	- Recombinant expression of EclA-M14A from *E. cloacae* subsp. *cloacae* DSM 30054	Beshr et al., (2025)	EC92
E. coli* BL21 (DE3) pET22b-*eclA-C	- Recombinant expression of EclA C-terminus from *E. cloacae* subsp. *cloacae* DSM 30054	Beshr et al., (2025)	EC100
E. coli* BL21(DE3) pET22b-*eclA-N-tag	- Recombinant expression of His-tagged EclA N-terminus from *E. cloacae* subsp. *cloacae* DSM 30054	Beshr et al., (2025)	EC96
E. coli* BL21 (DE3) pET25-*pa2L	- Recombinant expression of LecB from *P. aeruginosa* PAO1	Stock collection	EC15

SI Table 9: Plasmid cloning and transformation strains used.

Cloning Strains + Plasmids	Note	Reference	CBCH Stock Collection Code
***E. coli* BW19610 pKNG101**	-	Stock collection	EC13
***E. coli* BW19610 pKNG101_16657**	-	This work	EC104
***E. coli* BW19610 pKNG101_16657**	-	This work	EC105
***E. coli* TransforMax™ EC100D™ pir-116 pKNG101_30054_GmR**	-	AG Luzhetskyy	EC122
***E. coli* DH5α pMP7605**	-	Stock collection	EC67
***E. coli* HB101 pRK600**	- Helper strain for triparental conjugation	(Keen et al., 1988) (Boyer & Roulland-dussoix, 1969)	EC19

SI Table 10: Plasmids used.

Plasmids	Resistance Marker	Note	Other designations	Reference
pMP7605	Gentamicin	- Codes for mCherry for red fluorescence labeling	pMP7605	Lagendijk et al., (2010)
pKNG101	Streptomycin	- Suicide vector facilitating double recombination events	pKNG101	Kaniga et al., (1991)
pKNG101_16657	Streptomycin	- Suicide vector for *eclA* knockout in *E. cloacae* subsp. *dissolvens* DSM 16657	pKNG101_16657/ pKNG_S1	This work
pKNG101_30054	Streptomycin	- Incompatible suicide vector for *eclA* knockout in *E. cloacae* subsp. *cloacae* DSM 30054	pKNG101_30054/ pKNG_S2	This work
pKNG101_30054_GmR	Gentamicin	- Suicide vector for *eclA* knockout in *E. cloacae* subsp. *cloacae* DSM 30054	pKNG101_30054_GmR_SpeI_Nico2/ pKNG_S2	This work

SI Table 11: Primers used.

Primers	Reverse/ Forward	Sequence	Hybridization	Reference	CBCH Stock Collection Code
MF05	Reverse	gccgatattgagaggata	- 128 base pairs downstream *eclA* in *E. cloacae* subsp. *dissolvens* DSM 16657	This work	#1102
MF06	Forward	cgcctgactattctcatt	- 146 base pairs upstream eclA in *E. cloacae* subsp. *dissolvens* DSM 16657	This work	#1103
MF07	Forward	gatgatgagaagttcgtg	- 87 base pairs downstream *eclA* in *E. cloacae* subsp. *cloacae* DSM 30054	This work	#1104
MF08	Reverse	cagacaggtcttgtatcg	- 149 base pairs upstream *eclA* in *E. cloacae* subsp. *cloacae* DSM 30054	This work	#1105
MF17.1	Forward	aaaaaactagtccgcatgatgaacctgaatcgc	- 301 base pairs upstream the gentamicin resistance gene coding for gentamicin-3-acetyltransferase (NCBI AAB06696.1) in pMP7605 - Contains an optimized SpeI site	This work	#1115
MF18.1	Reverse	aaaaaactagtccttgaatcgggatatgcaggc	- 195 base pairs downstream the gentamicin resistance gene coding for gentamicin-3-acetyltransferase (NCBI AAB06696.1) in pMP7605 - Contains an optimized SpeI site	This work	#1117
#1001	Forward	tattaattgatctgcatcaacttaacg	- Upstream pKNG101's multiple cloning site	Stock collection	#1001

8. References

Adegbola, R. A., & Old, D. C. (1983). Fimbrial Haemagglutinins in Enterobacter Species. *Microbiology*, *129*(7), 2175-2180. https://doi.org/10.1099/00221287-129-7-2175

Ahmed, T., Lundgren, A., Arifuzzaman, M., Qadri, F., Teneberg, S., & Svennerholm, A.-M. (2009). Children with the Le(a+b−) Blood Group Have Increased Susceptibility to Diarrhea Caused by Enterotoxigenic *Escherichia coli* Expressing Colonization Factor I Group Fimbriae. *Infection and Immunity*, *77*(5), 2059-2064. https://doi.org/10.1128/IAI.01571-08

Akbari, M., Bakhshi, B., & Najar Peerayeh, S. (2016). Particular Distribution of Enterobacter cloacae Strains Isolated from Urinary Tract Infection within Clonal Complexes. *Iranian Biomedical Journal*, *20*(1), 49-55. https://doi.org/10.7508/ibj.2016.01.007

Anantharaman, V., Iyer, L. M., & Aravind, L. (2012). Ter-dependent stress response systems: novel pathways related to metal sensing, production of a nucleoside-like metabolite, and DNA-processing. *Molecular BioSystems*, *8*(12), 3142. https://doi.org/10.1039/c2mb25239b

Anderson, A. J. G., Morrell, B., Lopez Campos, G., & Valvano, M. A. (2023). Distribution and diversity of type VI secretion system clusters in Enterobacter bugandensis and Enterobacter cloacae. *Microbial Genomics*, *9*(12). https://doi.org/10.1099/mgen.0.001148

Annavajhala, M. K., Gomez-Simmonds, A., & Uhlemann, A.-C. (2019). Multidrug-Resistant Enterobacter cloacae Complex Emerging as a Global, Diversifying Threat. *Frontiers in Microbiology*, *10*. https://doi.org/10.3389/fmicb.2019.00044

Arcilla, M. B., & Sturgeon, P. (1971). Perinatal expression of the Lewis and secretor blood group systems. *Pediatric Research*, *5*(8), 422-423. https://doi.org/10.1203/00006450-197108000-00215

Augusto, L. A., Bourgeois-Nicolaos, N., Breton, A., Barreault, S., Alonso, E. H., Gera, S., Faraut-Derouin, V., Semaan, N., De Luca, D., Chaby, R., Doucet-Populaire, F., & Tissières, P. (2021). Presence of 2-hydroxymyristate on endotoxins is associated with death in neonates with *Enterobacter cloacae* complex septic shock. *IScience*, *24*(8), 102916. https://doi.org/10.1016/j.isci.2021.102916

Barnes, A. I., Ortiz, C., Paraje, M. G., Balanzino, L. E., & Albesa, I. (1997). Purification and characterization of a cytotoxin from *Enterobacter cloacae*. *Canadian Journal of Microbiology*, *43*(8), 729-733. https://doi.org/10.1139/m97-105

Beshr, G., Sikandar, A., Gläser, J., Fares, M., Sommer, R., Wagner, S., Köhnke, J., & Titz, A. (2025). A fucose-binding superlectin from *Enterobacter cloacae* with high Lewis and ABO blood group antigen specificity. *Journal of Biological Chemistry*, *301*(2), 108151. https://doi.org/10.1016/j.jbc.2024.108151

Beshr, G., Sikandar, A., Jemiller, E.-M., Klymiuk, N., Hauck, D., Wagner, S., Wolf, E., Koehnke, J., & Titz, A. (2017). Photorhabdus luminescens lectin A (PllA): A new probe for detecting α-galactoside-terminating glycoconjugates. *Journal of Biological Chemistry*, *292*(48), 19935-19951. https://doi.org/10.1074/jbc.M117.812792

Bhar, S., Edelmann, M. J., & Jones, M. K. (2021). Characterization and proteomic analysis of outer membrane vesicles from a commensal microbe, Enterobacter cloacae. *Journal of Proteomics*, *231*, 103994. https://doi.org/10.1016/j.jprot.2020.103994

Bjarnsholt, T. (2013). The role of bacterial biofilms in chronic infections. *APMIS*, *121*(s136), 1-58. https://doi.org/10.1111/apm.12099

Boman, H. G., & Hultmark, D. (1987). Cell-Free Immunity in Insects. *Annual Review of Microbiology*, *41*(1), 103-126. https://doi.org/10.1146/annurev.mi.41.100187.000535

Boyer, H. W., & Roulland-dussoix, D. (1969). A complementation analysis of the restriction and modification of DNA in Escherichia coli. *Journal of Molecular Biology*, *41*(3), 459-472. https://doi.org/10.1016/0022-2836(69)90288-5

Brenner, D. J., McWhorter, A. C., Kai, A., Steigerwalt, A. G., & Farmer, J. J. (1986). Enterobacter asburiae sp. nov., a new species found in clinical specimens, and reassignment of Erwinia dissolvens and Erwinia nimipressuralis to the genus Enterobacter as Enterobacter dissolvens comb. nov. and Enterobacter nimipressuralis comb. nov. *Journal of Clinical Microbiology*, *23*(6), 1114-1120. https://doi.org/10.1128/jcm.23.6.1114-1120.1986

Bruneau, A., Gillon, E., Furiga, A., Brachet, E., Alami, M., Roques, C., Varrot, A., Imberty, A., & Messaoudi, S. (2023). Discovery of potent 1,1-diarylthiogalactoside glycomimetic inhibitors of *Pseudomonas aeruginosa* LecA with antibiofilm properties. *European Journal of Medicinal Chemistry*, *247*, 115025. https://doi.org/10.1016/j.ejmech.2022.115025

Chang, C.-Y., Huang, P.-H., & Lu, P.-L. (2022). The Resistance Mechanisms and Clinical Impact of Resistance to the Third Generation Cephalosporins in Species of Enterobacter cloacae Complex in Taiwan. *Antibiotics*, *11*(9), 1153. https://doi.org/10.3390/antibiotics11091153

Chemani, C., Imberty, A., de Bentzmann, S., Pierre, M., Wimmerová, M., Guery, B. P., & Faure, K. (2009). Role of LecA and LecB Lectins in *Pseudomonas aeruginosa* -Induced Lung Injury and Effect of Carbohydrate Ligands. *Infection and Immunity*, *77*(5), 2065-2075. https://doi.org/10.1128/IAI.01204-08

da Silva, D. P., Matwichuk, M. L., Townsend, D. O., Reichhardt, C., Lamba, D., Wozniak, D. J., & Parsek, M. R. (2019). The Pseudomonas aeruginosa lectin LecB binds to the exopolysaccharide Psl and stabilizes the biofilm matrix. *Nature Communications*, *10*(1), 2183. https://doi.org/10.1038/s41467-019-10201-4

Davin-Regli, A., Lavigne, J.-P., & Pagès, J.-M. (2019). *Enterobacter* spp.: Update on Taxonomy, Clinical Aspects, and Emerging Antimicrobial Resistance. *Clinical Microbiology Reviews*, *32*(4). https://doi.org/10.1128/CMR.00002-19

Davin-Regli, A., & Pagès, J.-M. (2015). *Enterobacter aerogenes* and *Enterobacter cloacae*; versatile bacterial pathogens confronting antibiotic treatment. *Frontiers in Microbiology*, *6*. https://doi.org/10.3389/fmicb.2015.00392

de Oliveira, I. A., & Corvelo, T. C. de O. (2021). ABH and Lewis blood group systems and their relation to diagnosis and risk of Helicobacter pylori infection. *Microbial Pathogenesis*, *152*, 104653. https://doi.org/10.1016/j.micpath.2020.104653

Debroy, R., & Ramaiah, S. (2023). Translational protein RpsE as an alternative target for novel nucleoside analogues to treat MDR Enterobacter cloacae ATCC 13047: network analysis and molecular dynamics study. *World Journal of Microbiology and Biotechnology*, *39*(7), 187. https://doi.org/10.1007/s11274-023-03634-z

Di Martino, P. (2018). Extracellular polymeric substances, a key element in understanding biofilm phenotype. *AIMS Microbiology*, *4*(2), 274-288. https://doi.org/10.3934/microbiol.2018.2.274

Díaz-Pascual, F., Ortíz-Severín, J., Varas, M. A., Allende, M. L., & Chávez, F. P. (2017). In vivo Host-Pathogen Interaction as Revealed by Global Proteomic

Profiling of Zebrafish Larvae. *Frontiers in Cellular and Infection Microbiology*, *7*. https://doi.org/10.3389/fcimb.2017.00334

Diggle, S. P., Stacey, R. E., Dodd, C., Cámara, M., Williams, P., & Winzer, K. (2006). The galactophilic lectin, LecA, contributes to biofilm development in *Pseudomonas aeruginosa*. *Environmental Microbiology*, *8*(6), 1095-1104. https://doi.org/10.1111/j.1462-2920.2006.001001.x

Ejaz, M., Zhao, B., Wang, X., Bashir, S., Haider, F. U., Aslam, Z., Khan, M. I., Shabaan, M., Naveed, M., & Mustafa, A. (2021). Isolation and Characterization of Oil-Degrading Enterobacter sp. from Naturally Hydrocarbon-Contaminated Soils and Their Potential Use against the Bioremediation of Crude Oil. *Applied Sciences*, *11*(8), 3504. https://doi.org/10.3390/app11083504

Fares, M., Imberty, A., & Titz, A. (2025). Bacterial lectins: multifunctional tools in pathogenesis and possible drug targets. *Trends in Microbiology*. https://doi.org/10.1016/j.tim.2025.03.007

Farfour, E., Dortet, L., Guillard, T., Chatelain, N., Poisson, A., Mizrahi, A., Fournier, D., Bonnin, R. A., Degand, N., Morand, P., Janvier, F., Fihman, V., Corvec, S., Broutin, L., Le Brun, C., Yin, N., Héry-Arnaud, G., Grillon, A., Bille, E., … Vasse, M. (2022). Antimicrobial Resistance in Enterobacterales Recovered from Urinary Tract Infections in France. *Pathogens*, *11*(3), 356. https://doi.org/10.3390/pathogens11030356

Farsiani, H., Salimiyan Rizi, K., & Ghazvini, K. (2019). Published by: Mashhad University of Medical Sciences Salimiyan Rizi K, Ghazvini K, Farsiani H. Clinical and pathogenesis overview of Enterobacter infections. In *Clinical Medicine Rev Clin Med* (Vol. 6, Issue 4). http://rcm.mums.ac.ir

Ferry, A., Plaisant, F., Ginevra, C., Dumont, Y., Grando, J., Claris, O., Vandenesch, F., & Butin, M. (2020). Enterobacter cloacae colonisation and infection in a neonatal intensive care unit: retrospective investigation of preventive measures implemented after a multiclonal outbreak. *BMC Infectious Diseases*, *20*(1), 682. https://doi.org/10.1186/s12879-020-05406-8

Flores, E., Dutta, S., Bosserman, R., van Hoof, A., & Krachler, A.-M. (2023). Colonization of larval zebrafish (*Danio rerio*) with adherent-invasive *Escherichia coli* prevents recovery of the intestinal mucosa from drug-induced enterocolitis. *MSphere*, *8*(6). https://doi.org/10.1128/msphere.00512-23

Fornstedt, N., & Porath, J. (1975). Characterization studies on a new lectin found in seeds of Vicia ervilia. *FEBS Letters*, *57*(2), 187-191. https://doi.org/10.1016/0014-5793(75)80713-7

Frensch, M., Jäger, C., Müller, P. F., Tadić, A., Wilhelm, I., Wehrum, S., Diedrich, B., Fischer, B., Meléndez, A. V., Dengjel, J., Eibel, H., & Römer, W. (2021). Bacterial lectin BambL acts as a B cell superantigen. *Cellular and Molecular Life Sciences*, *78*(24), 8165-8186. https://doi.org/10.1007/s00018-021-04009-z

Frutos-Grilo, E., Kreling, V., Hensel, A., & Campoy, S. (2023). Host-pathogen interaction: Enterobacter cloacae exerts different adhesion and invasion capacities against different host cell types. *PLOS ONE*, *18*(10), e0289334. https://doi.org/10.1371/journal.pone.0289334

Gadar, K., & McCarthy, R. R. (2023). Using next generation antimicrobials to target the mechanisms of infection. *Npj Antimicrobials and Resistance*, *1*(1), 11. https://doi.org/10.1038/s44259-023-00011-6

Gan, Y., Zhao, G., Wang, Z., Zhang, X., Wu, M. X., & Lu, M. (2023). Bacterial Membrane Vesicles: Physiological Roles, Infection Immunology, and Applications. *Advanced Science*, *10*(25). https://doi.org/10.1002/advs.202301357

Ganbold, M., Seo, J., Wi, Y. M., Kwon, K. T., & Ko, K. S. (2023). Species identification, antibiotic resistance, and virulence in Enterobacter cloacae complex clinical isolates from South Korea. *Frontiers in Microbiology*, *14*. https://doi.org/10.3389/fmicb.2023.1122691

Garinet, S., Fihman, V., Jacquier, H., Corvec, S., Le Monnier, A., Guillard, T., Cattoir, V., Zahar, J.-R., Woerther, P.-L., Carbonnelle, E., Wargnier, A., Kernéis, S., & Morand, P. C. (2018). Elective distribution of resistance to beta-lactams among Enterobacter cloacae genetic clusters. *Journal of Infection*, *77*(3), 178-182. https://doi.org/10.1016/j.jinf.2018.05.005

Gasteiger, E., Hoogland, C., Gattiker, A., Duvaud, S., Wilkins, M. R., Appel, R. D., & Bairoch, A. (2005). Protein Identification and Analysis Tools on the Expasy Server. In J. M. Walker (Ed.), *The Proteomics Protocols Handbook* (1st ed., pp. 571-607). Humana Press. https://doi.org/10.1385/1592598900

Girlich, D., Ouzani, S., Emeraud, C., Gauthier, L., Bonnin, R. A., Le Sache, N., Mokhtari, M., Langlois, I., Begasse, C., Arangia, N., Fournier, S., Fortineau, N., Naas, T., & Dortet, L. (2021). Uncovering the novel Enterobacter cloacae complex species responsible for septic shock deaths in newborns: a cohort study. *The Lancet Microbe*, *2*(10), e536-e544. https://doi.org/10.1016/S2666-5247(21)00098-7

Glick, J., & Garber, N. (1983). The Intracellular Localization of Pseudomonas aeruginosa Lectins. *Microbiology*, *129*(10), 3085-3090. https://doi.org/10.1099/00221287-129-10-3085

Grimont, F., & Grimont, P. A. D. (2006). The Genus Enterobacter. In M. Dworkin, S. Falkow, E. Rosenberg, K. Schleifer, & E. Stackebrandt (Eds.), *The Prokaryotes* (pp. 197-214). Springer New York. https://doi.org/10.1007/0-387-30746-X_9

Guerrero-Mandujano, A., Hernández-Cortez, C., Ibarra, J. A., & Castro-Escarpulli, G. (2017). The outer membrane vesicles: Secretion system type zero. *Traffic*, *18*(7), 425-432. https://doi.org/10.1111/tra.12488

Hauck, D., Joachim, I., Frommeyer, B., Varrot, A., Philipp, B., Möller, H. M., Imberty, A., Exner, T. E., & Titz, A. (2013). Discovery of Two Classes of Potent Glycomimetic Inhibitors of *Pseudomonas aeruginosa* LecB with Distinct Binding Modes. *ACS Chemical Biology*, *8*(8), 1775-1784. https://doi.org/10.1021/cb400371r

Hennigs, J. K., Baumann, H. J., Schmiedel, S., Tennstedt, P., Sobottka, I., Bokemeyer, C., Kluge, S., & Klose, H. (2011). Characterization of Enterobacter cloacae Pneumonia: A Single-Center Retrospective Analysis. *Lung*, *189*(6), 475-483. https://doi.org/10.1007/s00408-011-9323-2

Hernandez-Alonso, E., Bourgeois-Nicolaos, N., Lepainteur, M., Derouin, V., Barreault, S., Waalkes, A., Augusto, L. A., Gera, S., Gleizes, O., Tissieres, P., Salipante, S. J., de Luca, D., & Doucet-Populaire, F. (2022). Contaminated Incubators: Source of a Multispecies Enterobacter Outbreak of Neonatal Sepsis. *Microbiology Spectrum*, *10*(4). https://doi.org/10.1128/spectrum.00964-22

Hmelo, L. R., Borlee, B. R., Almblad, H., Love, M. E., Randall, T. E., Tseng, B. S., Lin, C., Irie, Y., Storek, K. M., Yang, J. J., Siehnel, R. J., Howell, P. L., Singh, P. K., Tolker-Nielsen, T., Parsek, M. R., Schweizer, H. P., & Harrison, J. J. (2015). Precision-engineering the Pseudomonas aeruginosa genome with two-step allelic exchange. *Nature Protocols*, *10*(11), 1820-1841. https://doi.org/10.1038/nprot.2015.115

Hoffmann, H., & Roggenkamp, A. (2003). Population Genetics of the Nomenspecies *Enterobacter cloacae*. *Applied and Environmental Microbiology*, *69*(9), 5306-5318. https://doi.org/10.1128/AEM.69.9.5306-5318.2003

Hoffmann, H., Stindl, S., Ludwig, W., Stumpf, A., Mehlen, A., Heesemann, J., Monget, D., Schleifer, K. H., & Roggenkamp, A. (2005). Reassignment of Enterobacter dissolvens to Enterobacter cloacae as E. cloacae subspecies dissolvens comb. nov. and emended description of Enterobacter asburiae and Enterobacter kobei. *Systematic and Applied Microbiology*, *28*(3), 196-205. https://doi.org/10.1016/j.syapm.2004.12.010

Howe, K., Clark, M. D., Torroja, C. F., Torrance, J., Berthelot, C., Muffato, M., Collins, J. E., Humphray, S., McLaren, K., Matthews, L., McLaren, S., Sealy, I., Caccamo, M., Churcher, C., Scott, C., Barrett, J. C., Koch, R., Rauch, G.-J., White, S., … Stemple, D. L. (2013). The zebrafish reference genome sequence and its relationship to the human genome. *Nature*, *496*(7446), 498-503. https://doi.org/10.1038/nature12111

Kaniga, K., Delor, I., & Cornelis, G. R. (1991). A wide-host-range suicide vector for improving reverse genetics in Gram-negative bacteria: inactivation of the blaA gene of Yersinia enterocolitica. *Gene*, *109*(1), 137-141. https://doi.org/10.1016/0378-1119(91)90599-7

Keen, N. T., Tamaki, S., Kobayashi, D., & Trollinger, D. (1988). Improved broad-host-range plasmids for DNA cloning in Gram-negative bacteria. *Gene*, *70*(1), 191-197. https://doi.org/10.1016/0378-1119(88)90117-5

Keller, R., Pedroso, M. Z., Ritchmann, R., & Silva, R. M. (1998). Occurrence of Virulence-Associated Properties in *Enterobacter cloacae*. *Infection and Immunity*, *66*(2), 645-649. https://doi.org/10.1128/IAI.66.2.645-649.1998

Kim, S.-M., Lee, H.-W., Choi, Y.-W., Kim, S.-H., Lee, J.-C., Lee, Y.-C., Seol, S.-Y., Cho, D.-T., & Kim, J. (2012). Involvement of curli fimbriae in the biofilm formation of Enterobacter cloacae. *The Journal of Microbiology*, *50*(1), 175-178. https://doi.org/10.1007/s12275-012-2044-2

Kimmel, C. B., Ballard, W. W., Kimmel, S. R., Ullmann, B., & Schilling, T. F. (1995). Stages of embryonic development of the zebrafish. *Developmental Dynamics*, *203*(3), 253-310. https://doi.org/10.1002/aja.1002030302

Kremer, A., & Hoffmann, H. (2012). Prevalences of the Enterobacter cloacae complex and its phylogenetic derivatives in the nosocomial environment. *European Journal of Clinical Microbiology & Infectious Diseases*, *31*(11), 2951-2955. https://doi.org/10.1007/s10096-012-1646-2

Krzymińska, S., Koczura, R., Mokracka, J., Puton, T., & Kaznowski, A. (2010). Isolates of the Enterobacter cloacae complex induce apoptosis of human intestinal epithelial cells. *Microbial Pathogenesis*, *49*(3), 83-89. https://doi.org/10.1016/j.micpath.2010.04.003

Krzymińska, S., Mokracka, J., Koczura, R., & Kaznowski, A. (2009). Cytotoxic activity of *Enterobacter cloacae* human isolates. *FEMS Immunology & Medical Microbiology*, *56*(3), 248-252. https://doi.org/10.1111/j.1574-695X.2009.00572.x

Lagendijk, E. L., Validov, S., Lamers, G. E. M., De Weert, S., & Bloemberg, G. V. (2010). Genetic tools for tagging Gram-negative bacteria with mCherry for visualization in vitro and in natural habitats, biofilm and pathogenicity studies. *FEMS Microbiology Letters*, *305*(1), 81-90. https://doi.org/10.1111/j.1574-6968.2010.01916.x

Leslie, J. L., Weddle, E., Yum, L. K., Lin, Y., Jenior, M. L., Lee, B., Ma, J. Z., Kirkpatrick, B. D., Nayak, U., Platts-Mills, J. A., Agaisse, H. F., Haque, R., & Petri, W. A. (2021). Lewis Blood-group Antigens Are Associated With Altered Susceptibility to Shigellosis. *Clinical Infectious Diseases : An Official Publication*

of the Infectious Diseases Society of America, *72*(11), e868-e871. https://doi.org/10.1093/cid/ciaa1409
Leusmann, S., Ménová, P., Shanin, E., Titz, A., & Rademacher, C. (2023). Glycomimetics for the inhibition and modulation of lectins. *Chemical Society Reviews*, *52*(11), 3663-3740. https://doi.org/10.1039/D2CS00954D
Lewis, A. L., Szymanski, C. M., Schnaar, R. L., & Aebi, M. (2022). Bacterial and Viral Infections. In Varki A, Cummings RD, & Esko JD (Eds.), *Essentials of Glycobiology* (4th edn) (pp. 555-568). Cold Spring Harbor Laboratory Press.
Lindh, E., & Ursing, J. (1991). Genomic groups and biochemical profiles of clinical isolates of *Enterobacter cloacae*. *APMIS*, *99*(1-6), 507-514. https://doi.org/10.1111/j.1699-0463.1991.tb05183.x
Liu, H. Y., Prentice, E. L., & Webber, M. A. (2024). Mechanisms of antimicrobial resistance in biofilms. *Npj Antimicrobials and Resistance*, *2*(1), 27. https://doi.org/10.1038/s44259-024-00046-3
Liu, S., Chen, L., Wang, L., Zhou, B., Ye, D., Zheng, X., Lin, Y., Zeng, W., Zhou, T., & Ye, J. (2022). Cluster Differences in Antibiotic Resistance, Biofilm Formation, Mobility, and Virulence of Clinical Enterobacter cloacae Complex. *Frontiers in Microbiology*, *13*. https://doi.org/10.3389/fmicb.2022.814831
Lopez-Baez, J. C., Simpson, D. J., LLeras Forero, L., Zeng, Z., Brunsdon, H., Salzano, A., Brombin, A., Wyatt, C., Rybski, W., Huitema, L. F. A., Dale, R. M., Kawakami, K., Englert, C., Chandra, T., Schulte-Merker, S., Hastie, N. D., & Patton, E. E. (2018). Wilms Tumor 1b defines a wound-specific sheath cell subpopulation associated with notochord repair. *ELife*, *7*. https://doi.org/10.7554/eLife.30657
Maheswari, U., Palvai, S., Anuradha, P., & Kammili, N. (2013). Hemagglutination and biofilm formation as virulence markers of uropathogenic Escherichia coli in acute urinary tract infections and urolithiasis. *Indian Journal of Urology*, *29*(4), 277. https://doi.org/10.4103/0970-1591.120093
Marsh, E. K., & May, R. C. (2012). Caenorhabditis elegans, a Model Organism for Investigating Immunity. *Applied and Environmental Microbiology*, *78*(7), 2075-2081. https://doi.org/10.1128/AEM.07486-11
Meade, M. J., Nakas, J. P., & Tanenbaum, S. W. (1993). Highly viscous polysaccharide produced by an Enterobacter isolate on a hemicellulose hydrolysate. *Biotechnology Letters*, *15*(4), 389-392. https://doi.org/10.1007/BF00128282
Ménard, G., Rouillon, A., Cattoir, V., & Donnio, P.-Y. (2021). Galleria mellonella as a Suitable Model of Bacterial Infection: Past, Present and Future. *Frontiers in Cellular and Infection Microbiology*, *11*. https://doi.org/10.3389/fcimb.2021.782733
Meredith, T. C., Mamat, U., Kaczynski, Z., Lindner, B., Holst, O., & Woodard, R. W. (2007). Modification of Lipopolysaccharide with Colanic Acid (M-antigen) Repeats in Escherichia coli. *Journal of Biological Chemistry*, *282*(11), 7790-7798. https://doi.org/10.1074/jbc.M611034200
Merhi, G., Amayri, S., Bitar, I., Araj, G. F., & Tokajian, S. (2023). Whole Genome-Based Characterization of Multidrug Resistant Enterobacter and Klebsiella aerogenes Isolates from Lebanon. *Microbiology Spectrum*, *11*(1). https://doi.org/10.1128/spectrum.02917-22
Mezzatesta, M. L., Gona, F., & Stefani, S. (2012). *Enterobacter cloacae* Complex: Clinical Impact and Emerging Antibiotic Resistance. *Future Microbiology*, *7*(7), 887-902. https://doi.org/10.2217/fmb.12.61

Mikkelsen, H., McMullan, R., & Filloux, A. (2011). The Pseudomonas aeruginosa Reference Strain PA14 Displays Increased Virulence Due to a Mutation in ladS. *PLoS ONE*, *6*(12), e29113. https://doi.org/10.1371/journal.pone.0029113

Miller, W. R., & Arias, C. A. (2024). ESKAPE pathogens: antimicrobial resistance, epidemiology, clinical impact and therapeutics. *Nature Reviews Microbiology*, *22*(10), 598-616. https://doi.org/10.1038/s41579-024-01054-w

Mitchell, E. P., Sabin, C., Šnajdrová, L., Pokorná, M., Perret, S., Gautier, C., Hofr, C., Gilboa-Garber, N., Koča, J., Wimmerová, M., & Imberty, A. (2005). High affinity fucose binding of *Pseudomonas aeruginosa* lectin PA-IIL: 1.0 Å resolution crystal structure of the complex combined with thermodynamics and computational chemistry approaches. *Proteins: Structure, Function, and Bioinformatics*, *58*(3), 735-746. https://doi.org/10.1002/prot.20330

Moore, W. E. C., Stackebrandt, E., Kandler, O., Colwell, R. R., Krichevsky, M. I., Truper, H. G., Murray, R. G. E., Wayne, L. G., Grimont, P. A. D., Brenner, D. J., Starr, M. P., & Moore, L. H. (1987). Report of the Ad Hoc Committee on Reconciliation of Approaches to Bacterial Systematics. *International Journal of Systematic and Evolutionary Microbiology*, *37*(4), 463-464. https://doi.org/10.1099/00207713-37-4-463

Morand, P. C., Billoet, A., Rottman, M., Sivadon-Tardy, V., Eyrolle, L., Jeanne, L., Tazi, A., Anract, P., Courpied, J.-P., Poyart, C., & Dumaine, V. (2009). Specific Distribution within the *Enterobacter cloacae* Complex of Strains Isolated from Infected Orthopedic Implants. *Journal of Clinical Microbiology*, *47*(8), 2489-2495. https://doi.org/10.1128/JCM.00290-09

Mustafa, A., Ibrahim, M., Rasheed, M. A., Kanwal, S., Hussain, A., Sami, A., Ahmed, R., & Bo, Z. (2020). Genome-wide Analysis of Four Enterobacter cloacae complex type strains: Insights into Virulence and Niche Adaptation. *Scientific Reports*, *10*(1), 8150. https://doi.org/10.1038/s41598-020-65001-4

Naghavi, M., Vollset, S. E., Ikuta, K. S., Swetschinski, L. R., Gray, A. P., Wool, E. E., Robles Aguilar, G., Mestrovic, T., Smith, G., Han, C., Hsu, R. L., Chalek, J., Araki, D. T., Chung, E., Raggi, C., Gershberg Hayoon, A., Davis Weaver, N., Lindstedt, P. A., Smith, A. E., … Murray, C. J. L. (2024). Global burden of bacterial antimicrobial resistance 1990-2021: a systematic analysis with forecasts to 2050. *The Lancet*. https://doi.org/10.1016/S0140-6736(24)01867-1

Neu, T. R., Swerhone, G. D. W., & Lawrence, J. R. (2001). Assessment of lectin-binding analysis for in situ detection of glycoconjugates in biofilm systems. *Microbiology*, *147*(2), 299-313. https://doi.org/10.1099/00221287-147-2-299

Nishikawa, K., Oi, S., & Yamamoto, T. (1979). Induced Production of Acidic Polysaccharide by Benzalkonium Chloride in a Bacterium and Some Properties of the Acidic Polysaccharide Produced. *Agricultural and Biological Chemistry*, *43*(11), 2305-2310. https://doi.org/10.1080/00021369.1979.10863803

Nogaret, P., El Garah, F., & Blanc-Potard, A.-B. (2021). A Novel Infection Protocol in Zebrafish Embryo to Assess Pseudomonas aeruginosa Virulence and Validate Efficacy of a Quorum Sensing Inhibitor In Vivo. *Pathogens*, *10*(4), 401. https://doi.org/10.3390/pathogens10040401

Ogawara, H. (2021). Possible drugs for the treatment of bacterial infections in the future: anti-virulence drugs. *The Journal of Antibiotics*, *74*(1), 24-41. https://doi.org/10.1038/s41429-020-0344-z

Ostadfar, A. (2016). Fluid Mechanics and Biofluids Principles. In *Biofluid Mechanics* (pp. 1-60). Elsevier. https://doi.org/10.1016/B978-0-12-802408-9.00001-6

Ponnusamy, D., & Clinkenbeard, K. D. (2015). Role of Tellurite Resistance Operon in Filamentous Growth of Yersinia pestis in Macrophages. *PLOS ONE*, *10*(11), e0141984. https://doi.org/10.1371/journal.pone.0141984

Pont, S., & Blanc-Potard, A.-B. (2021). Zebrafish Embryo Infection Model to Investigate Pseudomonas aeruginosa Interaction With Innate Immunity and Validate New Therapeutics. *Frontiers in Cellular and Infection Microbiology*, *11*. https://doi.org/10.3389/fcimb.2021.745851

Poplimont, H., Georgantzoglou, A., Boulch, M., Walker, H. A., Coombs, C., Papaleonidopoulou, F., & Sarris, M. (2020). Neutrophil Swarming in Damaged Tissue Is Orchestrated by Connexins and Cooperative Calcium Alarm Signals. *Current Biology*, *30*(14), 2761-2776.e7. https://doi.org/10.1016/j.cub.2020.05.030

Rahal, A., Andreo, A., Le Gallou, F., Bourigault, C., Bouchand, C., Ferriot, C., Corvec, S., Guillouzouic, A., Gras-Leguen, C., Launay, E., Flamant, C., & Lepelletier, D. (2021). Enterobacter cloacae complex outbreak in a neonatal intensive care unit: multifaceted investigations and preventive measures are needed. *Journal of Hospital Infection*, *116*, 87-90. https://doi.org/10.1016/j.jhin.2021.07.012

Ramesh, A., Sharma, S. K., Sharma, M. P., Yadav, N., & Joshi, O. P. (2014). Plant Growth-Promoting Traits in Enterobacter cloacae subsp. dissolvens MDSR9 Isolated from Soybean Rhizosphere and its Impact on Growth and Nutrition of Soybean and Wheat Upon Inoculation. *Agricultural Research*, *3*(1), 53-66. https://doi.org/10.1007/s40003-014-0100-3

Ramirez, D., & Giron, M. (2025). Enterobacter Infections. In *StatPearls*. StatPearls Publishing. https://www.ncbi.nlm.nih.gov/books/NBK559296/

Rayner, C. R., Ioannides-Demos, L. L., Brien, J.-A. E., Liolios, L. L., & Spicer, W. J. (1998). Initial Concentration-Time Profile of Gentamicin Determines Efficacy against *Enterobacter cloacae* ATCC 13047. *Antimicrobial Agents and Chemotherapy*, *42*(6), 1370-1374. https://doi.org/10.1128/AAC.42.6.1370

Ren, Y., Ren, Y., Zhou, Z., Guo, X., Li, Y., Feng, L., & Wang, L. (2010). Complete Genome Sequence of *Enterobacter cloacae* subsp. *cloacae* Type Strain ATCC 13047. *Journal of Bacteriology*, *192*(9), 2463-2464. https://doi.org/10.1128/JB.00067-10

Rosen H.R. (1922). The bacterial pathogen of corn stalk rot. *Phytopathology*, *12*, 497-499.

Roy, P., Horswill, A. R., & Fey, P. D. (2021). Glycan-Dependent Corneocyte Adherence of Staphylococcus epidermidis Mediated by the Lectin Subdomain of Aap. *MBio*, *12*(4), e02908-20. https://doi.org/10.1128/mBio.02908-20

Sartorio, M. G., Pardue, E. J., Feldman, M. F., & Haurat, M. F. (2021). Bacterial Outer Membrane Vesicles: From Discovery to Applications. *Annual Review of Microbiology*, *75*, 609-630. https://doi.org/10.1146/annurev-micro-052821-031444

Sauer, K., Stoodley, P., Goeres, D. M., Hall-Stoodley, L., Burmølle, M., Stewart, P. S., & Bjarnsholt, T. (2022). The biofilm life cycle: expanding the conceptual model of biofilm formation. *Nature Reviews Microbiology*, *20*(10), 608-620. https://doi.org/10.1038/s41579-022-00767-0

Schenkel-Brunner, H. (2007). Blood Group Antigens. In H. Kamerling (Ed.), *Comprehensive Glycoscience* (pp. 343-372). Elsevier. https://doi.org/10.1016/B978-044451967-2/00039-8

Schmitz, D. A., Wechsler, T., Li, H. B., Menze, B. H., & Kümmerli, R. (2024). A new protocol for multispecies bacterial infections in zebrafish and their monitoring through automated image analysis. *PLOS ONE*, *19*(8), e0304827. https://doi.org/10.1371/journal.pone.0304827

Scott, C. A., Carney, T. J., & Amaya, E. (2022). Aerobic glycolysis is important for zebrafish larval wound closure and tail regeneration. *Wound Repair and Regeneration*, *30*(6), 665-680. https://doi.org/10.1111/wrr.13050

Sommer, R., Exner, T. E., & Titz, A. (2014). A Biophysical Study with Carbohydrate Derivatives Explains the Molecular Basis of Monosaccharide Selectivity of the Pseudomonas aeruginosa Lectin LecB. *PLoS ONE*, *9*(11), e112822. https://doi.org/10.1371/journal.pone.0112822

Sommer, R., Wagner, S., Varrot, A., Nycholat, C. M., Khaledi, A., Häussler, S., Paulson, J. C., Imberty, A., & Titz, A. (2016). The virulence factor LecB varies in clinical isolates: consequences for ligand binding and drug discovery. *Chemical Science*, *7*(8), 4990-5001. https://doi.org/10.1039/C6SC00696E

Soria-Bustos, J., Ares, M. A., Gómez-Aldapa, C. A., González-y-Merchand, J. A., Girón, J. A., & De la Cruz, M. A. (2020). Two Type VI Secretion Systems of Enterobacter cloacae Are Required for Bacterial Competition, Cell Adherence, and Intestinal Colonization. *Frontiers in Microbiology*, *11*. https://doi.org/10.3389/fmicb.2020.560488

Stowell, C. P., & Stowell, S. R. (2019). Biologic roles of the <scp>ABH</scp> and Lewis histo-blood group antigens Part I: infection and immunity. *Vox Sanguinis*, *114*(5), 426-442. https://doi.org/10.1111/vox.12787

Šulák, O., Cioci, G., Lameignère, E., Balloy, V., Round, A., Gutsche, I., Malinovská, L., Chignard, M., Kosma, P., Aubert, D. F., Marolda, C. L., Valvano, M. A., Wimmerová, M., & Imberty, A. (2011). Burkholderia cenocepacia BC2L-C Is a Super Lectin with Dual Specificity and Proinflammatory Activity. *PLoS Pathogens*, *7*(9), e1002238. https://doi.org/10.1371/journal.ppat.1002238

Sutton, G. G., Brinkac, L. M., Clarke, T. H., & Fouts, D. E. (2018). Enterobacter hormaechei subsp. hoffmannii subsp. nov., Enterobacter hormaechei subsp. xiangfangensis comb. nov., Enterobacter roggenkampii sp. nov., and Enterobacter muelleri is a later heterotypic synonym of Enterobacter asburiae based on computational analysis of sequenced Enterobacter genomes. *F1000Research*, *7*, 521. https://doi.org/10.12688/f1000research.14566.2

Sych, T., Omidvar, R., Ostmann, R., Schubert, T., Brandel, A., Richert, L., Mely, Y., Madl, J., & Römer, W. (2023). The bacterial lectin LecA from P. aeruginosa alters membrane organization by dispersing ordered domains. *Communications Physics*, *6*(1), 153. https://doi.org/10.1038/s42005-023-01272-3

Taylor, M. E., Drickamer, K., Imberty, A., van Kooyk, Y., Schnaar, R. L., Etzler, M. E., & Varki, A. (2022). Discovery and Classification of Glycan-Binding Proteins. In A. Varki, R. Cummings, & J. Esko (Eds.), *Essentials of Glycobiology* (4th edn) (pp. 375-386). Cold Spring Harbor Laboratory Press.

Tielker, D., Hacker, S., Loris, R., Strathmann, M., Wingender, J., Wilhelm, S., Rosenau, F., & Jaeger, K.-E. (2005). Pseudomonas aeruginosa lectin LecB is located in the outer membrane and is involved in biofilm formation. *Microbiology*, *151*(5), 1313-1323. https://doi.org/10.1099/mic.0.27701-0

Toptchieva, A., Sisson, G., Bryden, L. J., Taylor, D. E., & Hoffman, P. S. (2003). An inducible tellurite-resistance operon in Proteus mirabilis. *Microbiology*, *149*(5), 1285-1295. https://doi.org/10.1099/mic.0.25981-0

Van der Vaart, M., Spaink, H. P., & Meijer, A. H. (2012). Pathogen Recognition and Activation of the Innate Immune Response in Zebrafish. *Advances in Hematology*, *2012*, 1-19. https://doi.org/10.1155/2012/159807

Varas, M., Fariña, A., Díaz-Pascual, F., Ortíz-Severín, J., Marcoleta, A. E., Allende, M. L., Santiviago, C. A., & Chávez, F. P. (2017). Live-cell imaging of Salmonella

Typhimurium interaction with zebrafish larvae after injection and immersion delivery methods. *Journal of Microbiological Methods*, *135*, 20-25. https://doi.org/10.1016/j.mimet.2017.01.020

Vávrová, S., Grones, J., Šoltys, K., Celec, P., & Turňa, J. (2024). The tellurite resistance gene cluster of pathogenic bacteria and its effect on oxidative stress response. *Folia Microbiologica*, *69*(2), 433-444. https://doi.org/10.1007/s12223-024-01133-8

Wang, F., Yang, H., & Wang, Y. (2013). Structure characterization of a fucose-containing exopolysaccharide produced by Enterobacter cloacae Z0206. *Carbohydrate Polymers*, *92*(1), 503-509. https://doi.org/10.1016/j.carbpol.2012.10.014

WHO. (2024). *2023 Antibacterial agents in clinical and preclinical development: an overview and analysis*.

Yang, H.-F., Pan, A.-J., Hu, L.-F., Liu, Y.-Y., Cheng, J., Ye, Y., & Li, J.-B. (2017). Galleria mellonella as an in vivo model for assessing the efficacy of antimicrobial agents against Enterobacter cloacae infection. *Journal of Microbiology, Immunology and Infection*, *50*(1), 55-61. https://doi.org/10.1016/j.jmii.2014.11.011

Yang, R., Han, S., Yu, Y., Li, H., Helmann, J. D., Schaufler, K., Johnson, M. D. L., Yang, Q. E., & Rensing, C. (2025). The *Klebsiella pneumoniae* tellurium resistance gene *terC* contributes to both tellurite and zinc resistance. *Microbiology Spectrum*, *13*(5). https://doi.org/10.1128/spectrum.02634-24

Zahorska, E., Denig, L. M., Lienenklaus, S., Kuhaudomlarp, S., Tschernig, T., Lipp, P., Munder, A., Gillon, E., Minervini, S., Verkhova, V., Imberty, A., Wagner, S., & Titz, A. (2024). High-Affinity Lectin Ligands Enable the Detection of Pathogenic *Pseudomonas aeruginosa* Biofilms: Implications for Diagnostics and Therapy. *JACS Au*. https://doi.org/10.1021/jacsau.4c00670